



UNIVERSITÀ
degli STUDI
di CATANIA



Department of Biomedical and Biotechnological Sciences

Ph.D. in Biotechnology

curriculum in Biomedical and preclinical sciences

XXXIII Cycle

FILIPPO TORRISI

SRC inhibition combined with radiotherapy and proton therapy

A synergistic strategy for glioblastoma treatment

PhD Thesis

Tutor: *Prof. Rosalba Parenti*

Coordinator: *Prof. Vito De Pinto*

ACADEMIC YEARS 2017/2020

TABLE OF CONTENTS

1. ABSTRACT.....	1
2. KEYWORDS AND ABBREVIATIONS.....	2
3. AFFILIATIONS.....	3
4. PREFACE.....	4
5. INTRODUCTION.....	7
Epidemiology of Glioblastoma (GBM).....	7
Histopathological and molecular features of GBM.....	9
Current approaches for GBM treatment.....	10
Current limitations of radiation treatment.....	18
Targeting of SRC proto-oncogene non-receptor tyrosine kinase (SRC).....	22
6. AIMS.....	30
7. RESULTS.....	32
<i>PAPER 1:</i> Preliminary study of novel SRC tyrosine kinase inhibitor and proton therapy combined effect on glioblastoma multiforme cell line: <i>In vitro</i> evaluation of target therapy for the enhancement of protons effectiveness	
<i>PAPER 2:</i> Proton Therapy and SRC Family Kinase Inhibitor Combined Treatments on U87 Human Glioblastoma Multiforme Cell Line	
<i>PAPER 3:</i> SRC Tyrosine Kinase Inhibitor and X-rays Combined Effect on Glioblastoma Cell Lines	
<i>PAPER 4:</i> The Role of Hypoxia and SRC Tyrosine Kinase in Glioblastoma Invasiveness and Radioresistance	
8. DISCUSSION AND CONCLUDING REMARKS.....	93
9. APPENDIX: MATERIALS AND METHODS.....	97
10. REFERENCES.....	104
11. LIST OF PUBLISHED PAPERS AND CONGRESS CONTRIBUTION.....	111
12. ACKNOWLEDGMENTS.....	116

1. ABSTRACT

In the field of neuroncology, radiation therapy has clearly acquired a central role for the treatment of aggressive tumors, such as Glioblastoma (GBM). GBM is the most common malignant and radioresistant brain tumor in adults, characterized by an exiguous life expectancy, with median survival of 6–12 months after diagnosis. The radioresistance of GBM is mainly determined by the occurrence of hypoxic regions, where the indirect effects of ionizing radiation are largely reduced. Moreover, hypoxia is involved in the activation of intracellular signaling pathways mediated by SRC proto-oncogene non-receptor tyrosine kinase (SRC), that leads to proliferation, migration and invasion effects. For this reason, new molecularly targeted drugs for SRC inhibition combined with radiation therapy could increase the effect of ionizing radiation (X-rays for radiotherapy and protons for proton therapy or hadrontherapy), blocking specific pathways of radioresistance.

The aim of this project was to evaluate the synergic radiosensitive effect of a new SRC inhibitor (Si306, Lead Discovery Siena) in combination with radiation therapy for GBM treatment. In a first work, Si306 was tested with proton therapy, demonstrating a radiosensitive effect. Proton therapy experiments were performed at the National Institute for Nuclear Physics, Laboratori Nazionali del Sud, (INFN-LNS) in Catania. Clonogenic assay and molecular pathways analysis were performed to evaluate the surviving fraction and the cell network modulation respectively, confirming the effectiveness of proton therapy in combination with the Si306. In a second work, the radiosensitive effect of Si306, in combination with X-rays irradiation, was evaluated comparing normoxic (21% of oxygen) and hypoxic (1% of oxygen) conditions. In addition to clonogenic assay, γ H2AX molecular marker detection by immunofluorescence was performed to quantify the radiation-induced DNA double-strand break formation and the DNA damage repair ability. The role of SRC inhibition on migration was also evaluated by wound healing assay. These experiments were performed at the research unit “*Imagerie et Stratégies Thérapeutiques des pathologies Cérébrales et Tumorales*” (ISTCT), located in the Cyceron center of Caen, France. It was demonstrated that Si306 exhibited a synergistic effect with X-rays, decreasing radioresistance induced by hypoxia.

In conclusion, while further *in vitro* and *in vivo* investigations are required, the encouraging data confirms Si306 as a novel putative drug to overcome GBM radioresistance.

2. KEYWORDS AND ABBREVIATIONS

Keywords: Glioblastoma; ionizing radiation; radiation therapy; proton therapy; X-rays; gene signatures; hypoxia; radioresistance; radiosensitive; invasion; SRC tyrosine kinase; surviving fraction; DNA damage; combined treatments; targeted therapy

List of abbreviations:

DMF	Dose modifying factor
ECM	Extracellular matrix
EGFR	Epidermal growth factor receptor
FAK	Focal adhesion kinase
GBM	GlioBlastoMa
GSCs	Glioblastoma stem cells
IR	Ionizing radiation
LET	Linear energy transfer
LQ	Linear-quadratic
MMP	Matrix metalloproteinase
nRTK	Non receptor tyrosine kinase
OER	Oxygen enhancement ratio
PE	Plating efficiency
PT	Proton therapy
RBE	Relative biological effectiveness
RT	Radiation therapy
SRC tyrosine kinase	SRC
SF	Surviving fraction
TMZ	Temozolomide

3. AFFILIATIONS

Laboratory of Molecular & Cellular Physiology, Department of Biomedical and Biotechnological Science (BIOMETEC), University of Catania, Via S. Sofia, 89, 95123 Catania, Italy.

Collaborations:

- a) Center for Advanced Preclinical in vivo Research (CAPIR), University of Catania, Via Santa Sofia 89, 95123 Catania, Italy.
- b) Institute of Molecular Bioimaging and Physiology, National Research Council (IBFM-CNR), c/o Fondazione Istituto G. Giglio di Cefalù, Contrada Pietrapollastra-Pisciotta, 90015 Cefalù, Italy.
- c) National Institute for Nuclear Physics, Laboratori Nazionali del Sud (INFN-LNS), Via S. Sofia 62, 95125 Catania, Italy.
- d) Université de Caen Normandie (UNICAEN), Atomique Energie Commission (CEA), Centre national de la recherche scientifique (CNRS), Imagerie et Stratégies Thérapeutiques des pathologies Cérébrales et Tumorales/CERVOxy Group, Cyceron Groupement d'Intérêt Public (GIP), Boulevard Henri Becquerel, 14000 Caen, France. (Periodo di attività di ricerca svolta da giorno 11/03/2019 al 30/09/2019).
- e) Lead Discovery Siena s.r.l. (LDS), via Vittorio Alfieri, 31, Castelnuovo Berardenga, 53019 Siena, Italy
- f) Departments of Nuclear Medicine, Azienda Ospedaliera per l'Emergenza (AOE) Cannizzaro, Via Messina 829, 95126 Catania, Italy.

4. PREFACE

During the last decades, radiobiology research has led to several advancements in the area of radiation oncology, and recent preclinical discoveries are contributing to improve the radiation therapeutic effects in the clinical setting . Radiobiology, also known as radiation biology, is a branch of science which analyzes the effects of radiations on biological tissues and living organisms (Kirsch et al., 2018). The radiations of the whole electromagnetic spectrum which take part in radiobiological studies for clinical purposes are comprised between gamma rays ($\lambda=10^{-12}$ m and $\nu=10^{20}$ Hz) and the high frequency portion of ultraviolet ($\lambda= 10^{-8}$ m and $\nu=10^{16}$ Hz); these radiations are grouped in the class of ionizing radiation (IR) because they have a sufficient energy (>33 eV) to ionize the biological components. The application of IR started in the 1896, when the German physics professor, Wilhelm Conrad Roentgen, published his discoveries about a new type of radiations, called X, for their unknown properties. Since that time, new discoveries have been made over the years and the medical approaches of IR aimed to treat cancer lead to radiation therapy (RT) (Wojcik and Harms-Ringdahl, 2019) Indeed, it is well known that RT is definitely one of the most effective therapeutic strategies for the treatment of tumors, inducing cancer cells death and increasing disease-free survival. However, despite progresses have been made in the technology-driven treatment modality of radiations, a fully effective cure for some radioresistant and aggressive tumors, such as Glioblastoma (GBM), has not been found yet. Indeed, advances in radiation oncology and neurosurgery still failed to improve GBM prognosis, that at the present remains an incurable tumor, characterized by an excessively dismal life expectancy (Wen et al., 2020) It is therefore of interest to investigate new synergistic therapeutic approaches improving the efficacy of RT by targeted molecules that block GBM hallmarks implicated in the aggressiveness and radioresistance.

In this context, the SRC proto-oncogene tyrosine-protein kinase (SRC) represents a key molecular target, because several data suggest its involvement in mediating a cellular response derived from the interaction between external signals, surface growth factor receptors and the activation of intracellular molecular pathways that lead to radioresistance (Cirotti et al., 2020). The collaboration with the pharmaceutical company Lead Discovery Siena (LDS, Italy), allowed the development of the research project to evaluate the combined therapy between RT and SRC inhibition. LDS group designed and synthesized a wide library of compounds belonging to the aromatic heterocyclic family pyrazole[3,4-d] pyrimidine, identifying a specific SRC inhibitor, called Si306 (Tintori et al., 2015) .

Thanks to the collaboration between University of Catania and Laboratori Nazionali del Sud (LNS), I had the opportunity to perform a part of my radiobiological activities in The Center of Hadrontherapy and Advanced Nuclear Application (CATANA) of the National Institute for Nuclear Physics-LNS. In this facility, in addition to the Superconducting Cyclotron, that is able of accelerating protons at energy levels of up to 80 MeV/A, many devices for precise beam transport and for accurate control of the main beam parameters are provided in order to perform proton irradiation and radiobiological experiments. Cell sample irradiations with proton beams are carried out with high level of dosimetric precision and at different dose rates. In addition, a remotely controlled position system is provided in order to irradiate several cell samples in a single experimental session, sensibly reducing the irradiation time. The system is versatile so that different sample shapes and sizes can be irradiated with a sub-millimetric precision.

Moreover, during my experience abroad, I also performed radiobiological studies using X-ray radiation system, in the research unit “Imagerie et Stratégies Thérapeutiques des pathologies Cérébrales et Tumorales” (ISTCT) of the Cyceron center (Caen, France). The fashionable point of the studies at Cyceron center is not only related to the X-rays system of irradiation, but also to the possibility to perform the radiobiological experiments in hypoxic chamber, where cells are grown and conditioned with the desired oxygen concentration for the whole duration of the experiments, simulating the typical hypoxic conditions that characterize the GBM microenvironment.

** * **

An introduction is included in the first section to describe the current state of the art of the research field, the context and the significance of the work. In particular, the first part is an overview of the GBM, describing the epidemiology and the histological and molecular characteristics. The report of the therapeutic approaches for the current treatment of GBM will be followed by the evidences of the RT limitation, focusing the role of hypoxic condition in the radioresistance and elucidating the aggression mechanisms induced by the response to RT treatment. In the final part, the general role and function of SRC is described, subsequently with its involvement in the aggressiveness of GBM and in the mechanisms that reduce the effectiveness of RT. A specific section with the aims is proposed before the results, to recapitulate the key points regarding the evaluation of SRC inhibitor combined with RT. The results of the project are showed in the published articles which are fully attached in the “7. Results” section: it should be noted that in the first work, some initial activities for the evaluation of PT and Si306 treatment are published as conference proceeding; then, in the next work, the full data with the survival curves and the radiobiological parameter calculation are showed, in addition to the gene expression profiling and the gene signatures identification. In the third work, the survival curves, the repair capability from

DNA damage and the migration ability after SRC inhibitor and X-rays combined effect, are showed comparing normoxic and hypoxic condition. These two published articles are the core of the experimental results, and even though they are independent and self-standing studies, they are certainly connected by the univocal purpose and goal of evaluating the therapeutic synergy of the Si306 molecule with RT. Finally a Review is also included, with the aim to highlight the role of hypoxia and the SRC protein in GBM, revealing the direct and indirect correlation between these two factors in promoting invasion and radioresistance mechanisms. The discussion with concluding remarks is dedicated to the summary of research goals obtained in view of the current state of art and to the definition of future perspectives.

PREFACE REFERENCES

- Kirsch, D.G., et al., *The Future of Radiobiology*, in *J Natl Cancer Inst.* 2018. p. 329-340.
- Wojcik, A. and M. Harms-Ringdahl, *Radiation protection biology then and now*. *Int J Radiat Biol*, 2019. 95(7): p. 841-850.
- Wen, P.Y., et al., *Glioblastoma in adults: a Society for Neuro-Oncology (SNO) and European Society of Neuro-Oncology (EANO) consensus review on current management and future directions*. *Neuro Oncol*, 2020. 22(8): p. 1073-1113.
- Cirotti, C., C. Contadini, and D. Barilà, *SRC Kinase in Glioblastoma News from an Old Acquaintance*. *Cancers (Basel)*, 2020. 12(6)
- Tintori, C., et al., *Combining X-ray crystallography and molecular modeling toward the optimization of pyrazolo[3,4-d]pyrimidines as potent c-Src inhibitors active in vivo against neuroblastoma*. *J Med Chem*, 2015. 58(1): p. 347-61.

5. INTRODUCTION

5.1. Epidemiology of Glioblastoma (GBM)

Epidemiological analysis from National Cancer Institute reports that brain cancers account for 1.3% of all new cancer cases in the United States, with an annual age-adjusted rate of 3.19 per 100'000 people [1]. According to the Surveillance of Rare Cancer in Europe, GBM is included in the rare cancers group, with an incidence lower than 6/100'000/year, ranging from 3/100'000 in Eastern Europe to 5/100'000 in United Kingdom and Ireland. The mortality rate and the rate of new case of central nervous system (CNS) tumor are low, but they are close each other demonstrating the small incidence, but the poor life expectancy as well (Figure 3a). Therefore, the major issue for GBM is represented by poor prognosis, because both chemotherapeutic and radiotherapeutic or combined treatments are resulting in a median overall survival of 15-18 months and only small percentage of patients (5-6%) survive over 5 years [2] (Figure 1b).

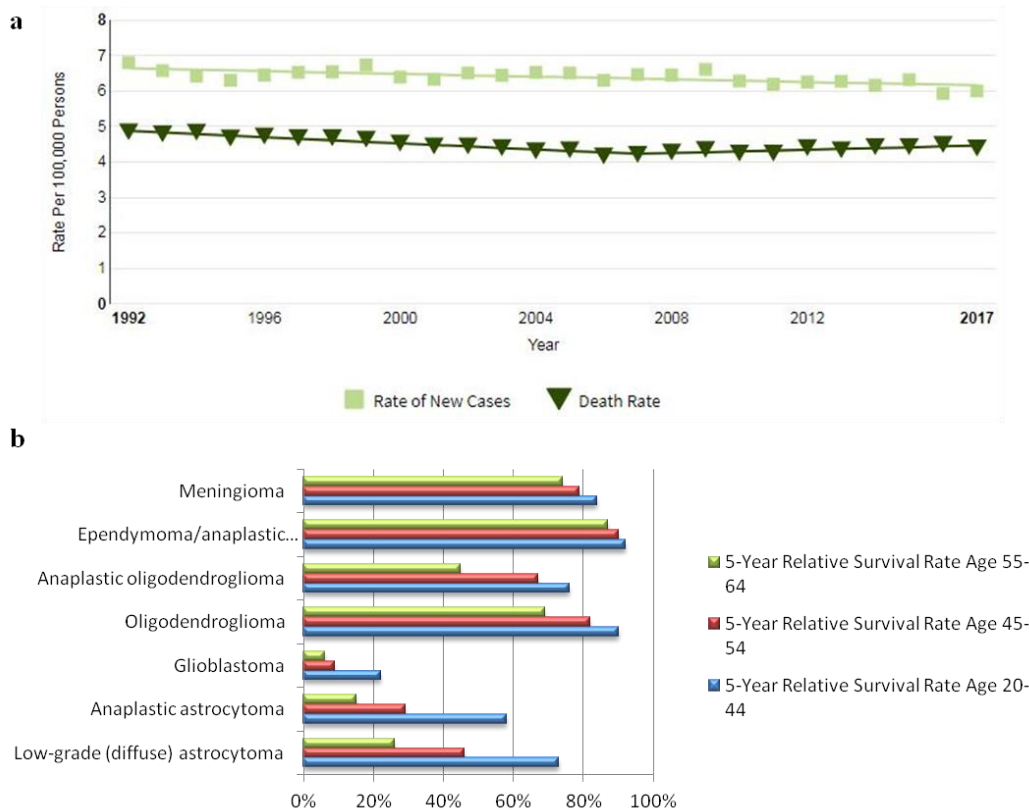


Figure 1. (a) Total number of deaths and new case of CNS tumor over 100.000 per year (adapted from National Cancer Institute website); **(b)** Percentage of people who survive five years after they were diagnosed with or started treatment in the most common types of brain and spinal cord tumors. The data are grouped based on age (data obtained from Central Brain Tumor Registry of the United States website)

The highest incidence is in the elderly age group with a peak at 55-60 years, whereas pediatric GBM incidence is of about 0.85/100'000 per year [3]. Indeed, 64 and 55 years old are the median age and the mean respectively at diagnosis of primary GBM compared to 40 years old that is the mean age at diagnosis of secondary GBM. DNA repair and immunological deficits are attributed to the increase of GBM incidence in elderly; in fact aging, associated with a low efficacy of the normal immunosurveillance and immunosuppression, is supposed to be the main cause of GBM occurrence due to the increase of immunosuppressive factors in brain, such as indoleamine 2,3 dioxygenase 1 (IDO), programmed death-ligand 1 (PD-L1), the dendritic cell surface marker and CD11c [4].

The analysis of rate of new cases based on sex reported that GBM is more frequent in males with an incidence of 1.6 times higher compared to females [5]. Sex differences were also found to be prognostic factor, because female patients are associated with better outcome; a possible explanation of sex differences in the response to treatment was provided from a recent study that analyzed the therapeutic response to standard treatment in association with transcriptomic data [6] [7].

Etiology of GBM remains unclear and risk factors are still under investigations [8]. However, some evidences identified the previous high dose IR exposition for therapeutic intent as confirmed risk which contribute to induce GBM [9]. No data supported the dose received for diagnostic procedures as biomarkers of exposition and no clear association has been found with non-IR from cell phones or electromagnetic field and with environmental factors. However, in a cohort study of Japanese–American patients, dietary levels of glucose and high carbon tetrachloride exposure were independently associated with development of GBM [10]. Genetic predisposition has been rarely observed, and 5% of all familial gliomas occur in association with Li-Fraumeni syndrome and neurofibromatosis type 1 [11].

Overall, unlike other cancers that are more common, the unpredictability and late diagnosis of GBM, give a limited opportunities for therapy and very low life expectancy as a consequence. These features, in addition to unknown risk factors and etiology make necessary further investigations aimed at finding new strategies to improve clinical outcome.

5.2. Histopathological and molecular features of GBM

GBM is the most aggressive type of malignant astrocytic gliomas that may occur in basically all brain regions, even if it is more common in the frontal and parietal lobes [12]. During the fast progression of cancer cells, GBM spreads from the primary site, with an infiltrating and irregular shape, making difficult, if not impossible, a complete surgical resection [13]. Histologically, GBM is a highly cellular glioma composed by glial cells with marked nuclear atypia and pleomorphism. Common peculiar diagnostic features are microvascular proliferation, often with glomerular-like appearance and palisading necrosis characterized by regular areas of necrosis surrounded by dense accumulations of neoplastic cells. Proliferative activity is usually prominent with a highly mitotic count. The evaluation of proliferation index is immunohistochemically determined by analyzing Ki67 positive cells that account for a total of about the 15-20% of GBM cells, but some tumors have a proliferation index greater than 50% [14].

In the 2007 classification, proposed by World Health Organization (WHO), GBM was also defined IV grade glioma, according to histopathological malignancy criteria (proliferative index, anaplastic nuclear features, microvascular proliferation, necrosis, response to treatment and survival time) [15]. In the 2016 edition, the WHO introduced for the first time a system to classify the brain tumor taking into account genotypical features in addition to morphological evidence [16]. The new classification provided specific molecular parameters in order to find a way to discriminate brain tumors, which might be appear similar in the diagnostic setting. For this reason GBM, included in the family of diffuse astrocytic and oligodendroglial tumors, was sub-classified in three groups, in relation to the mutation status of the isocitrate dehydrogenase gene (IDH1/2):

- 1) the GBM IDH-wildtype group, accounts for 90-95% of cases that are primary or *de novo* tumors with a worse prognosis [17]; in the same group were included the epithelioid GBM, giant cells GBM and gliosarcoma;

- 2) GBM IDH-mutated group, account for a minor part of cases (~12%) that are secondary from low grade GBM; however they can evolve over time reaching the highest grade; GBM IDH-mutated are characterized by lower aggressiveness and a better prognosis [18];

- 3) GBM, not otherwise specified (NOS), includes a category of IV grade astrocytomas with unknown IDH mutation status and which must be subject to future studies before further refinements in the classification [19].

The Cancer Genome Atlas (TCGA) offered a great contribute to integrate gene expression profile to the histological features of GBM. According to TCGA data, proneural, neural, classical and mesenchymal subtypes were identified, leading to GBM molecular stratification [20]. Most frequently mutated genes can be associated with each GBM subtypes: 1) epithelial growth factor

receptor (EGFR) and its mutated form EGFRvIII amplification with classical 2) platelet derived growth factor receptor alpha (PDGFRA) amplification and IDH1 mutations with proneural 3) neurofibromatosis type 1 (NF1) mutation with mesenchymal. In conclusion, the neuronal subtype, includes an expression pattern very close to the healthy condition and neuronal markers such as NEFL, GABRA1, SYT1 and SLC12A5 [20].

In view of these genomic and genetic based data, the Consortium to Inform Molecular and Practical Approaches to CNS Tumor Taxonomy (cIMPACT-NOW) approved the consideration of the molecular signature as necessary and sufficient condition to define GBM, even if morphologically it can resemble a low-grade glioma [21]. In the last version of cIMPACT-NOW, the term “Glioblastoma” was recommended for those diffuse astrocytic gliomas that are IDH-wildtype and have histologic or genetic features corresponding to WHO grade IV. Moreover, IDH-mutated were defined as astrocytoma grade 2, grade 3 or grade 4 in relation to the mitotic activity, microvascular proliferation, necrosis and cyclin-dependent kinase inhibitor 2A/B CDKN2A/B homozygous deletion [21]. However, the major issues for the clinical correlation with subtypes is the intra tumor “switching” and the coexistence of many subtypes in the same tumor due to the GBM heterogeneity [22]. In conclusion, despite none of these subtypes are strongly predictive for treatment response to current therapies, it helped to clarify the main genes mutation/amplification and deregulated pathways in GBM that may contribute to the development of new therapeutic strategies.

5.3. Current approaches for GBM treatment

5.3.1 Gold standard treatment of GBM

The investigation of pathological mechanisms and the elucidation of genetic and molecular state of art are still contributing to the development of therapies both in the pharmacological and RT fields. However, so far, the current standard treatment for newly diagnosed GBM is unchanged, including surgery, followed by the chemotherapy with the alkylating agent Temozolomide (TMZ) during and after conventional RT treatment [2]. Due to the infiltrating pattern of GBM, the application of intraoperative imaging may improve the maximal resection in order to avoid the loss of residual cancer cells, preventing the occurrence of post surgery complications and relapses. In spite of the complexity for the delicate anatomical site, the surgical resection is mandatory in the first-line setting according to the risk-benefit ratio and prognostic impact for each patients, because it has the aim to reduce the gross solid mass and to collect biopsy samples for grading and immunohistological analysis [23]. Analysis of patient-derived samples have a key role, not only for

stadiation, but also for the identification of predictive biomarkers. Indeed, in addition to IDH analysis, the evaluation of the methylation status of O⁶-methylguanine methyltransferase (MGMT) promoter has a predictive role for TMZ response treatment. Indeed, MGMT is a DNA repair enzyme that counteracts DNA alkylation induced by chemotherapy agents, such as TMZ; for this reason, the increase of progression free survival in patients was associated to the promoter methylation of MGMT that is not efficient to remove alkyl groups from DNA, leading to a better response to TMZ [24]. Despite the predictive role of MGMT, the methylation status may just offer the possibility to avoid TMZ in patients with poor functional status, especially when the chemotherapy benefit is minimal. Lomustine is another alkylating agent that has been tested in combination with TMZ, and a small clinical benefit in a recent small randomized phase III trial was showed [25].

For these reasons the standard treatment of GBM can not ensure a complete remission and more clinical trials are recommended [26]. However, the most of clinical trials and new treatment approaches has been proposed for GBM recurrences, that are the rule rather than exception [27]. According to U.S National library of medicine (available online at www.clinicaltrials.gov), for recurrent GBM, 491 trials has been completed and 229 trials are in the recruiting state, versus 227 and 180 respectively for newly diagnosed GBM. Beside the application of other chemotherapy agents, such as a rechallenge of TMZ and other nitrosureas, a large part of studies was performed to evaluate molecularly targeting drugs. Challenges included the formulation of specific drugs to block specific target that are responsible for the development of the primary hallmark of GBM. Among these, angiogenesis is one of the main factors associated with GBM expansion, because the endothelial proliferation and the neovascularization support the growth of GBM cells. Humanized vascular endothelial growth factor (VEGF) antibody Bevacizumab was approved in the United States and other countries, but not in the European Union, as monotherapy for recurrent GBM, because the improvements in progression free survival but not in the overall survival [28, 29]. Most of approaches are focused on targeting of factors that are implicated in altered pathways, such as RAS/MAPK and PI3K/mTOR, which are the downstream effectors of signaling for the tumor growth and death evasion of GBM; specific inhibitors were produced for EGFR, mTOR and CDKs and were tested in several clinical trials [30]. To date, clinical trials are still performed with this rationale, but little results have been obtained. Possible hypotheses to explain the failures include the multiple signaling pathways and their cross-interactions, as well as the presence of biological mechanisms of radioresistance in addition to the pharmacological difficulty to overcome the blood brain barrier.

For this reason, the international guidelines are still encouraging the investigation of targeted therapy which may enhance RT for the treatment of GBM. Therefore, the development of targeted therapies remains one of the main fields of investigation in the improvement of therapeutic synergies for GBM.

Many attempts with immunotherapy approaches are still ongoing in order to find a way to overcome the immunosuppression and immunoresistance or to enhance the effector immune infiltrate into the microenvironment. Chimeric antigen receptor (CAR) T-cells, oncolytic virus and vaccines combined with checkpoint inhibitors or RT are current under investigation [30].

5.3.2 Radiotherapy for GBM treatment

Clinical data reported that 60 Gy for 30 fractions (2 Gy/day) of X-rays with concurrent and adjuvant TMZ is a positive prognostic factor on the survival of patients, as compared to patients that receive surgery or chemotherapy alone [31]. The Advisory Committee on Radiation Oncology Practice, the European Society for Radioterapy and Oncology and the American Society for Radiation Oncology (ASTRO) cooperate to recommend many indications for the treatment of GBM with radiotherapy, aimed to reduce heterogeneity and to standardize procedures. Four principal key questions were elucidated in the ASTRO Evidence-Based Clinical Practice Guideline [32], providing recommendations whose strength or weakness were defined in relation to the evidence that explain the risk/benefit balance: 1) the role of post-surgery radiotherapy; 2) the optimal dose/fraction ratio; 3) the definition of the ideal target volume; 4) the role of radiotherapy in recurrences.

To date, despite the large histological/molecular characterization, there are no clinical indications to modulate the radiation treatment in relation to GBM subtypes. Indeed, the ASTRO guidelines take into account only the age and the performance status to discriminate the schedule of treatment with radiotherapy; there are no clinical evidences demonstrating an overall survival improvement with X-ray radiation dose above the standard of 60 Gy. One institutional phase 2 study of 23 patients treated with a dose escalation to 90 Cobalt Gy equivalent extended the median survival to 20 months but significant radiation necrosis and toxicity were considered too much elevated [33]. Hypofractionated treatment of 40 Gy in 15 fractions over 3 weeks is suggested only for patients older than 70 years old and with poor performance status, but just to improve the convenience of fewer fractions administered over a shorter period. There are no data supporting the application of hyperfractionation or accelerated fractionation (a larger number of fractions in a smaller interval of time, more than once a day up to four per day) aimed to enhance the radiobiological impact on

tumors versus normal tissues, which repair damage more quickly. Although the infiltrating pattern of GBM, it has been reported that survival in patients with partial brain radiation therapy wasn't worse than in those irradiated to the whole brain. Moreover, the partial brain irradiation determined a better performance status, suggesting a decrease of toxicity. However, the attempts in clinical imaging to delineate the tumor volume are complicated by the not specific signals which are made of simply edema rather than infiltrating cancer cells, determining a variation on the consensus regarding the target volume identification. Imaging technologies tried to detect three target regions:

- 1) gross tumour volume (GTV) is the visible macroscopic tumor;
- 2) clinical target volume (CTV) consists of GTV plus a volume of suspected microscopic spread including anatomical compartments with a high risk of residual cancer cells;
- 3) PTV consists CTV plus a margin for technical or positioning uncertainties, including movement of target volumes [34].

According to the European Organization for Research and Treatment of Cancer (EORTC), GTV delineation should be include the resection cavity with any residual enhancing tumor, without inclusion of surrounding edema that, conversely, is included by Radiation Therapy Oncology Group (RTOG). Both institutions recommend the same CTV and PTV as GTV plus a margin of 2 cm and CTV plus a margin of 3–5 mm respectively. According to this target volume definition, the X-ray treatment planning is proposed in one or two phases: the one phase strategy is adopted by EORTC delivering 60 Gy in CTV that includes gross residual tumor/resection cavity with wide margins, without specifically targeting edema; the two phase, approved by RTOG, separate a first CTV that includes a primary target volume encompasses edema where the dose is delivered with 46 Gy for 23 fractions and a second CTV that represents a boost target volume irradiated with 14 Gy in 7 fractions only at the resection cavity and gross residual tumor [35].

Concerning the recurrences, focal re-irradiation is suggested in order to improve outcomes, especially in younger patients with a good performance status. The urgent need for technology-driven improvement of radiation dose conformity is mentioned only in this context by ASTRO guidelines, because it has been observed a reduction of the probability of healthy brain necrosis [36]. So far, the conformal treatment options with X-ray that are suggested for recurrent GBM are the following: three-dimensional conformal radiotherapy, fractionated stereotactic radiotherapy, stereotactic radiosurgery, brachytherapy and intensity-modulated radiotherapy [37]. Unfortunately, to date, conformational irradiation techniques in radiotherapy have the limited benefit to avoid the damage of organs at risk, but a total remission of the GBM is not still ensured.

5.3.3 *The biophysical rationale of radiotherapy and hadrontherapy for GBM treatment*

The main difference between radiotherapy and hadron therapy is that X-ray radiation uses massless photon, while hadrons (from Greek, adros=strong) is made of quark that may be charged (such as protons, helium and carbon ions) or neutral (such as neutron) [38]. Even if all these particles are collected in the group of hadron therapy, protons are lighter than carbon ions; for this reason, protons and carbon ions are also defined light and heavy particles respectively.

All the conformal irradiation modalities for X-rays extended technological instrumental attributes, such as the different positioning, the irradiation from different angles and the modulation of the fractions in order to irradiate in a less invasive manner. However, the improvements of the technological qualities in irradiation structures can not solve all the issues because the dose deposition on the tumor is dependent by the physic properties of photons: the interaction of X-ray radiation is defined probabilistic, because the energy is not released continuously and the global attenuation of the beam as a function of penetration in the biological target should be considered. Therefore, in the conventional external beam radiation X-ray-based, a number of primary photons is lost during the interaction with the biological components [39].

In opposition to X-ray systems, the higher dose conformity of charged particles, such as protons is related to physical basis, regardless of the technological structure. First of all, protons release their energy to the atomic electrons of biological targets continuously, increasing their kinetic energy and leading to direct ionization or excitation [40]. Hence, due to coulomb interaction, the loss of energy per unit of track length is inversely proportional to the square of the speed: in the first part of penetration, the particle has a higher speed, the loss of energy is low and approximately constant; at the end of the range the particle slows down and the loss of energy increases until it reaches a peak. For this reason, the dose deposition of protons has the particular trend of the “Bragg curve”, where the maximum loss of energy occurs at the end of the range, in the so called *Bragg peak*, after which the radiation is characterized by a steep dose fall-off [41]. Moreover, the Bragg peak is spread out to cover the entire tumor region, contributing to reach a conformal dose on the tumor target and sparing the organs at risk (Figure 2).

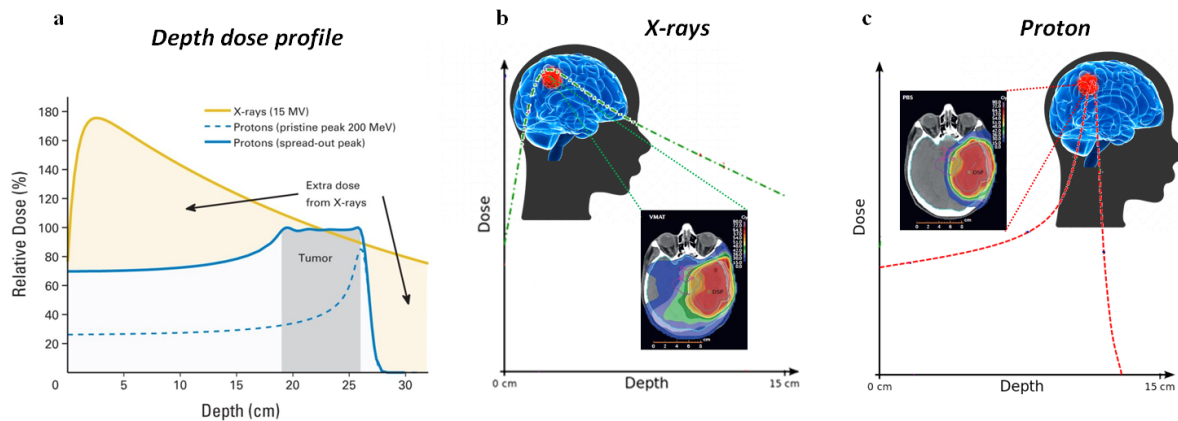


Figure 2. (a) The dose distribution of photon (yellow line), single proton beam (dashed blue line) and spread-out proton beam (blue line) as a function of penetration depth in tumor (adapted from “Proton-Beam Therapy Versus Photon-Beam Therapy: The Debate Continues” by Cynthia L. Kryder in IASLC Lung Cancer News). (b) X-rays dose deposition increases rapidly in the first part of the path and decreases along the depth covering a large part of the healthy tissues; (c) the protons dose deposition occurs slowly in the first part, increase in the Bragg peak and decrease rapidly sparing the healthy tissues (Copyright by F.Torrisi, Parenti Lab). The representation of brain areas exposed to radiation in proton and conventional radiotherapy were provided from “Radiation oncology in the era of precision medicine” by Baumann et al. in Nature Reviews Cancer 2016.

Thanks to their favourable physical properties, accelerated proton beams represent a cutting-edge technique by hadrontherapy in radiation oncology. From the first clinical application of protons in 1957 to treat a cervical cancer with the cyclotron of the Gustaf Werner Institute in Uppsala, by Börje Larsson, more centres for PT have subsequently been built in Europe and worldwide. According to the newest updates of the Particle Therapy Co-Operative Group (PTCOG), nowadays 110 particle therapy facilities are currently in operation worldwide, and this number goes to extend within the next five years, because 36 PT centers are under construction and 15 are in the planning stage (data from <https://www.ptcog.ch/>).

Many efforts have been made in order to take advantage of the protons conformational capacity, increasing the dose delivered in the target tissues, but the improvements, at the level of biological effectiveness, have not been so significant to strongly recommend PT in substitution of X-ray radiation for GBM treatment [42]. Therefore, the benefit offered by the peculiar depth-dose profile of protons has still a limited application for the treatment of pediatric cancers, in order to avoid side effects, but it is still not sufficient to treat radioresistant and hypoxic tumors, such as GBM, that remain incurable regardless the types of radiation treatment. Moreover, even with PT, the high

radioresistance of the GBM can not be overcome only with the dose escalation attempts because, despite the major dose conformity, risks of side effects exceed the benefit for patients. The reduced dose and toxicity in healthy tissues of protons is affected by a clear limitation which may be explained in relation to the physical parameter of IR that determine the biological response. One of the main features of IR is the linear energy transfer (LET), that is a measure of the ionization density and it is defined as the average energy (keV) transferred by a ionizing particle along a path of 1 μm [43]. The biological effects are strictly dependent to the LET, because a high ionization density determines a greater probability of triggering damage to biological macromolecules and therefore of killing cancer cells. To simplify, considering the DNA, IR with high LET creates the formation of clustered double strand breaks that lead to cell death because the cellular repair systems struggle to fix them. The LET variations are therefore reflected in terms of biological response. For this reason, the relative biological effectiveness (RBE) parameter has been introduced in radiobiology. It is defined as the ratio of the dose required by a reference radiation (commonly low LET, 250 kVp X-rays or ^{60}Co γ -rays) and the dose required by a test radiation to cause the same level of biological effect (i.e. cell death) [44]. RBE of protons is commonly approximated to ≈ 1.1 compared to X-rays (10% difference in biological effect), because they have a similar LET as photons [45, 46]. For this reason, the investigation about radioresistance mechanisms is necessary in order to use synergistic therapies that can enhance the effect of RT, both for X-rays and protons irradiation.

5.3.4 Targeted Molecular Therapies as combined approach with RT

Finding solutions that improves RT efficacy for GBM treatment by therapeutic synergies, implicate the investigation of deregulated molecular pathways, involved in radioresistance mechanisms, with the aim to obtain targeted molecular therapies. The knowledge of the GBM molecular characteristics have significantly improved the identification of potential targets. Several lines of evidences suggest that multiple signaling pathways may be involved in the radioresistance of GBM [47]. In particular, it is clear that GBM acquire self-sufficiency in growth signals thanks to a cascade of signal transduction molecules freed from checkpoints and dependence upon external signals. Many proteins involved in signal transduction for GBM progression were identified in order to the development of targeted therapies such as: receptorial tyrosine kinase inhibitors (RTKi), PI3K/Akt/mTOR inhibitors, PARP inhibitor and upstream or downstream factors [48]. (Figure 3)

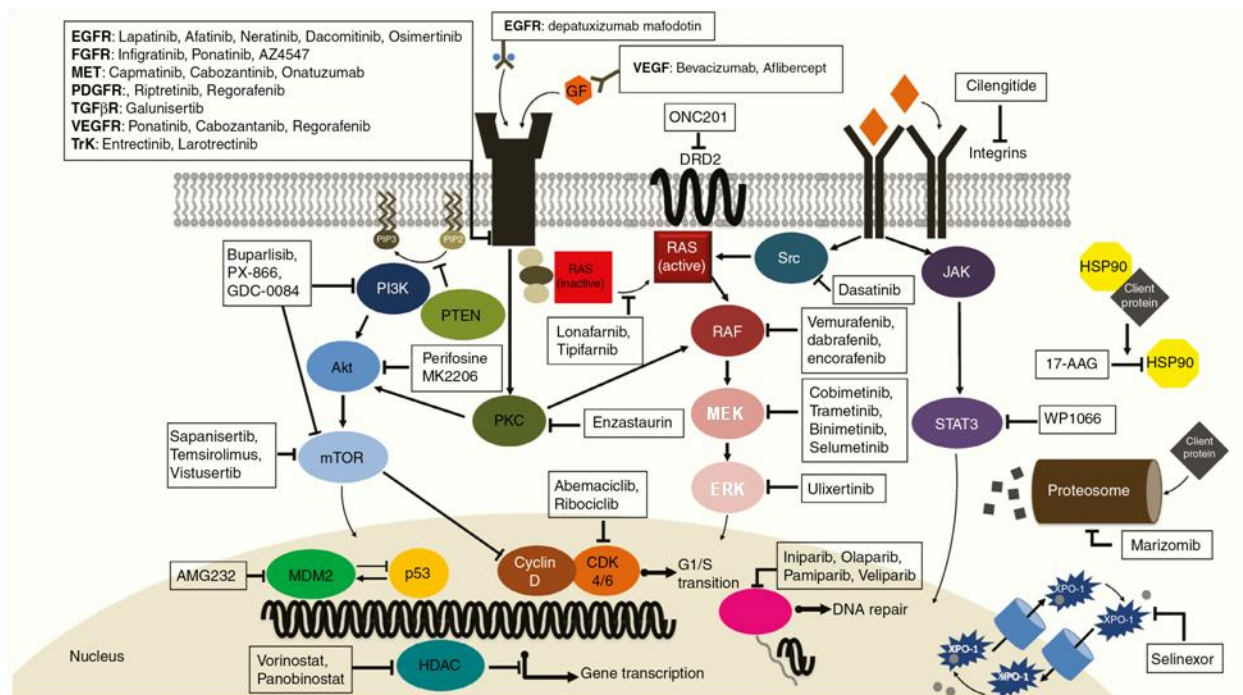


Figure 3. Schematic representation of the most important pathways and targeted molecules for GBM treatment (adapted from “Glioblastoma in adults: a Society for Neuro-Oncology (SNO) and European Society of Neuro-Oncology (EANO) consensus review on current management and future directions” by Wen P., Weller M. et al. in *Neuro-Oncology*, Volume 22, Issue 8, August 2020).

Targeted therapy is offering the possibility to reduce the radiation dose in order to obtain the same biological effect (i.e. synergistic interaction); indeed, such a concept in radiobiology is expressed as dose modifying factor (DMF) or sensitized enhancement ratio (SER), both indicating the ratio between the dose alone and in combination with a specific agent to determine the same biological effect [49]. An emerging strategy is the targeting of deregulated pathway that contribute for the conservation of the genomic integrity after the genotoxic damages that are induced by IR. For instance, interactions of many factors and pathways are involved in the generation of the DNA damage response (DDR), that is a complex mechanism that regulate the cell destiny after DNA strands breaks, and it implicated in the radioresistance of many tumors, including GBM [50] [51]. Targeted molecular therapies are applied to inhibit PARP, ATM, DNA-PK and Wee1, which are biomarkers involved in different phases of DDR machinery. In particular, PARP identify single strand DNA breaks and belong to the sensors of DNA damages; DNA-PK is a kinase mediating the activation of transducer proteins, such as ATM. Wee1 is a downstream cell cycle checkpoints inhibitors [52]. To date, most of clinical trials testing DDR inhibitor are in the recruiting status and studies are ongoing [30].

5.4 Current limitations of radiation treatment

Beyond the limitations of RT, described in the above section from a physical point of view (LET and RBE relationship), there are biological characteristics that determine the reduced effectiveness of RT. The main limitation of RT is related to radioresistance and to cancer hallmarks activation, which depend on two main factors: the hypoxic condition and the presence of de-regulated molecular pathways. Both issues are even more correlated, because hypoxia can trigger mechanism of radioresistance and tumor progression [53]. Moreover, the activation of these pathways may also result in cancer cells response to the IR itself. Indeed, it has been observed that several GBM hallmarks, especially those related to the invasion processes, are closely linked to mechanisms induced by IR [54]. For this reason, the investigation of molecular basis of radioresistance induced by hypoxia and IR can encompass very important therapeutic implications.

5.4.1 Hypoxia and radioresistance

Hypoxia is one of the main pathological hallmarks and a negative prognostic marker in GBM [55]. Intratumoral oxygen pressure (pO_2) values in GBM represents a critical aspect when considering an IR-based approach. The aerobic value of the brain tissue is of about 40 mmHg in physiological conditions, whereas it has been shown to be significantly lower in GBM [56]. Qualitative and quantitative information have been reported about hypoxia in GBM. Qualitatively, GBM may be characterized by acute or intermittent and chronic hypoxia. The acute/intermittent trait of hypoxia is due to the altered function and structure of the blood vessels, which generate intervals of re-oxygenation; kinetics are variable by short cycles within one hour in cycles lasting for hours or days. Chronic hypoxia is mostly associated to necrotic core, less irradiated due to tumor growth [57]. From a quantitative point of view, the lowest pO_2 to define a tissue as normoxic is 10 mmHg; in GBM, hypoxia is ranging from mild ($pO_2 = 20$ to 4mmHg) to severe condition (4 to 0.75mmHg), especially in necrotic and micronecrotic areas [58].

Hypoxic niches promote the tumor growth and progression inducing the expansion of GSCs with a crosstalk and a reciprocal signaling that sustain proliferation, invasion, angiogenesis and suppression of anti-tumor immune responses [59, 60]. In addition to GSCs and the acquisition of malignant phenotype, hypoxia is responsible for radioresistance in GBM due to radiobiological mechanisms regarding the interaction between the IR and the macromolecules. IR can determine direct damage to all organelles and macromolecules such as DNA, inducing single or double strand breaks, which are difficult to repair and are associated with oxygen-independent-cell death [61].

Vice versa, indirect damage is closely linked to the presence of oxygen. Indeed, IR interaction with water molecules induces the formation of reactive oxygen species (ROS) through a radiolysis reaction, that would be more efficient in well oxygenated tissues, because it can facilitate the formation of superoxide radical and hyperoxide, leading to the amplification of damage and increased RT efficiency [62]. In particular, according to *oxygen fixation hypothesis*, increasing concentration of ROS induces the so-called “fixed damage from oxygen” on DNA, invariably leading to cell death [63]. In hypoxic areas, the effect of cell death induced by ROS and oxygen reactions is less efficient, with a consequent increase of radioresistance. In view of the crucial significance of the GBM hypoxic condition, the "oxygen effect" and the response to RT treatment is assessed by the oxygen enhancement ratio (OER) parameter, which is defined as the ratio between the dose in hypoxia and normoxia to reach the same biological effect (Figure 4) [64].

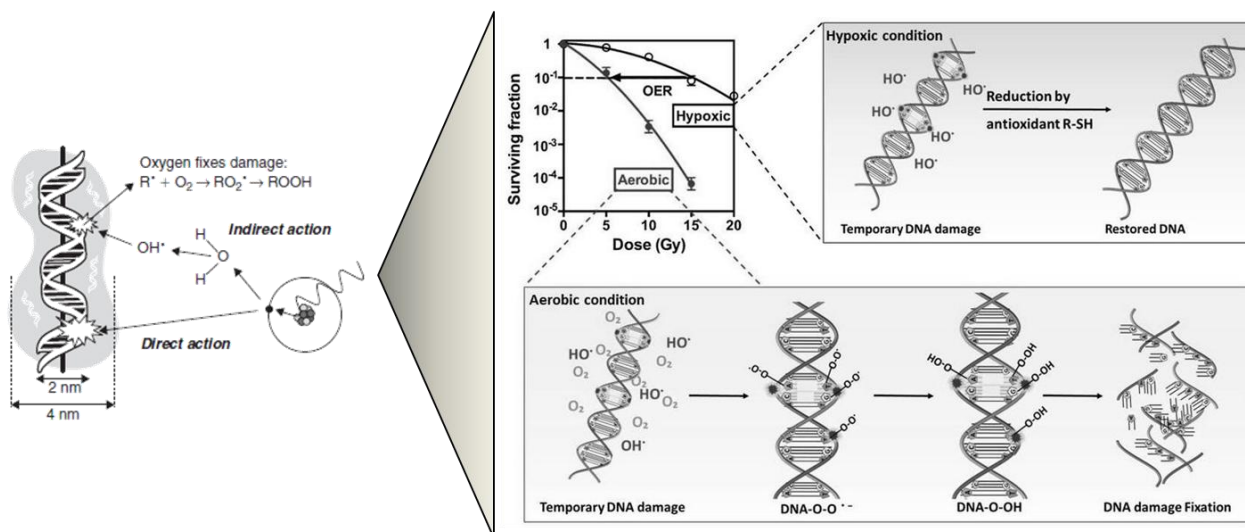


Figure 4. Schematic representation of the oxygen effect, where in hypoxic condition, DNA radicals that are created by indirect action of ionizing radiation may be reduced by compounds containing sulfhydryl groups, which restore the DNA damage. Otherwise, in normoxic condition, DNA damage and strand breaks make the radiation lesion permanent, leading to a shift in the surviving fraction (adapted from the Review “Hypoxic Radioresistance: Can ROS Be the Key to Overcome It?” by Wang H., et al in *Cancers* 2019 and “Basic Clinical Radiobiology” 4th edition by Michael C. Joiner and Albert van der Kogel 2009).

5.4.2 Hypoxia and invasion

GBM is a highly infiltrating tumor characterized by a high proliferation, ability to invade surrounding tissue and a remodelling of a number of biological pathways operating in both the intra- and extra-cellular microenvironment. Among the most crucial alterations, the dysfunction of cellular metabolism leads to a series of consecutive events which invariably affect the degree of malignancy. In particular, hypoxia characterizes tumor microenvironment and it is well known to trigger HIF-1 α /HIF-1 β complex, which translocate to the nucleus to control the expression of target genes [65], especially influencing the invasive ability of GBM cells [66, 67]. Hypoxia also supports a complex remodelling of cytoskeleton, which includes a number of linked events, such as alteration of cell adhesion, activation of cell motility and production of proteolytic enzymes.

The modification of cell adhesion occurs through the modulation of E-cadherin expression, which are commonly altered in tumors [68], generally as a result of mutation or hypermethylation-induced gene suppression [69]. It has been reported that E-cadherin expression is reduced in high grade brain tumor as compared to healthy tissue [70]. In particular, a shift occurs from E-cadherin to N-cadherin expression, which increases interaction between cancer and stromal cells, promoting the activation of cell motility as part of the complex epithelial-mesenchymal transition (EMT) [71]. In this context, it has been demonstrated that hypoxia induces an up-regulation of Zinc finger E-box binding Homebox 1 (ZEB1), which in turn promotes N-cadherin to cytoskeleton binding through downstream roundabout guidance receptor 1 (ROBO1) modulation [72], supporting EMT process [73].

After cell adhesion loss, cancer cells increase their motility by a number of processes, such as cytoskeleton activity stimulation, autocrine/paracrine chemotaxis or proteolysis activity and extracellular matrix degradation [74]. Tumor cells migrate via interactions between adhesion molecules (i.e. integrins) and extracellular matrix degradation products. Under hypoxic condition, GBM cells over-expressing EGFRvIII mutation, exhibit an increased rate of integrins interaction and recruitment (i.e. integrins α v β 3 and α v β 5) at the level of cell membrane strengthening the bind with the surrounding tissue [75-77]. Such a process generates a structure called adhesion plate, where integrins interacts with focal adhesion kinase (FAK) promoting cytoskeleton contraction and proliferative effects by intracellular signal transduction [78].

The production of proteolytic enzymes is a crucial event during invasion. In particular, increased activity of matrix metalloproteases (MMPs) is associated with higher grade glioma and correlated with shorter overall survival in GBM patients [79, 80]. On this aspect, a well-characterized effect is mediated by hypoxia. Indeed, low oxygenation indirectly promotes MMP-9 and MMP-2 up-

regulation and increased proteolytic activity, by reducing pH levels in tumor microenvironment. This condition is related to the increased metabolic activity of the tumor, which relies on glycolysis in hypoxic conditions, inducing lactic acid accumulation, thus reducing the pH [81]. In addition, activation of type A lactate dehydrogenase (LDH-A), which in turn regulates the transforming growth factor- β 2 (TGF- β 2), has been shown to trigger the cascade of transcriptional regulation of MMP-2 and integrin $\alpha\beta$ 3 expression, strongly influencing the tumor invasiveness process [82]. It is noteworthy that tissue inhibitor of metalloproteases (TIMP) and TIMP-like molecules, which are synthesized and released by resident cells, counteract extracellular matrix degradation thus inhibiting GBM invasion [83, 84].

5.4.3. Changes in the tumor microenvironment induced by IR

Recurrences of GBM after irradiation represents a key limitation of RT, in addition to radiation-mediated necrosis and damages observed on healthy tissues. Indeed, many evidences suggested that brain tumors, including GBM, occur in previously irradiated areas, determining the so-called radiation-induced gliomas [9]. The molecular basis of this phenomenon is associated to the upregulation of invasion and cell migration, which take place with a crosstalk between ECM and the tumor microenvironment of GBM [54]; indeed, it was reported that irradiation lead to the upregulation of specific proteins involved in ECM composition and biosynthesis, ECM-glioma cell (ligand-receptor) interaction and ECM degradation [54]. Changes or loss of structural proteins, such as cell-to-cell junctions and integrins respectively, lead to epithelial-to-mesenchymal transition (EMT), that is one of the main hallmark of tumor invasion [85]; a shift from proneural to mesenchymal phenotype was reported by TCGA in recurrences, with the accumulation of stem cell markers and the activation of NOTCH pathway and WNT/ β -catenin signaling [86]. Moreover, EMT is mediated by transcriptional regulator, such as Snail, that was found elevated in irradiated GBM cells [87]. Furthermore, ECM modulation is not the only event occurring in response to irradiation, as regulation of DNA repair processes [88], cell death evasion [89], senescence-associated secretory phenotype [90], inflammation [91] and angiogenesis [92] has also been observed. It is therefore clear that IR can trigger a number of processes that may represent druggable and promising target to promote IR efficacy and limiting side-effects and recurrences.

5.5. Targeting of SRC for GBM treatment

5.5.1 SRC proto-oncogene non-receptor tyrosine kinase

The proper physiological functioning and the maintenance of homeostasis is controlled by the cellular ability to perceive and correctly respond to specific signals derived from cell-to-cell and cell-microenvironment communication. The correct operation of these processes are under the control of signaling pathways, where receptor tyrosine kinases (RTKs) have a key role in the transduction mechanisms that lead to many cellular effects [93]. Since these processes are implicated in the regulation of several physiological cellular functions (proliferation, cell cycle, apoptosis regulation etc), RTKs alteration can generate pathological mechanisms that lead to the development of diseases, including cancer [94]. Indeed, RTKs are transiently activated by binding of the specific growth factors, followed rapidly by receptor dimerization and tyrosine phosphorylation of several substrates that are a part of the signaling cascade. In the oncogenic version, due to mutation or deregulation, a constitutive activation occurs, even without agonist activation, inducing continuous mitogenic signals [95].

RTKs are formed by extracellular domain that recognizes a specific ligand, otherwise, if the proteins are entirely in the cytoplasm, they are defined as cytoplasmic or non-RTKs (nRTKs) [96]. Among the nRTKs, the SRC family kinase is composed by nine members, of which SRC (known also as c-Src) was defined as proto-oncogene after its first identification in Rous sarcoma virus of chicken (v-SRC) [97]. It was found to be over-expressed and highly activated in various types of human cancers, including breast cancer, pancreatic cancer, colon cancer and brain cancer [98]. SRC is composed of 4 SRC homology domains (SH): the SH4 is linked to N-terminal with a 14-carbon myristic acid moiety, a unique domain different for all members and whose function is not yet known, two homologous SH3 and SH2 that are linked with a SH2-kinase linker to SH1 domain, containing the tyrosine action kinase (Tyr419) and a C-terminal negative regulatory domain (Tyr530) [99]. The autophosphorylation of Tyr419 determines the protein activation, whereas the phosphorylation of Tyr527 determines its inhibition. The SH1 catalytic domain contains the ATP and substrate-binding sites reside. Tyr527 residue phosphorylation determines a salt bridge with SH2 domain and the interaction of the SH3 domain with SH2-kinase linker is stabilized in a restrained state, that results inaccessible to external ligands (Figure 5).

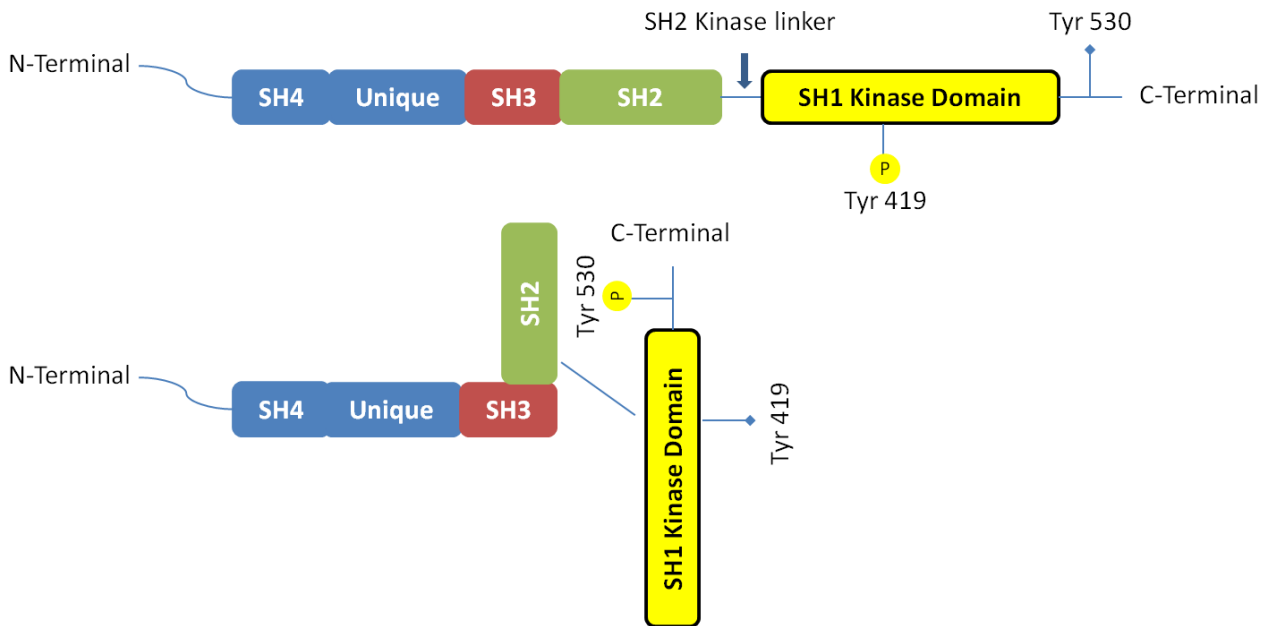


Figure 5. Schematic representation of SRC structure. SRC structural properties are showed from N-terminal myristoyl group to C-terminal regulatory segment. In the active form of SRC, the Tyr419 of SH1 domain is autophosphorylated promoting kinase activity; in the closed conformation, the phosphorylation of Tyr530 on C-terminal creates a link with the SH2 and the catalytic site, which is positioned on SH1, become not accessible for the substrates. (Copyright by F.Torrisi, R. Parenti Lab.)

There are various hypotheses to explain the activation mechanisms of SRC, mostly related to the destabilization of the SH2 - SH3 - SH2 linker - SH1 interactions. Upstream kinases or phosphatases are implicated in structural alteration for the SRC activation, that lead to pleiotropic effects such as adhesion, migration, invasion, cell morphology, differentiation, proliferation and survival. The Tyr530 dephosphorylation mediated by a protein kinase phosphatase- α is responsible for the reactivation of the SRC, by mean a conformational change that make the kinase domain accessible to substrates and ATP. SRC protein can be activated by the direct binding of the SH2 and SH3 domains with other surface receptors, like integrin or with cytoplasmatic tyrosine kinases, such as focal adhesion kinases (FAK), and with the cytoplasmic portion of RTKs, which hinder the inhibitory SRC interactions [100].

SRC/FAK/Integrin axis regulates intercellular and cell-to-ECM interactions. Integrins are surface proteins located at the level of focal adhesions allowing anchoring of cells to the ECM. Therefore, integrins have a key role in regulating cell adhesion, migration and invasion through their binding with specific proteins, such as FAK; FAK colocalize with the integrins on the focal adhesions, and SH2-SH3 domains are sites with high affinity of binding with the

autophosphorylation site and with proline-rich regions of the FAK. On one side, FAK binding to the SH2 domain of SRC displaces Tyr530 binding to it, relieving the auto-inhibitory interaction and leading to activation of SRC. After SRC-FAK bond, SRC phosphorylates two tyrosine residues on the FAK kinase domain, further increasing their kinase activity. These interactions regulate the structural organization of the cytoskeleton for adhesion, motility and cell division. In addition, SRC phosphorylates tyrosine residues the C-terminal of FAK, which acts as an attack site for other molecules that regulate communication signaling between cells or between cells and ECM [101]. Furthermore, the activation of SRC mediated by other RTKs lead to downstream multiple effectors, such as PI3K/Akt, Ras/Raf/MAPK, STAT3/STAT5B, and p130Cas pathway which are respectively involved in survival, proliferation, angiogenesis and motility [102].

5.5.2. SRC deregulation in GBM

Western blotting analysis on GBM samples compared to healthy brain tissues revealed high levels of SRC kinase activity, although the absence of amplifications or genetic mutations, as been reported by the TGCA [103]. In GBM, the absence of gene amplification and mutation confirmed that SRC hyperactivation is linked to aberrant activation of RTKs and surface receptors [104]. Indeed, FAK and other RTKs, including EGFR, platelet-derived growth factor receptor (PDGFR) and vascular endothelial growth factor receptor (VEGFR), determine the loss of SRC interdomains interactions involved in SRC inhibition, resulting in GBM-associated hallmarks activation (i.e. proliferation, survival, migration and angiogenesis) [105, 106]. Several *in vitro* and preclinical studies have shown that inhibition of SRC-mediated pathway mediates a decrease in the hallmarks listed above [104]. SRC was found highly expressed in GSCs, where they can enhance the migratory ability [107] and potentiate the stemness properties being a downstream target, together with transcription 3 (STAT3)-Kirsten rat sarcoma viral oncogene homolog (KRAS), in the MerTK pathway. Indeed, MerTK is upregulated in GBM and it was reported that the silencing of KRAS and SRC suppressed mesenchymal markers and GSCs features in MerTK-overexpressing X01 GBM stem-like cells [108].

5.5.3. Hypoxia-RT-SRC axis promotes GBM aggressiveness

Hypoxia plays a major role in the SRC tyrosine-kinase pathways [109-111]. Indeed, most of the RTKs, are also upstream or downstream factors of hypoxia-inducible factor-1 α (HIF-1 α) regulation, which is induced under conditions of low oxygen and acts as a master regulator of numerous

hypoxia-inducible genes [112]. Indeed, as early as 1995, it has been shown that phosphorylated SRC protein is highly active in GBM cells, particularly under hypoxic conditions [113]. In this study, it has also been shown that SRC activity in hypoxic conditions mediates a VEGF upregulation [113]. Moreover, in subsequent studies, a correlation between angiogenesis and hypoxia was also sustained by the observation of a marked increase in vascularisation related to hypoxia-signalling pathway involving the upregulation of integrin, that, as reported before, have a key role in the interaction with SRC [114]. Integrins overexpression in hypoxic GBM cells was correlated to the activation of FAK, promoting the activation of smallGTPase such as RhoB. RhoB increases the phosphorylation, leading to the inhibition of glycogen synthase kinase-3 pathway, involved in the degradation of HIF-1 α [75]. These evidences, represented the rational to target angiogenesis as a potential strategy for GBM therapy; however, it has been shown that therapeutic approach using anti-VEGF antibody (i.e. Bevacizumab) induces compensatory cellular mechanisms that also rely on SRC signalling activation [115]. The robust invasion in response to anti-VEGF may be, at least partially, associated with neo-vascular loss, low perfusion, and consequent hypoxia, which induces SRC activation [116].

Hypoxia-induced SRC pathway were also found to foster invasiveness. The EGFRvIII / integrin β 3 / FAK / SRC axis leads to the activation of the intracellular signaling pathway ERK1/2, MAPK, AKT, and STAT3, which determines the upregulation of MMP-2 and MMP-9, further promoting cell invasion [117]. It is also interesting that the SRC-induced TGF β pathway activation via α -SMA in hypoxic condition was associated with the promotion of cancer-associated fibroblasts (CAFs), which further increase chemotactic mediated migration of GBM cells [111, 118].

Besides being active during hypoxia, SRC activation has been found to promote invasiveness and motility of cancer cells in response to RT. The activation of malignant phenotypes of GBM in response to radiation was reported through the induction of MMP-2, involving pathways mediated by the interaction of SRC with EGFR [119]. In this study, it has been reported that IR induced phosphorylation of SRC kinase and that SRC inhibition by a pyrazolopyrimidine compound (PP2), reduced MMP-2 secretion, AKT activation, and SRC phosphorylation in irradiated cells. Moreover, PP2 was able to block IR-induced EGFR phosphorylation, whereas inhibition of EGFR did not affect the phosphorylation of SRC, identifying the possibility that radiation may stimulate the SRC activation regardless of EGFR/AKT pathway [119]. It has been also reported that IR-induced invasion modulating the ECM protein, is not only due to MMP action, but also to high production of other components such as hyaluronic acid, which acts as an extracellular signalling molecule for the mesenchymal shift of GBM, in response to radiation; hyaluronic acid is recognized by the CD44 receptor, which is a clear marker of the mesenchymal subtype. The interaction of hyaluronic acid

and CD44 receptor, leads to SRC activation, promoting tumor progression and radioresistance [120]. Moreover, IR-induced SRC activation promotes invasion also throughout FAK, ephrin type-A receptor 2 (EphA2) and EGFRvIII signalling [121]. The EGFRvIII expressing cells have been shown to release ligands such as hepatocyte growth factor (HGF) and interleukin 6 (IL6), activating SRC in EGFR expressing cells, thus increasing diffusion and infiltration [122].

The SRC pathways induced by IR have been also evaluated in relation to the intercellular communication systems in the context of signal molecules transmission by connexin-based channel and extracellular vesicles [123]. It has been shown in vitro that connexin 43 (Cx43)-based gap junctions and hemichannels through interactions with partners, such as SRC, are implicated in invadopodia formation and are responsible for invasion capacity and MMP-2 activity [124]. It has also been shown that following irradiation, GBM cells can release exosomes, which stimulate the upregulation of SRC and the migration of recipient cells [125].

Overall, SRC regulates the main pathways involved in proliferation, survival, migration and angiogenesis, which can also be interconnected. Both hypoxia and RT response modulate several factors through mechanisms coordinated by SRC (Figure 6).

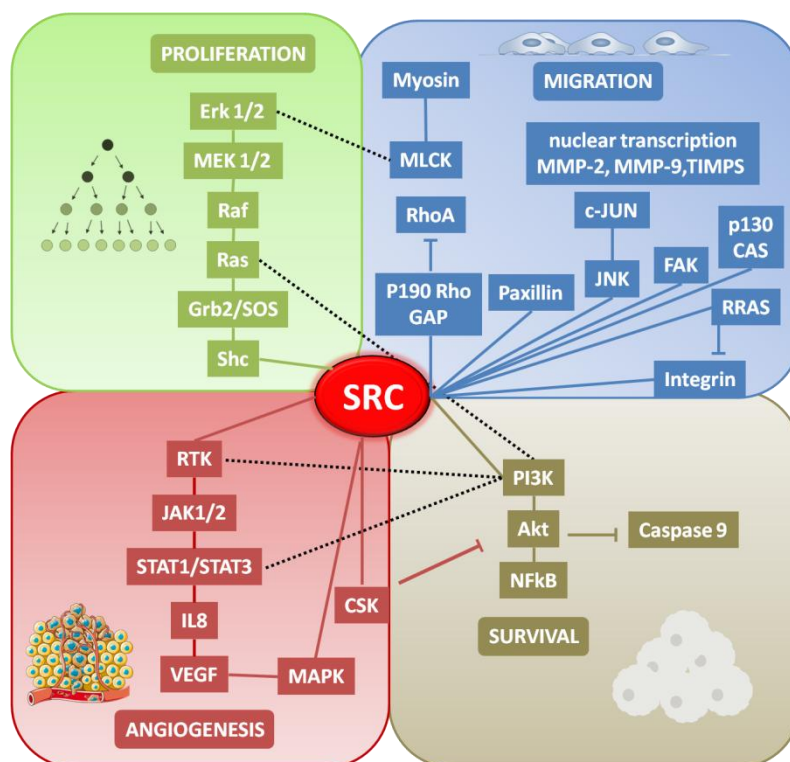


Figure 6. Schematic representation of SRC pathway stimulation under hypoxia and RT contributing to the deregulation of the principal events required for proliferation, survival, migration and angiogenesis. The complexity of the network is also determined by the cross talk between the factors of each signaling (Copyright by F.Torrisi, R. Parenti Lab.).

5.5.4 Si306 molecule: a Pyrazolo[3,4-d]Pyrimidine derivative for SRC inhibition

Recently, anticancer properties of pyrazole-pyrimidine derivatives has been confirmed against several human tumor cell lines, drawing a considerable attention for cancer treatment, including GBM [126, 127]. The research group of Lead Discovery Siena has designed and synthesized a wide library of pyrazolo[3,4-d]pyrimidines active as kinase inhibitors, identifying a potent inhibitors of the tyrosine kinases SRC. This molecule was called Si306 and it has been shown anticancer effects on different GBM cell lines.

The Si306 synthesis and its *in vitro* and *in vivo* characterization had a long course, that started from the production of pyrazolo[3,4-d]pyrimidine derivatives, evaluating the SRC activity in human epidermoids A431 cell line and in human breast cancer 8701-BC cell line [128]. The series of compounds was able to inhibit the Tyr419 phosphorylation site of SRC in a micro and sub-micromolar range, with an equivalent efficacy compared to the reference selective SRC inhibitor molecule, PP2 [128]. It was demonstrated that these compounds were able to block cell cycle progression and to promote apoptosis in both cell lines. The cell growth inhibition mechanism was also assessed by cell-free assay and inhibitory activity was found by competition with the ATP substrate. Molecular docking studies were conducted to evaluate the interaction between the SRC inhibitor compounds, applying the same protocol that was used at the outset for PP2. These docking studies revealed that the newly synthesized compounds showed superimposable molecular orientation and interactions with SRC comparable to those of PP2, with binding modalities similar to the specific substituents of the pyrazole-pyrimidine ring [128]. Further crystallography studies were performed using the Monte Carlo free energy perturbation (MC/FEP) calculations, which allowed to identify the preliminary structure of the Si306 molecule (previously called LDS001), among the series of inhibitors belonging to the pyrazolo [3,4-d]-pyrimidine family. The key interactions between molecule and pharmacological target were analyzed, optimizing the inhibitory effect through competition for the ATP site binding. This structure allowed to identify key interactions between LDS001 chemical series molecules and SRC leading to the subsequent optimization until the definitive Si306 molecule was obtained (Figure 7).

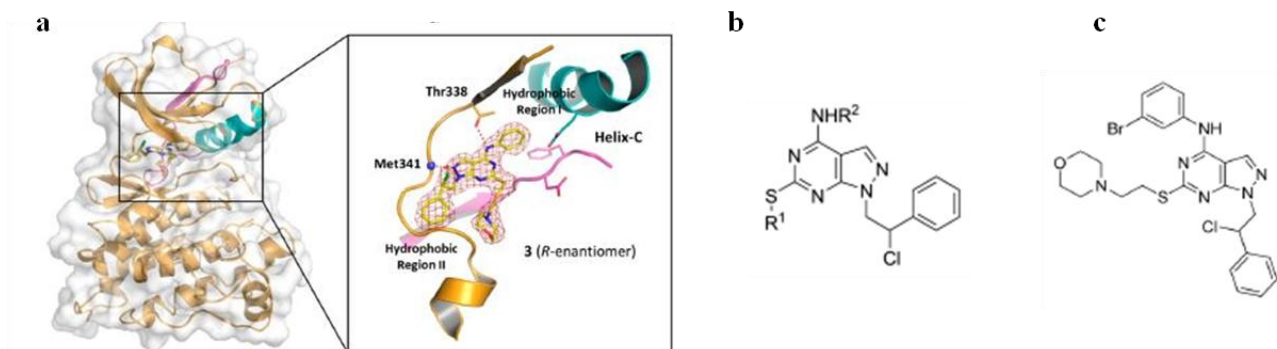


Figure 7. (a) Crystallographic structure of an analogue of LDS001 with the SRC kinase. (b) Chemical structure of pyrazolo[3,4-d]pyrimidine derivatives (c) and final chemical structure of Si306 (adapted from “Tintori C. et al.; J Med Chem. 2015”).

Furthermore, pharmacokinetic studies were performed in order to evaluate the absorption and aqueous solubility by parallel artificial membrane permeability (PAMPA) and human liver microsomes (HLM) assays. These studies have shown a high metabolic stability, good aqueous solubility, and effective membrane permeability. In a first phase, these data led to *in vitro* and *in vivo* studies to evaluate the effect of SRC inhibition on neuroblastoma models; Si306 revealed a high ability to inhibit the proliferation and to increase apoptosis of neuroblastoma SH-SY5Y cell line; no significant differences were observed with the gold standard for SRC inhibition, Dasatinib. The same cell line was tested in xenograft neuroblastoma models, where it was showed that the Si306 was able to inhibit tumor growth 60 days after oral treatment with a 50% mass reduction [129].

Promising results were obtained in a first study, testing the Si306 efficacy on *in vitro* GBM cell lines and *in vivo* GBM model. First, the western blot analysis revealed that both the U87-MG and U251-MG cell lines expressed the SRC protein in its Tyr 416/419 phosphorylated isoforms and that it was inactive following treatment with 1 $\mu\text{mol/L}$ of Si306 for 48 hours. It was also observed that the inhibition of SRC reduced the expression of the active β -PDGFR in U87-MG cell line, known to be one of key RTKs involved in the SRC modulation to promote GBM progression. Si306 was compared to PP2 for the evaluation of migration and survival effects. Under the EGF stimulus, Si306 blocked the migration in a comparable manner observed with PP2. A greater reduction in cell proliferation and a lower dose-response survival were obtained with Si306 compared to PP2 [111].

Moreover, pharmacokinetic studies were performed to verify the ability of Si306 to cross the blood brain membrane: it was reported that the accumulation of the Si306 in the brain increased progressively over the 24 hours. In conclusion, results from acute toxicity study showed that a

single intravenous administration at the highest dosage did not cause any adverse effects in the treated animals (mice) both in terms of behavioral symptoms and as regards organ injuries (liver, kidneys, brain) [111].

Finally, Si306 was demonstrated to overcome the multidrug resistance mechanisms, related to the presence of ATP-binding cassette transporters in endothelial cells of the blood-brain barrier, that affect drug delivery and efficacy in target tumor cells. Indeed, the P-glycoprotein and breast cancer resistance protein (BCRP) efflux transporters, represented the key pharmacokinetic limitation for the effectiveness of Dasatinib, that has been a good candidate for GBM treatment. Si306 showed an excellent pharmacodynamic profile and it was able to significantly inhibit GBM cells growth in highly P-gp expressing cells as compared to Dasatinib [130]. These findings led to a deeper investigation of Si306 as valuable strategy for GBM treatment in combination with RT.

6. AIMS

The investigation of new therapeutic strategies in radiobiology is still a very challenging field of research. The realization of this research project come from the necessity to find new strategies for GBM treatment that may help to eradicate completely tumor cells after a possible surgical resection, increasing RT therapeutic potential.

Intrinsic radioresistance mechanisms are the main reasons for the unsuccessful use of radiation to treat GBM. The arrest of malignancy processes by molecularly targeted therapies may represent a good strategy to enhance the RT efficacy for a dual advantage: decrease the dose required to eradicate cancer cells, reducing the toxicity of the treatment for surrounding healthy tissues.

The achievement of these aims deal with two primary issues that should be overcome: 1) hypoxic microenvironment; 2) activation of molecular mechanisms of radioresistance [48]. These two key aspects are responsible for additional issues that support the radioresistance mechanisms in GBM; indeed, they are related each other because radioresistance pathways can be induced by hypoxia and by IR response. Hypoxia and radiation-enhanced malignancy mechanisms have been associated to the activation of cell surface receptors and the overexpression of growth factors, but the complex interplay of multiple signaling pathways made difficult the identification and the design of molecularly targeted agents [131].

In this scenario, the elevated enzymatic activity of SRC in GBM is responsible of pleiotropic action for the development of several hallmarks of GBM, but also, the activation of SRC-mediated pathway of radioresistance and aggression are linked to the hypoxic microenvironment and to RT treatment response [104]. Therefore, the rationale for the selection of SRC as molecular target for a based therapeutic approach in combination with RT, has been guided by the hypothesis that SRC/hypoxia/IR response axis is involved in the GBM radioresistance and aggressive phenotypes. Targeting SRC represents a strong strategy to increase the efficacy of RT and a potential treatment option.

The general aim of the thesis was to investigate the effects of a synergistic therapy to improve the radiosensitivity of human GBM cell lines, combining RT with a molecule SRC inhibitor (Si306).

More in detail, the main aims were:

- I. Evaluate the synergistic effect of the Si306 molecule with proton therapy.
- II. Analyze the gene expression profile and molecular mechanisms induced by Si306 combined with protons, to identify cell signaling pathways involved in the modulation of radioresistance/radiosensitivity.
- III. Evaluate the ability of the Si306 molecule to overcome the radioresistance induced by hypoxia following X-rays treatment.

The research questions and the purpose are summarized in the figure below (Figure 8).

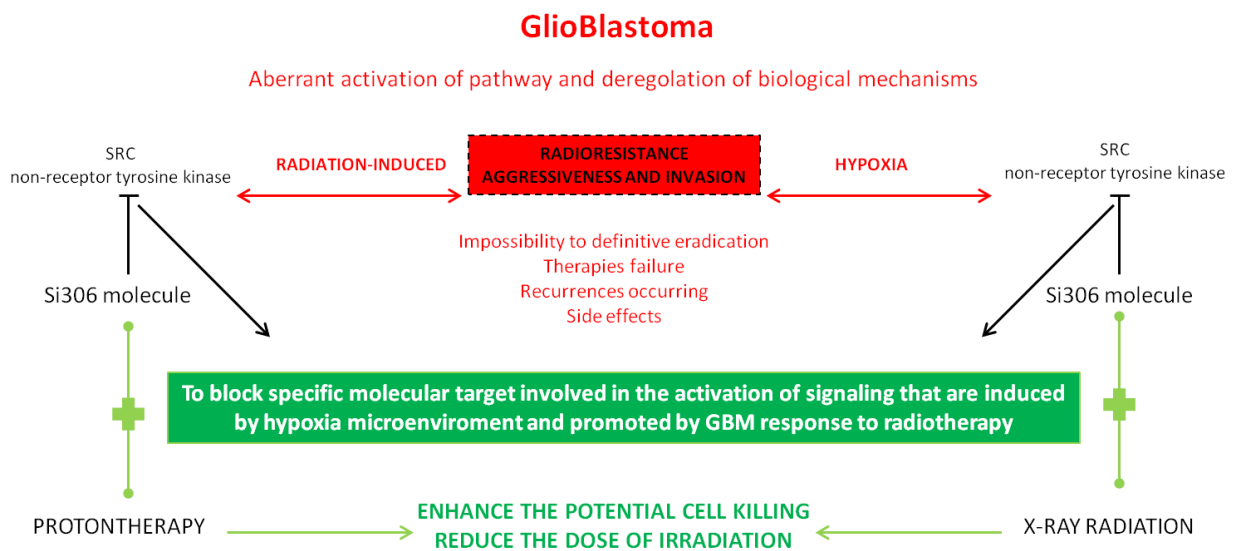


Figure 8. Schematic representation of the research project aim. Research questions focus on deregulated pathways in GBM that are generated both by hypoxia and by the response to RT (red bidirectional arrows) with the involvement of SRC. The aim of the research is represented by the inhibition of SRC (T bars) in synergy with X-rays and protons (green connector with plus sign) to enhance the RT effectiveness and to reduce the delivered dose (green arrows).

7. RESULTS

PAPER 1

IL NUOVO CIMENTO 41 C (2018) 203

DOI 10.1393/ncc/i2018-18203-8

Preliminary study of novel SRC tyrosine kinase inhibitor and proton therapy combined effect on glioblastoma multiforme cell line: In vitro evaluation of target therapy for the enhancement of protons effectiveness

LUIGI MINAFRA(*^{1,2}), FRANCESCO P. CAMMARATA(*^{1,2}), FILIPPO TORRISI(**^{2,3}), GIUSI I. FORTE(^{1,2}), VALENTINA BRAVATÀ(^{1,2}), MARCO CALVARUSO(¹), PIETRO PISCIOTTA(^{1,2}), CARMELO MILITELLO(^{2,3}), GIADA PETRINGA(²), GIUSEPPE A. P. CIRRONE(²), ANNA L. FALLACARA(^{4,5}), LAURA MACCARI(^{4,5}), MAURIZIO BOTTA(^{4,5}), GIACOMO CUTTONE(²) AND GIORGIO RUSSO(^{1,2})

(*) These authors contributed equally to this work.

(**) corresponding author. E-mail: filippo.torrisci@unict.it

(1) Institute of Molecular Bioimaging and Physiology, IBFM-CNR - Cefal`u, Italy

(2) National Institute for Nuclear Physics, Laboratori Nazionali del Sud, INFN-LNS Catania, Italy

(3) Department of Biomedical and BioTechnological Science (BIOMETEC), University of Catania - Catania, Italy

(4) Lead Discovery Siena (LDS) - Siena, Italy

(5) University of Siena - Siena, Italy

received 4 December 2018

Summary.

The aim of this work was to evaluate proton therapy effectiveness in combination with a molecule SRC protein inhibitor for glioblastoma multiforme treatment. The role of this novel compound, Si306, is to interfere with glioblastoma carcinogenesis and progression, creating a radiosensitivity condition. The experiments were performed on U87 human glioblastoma multiforme cell line. Molecule concentrations of 10 μ M and 20 μ M were tested in combination with proton irradiation doses of 2, 4, 10 and 21Gy. Cell survival evaluation was performed by clonogenic assay. The results showed that Si306 increases the efficacy of proton therapy reducing the surviving cells fraction significantly compared to treatment with protons only. These studies will support the

preclinical phase realization, in order to evaluate proton therapy effects and molecularly targeted drug combined treatments.

1. – Introduction

Glioblastoma multiforme (GBM) belongs to the group of diffuse astrocytic and oligodendroglial tumor of the gliomas family. The highest grade (IV grade) is assigned to GBM, according to the World Health Organization (WHO) classification based on malignancy histological criteria, proliferation index, aggressiveness, response to therapy and life expectancy [1].

The current standard treatment establishes conventional radiotherapy (RT) of 2 Gy for 30 fractions with the alkylating agent temozolomide (TMZ) both concomitantly and RT adjuvant [2]. At present, these treatments are not curative and the median overall survival (OS) is only 14–15 months after diagnosis [3]. Furthermore, radionecrosis and neurocognitive dysfunctions are the main causes of late tissue toxicities of the surrounding organs [4]. Proton therapy (PT), unlike conventional RT, shows physical characteristics which contribute to an overall improved risk-benefit profile in radiotherapy. The reverse depth dose profile of protons allows to hit the cancerous target sparing healthy tissues [5]. For this reason, PT can avoid side effects and increase median OS by means of protocols with dose escalation such as hyperfractionated treatments [6]. Actually, although the demonstration of an overall improved risk-benefit profile and an extension of the OS emerging from clinical trials, some aspects still need to be clarified. In particular, the excessive radiation necrosis and radioresistance phenomena are key features of GBM under investigation [7]. To date, the cellular pathways involved in radioresistance are not fully known. SRC protein non-receptor kinase is one of the main molecular targets involved in GBM radioresistance. In fact, SRC is a key factor which contributes to regulate the main hallmarks of GBM, such as cell morphology, adhesion, migration, invasion, proliferation, differentiation and cell survival [8]. For this reason, the SRC inhibitor compound Si306, has been designed to block the SRC protein activity, with the aim to enhance PT effectiveness and to reduce radioresistance. Computational and modelling analysis have revealed that Si306, can specifically bind the ATP site of the SRC protein making it inactive [9]. In particular, in previous studies it has been demonstrated that Si306 determines a significant reduction in glioblastoma cell proliferation, migration and an enhancement in growth inhibition. Antiproliferative effect of Si306, has been tested in association with X-ray both in vitro and in vivo. It has been observed that the combination effect of Si306, and RT reduced significantly colony numbers in vitro in low-density growth assay compared to the cells treated with only RT. For the in

vivo studies the combination treatment determined a significant reduction of the tumor growth compared to untreated group [10]. The aim of this preliminary study was to evaluate PT effects in combination with the compound Si306. In our study we tested two concentrations of Si306, 10 μ M and 20 μ M, combined with PT delivering four doses, 2, 4, 10 and 21 Gy, on U87 human glioblastoma cell line. Our results show an enhancement effect on cell killing by Si306 with proton beam.

2. – Materials and methods

2.1. Cell culture. – The U87 MG human glioblastoma cell line was purchased from American Type Culture Collection (ATCC, Manassas, VA, USA). The cell line was cultured according to ATCC, in Basal Medium Eagle (BME) supplemented with 10% FBS, 1% penicillin/streptomycin, 1% glutamine, 1% non-essential amino acids and sodium pyruvate. Cells were maintained in an exponentially growing culture condition in incubator at 37 °C in a humidified atmosphere (95% air and 5% CO₂) and were routinely sub cultured in 25 cm² (T25) standard tissue culture flasks.

2.2. Si306 treatment. – The compound Si306 was kindly provided by Lead Discovery Siena (Siena, Italy). It was dissolved in Dimethylsulfoxid (DMSO, Sigma-Aldrich) with final concentrations not exceeding 0.5% of DMSO. According to IC₅₀ (drug concentration that determined the 50% of growth inhibition) previously calculated [10], U87 cells were pretreated with Si306 concentrations of 10 μ M and 20 μ M for 24 h. After incubation time, the medium was removed, cells were rinsed two times with phosphate buffered saline (PBS) and fresh medium was added before the irradiations with a proton beam.

2.3. Proton irradiation. – The proton beam irradiation was performed at the CATANA (Centro di Adroterapia ed Applicazioni Nucleari Avanzate) facility of INFN-LNS (Catania, Italy) [11]. It is the first Italian proton therapy facility and it has been in operation since 2002. Here, using 62 MeV of proton beams accelerated by a cyclotron superconducting, patients affected by ocular melanoma are treated. The beamline is composed of several passive elements optimized for the clinical application: scattering foils to spread the beam laterally, collimators to define the beam profile in accordance to the tumor shape and monitor chambers to measure the dose delivered. In order to irradiate the entire T25 flask, a motorized system for biological samples irradiation was used. Radiochromic film detectors were adopted to check lateral dose distribution before each irradiation. The dosimetric system was calibrated under reference conditions according to the International

Atomic Energy Agency Technical Reports Series No. 398 “Absorbed Dose Determination in External Beam Radiotherapy” [12, 13]. For combined treatments with 10 μ M and 20 μ M of Si306, U87 cell line irradiations were carried out using four dose values of 2, 4, 10 and 21Gy. The same irradiation treatments were performed without the compound Si306, including also dose values of 1, 3 and 6 Gy in order to obtain a clonogenic survival curve as control. Cell irradiations were conducted placing the cell at the middle spread-out Bragg peak, to simulate a clinical condition, with a dose rate of 15 Gy/min.

2.4. Clonogenic assay. – Two days before treatments, U87 cells were seeded in T25 flasks at a density of 3×10^5 /flask and maintained at subconfluence. After irradiation, the cell survival was performed by clonogenic assay according to the protocol of Franken et al. [14] Briefly, after irradiation, U87 cells were detached, counted by haemocytometer and seeded in a 6-well plate in triplicate at a density of 50–2000 cells per well according to the dose delivered to assay the surviving fraction (SF). The number of cells plated was chosen to yield at least 50 colonies per flask. After an incubation time of 12 or 14 days, cells were fixed with 50% methanol for 20 min and stained with 0.5% crystal violet (both from Sigma-Aldrich, St. Louis, MO, USA). Colonies with more than 50 cells were counted as clonogenic and SF determined according to the plating efficiency (PE) of untreated cells (control).

3. – Results

The effect of Si306 alone and in combination with PT was assessed in U87 cells. After cell exposure with Si306 alone at concentration of 10 μ M and 20 μ M, we observed a SF of 80% and 60%, respectively, showing a dose-response relationship. Following proton irradiation with doses of 2, 4, 10 and 21 Gy, the SF of the U87 cells without the drug obtained were as follows: 40%, 21%, 7% and 3%. Cell survival was further reduced after the pre-treatment with Si306 combined with the irradiation treatment. SF obtained after combined treatments were as follows at the same irradiation doses: 28%, 20%, 5% and 3% for the setting with 10 μ M of Si306; 16%; 10%, 4% and 2% for the setting with 20 μ M of Si306. The results of clonogenic assays for U87 cell lines after irradiation with protons alone and in combination with Si306 are shown in fig. 1.

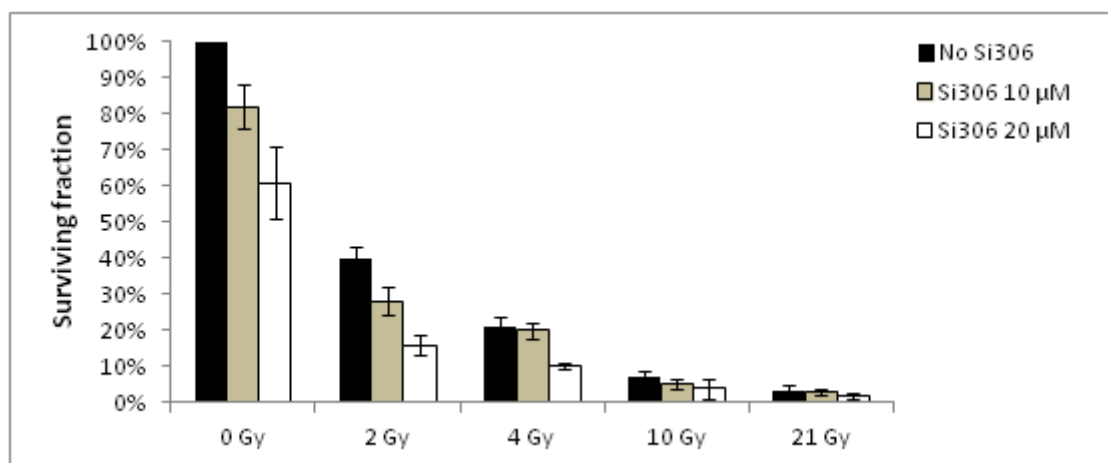


Fig. 1. – Effect of Si306 in combination with proton therapy on the human U87 glioblastoma cell line. Bar diagrams of surviving fraction are in percentage. The data are mean±SD of three independent experiments.

4. – Discussion

In this study, we evaluated the effect of PT combined with a novel molecule inhibitor of SRC on the glioblastoma cell line using clonogenic assay. The work shows that pretreatment with the compound Si306 contribute to weak clonogenic activity of glioblastoma cells irradiated with proton beams. In addition to the radiosensitivity evaluation, one of our main goals is to investigate IR-induced radioresistance at molecular level since gene expression profiling may reflect different clinical outcomes by assuming a significant prognostic value of gene signatures to predict a glioblastoma response to the radiation treatment. Therefore, gene expression analyses by whole-genome cDNA microarray are in progress in order to evaluate ionizing radiation-induced pathways that can be modulated by Si306 activity. There are no available studies about gene signatures proton-induced, especially in combination with targeted molecules.

From a clinical perspective, PT might be a promising treatment for patients with GBM and the inhibition of SRC tyrosine kinase proteins is a favourable strategy to overcome invasion, migration and other mechanisms involved in radioresistance of GBM.

Previous studies have shown that inhibition of SRC proteins reduces the expression of vascular endothelial growth factor (VEGF) and invasive processes that can be triggered by direct inhibitors of VEGF, such as bevacizumab or by exposure to IR itself [15-17].

Over recent years, few in vitro studies have been performed about the proton effects in association with molecular targeted drugs for GBM treatment. Among the studies with particle therapies, most of the information is related to the evaluation of the effect of high-LET particles,

such as carbon ions combined with TMZ or other chemotherapeutic agents [18-20]. Although a greater radiobiological efficacy of carbon ions has been shown for glioblastoma cell lines compared to photon irradiation, we encourage to implement studies that guide towards a new clinical trial for PT. One of the main reasons is the limited availability of dedicated facilities for carbon ion therapy compared to PT centres: more than 100,000 patients have been already treated in 50 centres for cancer treatment with protons. Carbon ion centres instead are located in few countries, since only two of them are in Europe: Heidelberg Ion-Beam Therapy Centre (HIT) in Heidelberg, Germany and Centro Nazionale di Adroterapia Oncologica (CNAO) in Pavia, Italy [21, 22].

This work shows for the first time the effects following the combination of proton irradiation with a molecular targeted agent blocking SRC protein in the GBM cell line.

Therefore, our in vitro results represent radiobiological data useful for subsequent preclinical steps, as well as clinical applications, contributing to define a personalized biologically driven treatment plan.

* * *

This work was supported by the National Institute for Nuclear Physics (INFN)-LNS - funded MoVeIT project “Modeling and Verification for Ion beam Treatment planning” and Prof. Rosalba Parenti, Dottorato in Biotecnologie - Dipartimento di Scienze Biomediche e Biotecnologiche (BIOMETEC) - XXXIII Ciclo.

REFERENCES

- [1] Louis D. N. et al., *Acta Neuropathol.*, 131 (2017) 6.
- [2] Stupp R. et al., *N. Engl. J. Med.*, 352 (2005) 10.
- [3] Hanif F. et al., *Asian Pac. J. Cancer Prevention*, 18 (2017) 3.
- [4] Justin M. et al., *Front. Neurol.*, 748 (2017) 8.
- [5] Tommasino F. et al., *Cancers*, 7 (2015) 1.
- [6] Cabrera A. R. et al., *Pract. Radiat. Oncol.*, 6 (2016) 4.
- [7] Gladson C. L. et al., *Annu. Rev. Pathol.*, 5 (2010) 33.
- [8] Ahluwalia M. S. et al., *Cancer Lett.*, 298 (2010) 2.
- [9] Tintori C. et al., *J. Med. Chem.*, 58 (2015) 1.
- [10] Calgani A. et al., *Mol. Cancer Ther.*, 15 (2016) 7.
- [11] Cirrone G. A. P. et al., in *Proceedings of the IEEE Nuclear Science Symposium and Medical Imaging Conference, Roma (Italy) 16–22 October 2004*, in *IEEE Nucl. Sci. Symp. Conf. Rec.*, Vol. 4 (IEEE) 2004.

- [12] Cirrone G. A. P. et al., Nucl. Phys. B Proc. Suppl., 150 (2006) 1.
- [13] Russo G. et al., Nucl. Instrum. Methods Phys. Res. Sect. A, 846 (2017) 126.
- [14] Franken et al., Nat Protoc., 1 (2006) 5.
- [15] Huvelde D. et al., PLoS ONE, 8 (2013) 2.
- [16] Arscott W. T. et al., Transl. Oncol., 6 (2013) 6.
- [17] Park C. M. et al., Cancer Res., 66 (2006) 17.
- [18] Combs S. E. et al., Int. J. Radiat. Biol., 85 (2009) 2.
- [19] Combs S. E. et al., Radiat Oncol., 7 (2012) 9.
- [20] Barazzuol L. et al., Radiat Res., 177 (2012) 5.
- [21] Hadziahmetovic M. et al., Future Oncol., 7 (2011) 10.
- [22] Pirtoli L. et al., Current Clinical Pathology, 1st edition (Springer, Switzerland) 2016.



Proton Therapy and Src Family Kinase Inhibitor Combined Treatments on U87 Human Glioblastoma Multiforme Cell Line

Francesco P Cammarata^{1,2†}, Filippo Torrisi^{2,3†}, Giusi I Forte^{1,2}, Luigi Minafra^{1,2*}, Valentina Bravatà^{1,2}, Pietro Pisciotta^{2,4}, Gaetano Savoca¹, Marco Calvaruso^{1,2}, Giada Petringa^{2,3}, Giuseppe A P Cirrone², Anna L Fallacara^{5,6}, Laura Maccari⁵, Maurizio Botta^{5,6}, Silvia Schenone⁷, Rosalba Parenti³, Giacomo Cuttone², Giorgio Russo^{1,2}

¹Institute of Molecular Bioimaging and Physiology, National Research Council, IBFM-CNR, 90015 Cefalù, Italy; francesco.cammarata@ibfm.cnr.it (F.P.C.); filippo.torrisi@unict.it (F.T.); giusi.forte@ibfm.cnr.it (G.I.F.); valentina.bravata@ibfm.cnr.it (V.B.); savoca.gaetano@gmail.com (G.S.); marco.calvaruso@ibfm.cnr.it (M.C.); giorgio.russo@ibfm.cnr.it (G.R.)

²National Institute for Nuclear Physics, Laboratori Nazionali del Sud, INFN-LNS, 95123 Catania, Italy; pietro.pisciotta@lns.infn.it (P.P.); giada.petringa@lns.infn.it (G.P.); pablo.cirrone@lns.infn.it (G.A.P.C.); cuttone@lns.infn.it (G.C.)

³Department of Biomedical and Biotechnological Sciences (BIOMETEC), University of Catania, 95123 Catania, Italy; parenti@unict.it

⁴Departments of Physics and Astronomy, University of Catania, 95123 Catania, Italy

⁵Lead Discovery Siena s.r.l. (LDS), 53100 Siena, Italy; al.fallacara@gmail.com (A.L.F.); l.maccari@leaddiscoverysiena.it (L.M.); maurizio.botta@unisi.it (M.B.)

⁶Department of Biotechnology, Chemistry and Pharmacy, Università degli Studi di Siena, 53100 Siena, Italy

⁷Department of Pharmacy, Università degli Studi di Genova, 16126 Genova, Italy; schenone@difar.unige.it

* Correspondence: luigi.minafra@ibfm.cnr.it

† These authors contributed equally to this work.

Received: 3 September 2019; Accepted: 24 September 2019; Published: 24 September 2019

Abstract: Glioblastoma Multiforme (GBM) is the most common of malignant gliomas in adults with an exiguous life expectancy. Standard treatments are not curative and the resistance to both chemotherapy and conventional radiotherapy (RT) plans is the main cause of GBM care failures. Proton therapy (PT) shows a ballistic precision and a higher dose conformity than conventional RT.

In this study we investigated the radiosensitive effects of a new targeted compound, SRC inhibitor, named Si306, in combination with PT on the U87 glioblastoma cell line. Clonogenic survival assay, dose modifying factor calculation and linear-quadratic model were performed to evaluate radiosensitizing effects mediated by combination of the Si306 with PT. Gene expression profiling by microarray was also conducted after PT treatments alone or combined, to identify gene signatures as biomarkers of response to treatments. Our results indicate that the Si306 compound exhibits a radiosensitizing action on the U87 cells causing a synergic cytotoxic effect with PT. In addition, microarray data confirm the SRC role as the main Si306 target and highlights new genes modulated by the combined action of Si306 and PT. We suggest, the Si306 as a new candidate to treat GBM in combination with PT, overcoming resistance to conventional treatments.

Keywords: glioblastoma multiforme; proton therapy; combined treatments; gene signatures

1. Introduction

Glioblastoma multiforme (GBM) is a central nervous system tumor classified as grade IV of highgrade malignant gliomas (HGG), according to the World Health Organization (WHO) guidelines [1]. GBM belongs to the group of diffuse astrocytic and oligodendroglial tumor, joining oligodendrocytomas, ependymomas, and mixed gliomas, under the glioma classification [2].

According to the ASTRO guidelines statements, the current standard care for GBM is surgical resection to the feasible extent, followed by conventional radiotherapy (RT) of 60 Gy delivered by fractions of 2 Gy, up to seven weeks. Moreover, chemotherapy is concurrent to RT with daily temozolomide (TMZ) administration [3–5]. These treatment modalities are not currently curative and the resistance to both chemotherapy and RT plans is the main cause of GBM care failures (the median survival time is 14.6 months) [6]. Moreover, the percentage of relapses and side effects post TMZ and RT treatments is more than 90% [7]. More precisely, even if the application of TMZ has significantly improved clinical GBM outcomes, cases of drug resistance related to the activity of the enzyme methyl guanine methyl transferase (MGMT) have been observed [8]. The hypermethylation of its promoter, is indeed associated with a better survival rate in patients receiving TMZ with or without RT [9]. In addition, the dose release onto healthy brain tissue or surrounding organs at risk during irradiation may, substantially, contribute to late tissue toxicities, such as radionecrosis and neurocognitive dysfunction, because of their limited dose tolerance.

In recent years, different dose fractionation schedules have been improved to have a better prognosis, avoiding the large side effect even in case of focal re-irradiation of recurrences. In this scenario, proton therapy (PT) could be used as a successful strategy for GBM treatment, being able to regulate the balance between tumor control and the normal tissue tolerance [10–14]. In particular, when heavy particles cross the tissues, they deposit a minimal radiation dose on their track to the tumor. The depth-dose distribution, described by the Bragg peak trend, gradually increases as a function of the depth. So, the so-called spread-out Bragg peak (SOBP) lead to a complete irradiation of the target volume and a more conformal dose distribution, sparing the surrounding healthy tissues from damage [15,16]. This specific dose distribution curve represents a key topic for GBM tumor treatments in which the sparing of healthy tissue is a key factor for the patient's quality of life. Therefore, there is a robust scientific rationale motivating the need to enlarge studies that guide towards new clinical trials for PT combined with targeted therapy rather than conventional RT with photons or electrons [17,18].

Today, in the context of personalized medicine, prognostic and predictive molecular biomarkers are useful to select cancer therapeutic planning [19,20]. A critical point in RT success is the prediction of cancer radiosensitivity. At the molecular level, the idea that genes may behave as biomarkers of a disease response represents the base for the development of gene signatures, to predict response to cancer radiation treatments [21]. Several genes have been shown to be responsive to radiation exposure and thanks to the use of high-throughput technologies, such as gene expression profiling (GEP) by microarray, radiosensitivity assays have been developed with gene signatures predicting radioresponse in many cancer types, including GBM [22]. However, the response to radiation is highly cell-line dependent and some specific genes and pathways may be linked both to tumor subtypes and dose delivered [23–25].

Actually, few published studies have evaluated the effectiveness of radiosensitizing agents combined with PT in GBM and none of them consider genes and response pathways induced by RT. Most studies have demonstrated that different genetic pathways and molecular features can provide reliable prognostic biomarkers, overlooking the treatment responses and predictive outcomes. However, according to WHO guidelines, IDH1/IDH2 gene status distinguishes a more radioresistant tumor type (primary GBM, IDH-wild type) from a more sensitive one (secondary GBM, IDH-mutant). IDH mutation is correlated with epigenetic modifications of the MGMT gene and assumes a prognostic value together with other biomarkers such as, the presence of LOH 10q, epidermal growth factor receptor (EGFR) amplification, p16INK4a deletion, TP53 mutation, PTEN mutation, and the codeletion of 1p/19q [26–28].

Based on this evidence, a large group of molecularly targeted agents have been designed, but none of them seem to overcome tumor radioresistance [29]. Previous studies support an involvement of the SRC-family protein kinases in the irradiation induction of radioresistance mechanisms. SRC protein is a non-receptor tyrosine kinase that interacts with many intracellular proteins involved in GBM carcinogenesis and progression. In addition, in vitro and in vivo studies confirmed the

correlation between SRC activity and GBM carcinogenesis. [30].

In this work we analyzed the GEP on the U87 MG human glioblastoma cell line after treatment with PT alone or in combination with a new targeted compound, named Si306 (Lead Discovery Siena, Siena, Italy), inhibiting SRC proteins. The Si306 molecule is a new TKI, chosen among the family of pyrazolo[3,4-d]pyrimidines, that exhibited the ability to specifically bind the ATP site of SRC protein, making it inactive. Furthermore, previous *in vitro* and *in vivo* studies have shown that the Si306 determines a significant reduction of the β -PDGFR active phosphorylated form and a greater loss of the migratory ability in GBM cells stimulated by Epidermal Growth Factor (EGF). In addition, the antiproliferative effect of Si306 has been tested in association with conventional RT treatments both *in vitro* and *in vivo* [31].

Here, in order to clarify the Si306 activity in GBM cells exposed to PT, we firstly evaluated radiosensitive effects of different amounts of the Si306 compound on the U87 cell line in combination with PT exposed at the doses of 1, 2, 3, 4, 10, and 21 Gy. Clonogenic assay and dose modifying factor (DMF) calculations were performed. We also analyzed the U87 cell radiosensitivity by applying the radiobiological linear-quadratic (LQ) model and calculated the α , β , and α/β ratio, commonly used to predict radiosensitivity of normal and tumor cells [32].

In addition, at molecular level we selected 2 and 10 Gy of proton radiation doses combined with the Si306 to evaluate GEP induced responses, by using whole genome cDNA microarray. We described networks and specific gene signatures of response to both treatments, highlighting for the first time, the cell pathways induced by Si306.

2. Results

2.1. IC50 Determination

In order to evaluate cytotoxicity ability of Si306 in term of concentration that determined the 50% of growth inhibition (IC50), U87 cells were incubated with Si306 at increasing concentrations of 0.1, 1.0, 10, and 100 μ M for 24, 48, and 72 h under normal cell culture conditions. Cell numbers and viability were evaluated and the IC50 values calculated at each time points (Table 1).

Table 1. IC50 values calculated after 24, 48, and 72 h of treatment with Si306 on U87 glioblastoma cell line

IC50	IC50	IC50
24 h	48 h	72 h
17.3 μ M	6.8 μ M	1.98 μ M

2.2. Cell Radiosensitization Following Combined Treatments with Protons and Si306

To evaluate the radiosensitizing ability of Si306 compound, we investigated the combined effects of this molecule on U87 cells exposed to different proton doses (1, 2, 3, 4, 10, and 21 Gy). Surviving fraction values, obtained by clonogenic assay, after irradiation with protons alone or after pretreatment with 10 and 20 μ M Si306, are shown in Table 2. These surviving fraction (SF) values were plotted to obtain dose-response curves with the exception of the 10 Gy and 21 Gy doses because of the lack of LQ model validity at high doses (Figure 1). We then calculated the DMF, which represents the relative reduction of dose to be delivered following a combined treatment with Si306 to get the isoeffect of SF = 0.5 compared to radiation treatment without modification. The DMF values were 1.09 (10 μ M of Si306) and 1.21 (20 μ M of Si306), showing a radiosensitive effect at both concentrations (Table 3).

Table 2. Surviving fraction (SF) values of U87 cells after irradiation with only protons and after combined treatments with 10 and 20 μM of Si306

Dose (Gy)	SF (Only Protons)	SF (Protons + 10 μM Si306)	SF (Protons + 20 μM Si306)
0	1.000 \pm 0.185	1.000 \pm 0.121	1.000 \pm 0.127
1	0.756 \pm 0.126	0.722 \pm 0.107	0.694 \pm 0.104
2	0.516 \pm 0.066	0.509 \pm 0.088	0.474 \pm 0.078
3	0.409 \pm 0.069	0.342 \pm 0.057	0.305 \pm 0.051
4	0.257 \pm 0.050	0.239 \pm 0.050	0.216 \pm 0.044
10	0.109 \pm 0.022	0.072 \pm 0.018	0.064 \pm 0.018
21	0.056 \pm 0.015	0.039 \pm 0.009	0.035 \pm 0.012

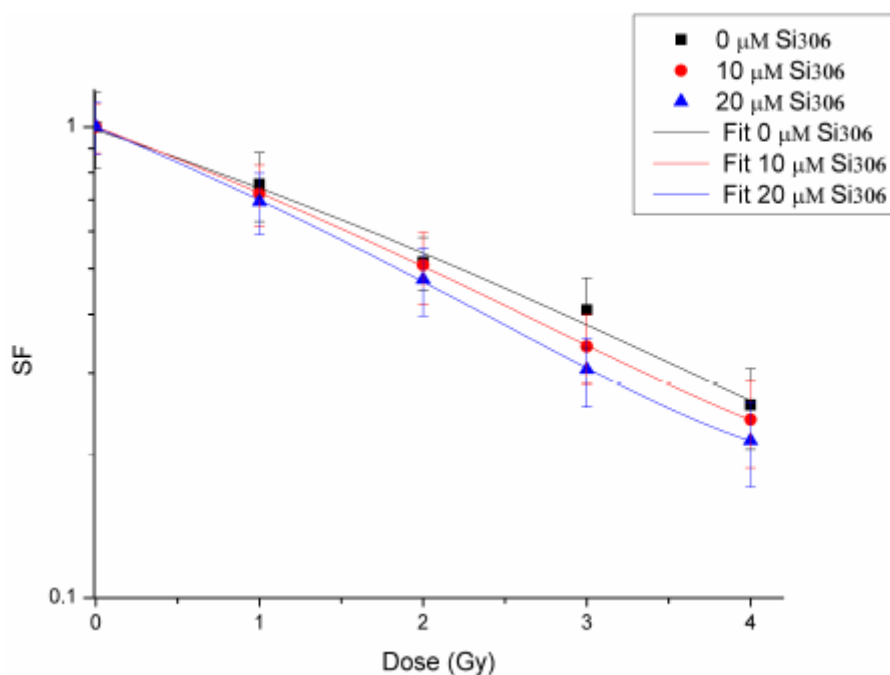


Figure 1. Cell survival curves of U87 cells. Cells treated with protons only (black line), protons plus 10 μM of Si306 (red line), and protons plus 20 μM of Si306 (blue line).

Table 3. Dose modifying factor (DMF) values calculated as isoeffective dose at surviving fraction of 0.5.

Treatment	SF 50% (Gy)	DMF
Protons	2.22	1
Protons + 10 μM Si306	2.03	1.09
Protons + 20 μM Si306	1.84	1.21

2.3 LQ model

We calculated LQ parameters α and β of U87 cells, which provided information about the intrinsic cell radiosensitivity. Together with α/β ratio they have a pivotal role for a reliable estimation of radiation response, although most of the studies reported a large heterogeneity in LQ parameters and limited data is published about PT [33,34]. The U87 fitted survival curve, generated after only protons administration, gives us the values of 0.292 Gy⁻¹ for α and of 0.010 Gy⁻² for β , that result in an α/β ratio of 28.6 Gy (Table 4).

The higher α/β ratio showed, when the Si306 is added, especially at higher concentrations, determines a more linear cell survival as reasonably expected and demonstrates the molecule radiosensitivity role. Moreover, the shape variations at the origin of survival curves are linked with the DMF values. Other points

are evident for the relationship between the LQ parameters and survival curve. Si306 affects substantially the linear component (α), whereas the quadratic component (β) is slightly decreased at higher concentrations. These results can be interpreted according to the LQ model, in which the cell death is lead, in our case, to the greater accumulation of lethal lesions. The use of Si306, both at concentrations of 10 and 20 μM , combined with PT contributes to sensitize GBM cells to protons exposure with an increase in cell killing.

Table 4. Values of the α and β parameters estimated by fitting the cell survival to the linear-quadratic (LQ) model.

Treatment	α (Gy-1)	β (Gy-2)	α/β (Gy)
Proton	0.292 ± 0.036	0.010 ± 0.003	28.6
Proton + 10 μM Si306	0.322 ± 0.011	0.010 ± 0.003	32.2
Proton + 20 μM Si306	0.372 ± 0.018	0.004 ± 0.001	93.0

2.4. Gene Expression Profiles (GEP) Experiments

As a second aim of this work, here we have reported GEP data obtained applying a Two-Color cDNA Microarray-Based Gene Expression Analysis (Agilent technologies) on U87 cells exposed to PT, with or without 10 μM Si306 compound. Comparative differential gene-expression analysis revealed that multiple deregulated genes (DEG) were significantly altered, by 2-fold or greater according to the specific experimental configuration reported as follows.

In addition, as described by several authors and also by our group [35,36], we have studied GEP lists, using PubMatrix, a tool for multiplex literature mining, in order to confirm our assumptions and to test their involvement in selected queries, radiation related, to draw assumptions described in the “Discussion” section. In this way, lists of terms, such as gene names, were assigned to a genetic, biological, or clinical relevance in a flexible systematic fashion in order to confirm our hypothesis, highlighting the involvement of known and lesser known genes able to drive cell radiation responses (Table S1).

2.4.1. GEP Induced by Proton Irradiation in U87 Glioblastoma Cells

Firstly, we analyzed the gene expression changes uniquely induced by protons irradiation with 2 and 10 Gy of IR doses. It should be remembered that 2 Gy is the daily dose delivered in fractionated RT treatments, so it is a dose of clinical interest, while 10 Gy represents a high dose of interest for comparisons with high-dose GEP studies of our research group [36].

In particular, U87 cell line treated with 2 Gy changed the expression levels of 936 genes (215 down regulated and 721 up regulated). On the other hand, 1018 DEGs were selected in U87 cells treated with 10 Gy and, among these, 251 were down regulated while 767 up regulated (Table 5).

Configuration	Number of Genes	Down	Up
U87 2 Gy versus U87 n.t	936	215	721
U87 10 Gy versus U87 n.t	1018	767	251
U87 +Si306 + 2 Gy versus U87 2 Gy	1419	563	856
U87 + Si306 + 10 Gy versus U87 10 Gy	969	353	616

Table 5. Number of genes significantly deregulated by 2-fold or greater in all the configuration modalities assayed in this work.

Deregulated transcripts obtained were grouped by using the DAVID tool [37,38] according to pathway analysis and the top-five molecular pathways selected are reported in Table 6. The analysis on DEGs induced by PT treatment with 2 Gy revealed the involvement of a set of factors controlling cellular processes, such as Hippo signaling pathway, cAMP signaling pathway, antigen processing and presentation, Wnt signaling pathway, and cell adhesion molecules (CAMs).

On the other hand, U87 glioblastoma cells exposed to 10 Gy of proton irradiation activate specific cell pathways as displayed in Table 6: PI3K-Akt signaling pathway, p53 signaling pathway, proteoglycans in cancer, Hippo signaling pathway, and cAMP signaling pathway. Finally, the GEP lists were analyzed by Venn diagrams in order to identify the overlapping deregulated genes (537 DEGs), between the two configurations of 2 and 10 Gy assayed (Figure 2A). Some genes were specifically deregulated following the dose provided, showing a dose-dependent transcriptional response. Moreover, cells respond to radiation treatment also in a common manner with activation of common genes and pathways, as displayed in Table 6 and listed as follows: Hippo signaling pathway; cAMP signaling pathway; proteoglycans in cancer; neuroactive ligand-receptor interaction; and antigen processing and presentation. Except for the neuroactive ligand-receptor interaction pathway, formed overall by molecules driving neuronal cell signaling, the involvement of these cellular processes in U87 cells proton exposed, has described above.

Table 6. Top-five statistically relevant pathways activated in U87 cells exposed to proton therapy (PT).

Table 6. Top-five statistically relevant pathways activated in U87 cells exposed to proton therapy (PT).

	Pathway Name	Genes Count	%	p Value	Genes
2 Gy	1 Hippo signaling pathway	19	0.016	0.000255	WNT5A, DVL3, WNT10A, NF2, FZD3, TCF7L2, LLLGL1, LATS2, TP73, DVL1, CTNNB1, PPP1CA, CCND3, CSNK1E, CCND2, DLG4, PARD6G, WNT6, BMP8B
	2 cAMP signaling pathway	18	0.015	0.012333	FXRD2, HCN2, VAV3, MAP2K2, GRIN1, GRIN2A, ATP1A4, VIPR2, ADORA1, AKT1, ATP2B2, PPP1CA, GRIN2D, ABCC4, CALML6, HCN4, PIK3R3, HTR1D
	3 Antigen processing and presentation	9	0.007	0.026474	CIITA, KLRC2, HLA-A, NFYC, HLA-C, HSPA1A, HLA-B, CTSB, HLA-E
	4 Wnt signaling pathway	13	0.011	0.029905	WNT5A, WNT10A, DVL3, FZD3, TCF7L2, DVL1, CTNNB1, SFRP1, CCND3, CSNK1E, CCND2, NFATC2, WNT6
	5 Cell adhesion molecules (CAMs)	13	0.011	0.036193	PVR, LRRC4, ITGAL, CD276, HLA-A, HLA-C, HLA-B, HLA-E, SDC4, NRCAM, SDC1, ITGB8, CLDN1
10 Gy	1 PI3K-Akt signaling pathway	31	0.025	0.000968	CSH1, PHLPP1, FGF7, PGF, KITLG, RPS6KB2, BCL2L1, GNG8, AKT1, COL6A5, COL6A3, TEK, COL6A2, COL6A1, PRKAA2, INSR, GHR, AKT2, FN1, TNXB, PKN2, HSP90B1, CDKN1A, EIF4E, CCND3, GNB2, CCND2, ITGA5, VEGFA, MDM2, LAMC2
	2 p53 signaling pathway	11	0.008	0.001175	PPM1D, CDKN1A, CCND3, CCND2, BBC3, BAX, MDM2, FAS, GADD45B, SESN1, TP73
	3 Proteoglycans in cancer	21	0.017	0.001320	ERBB2, RPS6KB2, IGF2, FLNC, FLNA, PXN, CTNNB1, AKT1, WNT7B, SDC1, PPP1CA, CDKN1A, MAPK12, ITGA5, VEGFA, MDM2, FAS, MSN, WNT6, FN1, AKT2, NF2, TEAD1, TCF7L2, LATS2, TP73, DVL1, CTNNB1, WNT7B, PPP1CA, CCND3, BBC3, CCND2, PARD6G, WNT6, BMP8B
	4 Hippo signaling pathway	15	0.012	0.012836	FXRD2, HCN2, VAV3, GRIN1, HTR4, ATP1A4, VIPR2, ADORA1, AKT1, ATP2B2, FOS, PPP1CA, SSTR1, GRIN2D, HTR6, ABCC4, HCN4, AKT2
	5 cAMP signaling pathway	18	0.014	0.013410	PPP1CA, CCND3, NF2, CCND2, PARD6G, WNT6, TCF7L2, BMP8B, LATS2, TP73, CTNNB1, DVL1
Common between 2 and 10 Gy	1 Hippo signaling pathway	12	0.018	0.001636	HCN2, FXRD2, VAV3, GRIN1, ATP1A4, VIPR2, ADORA1, AKT1, ATP2B2, PPP1CA, GRIN2D, ABCC4, HCN4
	2 cAMP signaling pathway	13	0.019	0.004726	AKT1, PPP1CA, SDC1, MAPK12, ERBB2, IGF2, MSN, FLNC, WNT6, FLNA, PXN, CTNNB1
	3 Proteoglycans in cancer	12	0.018	0.013466	CSH1, PRLHR, GRIN1, DRD4, ADORA1, VIPR2, NTSR2, CRHR2, CHRM3, GALR3, GRIN2D, GALR2, UTS2R, CHRNA1
	4 Neuroactive ligand-receptor interaction	14	0.021	0.025160	NFYC, HLA-C, HSPA1A, HLA-B, CTSB, HLA-E
	5 Antigen processing and presentation	6	0.009	0.044750	

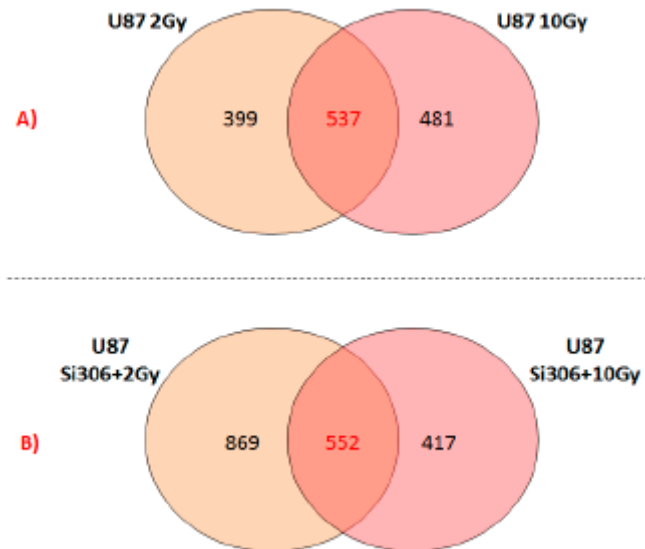


Figure 2. Venn diagrams showing the number of unique and shared differentially expressed genes after exposure to: (A) PT and (B) Si306 + PT combined treatments

2.4.2. GEP Induced by Si306 and Proton Combined Treatments in U87 Glioblastoma Cells

In a second step, we have evaluated the effect on GEPs after a combined administration of 10 μ M Si306 compound and PT using the doses of 2 and 10 Gy, hereafter named as follows: U87 Si306 + 2 Gy and U87 Si306 + 10 Gy, which were analyzed in comparison to the respective samples treated with PT alone (U87 2 Gy and U87 10 Gy). We selected a large amount of deregulated genes, caused by the Si306 compound addition to PT treatment: 1419 DEGs (563 down and 856 up regulated) in U87 Si306 + 2 Gy, while 969 DEGs (353 down and 616 up regulated) changed their expression levels in U87 Si306 + 10 Gy (Table 5). Thus, also for these experimental configurations, up and down regulated transcripts were grouped according to their involvement in specific biological pathways using DAVID tool [38]. The top-five statistically relevant molecular pathways of deregulated gene datasets are reported in Table 7. In particular, the Si306 + 2 Gy combined treatments deregulated the expression levels of genes controlling: Phagosome, antigen processing and presentation, cell adhesion molecules, inflammatory disease, and calcium signaling pathway.

Some of the above described pathways were also deregulated in U87 cells exposed to Si306 + 10 Gy and following reported and listed in Table 7: Proteoglycans in cancer, leukocyte transendothelial migration, phagosome, cell adhesion molecules, and autoimmune disease. Three out of the five pathways selected in U87 Si306 + 10 Gy (proteoglycans in cancer, phagosome, and cell adhesion molecules), were also deregulated in the other configurations analyzed, underling once again their interesting role in U87 cells response to radiation and/or to the Si306 molecule.

Finally, the Venn diagram shown in Figure 2B displays 552 deregulated common genes between the two configurations: U87 Si306 + 2 Gy and U87 Si306 + 10 Gy. The top-five statistically relevant pathways selected by DAVID tool using the 552 common gene list, are displayed in Table 7, and following listed: Autoimmune disease, antigen processing and presentation, proteoglycans in cancer, apoptosis, and inflammatory bowel disease.

Table 7. Top-five Statistically relevant pathways activated in U87 cells pretreated with Si306 and exposed to PT.

	Pathway Name	Genes Count	%	p Value	Genes
2 Gy	1 Phagosome	23	0.013	0.00014	HLA-DQB1, NOS1, HLA-DRB1, MRC2, HLA-A, HLA-C, HLA-B, ITGB3, SFTPA1, HLA-E, CLEC4M, FCAR, CD209, COMP, TUBAL3, HLA-DPA1, SCARB1, HLA-DPB1, HLA-DOA, TUBB1, ATP6V0D2, TUBB4A, HLA-DRA
	2 Antigen processing and presentation	15	0.009	0.00017	CIITA, HLA-DQB1, HLA-DRB1, HLA-A, HLA-C, HSPA1A, HLA-B, HLA-E, CD74, KIR3DL3, HSPA6, HLA-DPA1, HLA-DPB1, HLA-DOA, HLA-DRA
	3 Cell adhesion molecules (CAMs)	21	0.012	0.00036	PVR, HLA-DQB1, HLA-DRB1, SELL, CLDN5, HLA-A, NLGN1, CTLA4, HLA-C, HLA-B, HLA-E, CLDN15, ALCAM, NCAM2, SDC1, CD2, MADCAM1, HLA-DPA1, HLA-DPB1, HLA-DOA, HLA-DRA
	4 Inflammatory bowel disease (IBD)	13	0.007	0.00041	HLA-DQB1, HLA-DRB1, TBX21, RORC, STAT1, STAT3, IL12RB2, IL17A, IL1B, HLA-DPA1, HLA-DPB1, HLA-DOA, HLA-DRA
	5 Calcium signaling pathway	19	0.011	0.02473	ORAI2, PTGER1, NOS1, ERBB4, TNNC1, ERBB3, ERBB2, STIM2, OXTR, EDNRA, ATP2B2, P2RX1, CHR3M3, LTB4R2, GRPR, CHRNA7, CALML6, PLCB2, CACNA1B
10 Gy	1 Proteoglycans in cancer	22	0.019	0.000094	NANOG, ERBB4, ROCK2, HCLS1, ERBB2, FASLG, IGF2, FZD3, HGF, DCN, ITGB3, MMP2, PXXN, KDR, CTNND1, SMO, MAPK13, HPSE, PLCG2, HSPB2, PRKACA, TWIST1
	2 Leukocyte transendothelial migration	12	0.010	0.01064	ITGAL, ROCK2, MAPK13, PLCG2, CLDN5, CTNND1, MYLPP, RAPGEF3, JAM2, MMP2, PXXN, CTNND1
	3 Phagosome	14	0.012	0.01214	HLA-DQB1, HLA-DRB1, SFTPA1, ITGB3, COLEC11, TUBA8, CD36, FCGR2B, PIKFYVE, TUBAL3, HLA-DPA1, HLA-DPB1, TUBB1, TUBB4A
	4 Cell adhesion molecules (CAMs)	12	0.010	0.03671	HLA-DQB1, NRCAM, ITGAL, HLA-DRB1, CLDN5, NLGN1, CTLA4, HLA-DPA1, HLA-DPB1, JAM2, SELE, PDCD1LG2
	5 Autoimmune disease	6	0.005	0.06648	HLA-DQB1, HLA-DRB1, CTLA4, FASLG, HLA-DPA1, HLA-DPB1
Common between 2 and 10 Gy	1 Autoimmune disease	6	0.009	0.00768	HLA-DQB1, HLA-DRB1, CTLA4, FASLG, HLA-DPA1, HLA-DPB1
	2 Antigen processing and presentation	6	0.009	0.03468	HLA-DQB1, HLA-DRB1, KIR3DL3, HLA-DPA1, HLA-DPB1, CD74
	3 Proteoglycans in cancer	10	0.015	0.04961	ERBB4, MAPK13, ERBB2, FASLG, FZD3, HGF, ITGB3, MMP2, KDR, TWIST1
	4 Apoptosis	5	0.007	0.06011	DFFB, CYCS, CASP8, FASLG, IL3RA
	5 Inflammatory bowel disease (IBD)	5	0.007	0.06604	HLA-DQB1, HLA-DRB1, TBX21, HLA-DPA1, HLA-DPB1

3. Discussion

The first purpose of this study was to evaluate the radiosensitizing effects mediated by combination of the new compound, the Si306 targeting SRC proteins, with PT on the U87 human glioblastoma cell line. The IC50 evaluation showed that this cell line is sensitive to treatment with the Si306 compound. Based on the IC50 values, we tested the radiosensitizing effect of Si306, used at concentrations of 10 and 20 μ M, in combination with proton irradiation at increasing doses of 1,2, 3, 4, 10, and 21 Gy, in order to generate dose/response curves for the dose configurations tested.

The radiosensitizing effect was evaluated by calculating the DMF, obtained at the SF of 50%, in order to highlight the combined treatment capacity of enhancing tumor cells killing in respect of irradiation only [39]. Our data show that pretreatment with Si306 at both concentrations leads to a synergic cytotoxic effect with PT on the U87 cell line, further suggesting this compound as a new possible candidate to treat GBM in combination with PT. Indeed, the possibility to use drug/IR combined treatments, permits to increase the tumor control probability (TCP) even for radioresistant tumors, such as GBM. In addition, we also analyzed the U87 cell radiosensitivity by applying the radiobiological LQ model calculating the α , β parameters, and α/β ratio, which predict the radiosensitivity of normal and tumor cells [32]. The LQ model is considered to be the best-fitting model to describe cell survival and, therefore, is of great interest in radiation oncology to highlight the link existing between the α/β ratio and the following RT-induced tissue reactions [34,40,41]. The α/β ratio obtained on U87 cell line is in line with the α/β ratio calculated for a population of glioma cells

reported by Barazzuol et al., who used a mathematical model to extract radiobiological information from clinical GBM patients data [42]. In addition, our results showed a higher α/β ratio by using combined treatments of Si306 and protons. Therefore, we speculate that the clinical effect of using combined treatments of PT/Si306 administration, with an optimized Si306 pharmacological quantity for the patients, could be translated into the possibility of modifying the PT schedule treatment. Thus, all of this gains an efficacy in TCP, by using a more tolerable fractionated PT treatment plan and a reduced total dose delivered to the tumor [43,44].

As a second aim of this work, we carried out a transcriptomic study in order to define gene signatures as biomarkers of treatment response. GEP by whole genome cDNA microarray was firstly performed to analyze the gene expression changes uniquely induced by proton irradiation with 2 and 10 Gy of IR doses, which represent two clinical doses of interest and also for comparison with high-dose GEP studies of our research group [23,24,36,45].

In particular, the treatment of U87 with 2 Gy revealed that a large number of genes were deregulated and involved in the regulation of specific cellular processes (Table 6). One of the activated pathways was the Hippo signaling pathway, an emerging growth control and tumor suppressor pathway that regulates cell proliferation and stem cell functions; the hyperactivation of its downstream effectors (such as TAZ protein, up regulated in U87 2 Gy with a fold change of 1.89) contributes to the development of cancer including GBM, suggesting that pharmacological inhibition of these factors may be an effective anticancer strategy [46,47]. In turn, in GBM cells Yang et al. recently reported that the Hippo transducer TAZ promotes cell proliferation and tumor formation through the EGFR pathway [48]. In addition, Hippo and Wnt signaling, up regulated in U87 2 Gy cells, reciprocally regulate each other's activity through a variety of mechanisms that needs to be better clarified in GBM cells [49]. As known, Wnt/ β -catenin signaling plays important roles in maintaining the stemness of cancer stem cells in various cancer types and in promoting cellular invasiveness. Multimodality in vivo and in vitro studies revealed a key role of Wnt activation in GBM radiation resistance. In turn, literature data report a pivotal role of the Wnt/ β -catenin signaling pathway in IR-induced invasion of U87 GBM cells, indicating that β -catenin is a potential therapeutic target for overcoming evasive radioresistance [50,51].

In U87 2 Gy the involvement of cAMP signaling pathway was also observed. Existing evidence suggests that intracellular cAMP level and signaling may affect the survival of cancer cells, including resistant cancer cells to standard chemotherapeutic drugs. Suppression of the cAMP pathway is a common feature across different cancers including GBM. [52,53]. In addition, IR is known to be able to activate the transcription of genes, through the presence of cAMP responsive elements (CREs) in their promoters, in order to guide cell response and survival after radiation exposure [54].

Moreover, the activation of antigen processing and presentation pathway after proton exposure with dose of 2 Gy in GBM cells is sustained by an up regulation of genes belonging to the human leukocyte antigen (HLA) class family (probably activated by β -catenin), factors involved in antigen presentation. As reported by Ghosh et al., HLA genes increasing level, often caused by a hypoxic tumor microenvironment, is associated with evasion of immune responses in cancer cells [55]. Finally, an overall activation of several cell adhesion molecules was highlighted in U87 2 Gy cells, involved in the activation of inflammation process and in the regulation of cancer invasiveness.

On the other hand, U87 cells exposed to 10 Gy of proton irradiation activate specific cell pathways, including the phosphatidylinositol-3-kinase (PI3K)-protein kinase B (Akt) signaling pathway (Table 6). As known, the PI3K/AKT pathway is commonly activated in cancer initiation and progression, including GBM, as it regulates different processes, such as proliferation, apoptosis, and migration [56], therefore representing a key target for cancer therapeutics. Moreover, the activation of TP53 pathway was observed in U87 10 Gy and driven by TP53 gene that was significantly altered by 1.77-fold. As described, TP53, exerts a crucial role following IR-induced DNA damage because it

is able to cause cell cycle arrest, DNA repair, and apoptosis processes. Moreover, the influence of TP53 status on DNA damage repair after cell irradiation has been studied in several malignancies and also reported by our group in breast cancer cells after a high dose of electron irradiation [45,57]. Finally, in U87 10 Gy, an activation of proteoglycan signaling was observed. Proteoglycans are known to have many roles in tumor progression and are the main extracellular matrix (ECM) components of normal brain tissue, playing an

important role in brain development; an overproduction of different molecules of this family were found in GBM cells [58,59].

Interestingly, in U87 10 Gy Hippo and cAMP signaling pathways were activated, as above described in U87 2 Gy configuration, underling once again the important role of these processes in GBM cells after proton exposure.

In a second step, we evaluated the GEPs induced by Si306 molecule in U87 cells irradiated with 2 and 10 Gy of proton doses and we selected a large number of deregulated genes, grouped according to their involvement in specific biological pathways (Table 7). In particular, in U87 Si306 + 2 Gy combined treatments a deregulated expression level of genes controlling phagosome was observed.

In GBM an intensive autophagic activity regulated by several signaling pathways was described [60]. As recently reported by Yasui et al., an altered autophagic flux was described in GBM cell lines exposed to 10 Gy of γ -rays. Our data also confirms this trend after proton exposure. These altered fluxes represent a useful biomarker of metabolic stress induced by IR and provide a metabolic context for radiation sensitization [61]. Here the Si306 radiosensitization effect seems to act by stressing this molecular mechanism. In addition, in U87 Si306 + 2 Gy configuration the involvement of antigen processing and presentation and cell adhesion molecules pathways were observed, similarly to that shown in U87 cells proton treated with only 2 Gy. Therefore, the Si306 treatment seems to cause an overall down regulation of HLA molecules (up regulated in U87 2 Gy), suggesting the activation of immune surveillance escaping mechanism induced by Si306 [55,62].

The latest two pathways deregulated in U87 Si306 + 2 Gy were linked to inflammation and calcium signaling. As known, the inflammation process is often activated in cell exposed to radiation, affecting cell fate by the activation of key transcription factors (TFs), such as NF-KB and STATs (i.e., STAT1 and STAT3) [63]. Interestingly, the combined Si306 + 2 Gy treatment induced a down regulation of STAT1 and STAT3 proteins. Thus, we speculate that this inhibition could promote radiation sensitivity decreasing angiogenesis and cell survival as hypothesized in other malignancies by several authors [64,65]. Indeed, a number of studies confirm that selective inhibitors of these proinflammatory pathways driven by STAT TFs, could be combined to conventional radiation or chemotherapy to increase their effectiveness [66,67].

On the other hand, the combined treatment with Si306 and 2 Gy PT seem to affect survival/death balance by modulating the intracellular calcium levels, a mechanism known to be involved in regulating IR-induced cell cycle arrest, apoptosis, and chromatin structure modifications [45,68,69].

Some of these pathways were also deregulated in U87 cells exposed to Si306 + 10 Gy, such as: Proteoglycans in cancer, leukocyte transendothelial migration, phagosome, cell adhesion molecules, and autoimmune disease. Three of the five pathways (proteoglycans in cancer, phagosome, and cell adhesion molecules), were also deregulated in the other configurations analyzed, suggesting once again their important role in U87 cells in response to radiation and/or to Si306 molecule. The other two selected pathways in U87 Si306 + 10 Gy (i.e., leukocyte transendothelial migration and autoimmune disease), highlight the involvement of a complex immunological response induced by IR, as known from the literature, and by the Si306 compound addition, as observed in this study.

Finally, we reported the number of overlapping deregulated genes between the two configurations of the combined treatments, such as U87 Si306 + 2 Gy and U87 Si306 + 10 Gy (Figure 2B). The top-five statistically relevant pathways selected and displayed in Table 7, were previously described.

Summarizing, our GEP results show that combined treatments on U87 cells can activate multiple signal transduction pathways described, to our knowledge, for the first time, to be new targets of Si306. Finally, considering that the main target of Si306 is the tyrosine kinase SRC, we analyzed the known cellular target downstream to this transducer, in order to better clarify its role as molecular radiosensitizing. Thus, we observed that the combined treatment Si306 + protons (with 2 and 10 Gy) in U87 cells, is able to inhibit several signal transduction pathways, normally regulated by SRC as shown in Figure 3.

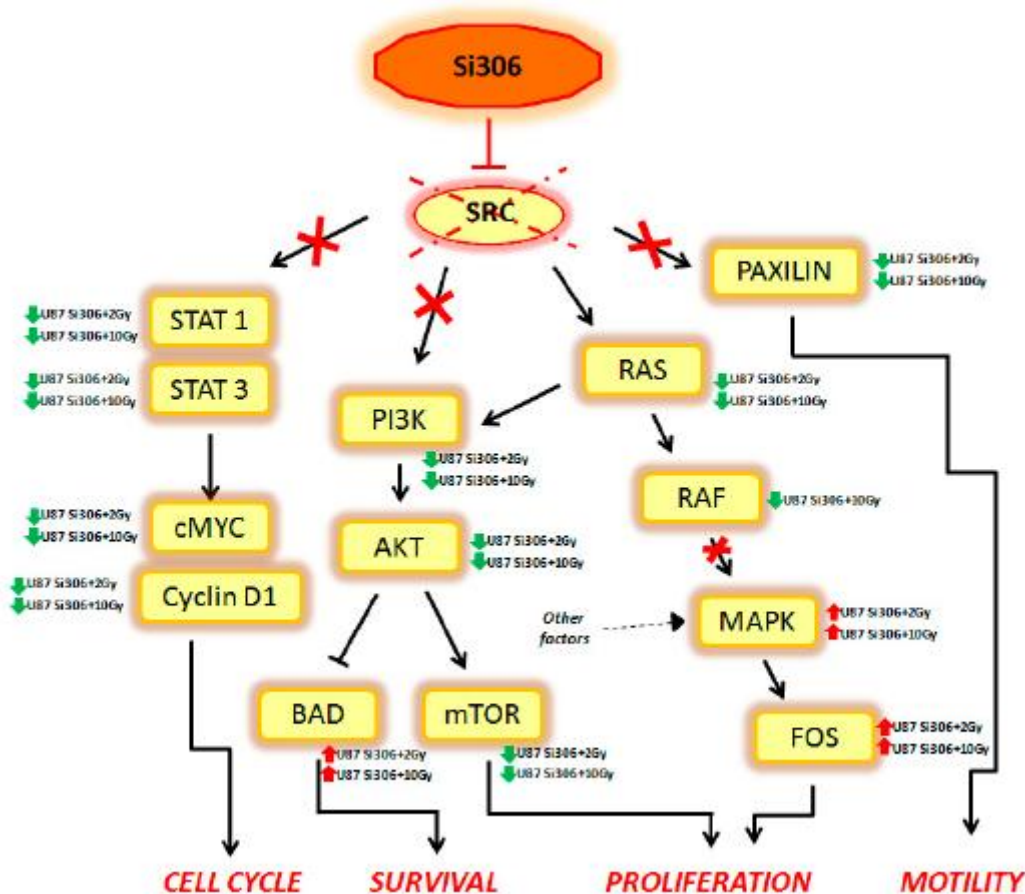


Figure 3. The figure displays the main targets of Si306 compound observed. The arrows define an activation and the T bars the inhibition. Red arrows define gene upregulation and green arrows gene downregulation.

In particular, the STAT1, STAT3, c-MYC, and Cyclin D1 genes, which are able to control the cell cycle, were downregulated in our analysis. Cell survival was negatively regulated by the downstream PI3K, AKT, and mTOR downregulation and by the BAD upregulation. In addition, Si306 is able to cause a partial inhibition of cell proliferation, downregulating RAS and RAF gene expression. However, the MAPK and FOS genes were not targets of Si306, so these factors (up regulated in our data), were probably activated by other cellular pathways. Finally, Si306 is also able to negatively regulate cell motility, through the downregulation of the paxilin gene.

These data confirm the SRC role as a main target of Si306 compound and highlight the transcriptional events occurring downstream of SRC inhibition by the combined treatments. The SRC blockage observed after Si306 and PT combined treatments seems to increase the single treatments effectiveness, thus promoting a radiosensitizing effect.

Today, very little data is available regarding the combination of molecularly targeted drugs and PT. Indeed, many studies debate about chemotherapeutic agents combined with high-linear energy transfer (LET) particle beams or protons for GBM treatment, overlooking the clinical perspective of target therapy [70,71].

The results obtained from this work have highlighted the radiosensitizing capacity of the Si306 targeted compound on U87 GBM cell line, acting in tandem with PT. Taking into account previously in vivo pharmacokinetic data, demonstrating that Si306 was able to reach the brain, overcoming the hurdle represented by the blood–brain barrier [31], this compound can be considered a new candidate for combined treatments of GBM. In addition, our GEP results confirm the important role of SRC as the main Si306 target and highlight new genes and pathways modulated by the combined action of Si306 and PT, which can be further explored as new radiosensitizing therapeutic targets in GBM.

4. Materials and Methods

4.1. Proton Irradiation Configuration and Cell Irradiation

The proton beam irradiation was performed at the CATANA (Centro di Adroterapia ed Applicazioni Nucleari Avanzate) facility of INFN-LNS (Catania, Italy) [72], using 62 MeV of proton beams accelerated by a cyclotron superconducting. The beamline is composed of several passive elements optimized for the clinical application: Scattering foils to spread the beam laterally, collimators to define beam profile in accordance to the tumor shape, and monitoring chambers to measure the dose delivered [73]. In order to irradiate the entire 25 cm² (T25) standard tissue culture flasks, a motorized system for biological samples irradiation was used. Radiochromic film detectors were adopted to check the delivered dose and the lateral dose distribution during each irradiation. The dosimetric system was calibrated under reference conditions according to the International Atomic Energy Agency Technical Reports Series No. 398 “Absorbed Dose Determination in External Beam Radiotherapy” [74].

For combined treatments with Si306, U87 irradiations were carried out using six dose values of 1, 2, 3, 4, 10, and 21 Gy. Cell irradiations were conducted placing the cell at the middle spread-out Bragg peak, to simulate a clinical condition, with a dose rate of 15 Gy/min.

4.2. Cell Culture and IC₅₀ Determination

In vitro experiments were carried out using the U87 MG human glioblastoma cell line. Cells were purchased from European Collection of Authenticated Cell Cultures (ECACC, Public Health England, Porton Down Salisbury, UK) and cultured as previously described [31]. Cells were maintained in an exponentially growing culture condition in an incubator at 37 °C in a humidified atmosphere (95% air and 5% CO₂) and were routinely sub-cultured in T25 standard tissue culture flasks.

To calculate IC₅₀ (drug concentration that determined the 50% of growth inhibition), 2.5 × 10⁴ U87 cells were plated in 12-well plates and incubated with Si306 dissolved in DMSO at increasing concentrations (0.1, 1.0, 10, and 100 μM) for 24, 48, and 72 h under normal cell culture conditions. Cell numbers and viability were evaluated using Z2 Coulter Counter (Beckman Coulter, Indianapolis, United States). IC₅₀ was calculated by GraphPad Prism 6.0 software (GraphPad Software, San Diego, CA, USA) using the best fitting sigmoid curve.

4.3. Clonogenic Survival Assay

Forty-eight hours before irradiations U87 cells were seeded in T25 flasks and the day after were incubated with the concentrations of 10 and 20 μM of Si306, chosen on the base of IC₅₀ results, for 24 h prior to radiation treatment. Cells were irradiated at subconfluence. Combined effects of Si306 and protons were evaluated by clonogenic survival assay, performed as previously described [45,57]. Briefly, after irradiation, U87 cells were detached, counted by hemocytometer and seeded into a sixwell plate in triplicate at a density of 50–2000 cells per well, by plating an increasing cell quantity according to the dose delivered raising, in order to assay the SF. Colonies were allowed to grow under normal cell culture conditions for two weeks and then were fixed with 50% methanol and stained 0.5% crystal violet (both from Sigma-Aldrich, St. Louis, MO, USA). Colonies with more than 50 cells were counted manually under Olympus CK30 phase-contrast microscope (Olympus, Tokyo, Japan) and also automatically with a computer-assisted methodology [75]. The calculation of SFs in U87 cells irradiated with protons and pre-treated with Si306 were determined taking into consideration the plating efficiency (PE) for all treatment modalities based on three independent experiments.

4.4. The Linear-Quadratic Model

The linear-quadratic model, introduced by Kellerer and Rossi in the 1970s [32], is the most widely used model in RT, in which a lethal event is supposed to be caused by one hit due to one particle track (the linear component αD) or two particle tracks (the quadratic component β^2).

The clonogenic survival data were analyzed by means of non-linear regression, which utilizes a multi-parameter equation for curves, whose form is: $S(D)/S(0) = e^{-\alpha D - \beta D^2}$, so we get α [Gy⁻¹] e β [Gy⁻²] with their own standard deviation.

4.5. Dose Modifying Factor Calculation

The parameter dose modifying factor was calculated in order to evaluate synergistic effect of protons combined with Si306 compound. This value, as the best measure of treatment effectiveness, was calculated at the SF of 50% and represents the relative dose of irradiation required to obtain the isoeffect of SF = 0.5 with radiation treatment alone in respect of combined treatments with a defined concentration of Si306 [39].

The SF data versus dose were plotted with the reported quadratic equation: $y = a + bx + cx^2$ where y is $\ln(SF)$ and x is the dose, considering the positive solution. The experimental samples (pretreated with 10 or 20 μ M of Si306 and proton irradiated) were normalized to coefficient a of the previous equation in order to start the survival curves from the same origin. The results were achieved with the software OriginPro 8.

The SF values take into account two errors: The first was derived from the equation $y = a + bx + cx^2$ and was calculated using error propagation; the second was derived from ratio normalization, but negligible compared to first one.

4.6. Whole Genome cDNA Microarray Expression Analysis

To study molecular pathways and cell networks activated at transcriptional level in U87 cells exposed to PT, with or without Si306 compound, we performed gene expression experiments by cDNA microarray. In particular, in this work we analyzed GEP of the following configurations: (i) U87 2 Gy versus U87 untreated cells; (ii) U87 10 Gy versus U87 untreated cells; (iii) U87 2 Gy + 10 Mm Si306 versus U87 2 Gy; and iv) U87 10 Gy + 10 μ M Si306 versus U87 10 Gy.

RNA extraction and analyses were performed as previously described [45,57]. Microarray experiments conducted by using the protocol Two-Color Microarray-Based Gene Expression Analysis (Agilent Technologies, Santa Clara, CA, USA), statistical analyzes carried out with GeneSpring GX 10.0.2 software (Agilent Technologies), and pathway analysis conducted by using DAVID database, were performed as previously described [76].

The data showed in this work were deposited in the Gene Expression Omnibus (GEO) database (NCBI) [38] and are available by using the GEO Series accession number: GSE127989.

5. Conclusions

The data here described, supported by DMF calculation and LQ model analyses, indicate that a new compound, the Si306 targeting SRC protein, exerts a radiosensitizing action on the U87 MG cell line causing a synergic cytotoxic effect when combined with PT. This compound can be considered a new possible candidate to treat GBM in combination with PT. In addition, we provide for the first time a description of GEPs induced by Si306 and PT combined treatments, highlighting the modulated cellular networks and confirming the important role of SRC as the main target of the compound. Taking together our encouraging data suggest the use of Si306 compound in targeted therapies in tandem with PT, to obtain a more successful treatment modality in GBM disease.

Supplementary Materials: Supplementary materials can be found at www.mdpi.com/xxx/s1.

Author Contributions: All authors participated in the conception, design, interpretation, and elaboration of the findings of the study, as well as in drafting and revising the final version. In particular, G.R., P.P., G.S., G.A.P.C. and G.P. studied the irradiation setup, simulations and dose distribution. F.P.C., F.T., M.C. and L.M. (Luigi Minafra), performed cell irradiations. F.P.C., L.M. (Luigi Minafra), G.I.F. and F.T. maintained cell cultures and carried out cell survival experiments. L.M. (Laura Maccari), A.L.F., and S.S. carried out the Si306 synthesis and IC50 determination. P.P. and G.S. performed DMF and LQ model analysis. V.B. performed whole-genome cDNA microarray experiments and gene expression profile network analyses. M.B, G.C., R.P., G.R. participated in the elaboration of the findings of the study, drafting and revising the final version. All authors read and approved the final content of the manuscript.

Funding: This work was partially supported by the National Institute for Nuclear Physics (INFN) Commissione Scientifica Nazionale 5 (CSN5) Call ‘MoVe-IT’.

Acknowledgments: The authors of this paper wish to pay their gratitude and respect to their colleague and coauthor M. Botta who passed away in August 2019. He was a dedicated Professor with a deep passion for science and research. He guided the discovery and the development of Si306, and contributed to the results showed in this paper.

Conflicts of Interest: The authors declare no conflict of interest. The funders had no role in the design of the study; in the collection, analyses, or interpretation of data; in the writing of the manuscript, or in the decision to publish the results

References

1. Hanif, F.; Muzaffar, K.; Perveen, K.; Malhi, S.M.; Simjee, S.U. Glioblastoma multiforme: A review of its epidemiology and pathogenesis through clinical presentation and treatment. *Asian Pac. J. Cancer Prev.* **2017**, *18*, 3–9.
2. Louis, D.N.; Perry, A.; Reifenberger, G.; Von Deimling, A.; Figarella-Branger, D.; Cavenee, W.K.; Ellison, D.W.; Ohgaki, H.; Wiestler, O.D.; Kleihues, P. The 2016 World Health Organization classification of tumors of the central nervous system: A summary. *Acta Neuropathol.* **2016**, *6*, 803–820.
3. Urbańska, K.; Sokołowska, J.; Szmidt, M.; Sysa, P. Glioblastoma multiforme—An overview. *Contemp. Oncol.* **2014**, *18*, 307–312.
4. Khosla, D. Concurrent therapy to enhance radiotherapeutic outcomes in glioblastoma. *Ann. Transl. Med.* **2016**, *4*, 54.
5. Cabrera, A.R.; Kirkpatrick, J.P.; Fiveash, J.B.; Shih, H.A.; Koay, E.J.; Lutz, S.; Reardon, D.A.; Petit, J.; Chao, S.T.; Brown, P.D.; et al. Radiation therapy for glioblastoma: An astro evidence-based clinical practice guideline. *Pract. Radiat. Oncol.* **2016**, *6*, 217–225.
6. Stupp, R.; Mason, W.P.; van den Bent, M.J.; Weller, M.; Fisher, B.; Taphoorn, M.J.; Belanger, K.; Brandes, A.A.; Marosi, C.; et al. Radiotherapy plus concomitant and adjuvant temozolomide for glioblastoma. *N. Engl. J. Med.* **2005**, *352*, 987–996.
7. Sherriff, J.; Tamangani, J.; Senthil, L.; Cruickshank, G.; Spooner, D.; Jones, B.; Brookes, C.; Sanghera, P. Patterns of relapse in glioblastoma multiforme following concomitant chemoradiotherapy with temozolomide. *Br. J. Radiol.* **2013**, *86*, 20120414.
8. Lee, S.Y. Temozolomide resistance in glioblastoma multiforme. *Genes Dis.* **2016**, *3*, 198–210.
9. Rivera, A.L.; Pelloski, C.E.; Gilbert, M.R.; Colman, H.; De La Cruz, C.; Sulman, E.P.; Aldape, K.D.; Bekele, B.N. MGMT promoter methylation is predictive of response to radiotherapy and prognostic in the absence of adjuvant alkylating chemotherapy for glioblastoma. *Neuro-oncology* **2010**, *12*, 116–121.
10. Fitzek, M.M.; Thornton, A.F.; Rabinov, J.D.; Lev, M.H.; Pardo, F.S.; Munzenrider, J.E.; Hedley-Whyte, E.T.; Okunieff, P.; Braun, I.; Hochberg, F.H.; et al. Accelerated fractionated proton/photon irradiation to 90

cobalt gray equivalent for glioblastoma multiforme: Results of a phase II prospective trial. *J. Neurosurg.* **1999**, *91*, 251–260.

11. Mizumoto, M.; Tsuboi, K.; Igaki, H.; Yamamoto, T.; Takano, S.; Oshiro, Y.; Sugahara, S.; Hayashi, U.; Hashii,

H.; Kanemoto, A.; et al. Phase I/II trial of hyperfractionated concomitant boost proton Radiotherapy for supratentorial glioblastoma multiforme. *Int. J. Radiat. Oncol. Biol. Phys.* **2010**, *77*, 98–105.

12. Mizumoto, M.; Yamamoto, T.; Ishikawa, E.; Matsuda, M.; Takano, S.; Ishikawa, H.; Tsuboi, K.; Okmura, T.; Sakurai, H.; Matsumura, A. Proton beam therapy with concurrent chemotherapy for glioblastoma multiforme: Comparison of nimustine hydrochloride and temozolomide. *J. Neurooncol.* **2016**, *130*, 165–170.

13. Matsuda, M.; Kohzuki, H.; Ishikawa, E.; Yamamoto, T.; Akutsu, H.; Takano, S.; Matsumura, A.; Mizumoto, M.; Tsuboi, K. Prognostic analysis of patients who underwent gross total resection of newly diagnosed glioblastoma. *J. Clin. Neurosci.* **2018**, *50*, 172–176.

14. Petr, J.; Platzek, I.; Hofheinz, F.; Mutsaerts, H.J.; Asllani, I.; van Osch, M.J.; Jentsch, C.; Maus, J.; Troost, E.G.C.; Baumann, M.; et al. Effects on brain tissue volume and perfusion. *Radiother. Oncol.* **2018**, *128*, 121–127.

15. Baumann, M.; Krause, M.; Overgaard, J.; Debus, J.; Bentzen, S.M.; Daartz, J.; Bortfeld, T.; Richter, C.; Zips, D. Radiation oncology in the era of precision medicine. *Nat. Rev. Cancer* **2016**, *16*, 234.

17. Combs, S.; Schmid, T.; Vaupel, P.; Multhoff, G. Stress response leading to resistance in glioblastoma-The need for innovative radiotherapy (iRT) Concepts. *Cancers* **2016**, *8*, doi:10.3390/cancers8010015.

18. Tsuboi, K. Advantages and Limitations in the Use of Combination Therapies with Charged Particle Radiation Therapy. *Int. J. Part. Ther.* **2018**, *5*, 122–132.

19. Hirst, D.G.; Robson, T. Molecular biology: The key to personalised treatment in radiation oncology? *Br. J. Radiol.* **2010**, *83*, 723–728.

20. Dalton, W.S.; Friend, S.H. Cancer biomarkers – An invitation to the table. *Science* **2006**, *312*, 1165–1168.

21. Speers, C.; Pierce, L.J. Molecular signatures of radiation response in breast cancer: Towards personalized decision-making in radiation treatment. *Int. J. Breast Cancer.* **2017**, *2017*, 4279724.

22. Meng, J.; Li, P.; Zhang, Q.; Yang, Z.; Fu, S. A radiosensitivity gene signature in predicting glioma prognostic via EMT pathway. *Oncotarget* **2014**, *5*, 4683–4693.

23. Bravatà, V.; Cammarata, F.P.; Minafra, L.; Pisciotta, P.; Scazzone, C.; Manti, L.; Savoca, G.; Petringa, G.; Cirrone, G.A.P.; Cuttone, G.; et al. Proton-irradiated breast cells: molecular points of view. *J. Radiat. Res.* **2019**, *60*, 451–465.

24. Minafra, L.; Bravatà, V.; Cammarata, F.P.; Russo, G.; Gilardi, M.C.; Forte, G.I. Radiation gene-expression signatures in primary breast cancer cells. *Anticancer Res.* **2018**, *38*, 2707–2715.

25. Bravatà, V.; Cava, C.; Minafra, L.; Cammarata, F.; Russo, G.; Gilardi, M.; Forte, G.; Castiglioni, I. Radiation-induced gene expression changes in high and low grade breast cancer cell types. *Int. J. Mol. Sci.* **2018**, *19*, 1084.

26. Yang, P.; Zhang, W.; Wang, Y.; Peng, X.; Chen, B.; Qiu, X.; Li, W.; Li, G.; Li, S.; Wu, C.; et al. IDH mutation and MGMT promoter methylation in glioblastoma: Results of a prospective registry. *Oncotarget* **2015**, *38*, 40896–40906, doi:10.18632/oncotarget.5683.

27. Szopa, W.; Burley, T.A.; Kramer-Marek, G.; Kaspera, W. Diagnostic and therapeutic biomarkers in glioblastoma: Current status and future perspectives. *BioMed Res. Int.* **2017**, *2017*, 8013575, doi:10.1155/2017/8013575.

28. Karsy, M.; Neil, J.A.; Guan, J.; Mahan, M.A.; Colman, H.; Jensen, R.L. A practical review of prognostic correlations of molecular biomarkers in glioblastoma. *Neurosurg. Focus* **2015**, *38*, E4, doi:10.3171/2015.1.

29. Sottili, M.; Gerini, C.; Desideri, I.; Loi, M.; Livi, L.; Mangoni, M. Tumor microenvironment, Hypoxia, and Stem Cell-Related Radiation Resistance. In *Radiobiology of Glioblastoma: Recent Advances and Related Pathobiology*; Current Clinical Pathology, 1st ed.; Springer: Berlin/Heidelberg, Germany, 2016; pp. 189–207.

30. Ahluwalia, M.; De Groot, J.; Liu, W.; Gladson, C.L. Targeting SRC in glioblastoma tumors and brain metastases: Rationale and preclinical studies. *Cancer Lett.* **2010**, *298*, 139–149.

31. Calgani, A.; Vignaroli, G.; Zamperini, C.; Coniglio, F.; Festuccia, C.; Di Cesare, E.; Botta, M.; Gravina, G.L.; Mattei, C.; Vitale, F.; et al. Suppression of SRC Signaling Is Effective in Reducing Synergy between Glioblastoma and Stromal Cells. *Mol. Cancer Ther.* **2016**, *15*, 1535–1544.

32. Chapman, J.D. Can the two mechanisms of tumor cell killing by radiation be exploited for therapeutic gain? *J. Radiat. Res.* **2014**, *55*, 2–9.
33. van Leeuwen, C.M.; Oei, A.L.; Crezee, J.; Bel, A.; Franken, N.A.P.; Stalpers, L.J.A.; Kok, H.P. The alfa and beta of tumours: A review of parameters of the linear-quadratic model, derived from clinical radiotherapy studies. *Radiat. Oncol.* **2018**, *13*, 96.
34. Bentzen, S.M.; Joiner, M.C. The linear-quadratic approach in clinical practice. *Basic Clin. Radiobiol.* **2009**, *4*, 120–134.
35. Becker, K.G.; Hosack, D.A.; Dennis, G., Jr.; Lempicki, R.A.; Bright, T.J.; Cheadle, C.; Engel, J. PubMatrix: A tool for multiplex literature mining. *BMC Bioinform.* **2003**, *4*, 61.
36. Bravatà, V.; Minafra, L.; Cammarata, F.P.; Pisciotta, P.; Lamia, D.; Marchese, V.; Petringa, G.; Manti, L.; Cirrone, G.A.; Gilardi, M.C.; et al. Gene expression profiling of breast cancer cell lines treated with proton and electron radiations. *Br. J. Radiol.* **2018**, *91*, 20170934.
37. Huang da, W.; Sherman, B.T.; Lempicki, R.A. Systematic and integrative analysis of large gene lists using DAVID bioinformatics resources. *Nat. Protoc.* **2009**, *4*, 44–57.
38. Barrett, T.; Wilhite, S.E.; Ledoux, P.; Evangelista, C.; Kim, I.F.; Tomashevsky, M.; Yefanov, A.; Marshall, K.A.; Phillippy, K.H.; Sherman, P.M.; et al. NCBI GEO: Archive for functional genomics data sets-update. *Nucleic Acids Res.* **2013**, *41*, D991–D995.
39. Medhora, M.; Gao, F.; Fish, B.L.; Jacobs, E.R.; Moulder, J.E.; Szabo, A. Dose-modifying factor for captopril for mitigation of radiation injury to normal lung. *J. Radiat. Res.* **2012**, *53*, 633–640.
40. Barendsen, G.W. Dose fractionation, dose rate and iso-effect relationships for normal tissue responses. *Int. J. Radiat. Oncol. Biol. Phys.* **1982**, *8*, 1981–1997.
41. Brenner, D.J.; Sachs, R.K.; Peters, L.J.; Withers, H.R.; Hall, E.J. We forget at our peril the lessons built into the α/β model. *Int. J. Radiat. Oncol. Biol. Phys.* **2012**, *82*, 1312–1314.
42. Barazzuol, L.; Burnet, N.G.; Jena, R.; Jones, B.; Jefferies, S.J.; Kirkby, N.F. A mathematical model of brain tumors response to radiotherapy and chemotherapy considering radiobiological aspects. *J. Theor. Biol.* **2010**, *262*, 553–565.
43. Nieder, C.; Baumann, M. *Re-Irradiation: New Frontiers, Medical Radiology*; Springer: Berlin/Heidelberg, Germany, 2011; pp. 13–24, doi:10.1007/174_2010_77.
44. Williams, M.V.; Denekamp, J.; Fowler, J.F. A review of a/b ratios for experimental tumours: Implications for clinical studies of altered fractionation. In *Basic Clinical Radiobiology*; Steel, G.G., Ed.; EdwardArnold: London, UK, 1985.
45. Bravata, V.; Minafra, L.; Russo, G.; Forte, G.I.; Cammarata, F.P.; Ripamonti, M.; Messa, C.; Casarino, C.; Augello, G.; Costantini, F.; et al. High dose ionizing radiation regulates gene expression changes in MCF7 breast cancer cell Line. *Anticancer Res.* **2015**, *35*, 2577–2591.
46. Johnson, R.; Halder, G. The two faces of Hippo: Targeting the Hippo pathway for regenerative medicine and cancer treatment. *Nat. Rev. Drug Discov.* **2014**, *13*, 63–79, doi:10.1038/nrd4161.
47. Orr, B.A.; Bai, H.; Odia, Y.; Jain, D.; Anders, R.A.; Eberhart, C.G. Yes-associated protein 1 is widely expressed in human brain tumors and promotes glioblastoma growth. *J. Neuropathol. Exp. Neurol.* **2011**, *70*, 568–577.
48. Yang, R.; Wu, Y.; Zou, J.; Zhou, J.; Wang, M.; Hao, X.; Cui, H. The Hippo transducer TAZ promotes cell proliferation and tumor formation of glioblastoma cells through EGFR pathway. *Oncotarget* **2016**, *24*, 36255–36265.
49. Bae, J.S.; Kim, S.M.; Lee, H. The Hippo signaling pathway provides novel anti-cancer drug targets. *Oncotarget* **2017**, *8*, 16084–16098.
50. Kim, S.; Jho, E.H. Merlin, a regulator of Hippo signaling, regulates Wnt/ β -catenin signaling. *BMB Rep.* **2016**, *49*, 357–358.
51. Dong, Z.; Zhou, L.; Han, N.; Zhang, M.; Lyu, X. Wnt/ β -catenin pathway involvement in ionizing radiation-induced invasion of U87 glioblastoma cells. *Strahlenther. Onkol.* **2015**, *191*, 672–680.
52. Wang, H.; Sun, T.; Hu, J.; Zhang, R.; Rao, Y.; Wang, S.; Bigner, D.D.; Chen, R.; McLendon, R.E.; Friedman, A.H.; et al. miR-33a promotes glioma-initiating cell self-renewal via PKA and NOTCH pathways. *J. Clin. Invest.* **2014**, *124*, 4489–4502.
53. Daniel, P.M.; Filiz, G.; Mantamadiotis, T. Sensitivity of GBM cells to cAMP agonist-mediated apoptosis correlates with CD44 expression and agonist resistance with MAPK signaling. *Cell Death Dis.* **2016**, *7*, e2494.

54. Meyer, R.G.; Küpper, J.H.; Kandolf, R.; Rodemann, H.P. Early growth response-1 gene (Egr-1) promoter induction by ionizing radiation in U87 malignant glioma cells in vitro. *Eur. J. Biochem.* **2002**, *269*, 337–346.
55. Ghosh, S.; Paul, A.; Sen, E. Tumor necrosis factor α -induced hypoxia-inducible factor 1 α - β -catenin axis regulates major histocompatibility complex class I gene activation through chromatin remodeling. *Mol. Cell Biol.* **2013**, *33*, 2718–2731.
56. Lino, M.M.; Merlo, A. PI3Kinase signaling in glioblastoma. *J. Neurooncol.* **2011**, *103*, 417–427, doi:10.1007/s11060-010-0442-z.
57. Minafra, L.; Bravata, V.; Russo, G.; Forte, G.I.; Cammarata, F.P.; Ripamonti, M.; Messa, C.; Candiano, G.; Cervello, M.; Giallongo, A.; et al. Gene expression profiling of MCF10A breast epithelial cells exposed to IOERT. *Anticancer Res.* **2015**, *35*, 3223–3234.
58. Iozzo, R.V.; Sanderson, R.D. Proteoglycans in cancer biology, tumour microenvironment and angiogenesis. *J. Cell Mol. Med.* **2011**, *15*, 1013–1031.
59. Kazanskaya, G.M.; Tsidulko, A.Y.; Volkov, A.M.; Kiselev, R.S.; Suhovskih, A.V.; Kobozev, V.V.; Grigorieva, E.V.; Gaytan, A.S.; Aidagulova, S.V.; et al. Heparan sulfate accumulation and perlecan/HSPG2 upregulation in tumour tissue predict low relapse-free survival for patients with glioblastoma. *Histochem. Cell Biol.* **2018**, *149*, 235–244.
60. Giatromanolaki, A.; Sivridis, E.; Mitrakas, A.; Kalamida, D.; Zois, C.E.; Haider, S.; Koukourakis, M.I.; Piperidou, C.; Pappa, A.; Gatter, K.C.; et al. Autophagy and lysosomal related protein expression patterns in human glioblastoma. *Cancer Biol. Ther.* **2014**, *15*, 1468–1478.
61. Yasui, L.S.; Duran, M.; Andorf, C.; Kroc, T.; Owens, K.; Allen-Durdan, K.; Becker, R.; Schuck, A.; Grayburn, S. Autophagic flux in glioblastoma cells. *Int. J. Radiat. Biol.* **2016**, *92*, 665–678.
62. Yaghi, L.; Poras, I.; Simoes, R.T.; Donadi, E.A.; Tost, J.; Daunay, A.; Moreau, P.; de Almeida, B.S.; Carosella, E.D. Hypoxia inducible factor-1 mediates the expression of the immune checkpoint HLA-G in glioma cells through hypoxia response element located in exon 2. *Oncotarget* **2016**, *7*, 63690–63707.
63. Di Maggio, F.M.; Minafra, L.; Forte, G.I.; Cammarata, F.P.; Lio, D.; Messa, C.; Bravata, V.; Gilardi, M.C. Portrait of inflammatory response to ionizing radiation treatment. *J. Inflamm.* **2015**, *12*, 14.
64. Kim, K.W.; Mutter, R.W.; Cao, C.; Albert, J.M.; Shinohara, E.T.; Sekhar, K.R.; Lu, B. Inhibition of signal transducer and activator of transcription 3 activity results in down-regulation of Survivin following irradiation. *Mol. Cancer Ther.* **2006**, *5*, 2659–2665.
65. Yu, H.; Pardoll, D.; Jove, R. STATs in cancer inflammation and immunity: A leading role for STAT3. *Nat. Rev. Cancer.* **2009**, *9*, 798–809.
66. Sun, Y.; Cheng, M.K.; Thomas, R.L.G.; T.; Kilian, M.J.; Kai, B.; Kriajevska, M.; Manson, M. Inhibition of STAT signalling in bladder cancer by diindolylmethane: Relevance to cell adhesion, migration and proliferation. *Curr. Cancer Drug Targets.* **2013**, *13*, 57–68.
67. Du, Y.C.; Gu, S.; Zhou, J.; Wang, T.; Cai, H.; MacInnes, M.A.; Chen, X.; Bradbury, E.M. The dynamic alterations of H2AX complex during DNA repair detected by a proteomic approach reveal the critical roles of Ca(2+)/calmodulin in the ionizing radiation-induced cell cycle arrest. *Mol. Cell. Proteom.* **2006**, *5*, 1033–1044.
68. Lao, Y.; Chang, D.C. Mobilization of Ca²⁺ from endoplasmic reticulum to mitochondria plays a positive role in the early stage of UV-or TNF α -induced apoptosis. *Biochem. Biophys. Res. Commun.* **2008**, *373*, 42–47.
69. Combs, S.E.; Bohl, J.; Elsässer, T.; Weber, K.J.; Schulz-Ertner, D.; Debus, J.; Weyrather, W.K. Radiobiological evaluation and correlation with the local effect model (LEM) of carbon ion radiation therapy and temozolomide in glioblastoma cell lines. *Int. J. Radiat. Biol.* **2009**, *85*, 126–137.
70. Combs, S.E.; Zipp, L.; Rieken, S.; Habermehl, D.; Brons, S.; Winter, M.; Weber, K.J.; Haberer, T.; Debus, J. In vitro evaluation of photon and carbon ion radiotherapy in combination with chemotherapy in glioblastoma cells. *Radiat. Oncol.* **2012**, *7*, 9, doi:10.1186/1748-717X-7-9.
71. Barazzuol, L.; Jena, R.; Burnet, N.G.; Jeynes, J.C.; Merchant, M.J.; Kirkby, K.J.; Kirkby, N.F. In Vitro Evaluation of Combined Temozolomide and Radiotherapy Using X Rays and High-Linear Energy Transfer Radiation for Glioblastoma. *Radiat. Res.* **2012**, *177*, 651–662.
72. Cirrone, G.A.P.; Cuttone, G.; Lojacono, P.A.; Lo Nigro, S.; Mongelli, V.; Patti, I.V.; Privitera, G.; Raffaele, L.; Rifuggiato, D.; Sabini, M.G.; Salamone, V.; Spatola, C.; Valastro, L.M. A 62-MeV proton beam for the treatment of ocular melanoma at laboratori nazionali del sud-INFN. *IEEE Transact. Nuclear Sci.* **2004**, *51*, 860–865.

73. Cirrone, G.A.P.; Cuttone, G.; Lo Nigro, S.; Mongelli, V.; Raffaele, L.; Sabini, M.G. Dosimetric characterization of CVD diamonds in photon, electron and proton beams. *Nuclear Physics B (Proc. Suppl.)* **2006**, *150*, 330–333.
74. Sartini, L.; Simeone, F.; Pani, P.; Lo Bue, N.; Marinaro, G.; Grubich, A.; Gasparoni, F.; Lobko, A.; Etiope, G.; Gapone, A.; et al. Nuclear Instruments and Methods in Physics Research Section A: Accelerators, Spectrometers, Detectors and Associated Equipment. *Nucl. Instrum. Methods Phys. Res. A* **2017**, *846*, doi:10.1016/j.nima.2010.06.248.
75. Militello, C.; Rundo, L.; Conti, V.; Minafra, L.; Cammarata, F.P.; Mauri, G.; Porcino, N.; Gilardi, M.C. Areabased cell colony surviving fraction evaluation: A novel fully automatic approach using general-purpose acquisition hardware. *Comput. Biol. Med.* **2017**, *89*, 454–465.
76. Minafra, L.; Porcino, N.; Bravatà, V.; Gaglio, D.; Bonanomi, M.; Amore, E.; Baglio, M.; Cammarata, F.P.; Russo, G.; Militello, C.; et al. Radiosensitizing effect of curcumin-loaded lipid nanoparticles in breast cancer cells. *Sci. Rep.* **2019**, *9*, 11134.



© 2019 by the authors. Licensee MDPI, Basel, Switzerland. This article is an open access article distributed under the terms and conditions of the Creative Commons Attribution (CC BY) license (<http://creativecommons.org/licenses/by/4.0/>).



Article

SRC Tyrosine Kinase Inhibitor and X-rays Combined Effect on Glioblastoma Cell Lines

Filippo Torrisi ^{1,†}, Luigi Minafra ^{2,3,†}, Francesco P. Cammarata ^{2,3,*}, Gaetano Savoca ^{2,3}, Marco Calvaruso ^{2,3}, Nunzio Vicario ¹, Laura Maccari ⁴, Elodie A. Pérès ⁵, Hayriye Özçelik ⁵, Myriam Bernaudin ⁵, Lorenzo Botta ⁴, Giorgio Russo ^{2,3}, Rosalba Parenti ^{1,*} and Samuel Valable ⁵

¹ Department of Biomedical and Biotechnological Sciences (BIOMETEC), University of Catania, 95123 Catania, Italy; filippo.torrisi@unict.it (F.T.); nunziovicario@unict.it (N.V.); parenti@unict.it (R.P.)

² National Institute for Nuclear Physics, Laboratori Nazionali del Sud, INFN-LNS, 95123 Catania, Italy; luigi.minafra@ibfm.cnr.it (L.M.); francesco.cammarata@ibfm.cnr.it (F.P.C.); savoca.gaetano@gmail.com (G.S.); marco.calvaruso@ibfm.cnr.it (M.C.); giorgio.russo@ibfm.cnr.it (G.R.)

³ Institute of Molecular Bioimaging and Physiology, National Research Council, IBFM-CNR, 90015 Cefalù, Italy; luigi.minafra@ibfm.cnr.it (L.M.); francesco.cammarata@ibfm.cnr.it (F.P.C.); savoca.gaetano@gmail.com (G.S.); marco.calvaruso@ibfm.cnr.it (M.C.); giorgio.russo@ibfm.cnr.it (G.R.)

⁴ Lead Discovery Siena s.r.l. (LDS), via Vittorio Alfieri, 31, Castelnuovo Berardenga, 53019 Siena, Italy; l.maccari@leaddiscoverysiena.it (L.M.); l.botta@leaddiscoverysiena.it (L.B.)

⁵ Normandie University, UNICAEN, CEA, CNRS, ISTCT/CERVOxy group, GIP Cyceron, 14074 Caen, France; peres@cyceron.fr (E.P.); ozcelik@cyceron.fr (H.O.); bernaudin@cyceron.fr (M.B.); samuel.valable@cnrs.fr (S.V.)

* Correspondence: francesco.cammarata@ibfm.cnr.it (F.P.C.); parenti@unict.it (R.P.)

† These authors contributed equally to this work.

Received: 12 May 2020; Accepted: 28 May 2020; Published: date

Abstract: Glioblastoma (GBM) is one of the most lethal types of tumor due to its high recurrence level in spite of aggressive treatment regimens involving surgery, radiotherapy and chemotherapy. Hypoxia is a feature of GBM, involved in radioresistance, and is known to be at the origin of treatment failure. The aim of this work was to assess the therapeutic potential of a new targeted c-SRC inhibitor molecule, named Si306, in combination with X-rays on the human glioblastoma cell lines, comparing normoxia and hypoxia conditions. For this purpose, the dose modifying factor and oxygen enhancement ratio were calculated to evaluate the Si306 radiosensitizing effect. DNA damage and the repair capability were also studied from the kinetic of γ -H2AX immunodetection. Furthermore, motility processes being supposed to be triggered by hypoxia and irradiation, the role of c-SRC inhibition was also analyzed to evaluate the migration blockage by wound healing assay. Our results showed that inhibition of the c-SRC protein enhances the radiotherapy efficacy both in normoxic and hypoxic conditions. These data open new opportunities for GBM treatment combining radiotherapy with molecularly targeted drugs to overcome radioresistance.

Keywords: Glioblastoma; ionizing radiation; hypoxia; DNA damage; combined treatments

1. Introduction

Radiotherapy (RT) represents a gold standard in the treatment of glioblastoma (GBM) that remains one of the most aggressive primary brain tumors with a high rate of recurrence [1]. Clinical data reported that RT is a positive prognostic factor on the survival of patients, as compared to patients that receive surgery or chemotherapy alone [2]. However, there are no clinical studies demonstrating an overall survival improvement with RT dosing above the standard of 60 Gy for 30 fractions (2 Gy/day), showing that there are

two main issues to overcome: i) Avoiding radiation side effects and ii) reducing GBM radioresistance. The hypoxic pattern of GBM has been widely described and represents one of the main factors inducing radioresistance [3]. Hypoxic microenvironment reduces non-repairable DNA damage mediated by RT, as described by the hypothesis of oxygen fixation. Indeed, under normoxic conditions, molecular oxygen permanently fixes the DNA damage induced by free radicals produced in water radiolysis (indirect effects of ionizing radiation), being very genotoxic. Such a role, under hypoxic conditions, is proportionally reduced, thus affecting indirect damage induced by RT and establishing so called GBM radioresistance, leading to non-repairable DNA double strand breaks [4,5]. Therefore, hypoxic microenvironment, particularly pronounced in GBM, represents a poor prognosis factor, as shown both in preclinical models [6] and in human GBM patients [3,7]. Moreover, hypoxia mediates a favourable microenvironment to the growth and renewal of GBM stem cells and to the activation of specific proteins, involved in cell proliferation, angiogenesis, migration and invasion, that are the biological basis of GBM recurrence [8,9]. Among these proteins, SRC proto-oncogene non-receptor tyrosine kinase (c-SRC), a member of non-receptor SRC family kinases (SFKs), drives GBM carcinogenesis and progression, and is involved in intracellular signalling pathways related with hypoxia [10]. Several factors are involved in the activation of c-SRC, including focal adhesion kinase (FAK), integrins or tyrosine kinase growth factor receptors, like epidermal growth factor receptor (EGFR) [11]. Hypoxia stimulates the interaction of vIIIIEGFR with the integrin β 3 in GBM cells, activating a signalling pathways c-SRC-dependent resulting in the up-regulation of the cancer cell invasion markers, like matrix metalloproteinase-2 (MMP-2) and matrix metalloproteinase-9 (MMP-9) [12]. Therefore, c-SRC and its related network represent a key protein for targeted therapy.

Si306 (Lead Discovery Siena, Siena, Italy) is a molecule of the pyrazolo[3,4-d]pyrimidines family, which has been shown to inhibit c-SRC kinase protein activity [13]. Previous preclinical studies confirmed that Si306 was able to cross the intact blood–brain barrier and to progressively accumulate into the brain for 24 h after the post-intravenous injection. Moreover, it has been demonstrated that Si306 in combination with X-rays showed a synergic anti-proliferative effect in both in vitro and in vivo GBM models [14].

Herein, we aimed at investigating the Si306 capability to increase the radiotherapy efficacy both in normoxic and hypoxic conditions on the GBM cells, increasing the current knowledge on radiosensitizing effects of the novel c-SRC inhibitor Si306. For this purpose, we investigated the radiosensitizing effect of Si306 on two GBM cell lines, U251-MG and U87-MG, irradiated with X-rays in both normoxic (21% of oxygen) and hypoxic (1% of oxygen) conditions, and evaluated the degree of proliferation and migration. In addition, γ H2AX foci detection by immunofluorescence was performed to quantify the radiation-induced DNA double-strand break formation and the DNA damage repair ability. Our results showed that c-SRC inhibition acted synergistically with radiation treatment, reducing clonogenic and migration ability and increasing DNA damage in GBM cells, in both normoxic and hypoxic conditions.

2. Results

2.1. c-SRC Inhibition Improves the Efficacy of Radiotherapy on U251-MG Cell Line

2.1.1. Evaluation of Cell Survival from Clonogenic Assay

In order to compare the effects of increasing doses of X-rays (0, 2, 4, 6, 8 Gy) on U251-MG cell survival in normoxic (21% O₂) and hypoxic (1% O₂) conditions and in combination with 10 μ M and 20 μ M of the Si306 molecule, we performed clonogenic assays on the U251-MG cell line. The surviving fraction (SF) values were plotted against the dose to obtain dose-response curves. Dose modifying factor (DMF) and oxygen enhancement ratio (OER) were also calculated to evaluate treatment efficiency. The results showed a radiation dose dependent decrease in clone number with a significant effect with the exposition concomitant to Si306 (Figure 1a,b). Of note, U251-MG cells exhibited hypoxia-induced radioresistance with an OER of 1.27 (Figure 2a,b and Table 1). In normoxic conditions, the exposure to Si306 combined with RT induced a decrease in SF values with a DMF of 1.38 at the concentration of 20 μ M (Figure 3a,b and Table 1). In hypoxic conditions, the effect of combined treatment was increased in culture exposed to Si306 versus control. The synergistic effect of Si306 and RT was further confirmed by the OER reduction of about 11%, demonstrating that c-SRC inhibition had a significant role as radiosensitizer in hypoxic conditions (Figure 4a,b and Table 1).

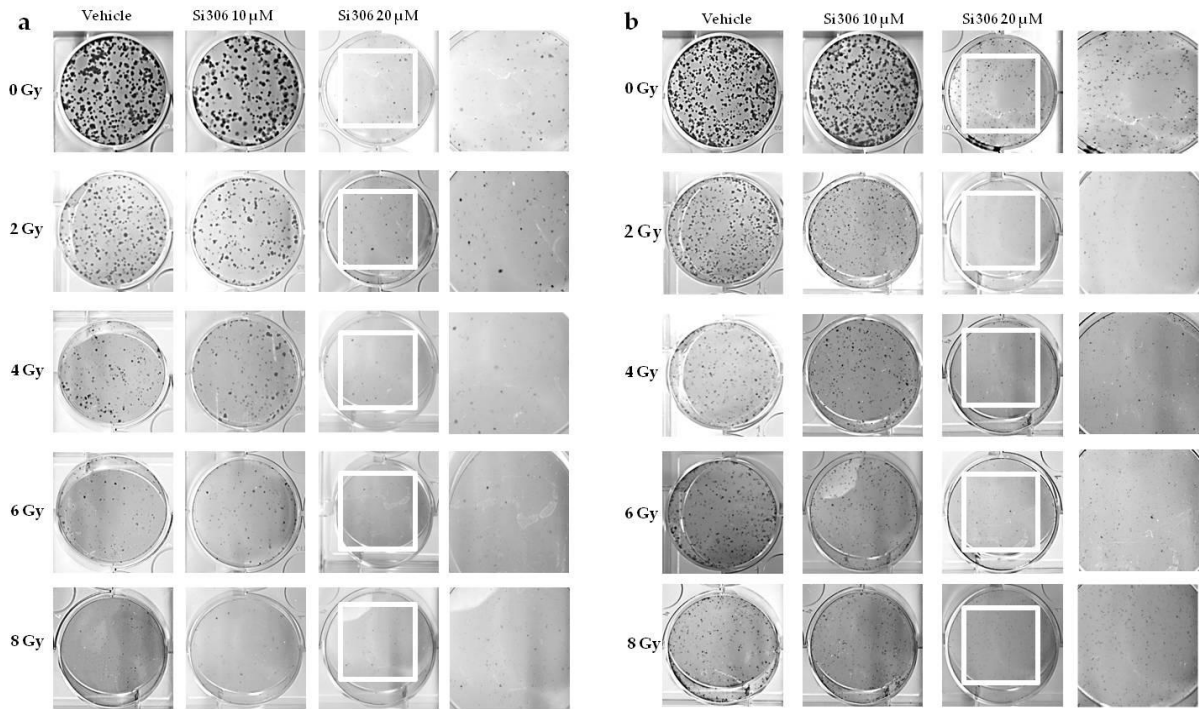


Figure 1. U251 clones after X-ray irradiation combined with Si306 in normoxia (21% oxygen) (a) and hypoxia (1% oxygen) (b).

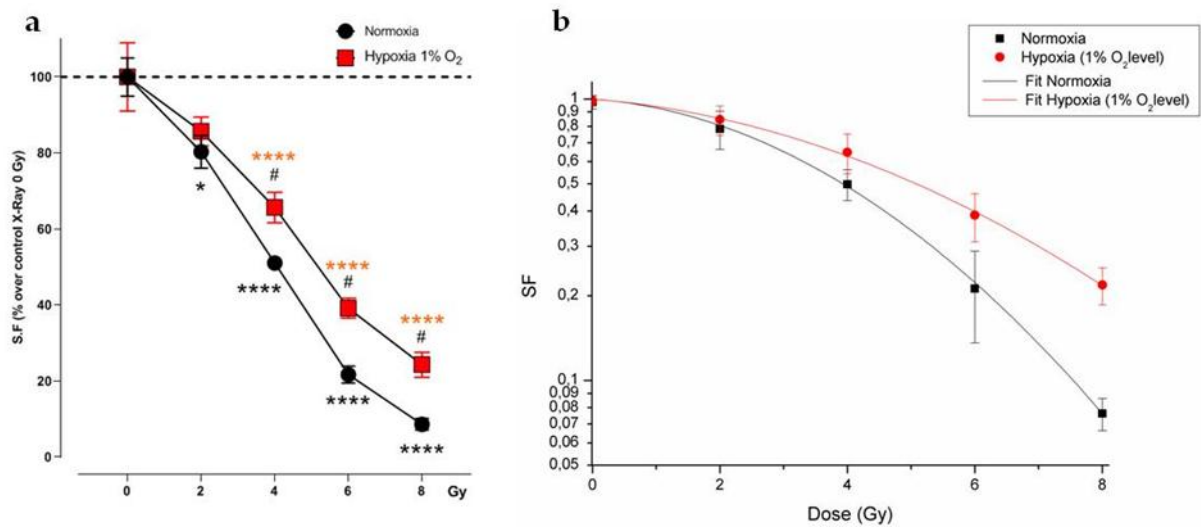


Figure 2. U251-MG irradiated cells in normoxia and hypoxia. (a) Surviving fraction (SF) plot of normoxic and hypoxic U251-MG cells exposed to 0, 2, 4, 6 and 8 Gy. Data are mean \pm SEM of $n = 3$ independent experiments. * p -value < 0.05 and **** p -value < 0.0001 versus normoxia 0 Gy; # p -value < 0.05 versus each dose in normoxia ($F_{\text{Si306conc.}} = 133.8$, p -value < 0.0001 ; $F_{\text{Gy}} = 15.49$, p -value = 0,0003; $F_{\text{Si306conc.} \times \text{Gy}} = 1.568$, p -value = 0.1973. Two-way ANOVA with Holm-Šidák post-hoc test). (b) Linear-quadratic adjustment of the data of U251 cell survival curves treated with X-rays in hypoxia and normoxia.

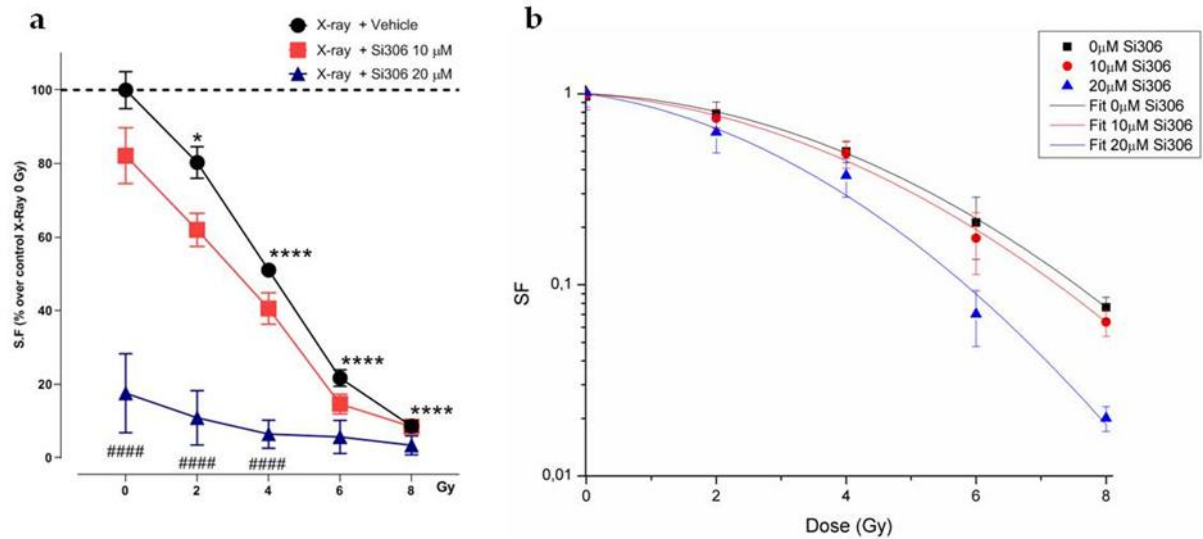


Figure 3. Cell survival of irradiated cells in normoxia with Si306 exposure. **(a)** SF plot of normoxic U251-MG cells exposed to 0, 2, 4, 6 and 8 Gy and treated with vehicle, 10 or 20 μM Si306. Data are mean ± SEM of $n = 3$ independent experiments. * p -value < 0.05 and **** p -value < 0.0001 versus 0 Gy in normoxia; ### p -value < 0.0001 versus only irradiated cells with 0, 2 and 4 Gy in normoxia ($F_{\text{Si306conc.}} = 89.17$, p -value < 0.0001; $F_{\text{Gy}} = 124.5$, p -value < 0.0001; $F_{\text{Si306conc.} \times \text{Gy}} = 14.64$, p -value < 0.0001. Two-way ANOVA with Holm-Šidák post-hoc test). **(b)** Linear-quadratic adjustment of the data of U251 cell survival curves treated with X-rays only and combined with Si306 in normoxia.

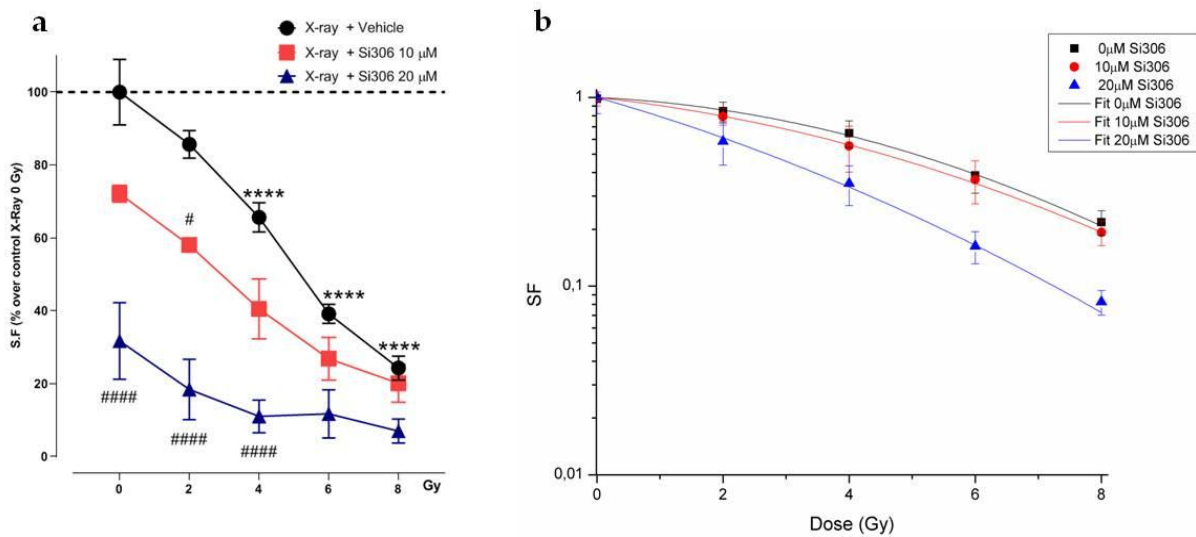


Figure 4. SF of irradiated cells with Si306 exposure in hypoxia. **(a)** Mean ± SEM, three independent experiments; *** p -value < 0.001 and **** p -value < 0.0001 versus 0 Gy in normoxia; # p -value < 0.05 and ### p -value < 0.0001 versus X-rays + vehicle at the same dose ($F_{\text{Si306conc.}} = 34.09$, p -value < 0.0001; $F_{\text{Gy}} = 77.95$, p -value < 0.0001; $F_{\text{Si306conc.} \times \text{Gy}} = 3.929$, p -value = 0.0012. Two-way ANOVA with Holm-Šidák post-hoc test). **(b)** Linear-quadratic adjustment of the data of U251 cell survival curves treated with X-rays only and combined with Si306 in hypoxia.

Table 1. Dose modifying factor (DMF) and oxygen enhancement ratio (OER) values calculated as isoeffective dose at surviving fraction of 0.5.

Treatment	Normoxia SF50% (Gy)	Hypoxia SF50% (Gy)	Normoxia DMF	Hypoxia DMF	OER
X-rays + vehicle	4.09	5.18	1	1	1.27
X-rays + 10 μ M Si306	3.86	4.53	1.05	1.15	1.17
X-rays+ 20 μ M Si306	2.54	2.67	1.38	1.94	1.05

2.1.2. Radiobiological Meaning of A, B and A/B Ratio Parameters

DMF and OER changes were also related to the α and β parameters analysis. These values displayed differences between groups (normoxia versus hypoxia) and treatment (vehicle versus Si306) (Tables 2 and 3). The Si306 treatment combined with X-rays induced an α value increase in both conditions, in particular in the hypoxic one. Indeed, 10 and 20 μ M Si306 showed α values of 0.092 ± 0.010 and 0.219 ± 0.025 , respectively, as compared to control cultures (α value = 0.037 ± 0.024). This means that, in hypoxia, the linear contribution to damage is higher than in normoxia. The increase in β value is greater in normoxia rather than in hypoxia after exposure to Si306 in combination with irradiation, maybe due to ROS decrease in hypoxic condition. However, the DNA direct damage associated with α component may contribute to the OER decrease. Moreover, our data provided important evidence on the α/β value meaning that is an inverse reflection of a tissue sensitivity to dose fractionation. According to the α/β ratio, tissues are classified as early (low α/β) or late (high α/β) responding [15]. Therefore, the significant increase in the α/β ratio observed in hypoxia may represent a change in cellular radiobiological response leading to tissue patterns with a reduced ability to repair damage and with a greater accumulation of lethal lesions.

Table 2. α and β parameters by fitting the cell survival to the linear-quadratic (LQ) model in normoxia. Values correspond to mean \pm SEM; three independent experiments.

Treatment Normoxia	α (Gy-1)	β (Gy-2)	α/β (Gy)
X-rays + vehicle	0.037 ± 0.011	0.036 ± 0.009	1.03
X-ray s+ 10 μ M Si306	0.060 ± 0.039	0.035 ± 0.009	1.71
X-rays+ 20 μ M Si306	0.077 ± 0.009	0.052 ± 0.005	1.48

Table 3. α and β parameters estimated by fitting the cell survival to the linear-quadratic in normoxia (LQ) model in hypoxia. Values correspond to mean \pm SEM; three independent experiments.

Treatment Hypoxia	α (Gy-1)	β (Gy-2)	α/β (Gy)
X-rays + vehicle	0.037 ± 0.024	0.020 ± 0.005	1.85
X-rays + 10 μ M Si306	0.092 ± 0.010	0.013 ± 0.002	7.07
X-rays + 20 μ M Si306	0.219 ± 0.025	0.014 ± 0.005	15.64

2.2. c-SRC Inhibition Sustains Radiation-Induced DNA Damage Over Time

The DNA damage was evaluated by γ H2AX immunofluorescence during the maximum of foci formation and also damage repair capacity (2 and 24 h after X-ray radiation, respectively) [9]. Immunofluorescence analyses showed that in normoxia and hypoxia, the exposure to Si306 in combination

with irradiation led to a signal increase that was not significant 2 h after irradiation compared to X-rays only (Figure 5a,b). The synergistic effect of the Si306 molecule with IR became significant 24 h after treatment, where the foci signal was maintained at high levels in the case of combined treatment, compared to irradiation alone: 48 % and 41% of U251 cells, exposed, respectively, with 10 μ M and 20 μ M of Si306, were still positive compared to 10% of only irradiated U251 cells in normoxia. More interestingly, in hypoxia we showed a persistence of 21% and 27% positive U251-MG cells, both irradiated and exposed to 10 μ M Si306 and 20 μ M of Si306, respectively, compared to 5% of only irradiated cells (Figure 6a,b). To further confirm this observation, the immunofluorescence assay was repeated on the U87-MG GBM cell line. The results obtained were similar, since the differences in the foci γ H2AX signal between the treatment conditions with vehicle and with Si306 were not significant 2 h after irradiation (Figure 7a,b). The increase in foci γ H2AX expression was statistically significant only 24 h after irradiation in the combined treatments: In normoxia, after irradiation and Si306 pre-treatment, 35% (10 μ M) and 31% (20 μ M) of U87 cells were positive versus 15% of only irradiated U87 cells; similar results were obtained in hypoxia, since 18% and 28% of irradiated and Si306 pre-treated U87 cells, respectively, with 10 μ M and 20 μ M, were positive compared to 10% of only irradiated U87 cells (Figure 8a,b).

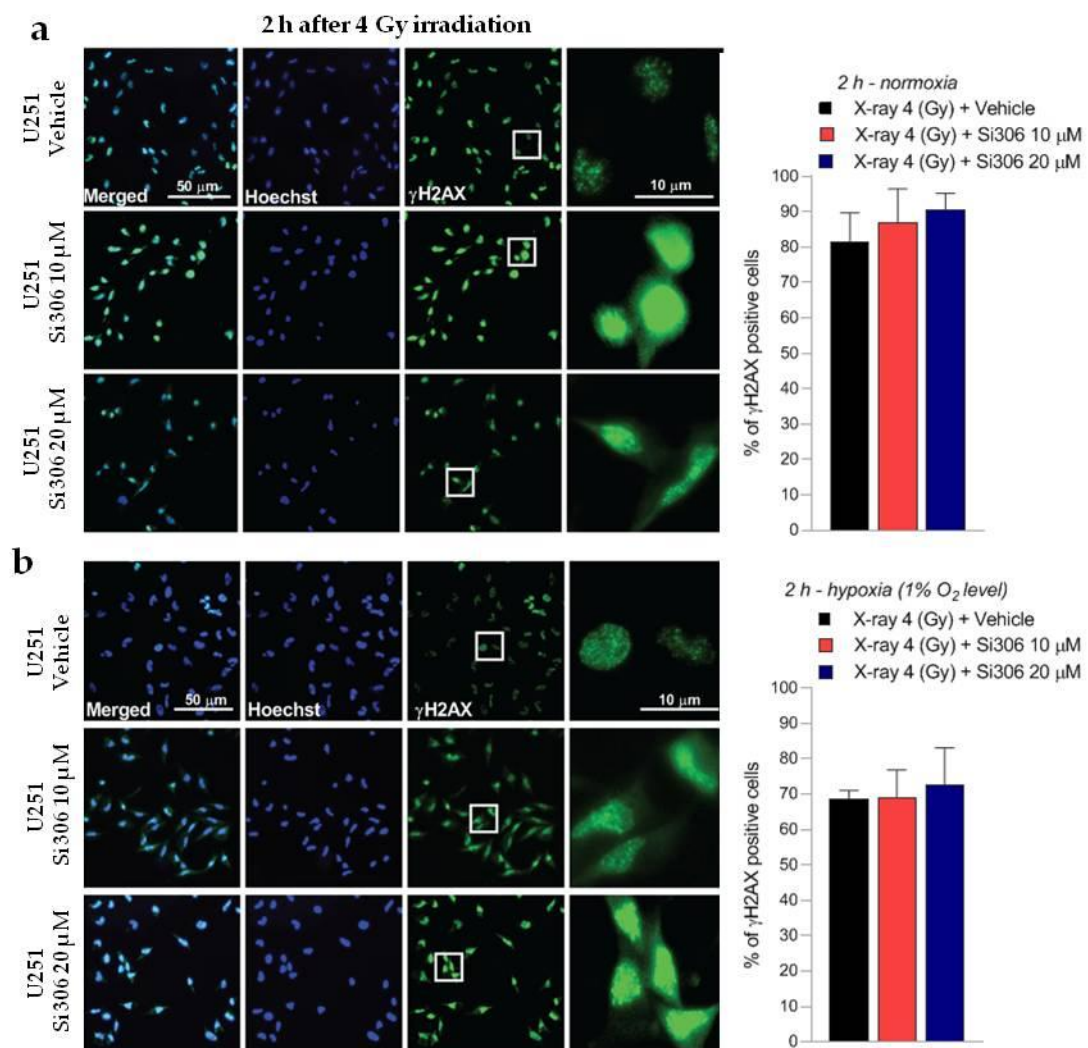


Figure 5. Representative pictures with inserts (white squares) and quantification of U251-MG positive cells for γ H2AX performed 2 h after 4 Gy irradiation in normoxia (**a**) and hypoxia (**b**). Data are mean \pm SD of $n = 3$ independent experiments; *** p -value < 0.001 and **** p -value < 0.0001 versus 4 Gy + vehicle; ($F_{\text{normoxia}} = 2.030$, p -value = 0.1564; $F_{\text{hypoxia}} = 0.5685$, p -value = 0.5798. One-way ANOVA with Holm-Šidák post-hoc test).

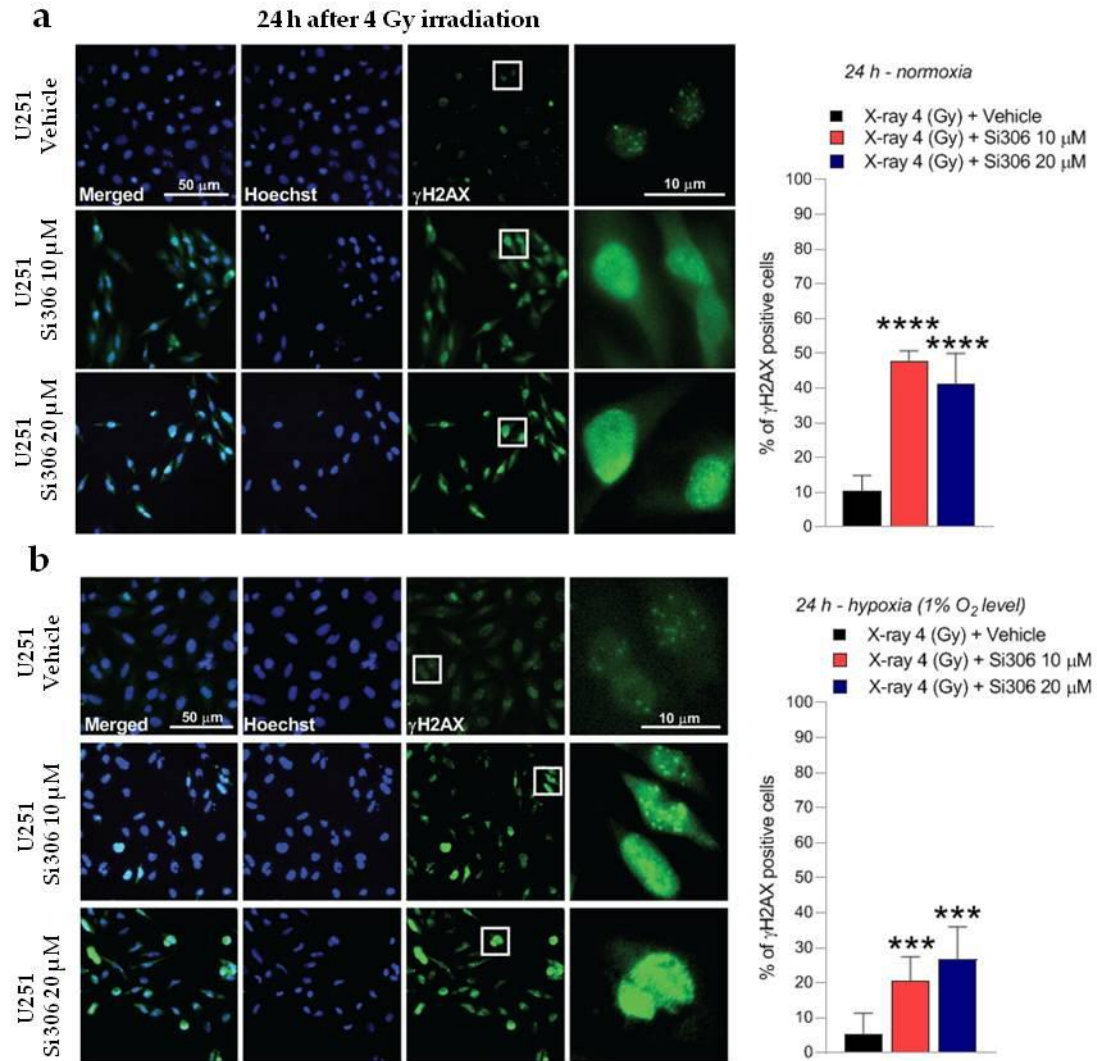


Figure 6. Representative pictures with inserts (white squares) and quantification of U251-MG positive cells for γH2AX realized 24 h after 4 Gy irradiation normoxia (a) and in hypoxia (b). Data are mean \pm SD of $n = 3$ independent experiments; *** p -value < 0.001 and **** p -value < 0.0001 versus 4 Gy + vehicle ($F_{\text{normoxia}} = 87.81$, p -value < 0.0001 ; $F_{\text{hypoxia}} = 18.87$, p -value < 0.0001). One-way ANOVA with Holm-Šídák post-hoc test).

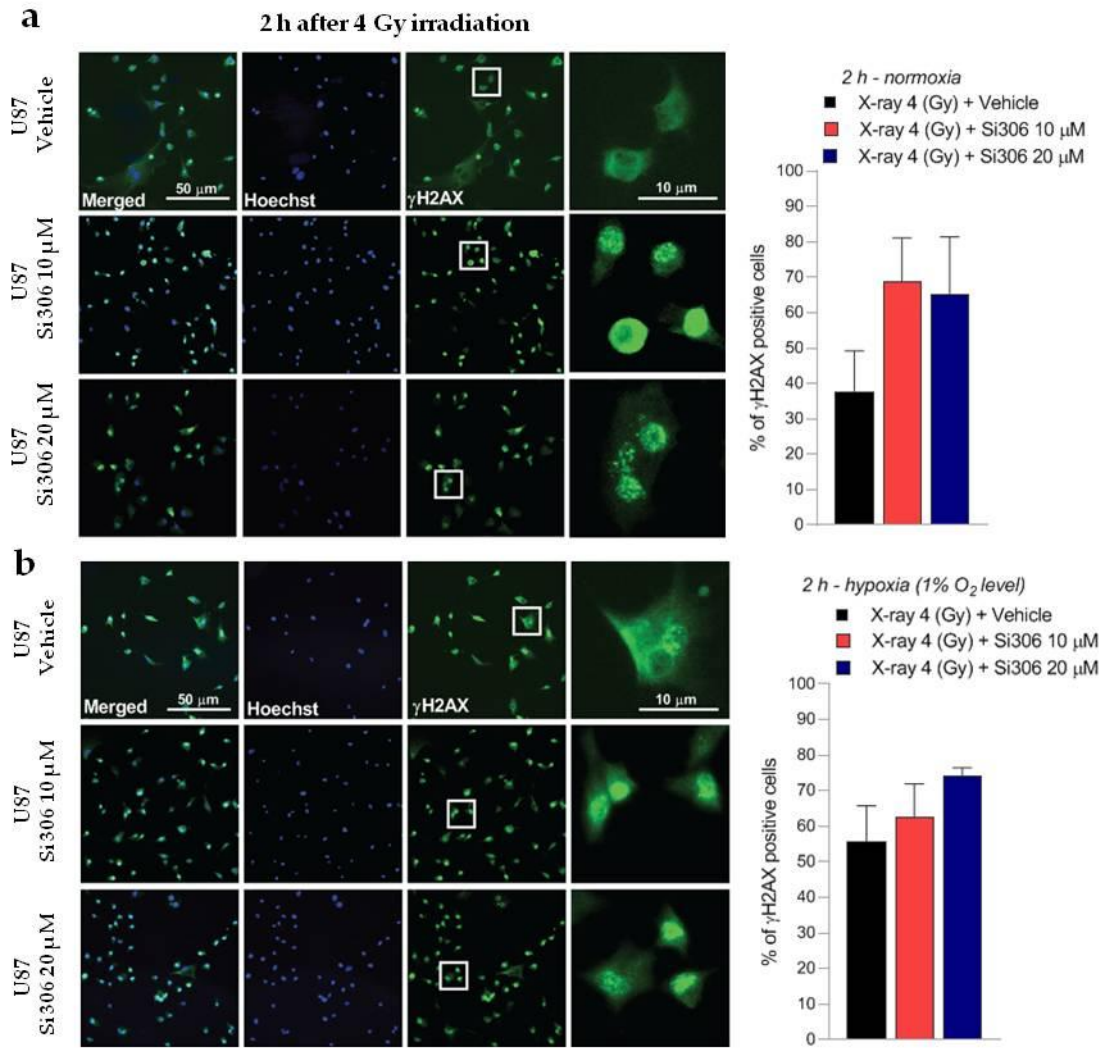


Figure 7. Representative pictures with inserts (white squares) and quantification of U87 positive cells for γH2AX performed 2 h after 4 Gy irradiation in normoxia **(a)** and hypoxia **(b)** Data are mean \pm SD of $n = 3$ independent experiments ($F_{\text{normoxia}} = 5.787$, $p\text{-value} < 0.0329$; $F_{\text{hypoxia}} = 4.048$, $p\text{-value} < 0.0557$. One-way ANOVA with Holm-Šidák post-hoc test).

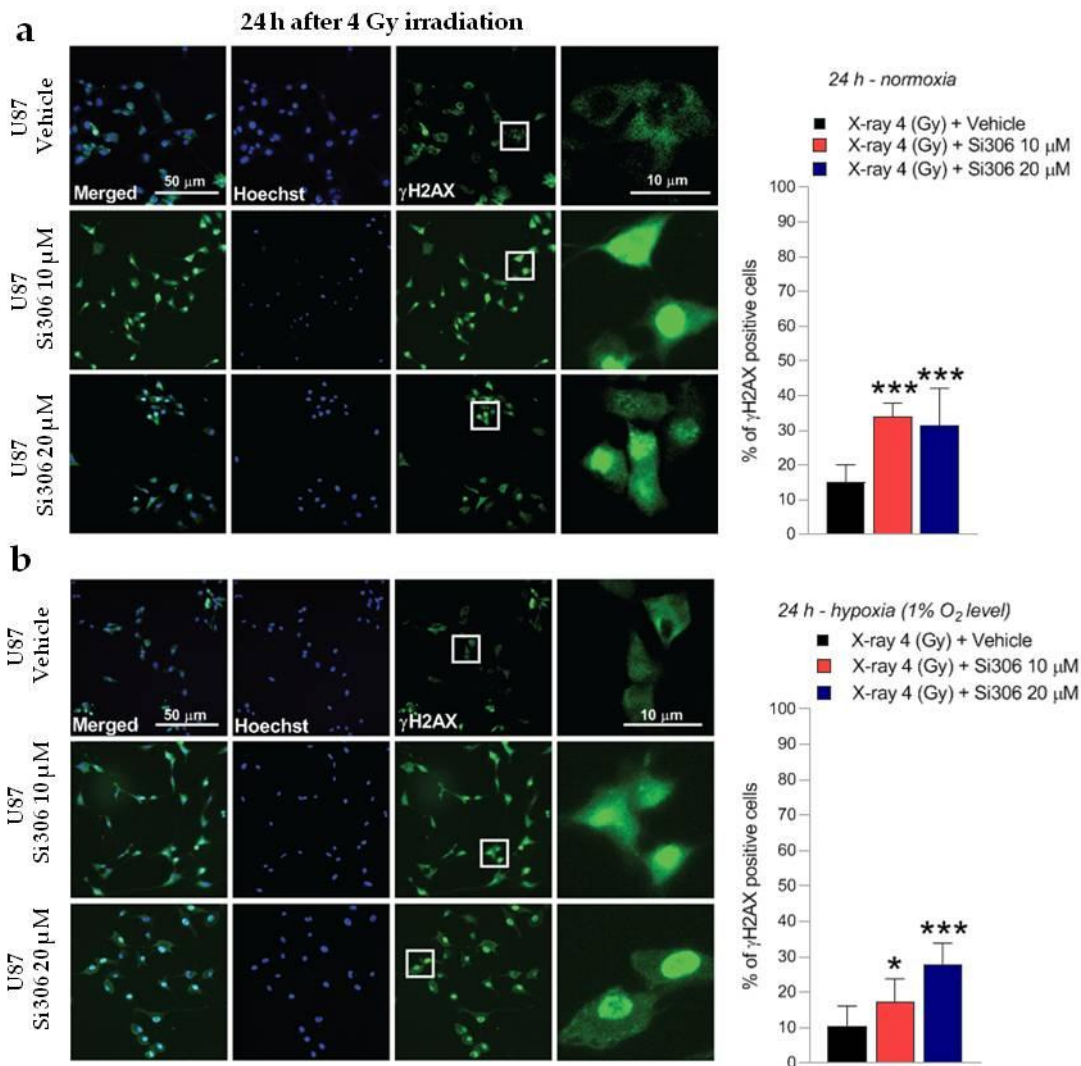


Figure 8. Representative pictures with inserts (white squares) and quantification of U87 positive cells for γ H2AX realized 24 h after 4 Gy irradiation in normoxia (a) and hypoxia (b). Data are mean \pm SD of $n = 3$ independent experiments; * p -value < 0.05 and *** p -value < 0.001 versus 4 Gy + vehicle ($F_{\text{normoxia}} = 16.82$, p -value < 0.0001; $F_{\text{hypoxia}} = 12.77$, p -value = 0.0004. One-way ANOVA with Holm-Šídák post-hoc test).

2.3. c-SRC Inhibition Reduces Cell Migration

Migration and invasion of malignant glioma play a key role in GBM progression. Therefore, we examined, by wound healing assay, the effect of c-SRC inhibition on migration in irradiated U251-MG cells, being highly invasive, as reported in previous studies [16]. The results of wound healing assay showed an inhibitory effect of the Si306 molecule on the migration of the U251-MG cells. The addition of the Si306 molecule at both concentrations of 10 μ M and 20 μ M reduced the migration index of cells compared to those not irradiated and irradiated with a vehicle, in both normoxic and hypoxic conditions (Figure 9a,b).

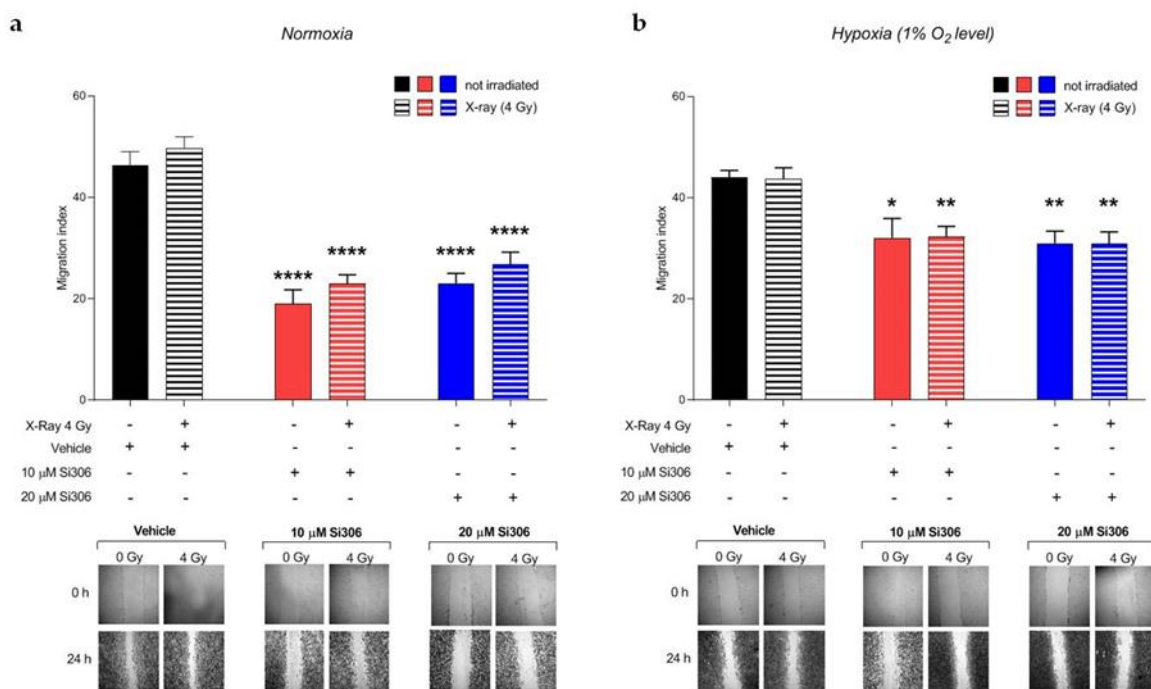


Figure 9. Effects of Si306 on migration of U251-MG cells in normoxia (a) and hypoxia (b). Data are mean \pm SEM of $n = 3$ independent experiments. * p -value < 0.05 , ** p -value < 0.01 and **** p -value < 0.0001 versus vehicle or vehicle + irradiation at 24 h after scratch ($F_{\text{normoxia}} = 32.59$, p -value < 0.0001 ; $F_{\text{hypoxia}} = 6.907$, p -value < 0.0001 . One-way ANOVA with Holm–Šidák post-hoc test).

3. Discussion

The poor prognosis of GBM represents an urgent clinical need and reinforces the necessity to explore and to develop novel therapeutic approaches. According to the clinical guidelines for the treatment of newly diagnosed GBM, only concomitant temozolomide with fractionated radiotherapy is indicated to significantly improve median survival (14.6 versus 12.1 months) and progression free survival (6.9 versus 5 months) as compared to RT alone, but high recurrences are still observed [17]. Therefore, specific cancer molecular targets are expected to have a synergistic effect to increase the efficacy of RT, overcoming radioresistance and modulating the irradiation dose delivered to enhance RT intrinsic sensitivity. During the last decade, molecular investigation on pathobiological mechanisms of GBM promoted research to develop molecularly targeted drugs (i.e., targeted therapy), including monoclonal antibodies (mAb) and tyrosine-kinase inhibitors (TKi), but their efficacy in the clinical practice is still limited as compared to conventional chemotherapy regimen [18]. c-SRC is a non-receptor tyrosine kinase (nRTK), interacting with many intracellular proteins, involved in GBM proliferation, invasion, motility and angiogenesis [10]. Previous evidence showed that hypoxia enhanced phosphorylation of tyrosine 416 in c-SRC, thus leading to protein-tyrosine kinase domain activation and to the downstream induction of VEGF expression, promoting angiogenesis [19]. Hypoxia may promote GBM progression and invasion throughout the integrin $\beta 3$ /FAK/SRC/EGFRvIII signalling axis, linking tumor cells and their surrounding environment [12]. Moreover, c-SRC activates HIF-1 α and glucose uptake, thus fostering GBM proliferation rate [20].

Recently, we investigated Si306 molecule, a member of the pyrazolo[3,4-d] pyrimidines family, which is able to selectively bind and inactivate the ATP site of c-SRC protein, acting as ATP competitive inhibitor type I/II [13]. Combined approaches with X-rays irradiation showed that Si306 is able to reduce proliferation, survival and clonogenic ability of GBM cell lines, also promoting carcinoma-associated fibroblasts

throughout TGF β [14]. We previously showed that a combination of Si306 and proton irradiation holds great potential to induce synergic cytotoxic effects and modulate the complex gene network in in vitro models of GBM [21]. Given the pronounced hypoxia observed during GBM development and progression, we aimed at studying the role of the Si306 and X-ray combination in hypoxic conditions, generating dose/response curves and calculating OER in addition to DMF to evaluate the relationship of these two parameters.

We first confirmed that Si306 was able to reduce cell survival in normoxia and, importantly, whether such an effect was preserved in hypoxic conditions. Notably, clonogenic assay revealed that c-SRC inactivation had a significant impact in hypoxic cells, leading to a higher DMF and a lower OER. The α and β values also support these data, showing that the robust increase in the α/β ratio in hypoxic conditions was related to an increase in α value, thus indicating improved non-repairable DNA damage [22]. A potential explanation of such a significant effect of Si306 in hypoxic GBM cells may be related to the intrinsic biological response to low oxygen levels [23]. Hypoxia induces radioresistance promoting GBM invasion and activating specific intracellular machinery that also relies on c-SRC activation [12,24]. Previous studies showed that RT itself may positively relate to activation of invasion and migration mechanisms involving c-SRC proteins [25,26]. Our evidence suggests that Si306 contributes to reducing efficacy of endogenous self-protective mechanisms that took place in hypoxic conditions, particularly sensitizing cell populations relying on c-SRC activation [27]. Furthermore, the analysis of the γ H2AX foci showed the c-SRC inhibition increases radiation-induced DNA damage and slows down the DNA repair abilities in both normoxic and hypoxic conditions. Importantly, Si306 treatment was also able to dramatically reduce cell migration in both normoxic and hypoxic conditions, thus indicating a substantial role of c-SRC pathway inhibition in GBM invasiveness.

Altogether, our data support the hypothesis that c-SRC inhibition may represent a promising approach to improve RT efficacy. Our evidences are in accordance with previous observations with the reference compound of c-SRC-family inhibitor PP2 [28] and with Si306 [14,29,30]. To date, the most important nTKI is the dual inhibitor c-SRC/Abl (Dasatinib) that was tested alone and in combination with mAb anti-VEGF (Bevacizumab), TKi of EGFR (Erlotinib) and alkylating agent (Lomustine) in clinical trials for recurrent GBM [31–34]. Results from randomized phase I/II trial of Dasatinib combined with Temozolomide and radiotherapy for newly diagnosed GBM does not show increased survival as compared to standard therapy alone [35]. The limitations of Dasatinib were associated to pharmacokinetics aspects due to efflux transporters P-glycoprotein, which are highly expressed in the blood–brain barrier and GBM cells [36]. On this aspect, recent evidence showed that Si306 hold higher cell growth inhibitory potential as compared to Dasatinib, and it was found to reduce P-gp activity in GBM cells with multidrug resistance phenotype in addition to an optimal brain penetration and accumulation on mice [37].

This work provided addition data supporting the benefit of c-SRC inhibition to enhance RT and, for the first time, investigated the efficacy of radiotherapy combined with c-SRC inhibition comparing normoxic and hypoxic conditions on GBM cell lines. Interestingly, our results indicated that Si306 molecule has a radiosensitizing effect on GBM cells both in normoxia and hypoxia, showing that it could be considered in a targeted strategy for GBM treatment.

4. Materials and Methods

4.1. Cell Culture and Hypoxia Experiments

The U251-MG and U87-MG human GBM cell lines were purchased from American Type Culture Collections (ATCC, Manassas, VA, USA) and cultured as previously described [21]. Cells were maintained in an exponentially growing culture condition, at 37 °C in a humidified atmosphere with 21% O₂ and 5% CO₂ (normoxic condition) and were subcultured in 75 cm² standard tissue culture flasks. The U87-MG cells were used as additional cell line only for γ -H2AX immunofluorescence analyses.

For hypoxic experiments, 15 h after seeding, cells were transferred in the hypoxic workstation (IN VIVO2 1000, Ruskinn; Awel International, Blain, France), balanced with 94% N₂ and 5% CO₂ to maintain a gas concentration of 1% O₂ at 37 °C (hypoxia). During experiment, cells were refilled with fresh medium previously equilibrated with the gas mixture containing 1% O₂ in order to maintain this concentration from the beginning of the treatment with the drug.

4.2. Irradiation and Drug Treatments

Irradiation was performed in a biological irradiator (CellRad®, Faxitron, Edimex Le Plessis Grammoire, France) with a dose rate of 2 Gy/min, 130 kV and 5.0 mA. GBM cell irradiation was carried out using dose values of 2, 4, 6 and 8 Gy for clonogenic assay. 4 Gy dose was used for γ -H2AX immunofluorescence and migration assay.

The compound Si306 was provided by Lead Discovery Siena (Siena, Italy) as a stock powder and was dissolved in Dimethylsulfoxide (DMSO, Saint Quentin Fallavier, France). The Si306 molecule was diluted at a final concentration of 10 μ M and 20 μ M with fresh medium, in which GBM cells were maintained for 24 h. After irradiation, cells were replaced with fresh medium in order to remove the Si306 and maintained in normoxia or hypoxia up to the end of the experiment. The control samples for all biological tests were supplemented with vehicle (i.e., 0.5% DMSO).

4.3. Clonogenic Assay

Cells were seeded in a 6-well plates in triplicate at a density of 80–420 cells/cm², according to the dose delivered and to the vehicle or drug concentration. Then, irradiation was performed using the dose values of 2, 4, 6 and 8 Gy. After irradiation, cells were incubated for 7 - 10 days in normoxia and hypoxia condition until the colony formation. The colonies were incubated with 0.05% crystal violet diluted in 20% ethanol (Saint Quentin Fallavier, France) for 30 min at room temperature. SF was determined according to the plating efficiency (PE) as we previously described [9]. Briefly, we calculated the PE, dividing the counted colony by the total plated cells. We then calculated the SF as a ratio of sample PE over control PE. For each experiment, the effect of each dose of radiation alone and combined with Si306 was evaluated on three individual wells of cell culture and each experiment was performed in triplicate.

4.4. Radiobiological Parameters Calculation

Surviving fraction values were adjusted according to the LQ model, which utilizes a multi-parameter equation for each individual experimental curve, the form of which is: $S(D)/S(0)=e^{-(\alpha D+\beta D^2)}$, where $S(D)$ is the fraction of cells that survive at a given dose (D) and $S(0)$ is the fraction of cells at 0 Gy; so we get α [Gy⁻¹] and β [Gy⁻²] with their own standard deviation [21,38]. The DMF, which represents the dose of irradiation required to obtain the isoeffect, was calculated as previously described [21]. The OER, which is defined as the ratio of dose given under hypoxic conditions to the dose resulting in the same effect when given under normoxia [39], was also calculated. For both values of DMF and OER, the surviving fraction of 50% was considered a biological isoeffect at 0 μ M, 10 μ M and 20 μ M of Si306.

4.5. γ -H2AX Immunofluorescence Analysis

Cells were seeded on sterile cover-glasses on 24 multiwell plates. After 8 h, cells were exposed to Si306 treatment for 24 h. Cells were then irradiated with 4 Gy and fixed in paraformaldehyde 4% at 2 and 24 h post-irradiation. Samples were then incubated with bovine serum albumin (BSA) 3% (Saint Quentin Fallavier, France), Tween 0.1% in PBS (Saint Quentin Fallavier, France) as blocking solution and to permeate cells for 30 min at room temperature. Indirect staining was performed using a primary antibody anti- γ H2AX (1/1000; Abcam, ab26350, Paris, France) dissolved in BSA 1%, Tween 0.1% in PBS overnight at 4 °C. Then, samples were washed three times with Tween 0.1% in PBS for 5 min. Samples were incubated with Alexa-488-conjugated anti-mouse secondary antibody (1/500; Thermofisher Scientific, A-21202, Montigny Le Bretonneux, France) for 1 h. Nuclei were counterstained adding Hoechst 33342 stain (10 μ g/mL; Saint Quentin Fallavier, France) for 1 h at room temperature. After three washes in PBS, samples were coverslipped and images were acquired using a Leica DM6000 microscope with a 20 \times objective. FITC and DAPI filter were used to detect foci γ -H2AX (in green) and nuclear signals (in blue), respectively. Quantifications were performed as previously described [40–42]. Briefly, images were analyzed using FIJI application software (version 2.0.0-rc-69/1.52p). Each region of interest was analyzed applying the iso-data threshold on immunofluorescence images of Hoechst and γ -H2AX and data are expressed as percentage of γ -H2AX positive nuclei over total Hoechst positive cells. Investigators blinded to the treatment groups performed all quantifications.

4.6. Migration Assay

Cells were seeded in 24 multiwell plates and incubated at both normoxic and hypoxic conditions. Following cell adhesion, Si306 molecule was added for 24 h. Mitomycin C (3 μ L/mL, Saint Quentin Fallavier, France) was used to block cell proliferation. Samples were irradiated with 4 Gy, and immediately after the irradiation a horizontal scratch was created using a sterile tip in the center of the cell monolayer. After 24 h samples were washed with PBS to remove floating cells and were stained with crystal violet solution as mentioned above. Images were acquired at 0 and 24 h post-scratch and the area between scratch edges was quantified. The scratch wound closure percentage was calculated as follows: $\frac{\text{The scratch area 0 h} - \text{the scratch area 24 h}}{\text{the scratch area 0 h}} \times 100\%$.

4.7. Statistical Analyses

All tests were performed in GraphPad Prism (version 5.00, GraphPad Software, San Diego, CA, USA). Data were tested for normality using a D'Agostino and Pearson omnibus normality test and subsequently assessed for homogeneity of variance. For comparison of $n > 3$ groups, one-way or two-way ANOVA was used where appropriate, followed by Holm–Šidák post-hoc test.

5. Conclusions

Further studies will help to better characterize the biological effects of Si306 in terms of cell toxicity and potential side effects. Taken together, the cell survival reduction, supported by DMF and LQ model, the DNA damage increase and the migration inhibition are all effects induced by the combination of a Si306 molecule and X-rays in both conditions of normoxia and hypoxia. For this reason, Si306 is a potential candidate as a new radiosensitizer in targeted therapy to overcome radioresistance in GBM disease.

Author Contributions: Conceptualization, F.T., L.M. (Luigi Minafra), F.P.C., S.V.; methodology, F.T., L.M. (Luigi Minafra), F.P.C., G.S., M.C., E.A.P., H.O., S.V.; investigation, F.T., L.M. (Luigi Minafra), S.V.; data curation and formal analysis, F.T., L.M. (Luigi Minafra), NV and S.V.; resources, L.M. (Laura Maccari), M.B., L.B., G.R., R.P., S.V.; writing—original draft preparation, F.T.; writing—review and editing, F.T., L.M. (Luigi Minafra), F.P.C., N.V., R.P., S.V.; supervision, F.T., L.M. (Luigi Minafra), F.P.C., M.B., G.R., R.P., S.V.; project administration, F.P.C., M.B., L.B., G.R., R.P., S.V.; funding acquisition, M.B., G.R., R.P., S.V.. All authors have read and agreed to the published version of the manuscript.

Funding: This work was partially supported by Institut National du Cancer (INCA 11699) and HABIONOR European project, co-funded by the Normandy County Council, the French State in the framework of the interregional development Contract “Vallée de la Seine” 2015-2020. This work was partially supported by the National Institute for Nuclear Physics (INFN) Commissione Scientifica Nazionale 5 (CSN5) Call ‘MoVe-IT’. This work was also supported by PBCT PRIN: Progetti di Ricerca di Rilevante Interesse Nazionale – PRIN 2017 – Prot. 2017XKWWK9. F.T. was supported by the ERASMUS+ Programme, Key Action 1, 2018/2019 – Student Mobility for Traineeship (Sapienza, University of Rome, Italy) and by the PhD programme in Biotechnology (Biometec, University of Catania, Italy). N.V. was supported by the PON AIM R&I 2014-2020 - E66C18001240007.

Conflicts of Interest: The authors declare no conflict of interest. The funders had no role in the design of the study; in the collection, analyses, or interpretation of data; in the writing of the manuscript, or in the decision to publish the results.

Abbreviations

GBM	Glioblastoma
RT	Radiotherapy
MMP-2	Matrix metalloproteinase-2
MMP-9	Matrix metalloproteinase-9
SFKs	SRC family kinases
FAK	Focal adhesion kinase
EGFR	Epidermal growth factor receptor
SF	Surviving fraction
PE	Plating efficiency
DMF	Dose modifying factor
OER	Oxygen enhancement ratio
LQ	Linear-quadratic
mAb	Monoclonal antibodies
TKi	Tyrosine-kinase inhibitors
nRTK	Non receptor tyrosine kinase
ECM	Extracellular matrix
DMSO	Dimethylsulfoxide
BSA	Bovine serum albumin

References

1. Wen, P.Y.; Weller, M.; Lee, E.Q.; Alexander, B.A.; Barnholtz-Sloan, J.S.; Barthel, F.P.; Batchelor, T.T.; Bindra, R.S.; Chang, S.M.; Chiocca, E.A.; et al. Glioblastoma in Adults: A Society for Neuro-Oncology (SNO) and European Society of Neuro-Oncology (EANO) Consensus Review on Current Management and Future Directions. *Neuro - Oncology*. **2020**, doi:10.1093/neuonc/noaa106.
2. Cabrera, A.R.; Kirkpatrick, J.P.; Fiveash, J.B.; Shih, H.A.; Koay, E.J.; Lutz, S.; Petit, J.; Chao, S.T.; Brown, P.D.; Vogelbaum, M.; et al. Radiation therapy for glioblastoma: Executive summary of an American Society for Radiation Oncology Evidence-Based Clinical Practice Guideline. *Pract. Radiat. Oncol.* **2016**, *6*, 217–225, doi:10.1016/j.prro.2016.03.007.
3. Gerstner, E.R.; Zhang, Z.; Fink, J.R.; Muzi, M.; Hanna, L.; Greco, E.; Prah, M.; Schmainda, K.M.; Mintz, A.; Kostakoglu, L.; et al. ACRIN 6684: Assessment of Tumor Hypoxia in Newly Diagnosed Glioblastoma Using 18F-FMISO PET and MRI. *Clin. Cancer Res.* **2016**, *22*, 5079–5086, doi:10.1158/1078-0432.CCR-15-2529.
4. Liu, C.; Lin, Q.; Yun, Z. Cellular and molecular mechanisms underlying oxygen-dependent radiosensitivity. *Radiat. Res.* **2015**, *183*, 487–496, doi:10.1667/RR13959.1.
5. Grimes, D.R.; Partridge, M. A mechanistic investigation of the oxygen fixation hypothesis and oxygen enhancement ratio. *Biomed. Phys. Eng. Express* **2015**, *1*, 045209, doi:10.1088/2057-1976/1/4/045209.
6. Valable, S.; Corroyer-Dulmont, A.; Chakhoyan, A.; Durand, L.; Toutain, J.; Divoux, D.; Barre, L.; MacKenzie, E.T.; Petit, E.; Bernaudin, M.; et al. Imaging of brain oxygenation with magnetic resonance imaging: A validation with positron emission tomography in the healthy and tumoural brain. *J. Cereb Blood Flow Metab.* **2017**, *37*, 2584–2597, doi:10.1177/0271678X16671965.
7. Ponte, K.F.; Berro, D.H.; Collet, S.; Constans, J.M.; Emery, E.; Valable, S.; Guillamo, J.S. In Vivo Relationship Between Hypoxia and Angiogenesis in Human Glioblastoma: A Multimodal Imaging Study. *J. Nucl. Med.* **2017**, *58*, 1574–1579, doi:10.2967/jnumed.116.188557.
8. Persano, L.; Rampazzo, E.; Della Puppa, A.; Pistollato, F.; Basso, G. The three-layer concentric model of glioblastoma: Cancer stem cells, microenvironmental regulation, and therapeutic implications. *Sci. World J.* **2011**, *11*, 1829–1841, doi:10.1100/2011/736480.
9. Peres, E.A.; Gerault, A.N.; Valable, S.; Roussel, S.; Toutain, J.; Divoux, D.; Guillamo, J.S.; Sanson, M.; Bernaudin, M.; Petit, E. Silencing erythropoietin receptor on glioma cells reinforces efficacy of temozolomide and X-rays through senescence and mitotic catastrophe. *Oncotarget* **2015**, *6*, 2101–2119, doi:10.18632/oncotarget.2937.
10. Ahluwalia, M.S.; de Groot, J.; Liu, W.M.; Gladson, C.L. Targeting SRC in glioblastoma tumors and brain metastases: Rationale and preclinical studies. *Cancer Lett.* **2010**, *298*, 139–149, doi:10.1016/j.canlet.2010.08.014.
11. Keller, S.; Schmidt, M.H.H. EGFR and EGFRvIII Promote Angiogenesis and Cell Invasion in Glioblastoma: Combination Therapies for an Effective Treatment. *Int. J. Mol. Sci.* **2017**, *18*, doi:10.3390/ijms18061295.
12. Liu, Z.; Han, L.; Dong, Y.; Tan, Y.; Li, Y.; Zhao, M.; Xie, H.; Ju, H.; Wang, H.; Zhao, Y.; et al. EGFRvIII/integrin beta3 interaction in hypoxic and vitronectin-enriching microenvironment promote GBM progression and metastasis. *Oncotarget* **2016**, *7*, 4680–4694, doi:10.18632/oncotarget.6730.
13. Schenone, S.; Radi, M.; Musumeci, F.; Brullo, C.; Botta, M. Biologically driven synthesis of pyrazolo[3,4-d]pyrimidines as protein kinase inhibitors: An old scaffold as a new tool for medicinal chemistry and chemical biology studies. *Chem. Rev.* **2014**, *114*, 7189–7238, doi:10.1021/cr400270z.
14. Calgani, A.; Vignaroli, G.; Zamperini, C.; Coniglio, F.; Festuccia, C.; Di Cesare, E.; Gravina, G.L.; Mattei, C.; Vitale, F.; Schenone, S.; et al. Suppression of SRC Signaling Is Effective in Reducing Synergy between Glioblastoma and Stromal Cells. *Mol. Cancer Ther.* **2016**, *15*, 1535–1544, doi:10.1158/1535-7163.MCT-15-1011.
15. O'Rourke, S.F.; McAnaney, H.; Hillen, T. Linear quadratic and tumour control probability modelling in external beam radiotherapy. *J. Math. Biol.* **2009**, *58*, 799–817, doi:10.1007/s00285-008-0222-y.
16. Hu, G.; Fang, W.; Liu, N.; Li, C. Effects of mir-128a on the invasion and proliferation of glioma U251 cells. *Oncol. Lett.* **2019**, *17*, 891–896, doi:10.3892/ol.2018.9651.

17. Stupp, R.; Mason, W.P.; van den Bent, M.J.; Weller, M.; Fisher, B.; Taphoorn, M.J.; Belanger, K.; Brandes, A.A.; Marosi, C.; Bogdahn, U., et al. Radiotherapy plus concomitant and adjuvant temozolomide for glioblastoma. *N. Engl. J. Med.* **2005**, *352*, 987–996, doi:10.1056/NEJMoa043330.
18. Buglione M., Triggiani L., Borghetti P., Pedretti S., Pasinetti N., Magrini S.M. The “Radioresistance” of Glioblastoma in the Clinical Setting, and the Present Therapeutic Options, In *Radiobiology of Glioblastoma*, Pirtoli L., Gravina G., Giordano A. (eds) Radiobiology of Glioblastoma. Current Clinical Pathology. Humana Press, Cham: Totowa, NJ, USA, 2016; pp. 15–27.
19. Mukhopadhyay, D.; Tsiokas, L.; Zhou, X.M.; Foster, D.; Brugge, J.S.; Sukhatme, V.P. Hypoxic induction of human vascular endothelial growth factor expression through c-Src activation. *Nature* **1995**, *375*, 577–581, doi:10.1038/375577a0.
20. Valle-Casuso, J.C.; Gonzalez-Sanchez, A.; Medina, J.M.; Tabernero, A. Hif-1 and C-Src Mediate Increased Glucose Uptake Induced by Endothelin-1 and Connexin43 In Astrocytes. *PLoS ONE* **2012**, *7*, e32448, doi:10.1371/journal.pone.0032448.
21. Cammarata, F.P.; Torrisi, F.; Forte, G.I.; Minafra, L.; Bravata, V.; Pisciotta, P.; Savoca, G.; Calvaruso, M.; Petringa, G.; Cirrone, G.A.P.; et al. Proton Therapy and Src Family Kinase Inhibitor Combined Treatments on U87 Human Glioblastoma Multiforme Cell Line. *Int. J. Mol. Sci.* **2019**, *20*, 4745, doi:10.3390/ijms20194745.
22. Choi, J.; Kang, J.O. Basics of Particle Therapy II: Relative Biological Effectiveness. *Radiat. Oncol. J.* **2012**, *30*, 1–13, doi:10.3857/roj.2012.30.1.1.
23. Plaks, V.; Kong, N.; Werb, Z. The Cancer Stem Cell Niche: How Essential Is The Niche in Regulating Stemness of Tumor Cells? *Cell Stem Cell* **2015**, *16*, 225–238, doi:10.1016/j.stem.2015.02.015.
24. Skuli, N.; Monferran, S.; Delmas, C.; Favre, G.; Bonnet, J.; Toulas, C.; Cohen-Jonathan Moyal, E. Alpha5beta3/Alpha5beta5 Integrins-Fak-RhoB: A Novel Pathway for Hypoxia Regulation in Glioblastoma. *Cancer Res.* **2009**, *69*, 3308–3316, doi:10.1158/0008-5472.CAN-08-2158.
25. Park, C.M.; Park, M.J.; Kwak, H.J.; Lee, H.C.; Kim, M.S.; Lee, S.H.; Park, I.C.; Rhee, C.H.; Hong, S.I. Ionizing Radiation Enhances Matrix Metalloproteinase-2 Secretion and Invasion of Glioma Cells Through Src/Epidermal Growth Factor Receptor-Mediated P38/Akt And Phosphatidylinositol 3-Kinase/Akt Signaling Pathways. *Cancer Res.* **2006**, *66*, 8511–8519, doi:10.1158/0008-5472.CAN-05-4340.
26. Roos, A.; Ding, Z.; Loftus, J.C.; Tran, N.L. Molecular and Microenvironmental Determinants of Glioma Stem-Like Cell Survival and Invasion. *Front. Oncol.* **2017**, *7*, 120, doi:10.3389/fonc.2017.00120.
27. Brown, J.M.; Wilson, W.R. Exploiting Tumour Hypoxia in Cancer Treatment. *Nat. Rev. Cancer* **2004**, *4*, 437–447, doi:10.1038/nrc1367.
28. Eom, K.Y.; Cho, B.J.; Choi, E.J.; Kim, J.H.; Chie, E.K.; Wu, H.G.; Kim, I.H.; Paek, S.H.; Kim, J.S.; Kim, I.A. The Effect of Chemoradiotherapy with SRC Tyrosine Kinase Inhibitor, PP2 and Temozolomide on Malignant Glioma Cells In Vitro and In Vivo. *Cancer Res. Treat.* **2016**, *48*, 687–697, doi:10.4143/crt.2014.320.
29. Carraro, F.; Naldini, A.; Pucci, A.; Locatelli, G.A.; Maga, G.; Schenone, S.; Bruno, O.; Ranise, A.; Bondavalli, F.; Brullo, C.; et al. Pyrazolo[3,4-D]Pyrimidines as Potent Antiproliferative and Proapoptotic Agents Toward A431 And 8701-Bc Cells in Culture Via Inhibition Of C-Src Phosphorylation. *J. Med. Chem.* **2006**, *49*, 1549–1561, doi:10.1021/jm050603r.
30. Tintori, C.; Fallacara, A.L.; Radi, M.; Zamperini, C.; Dreassi, E.; Crespan, E.; Maga, G.; Schenone, S.; Musumeci, F.; Brullo, C., et al. Combining X-Ray Crystallography and Molecular Modeling Toward the Optimization of Pyrazolo[3,4-D]Pyrimidines as Potent C-Src Inhibitors Active in Vivo Against Neuroblastoma. *J. Med. Chem.* **2015**, *58*, 347–361, doi:10.1021/jm5013159.
31. Lassman, A.B.; Pugh, S.L.; Gilbert, M.R.; Aldape, K.D.; Geinoz, S.; Beumer, J.H.; Christner, S.M.; Komaki, R.; DeAngelis, L.M.; Gaur, R.; et al. Phase 2 Trial of Dasatinib in Target-Selected Patients With Recurrent Glioblastoma (Rtog 0627). *Neuro Oncology* **2015**, *17*, 992–998, doi:10.1093/neuonc/nov011.
32. Galanis, E.; Anderson, S.K.; Twohy, E.L.; Carrero, X.W.; Dixon, J.G.; Tran, D.D.; Jeyapalan, S.A.; Anderson, D.M.; Kaufmann, T.J.; Feathers, R.W.; et al. A phase 1 and randomized, placebo-

- controlled phase 2 trial of bevacizumab plus dasatinib in patients with recurrent glioblastoma: Alliance/North Central Cancer Treatment Group N0872. *Cancer* **2019**, *125*, 3790–3800, doi:10.1002/cncr.32340.
33. Reardon, D.A.; Vredenburgh, J.J.; Desjardins, A.; Peters, K.B.; Sathornsumetee, S.; Threatt, S.; Sampson, J.H.; Herndon, J.E., 2nd; Coan, A.; McSherry, F.; et al. Phase 1 trial of dasatinib plus erlotinib in adults with recurrent malignant glioma. *Neuro oncolohy* **2012**, *108*, 499–506, doi:10.1007/s11060-012-0848-x.
 34. Franceschi, E.; Stupp, R.; van den Bent, M.J.; van Herpen, C.; Laigle Donadey, F.; Gorlia, T.; Hegi, M.; Lhermitte, B.; Strauss, L.C.; Allgeier, A.; et al. EORTC 26083 phase I/II trial of dasatinib in combination with CCNU in patients with recurrent glioblastoma. *Neuro Oncology* **2012**; *14*, 1503–1510, doi:10.1093/neuonc/nos256.
 35. Laack, N.N.; Galanis, E.; Anderson, S.K.; Leinweber, C.; Buckner, J.C.; Giannini, C.; Geoffroy, F.J.; Johnson, D.R.; Lesser, G.J.; Jaeckle, K.A.; et al. Randomized, placebo-controlled, phase II study of dasatinib with standard chemo-radiotherapy for newly diagnosed glioblastoma (GBM), NCCTG N0877 (Alliance). *J. Clin. Oncol.* **2017**, *33*, 2013.
 36. Agarwal, S.; Mittapalli, R.K.; Zellmer, D.M.; Gallardo, J.L.; Donelson, R.; Seiler, C.; Decker, S.A.; Santacruz, K.S.; Pokorny, J.L.; Sarkaria, J.N.; et al. Active efflux of Dasatinib from the brain limits efficacy against murine glioblastoma: Broad implications for the clinical use of molecularly targeted agents. *Mol. Cancer Ther.* **2012**, *11*, 2183–2192, doi:10.1158/1535-7163.MCT-12-0552.
 37. Fallacara, A.L.; Zamperini, C.; Podolski-Renic, A.; Dinic, J.; Stankovic, T.; Stepanovic, M.; Mancini, A.; Rango, E.; Iovenitti, G.; Molinari, A.; et al. A New Strategy for Glioblastoma Treatment: In Vitro and In Vivo Preclinical Characterization of Si306, a Pyrazolo[3,4-d]Pyrimidine Dual Src/P-Glycoprotein Inhibitor. *Cancers (Basel)* **2019**, *11*, 848, doi:10.3390/cancers11060848.
 38. Chapman, J.D. Can the Two Mechanisms of Tumor Cell Killing by Radiation Be Exploited for Therapeutic Gain? *J. Radiat. Res.* **2014**, *55*, 2–9, doi:10.1093/jrr/rrt111.
 39. Joiner, M.; van der Kogel, A.; *Basic clinical radiobiology*, 4th ed.; Taylor & Fransis Group: London, UK, 2009; p. 375.
 40. Vicario, N.; Bernstock, J.D.; Spitale, F.M.; Giallongo, C.; Giunta, M.A.S.; Li Volti, G.; Gulisano, M.; Leanza, G.; Tibullo, D.; Parenti, R.; et al. Clobetasol Modulates Adult Neural Stem Cell Growth via Canonical Hedgehog Pathway Activation. *Int. J. Mol. Sci.* **2019**, *20*, doi:10.3390/ijms20081991.
 41. Mauri, E.; Sacchetti, A.; Vicario, N.; Peruzzotti-Jametti, L.; Rossi, F.; Pluchino, S. Evaluation of RGD functionalization in hybrid hydrogels as 3D neural stem cell culture systems. *Biomater. Sci.* **2018**, *6*, 501–510, doi:10.1039/c7bm01056g.
 42. Gulino, R.; Vicario, N.; Giunta, M.A.S.; Spoto, G.; Calabrese, G.; Vecchio, M.; Gulisano, M.; Leanza, G.; Parenti, R. Neuromuscular Plasticity in a Mouse Neurotoxic Model of Spinal Motoneuronal Loss. *Int. J. Mol. Sci.* **2019**, *20*, doi:10.3390/ijms20061500.



© 2020 by the authors. Submitted for possible open access publication under the terms and conditions of the Creative Commons Attribution (CC BY) license (<http://creativecommons.org/licenses/by/4.0/>).

Review

The Role of Hypoxia and SRC Tyrosine Kinase in Glioblastoma Invasiveness and Radioresistance

Filippo Torrisi ^{1,†}, Nunzio Vicario ^{1,†}, Federica M. Spitale ¹, Francesco P. Cammarata ^{2,*}, Luigi Minafra ², Lucia Salvatorelli ³, Giorgio Russo ², Giacomo Cuttone ⁴, Samuel Valable ⁵, Rosario Gulino ¹, Gaetano Magro ³ and Rosalba Parenti ^{1,*}

¹ Department of Biomedical and Biotechnological Sciences (BIOMETEC), Section of Physiology, University of Catania, 95123 Catania; filippo.torrisi@unict.it (F.T.); nunziovicario@unict.it (N.V.); federica.spitale94@gmail.com (F.M.S.); rosario.gulino@unict.it (R.G.)

² Institute of Molecular Bioimaging and Physiology, National Research Council, IBFM-CNR, 90015 Cefalù, Italy; luigi.minafra@ibfm.cnr.it (L.M.); giorgio.russo@ibfm.cnr.it (G.R.)

³ Department G.F. Ingrassia, Azienda Ospedaliero-Universitaria “Policlinico-Vittorio Emanuele” Anatomic Pathology, University of Catania, 95125 Catania, Italy; lucia.salvatorelli@unict.it (L.S.); g.magro@unict.it (G.M.)

⁴ National Laboratory of South, National Institute for Nuclear Physics (LNS-INFN), 95125 Catania, Italy; cuttone@lns.infn.it (G.C.)

⁵ Normandie Université, UNICAEN, CEA, CNRS, ISTCT/CERVOxy group, GIP Cyceon, 14074 Caen, France; samuel.valable@cnrs.fr (S.V.)

† These authors equally contributed to this work as co-first.

* Correspondence: francesco.cammarata@ibfm.cnr.it (F.P.C.) and parenti@unict.it (R.P.).

Received: 3 September 2020; Accepted: 30 September; Published: date

Simple Summary: The biological pathways underlying glioblastoma malignancy and radioresistance are still unclear. In this review, we describe the role of the hypoxic microenvironment and SRC proto-oncogene non-receptor tyrosine kinase in the activation of radioresistance and invasion pathways of glioblastoma. We also highlight the hypoxia- and ionizing radiation-induced infiltration, providing updated evidences on the involvement of SRC in these processes. Optimizing radiotherapy and identifying druggable molecular players are crucial steps to improve current glioblastoma therapeutic strategies.

Abstract: Advances in functional imaging are supporting neurosurgery and radiotherapy for glioblastoma, which still remains the most aggressive brain tumor with poor prognosis. The typical infiltration pattern of glioblastoma, which impedes a complete surgical resection, is coupled with a high rate of invasiveness and radioresistance, thus further limiting efficient therapy, leading to inevitable and fatal recurrences. Hypoxia is of crucial importance in gliomagenesis and, besides reducing radiotherapy efficacy, also induces cellular and molecular mediators that foster proliferation and invasion. In this review, we aimed at analyzing the biological mechanism of glioblastoma invasiveness and radioresistance in hypoxic niches of glioblastoma. We also discussed the link between hypoxia and radiation-induced radioresistance with activation of SRC proto-oncogene non-receptor tyrosine kinase, prospecting potential strategies to overcome the current limitation in glioblastoma treatment.

Keywords: Glioblastoma; hypoxia; radioresistance; invasion; SRC tyrosine kinase; targeted therapy

1. Introduction

Glioblastoma (GBM) is the most frequent and aggressive primary brain tumor with an incidence of 5/100,000 per year and a median survival of 12–15 months after diagnosis, despite aggressive multimodal treatments [1]. Recent genetic and molecular advances on GBM cellular states provided both genetic and micro-environmental determinants, establishing four GBM subtypes recapitulating astrocyte-like, mesenchymal-like, neural-progenitor-like, and oligodendrocyte-progenitor-like phenotypes [2,3]. Such a classification specifies molecular and genetic profiles associated with GBM subtypes, thus providing additional information to the histopathological characterization in accordance with World Health Organization guidelines [4]. Histologically, GBM is a highly cellular glioma composed by glial cells with marked nuclear atypia and pleomorphism (Figure 1a). Common typical diagnostic features are microvascular proliferation (Figure 1b), often with glomerular-like appearance and palisading necrosis characterized by regular areas of necrosis surrounded by dense accumulations of neoplastic cells (Figure 1b). Proliferative activity is usually prominent with highly mitotic count. The proliferation index is evaluated immunohistochemically by analyzing the proportion of cells expressing the nuclear markers of proliferation Ki-67, accounting for a total of 15–20% of GBM cells, even if some tumors show a proliferation index greater than 50% (Figure 1c). Two different molecular types of GBM are recognized: GBM isocitrate dehydrogenase (IDH)-wildtype and GBM IDH-mutant, which are commonly associated with primary and secondary GBM, respectively. Indeed, based on mutation of other genes, in GBM IDH-wildtype, the gliomagenesis occurs early due to the amplification/mutation of epidermal growth factor receptor (EGFR) and the loss of the phosphatase and tensin homolog (PTEN) gene. In GBM IDH-mutant, the mutation of tumor protein p53 (TP53) and the deletion of 1p/19q determine the acquisition of the genetic alteration, resulting in a lower grade astrocytoma or oligodendroglioma.

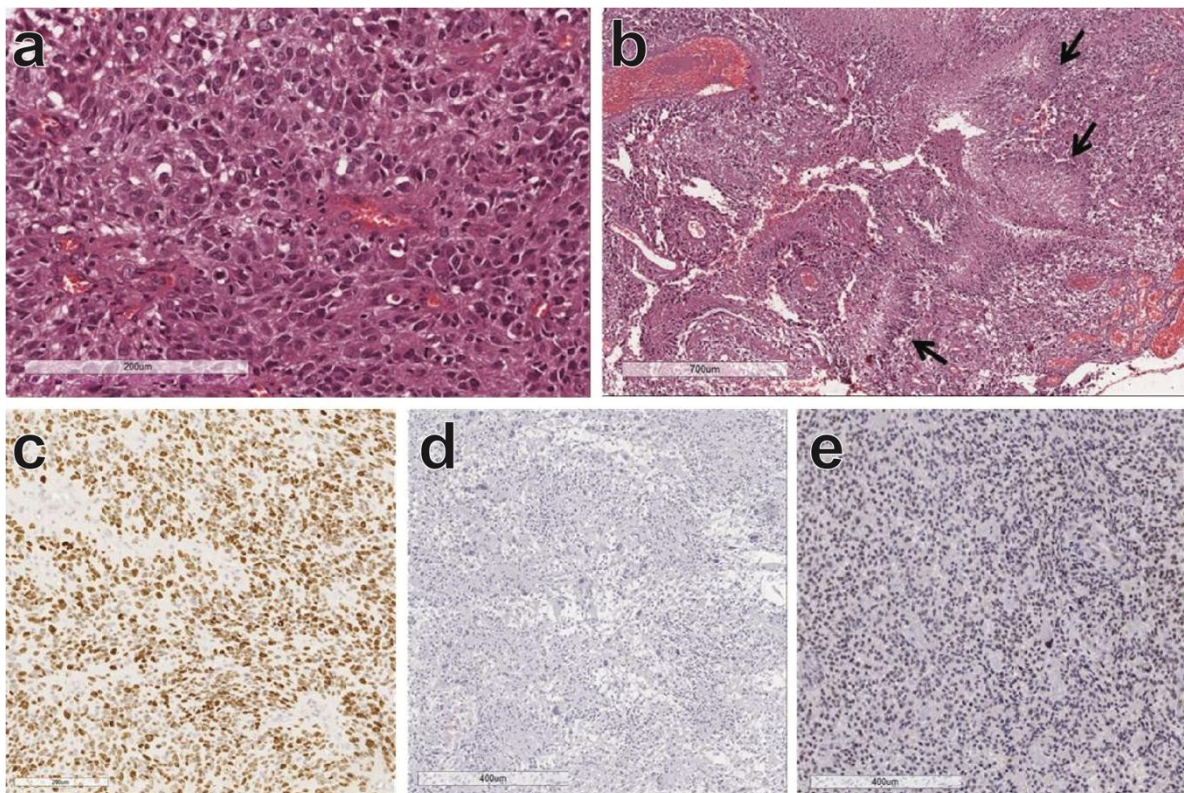


Figure 1. Glioblastoma, isocitrate dehydrogenase (IDH) wildtype. Highly anaplastic glial cells with nuclear atypia and pleomorphism (a); palisading necrosis (arrows) and microvascular proliferation (b); at immunohistochemistry the neoplastic cells show a high proliferation index (Ki67); (c) no immunostaining for IDH-1; (d) and retained ATRX chromatin remodeler (ATRX) (e).

GBM IDH-wildtype is more frequent, usually occurs in older patients (mean age: 62 years), and it is characterized by absence of mutated IDH-1 (Figure 1d) and expression of ATRX chromatin remodeler (ATRX, Figure 1e) is expressed. Conversely, GBM IDH-mutant, is less frequent and develops in significantly younger patients (mean age 45 years). It may arise from a lower grade glioma (diffuse or anaplastic astrocytoma) and shows IDH-1 mutation and loss of ATRX.

Many advances have been made to elucidate the biological mechanisms promoting GBM development and progression, including genetic mutations, metabolism, and the microenvironment role. A common denominator is the hypoxic microenvironment that characterizes this scenario, feeding the renewed players of the tumor set. Therefore, hypoxia and associated necrosis have provided this tremendous neoplasm with an identity card, showing salient marks of the different subtypes and stages of invasiveness and aggressiveness.

Despite recent evidence expanding the current knowledge on GBM, therapeutic options for newly diagnosed cases are still limited to surgery, standard chemotherapy (i.e., temozolomide), and radiotherapy [1]. Indeed, clinical reports showed that radiotherapy combined with temozolomide improves the overall survival of patients, after surgical resection [5]. Current guidelines indicate radiotherapy dosing up to 60 Gy for 30 fractions (2 Gy/day) as the best approach to reduce radiotherapy-induced side effects and to counteract radioresistance and recurrences [6]. Hypofractionated treatment of 40 Gy in 15 fractions over 3 weeks is suggested only for patients older than 70 years old and with poor performance status [7].

However, in this context, in order to reduce GBM aggressiveness and to simultaneously increase the effect of the radiation dose, there is an urgent clinical need to develop targeted therapy and radiosensitizing agents. Strategies to reach this aim should take into account two main features of GBM: hypoxia and invasiveness. These two features are also correlated with each other; indeed, hypoxia is known to support GBM radioresistance and it is also involved in increased GBM invasiveness and infiltration into the surrounding tissue [8].

In this sense, it is essential to dissect hypoxia-related events which play a central role in determining cancer cell invasiveness and infiltration into the surrounding tissue, and also in causing radioresistance. The investigation of molecular mechanisms may elucidate the relationship between GBM hallmarks and hypoxia, providing new key molecular targets.

In this review we describe the role of hypoxia and the molecular mechanisms involved in GBM invasiveness and radioresistance, focusing on the involvement of SRC proto-oncogene non-receptor tyrosine kinase (SRC). We also report potential strategies to improve efficacy of radiotherapy against hypoxia, invasiveness, and SRC activation.

2. SRC Proto-Oncogene Non-Receptor Tyrosine Kinase and Glioblastoma

Previous studies revealed that SRC is shaping GBM pathophysiology and features such as proliferation, migration, invasiveness, and angiogenesis [9]. SRC is composed of 4 SRC homology domains (SH): SH4 is linked to N-terminal with a 14-carbon myristic acid moiety, a unique domain different for all members and whose function is far to be fully elucidated, SH3 is a non-catalytic domain and SH2 linked, with a SH2-kinase linker, to the SH1 domain, containing a kinase domain involved in the activation of SRC autophosphorylation at the level of the tyrosine residue (Tyr419), followed by a C-terminal negative regulatory domain (Tyr530) [10]. In particular, the autophosphorylation of Tyr419 switches the protein from an inactive to an active conformation, whereas the phosphorylation of Tyr530 determines the binds of the SH2 domain and the inhibition of protein kinase activity. There are various hypotheses to explain the aberrant activation mechanisms of SRC in tumors that mostly concern the destabilization of the SH4-SH3-SH2-Linker-SH1, leading to the promotion of adhesion, invasion, and motility. Indeed, SRC protein can be activated by the direct binding of the SH2 and SH3 domains with other surface receptors, such as integrins, with cytoplasmic tyrosine kinases, such as focal adhesion kinase (FAK), or with the cytoplasmic portion of activated receptor tyrosine kinases (RTKs), which hinder the inhibitory SRC interactions [11]. The integrin/FAK/SRC axis regulates intercellular interaction and communication between cells and the extracellular matrix (ECM) in a signal transduction manner. Integrins and FAK colocalize on the focal adhesions, and SH2 and SH3 domains are respectively high affinity sites for binding with the autophosphorylation domain and with proline-rich regions of the FAK. On one side, the interaction of FAK

with the SH2 domain of SRC displaces the salt bridge formed after Tyr530 phosphorylation in the closed conformation and leads to activation of SRC. Conversely, following the SRC-FAK bond, SRC phosphorylates two tyrosine residues on the FAK kinase domain, increasing their kinase activity. The FAK-SRC complex phosphorylates the serine and threonine sites of paxilline, which regulates the Rho family of GTPases, such as RhoA, promoting actin-stress-fiber formation in order to regulate the structural organization of the cytoskeleton for adhesion, motility, and cell division [12]. In addition, SRC phosphorylates tyrosine residues of the C-terminal of FAK which acts as a binding site for other molecules that regulate communication signaling between cells or between cells and ECM [13]. In particular, these processes are mediated by the formation of the FAK-SRC complex that regulates guanine-exchange factors and GTPase-activating proteins, leading to membrane protrusion or cytoplasmatic projections formation such as filopodia [14]. Furthermore, the activation of SRC mediated by RTKs, through the interaction with SH2 domains or the recruitment of small GTPases Ras/Ral and the inhibition of the Csk negative regulator, leads to downstream multiple effectors, such as PI3K/Akt, Ras/Raf/MAPK, STAT3/STAT5B, and p130 Cas pathways, which are respectively involved in survival, proliferation, angiogenesis, and motility [15] (Figure 2).

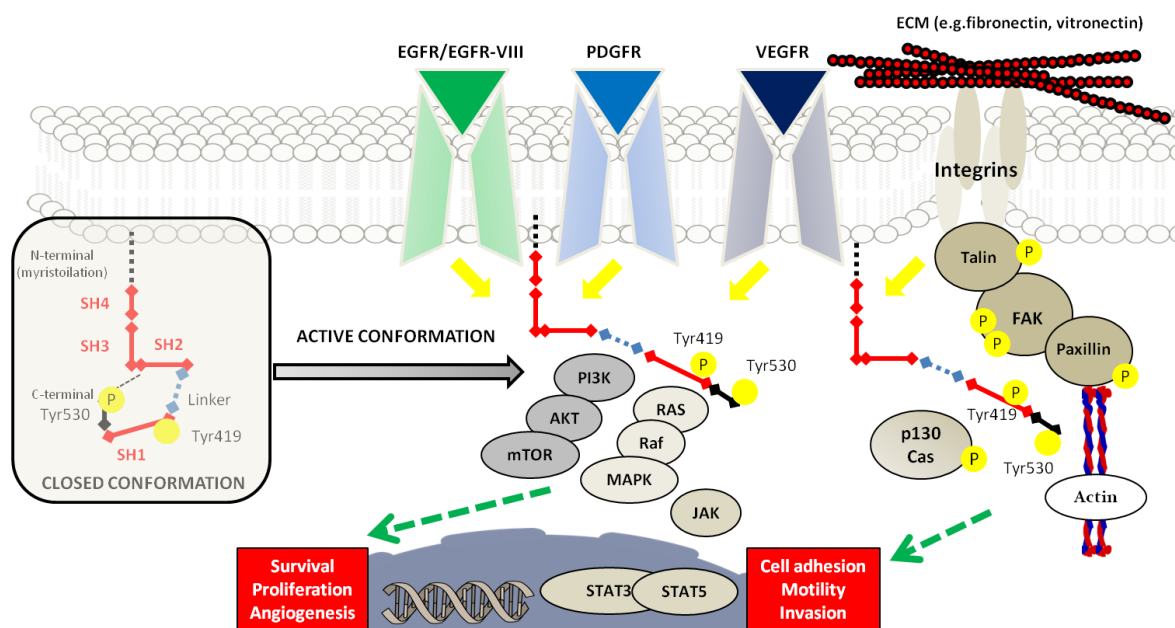


Figure 2. Schematic representation of SRC structure and regulation. The inactive form of SRC is illustrated on the left side, with the specification of each SH domain; in this closed conformation, the phosphorylation of Tyr530 on C-terminal creates a link with the SH2 and the catalytic site, which is positioned on SH1, becoming not accessible for the substrates. In the transition to the active form, the phosphorylation of Tyr419 is showed with the main pathways that act by downstream and upstream effectors. The conformational switch is mediated by many phosphatases, such as PTP α , PTP γ , SHP-1 and -2, and PTP1B, able to dephosphorylate SRC. The regulation of activated SRC is displayed with the RTKs and integrins signaling. In particular, the downstream effectors of RTKs/SRC interaction lead to target genes transcription for survival, proliferation, and angiogenesis sustainment. The interaction of integrins with ECM components and their localization on cell adhesion sites, determines the modulation of cell motility: The SRC signaling pathway induces a cascade that results in the phosphorylation of several proteins, such as FAK, talin, and paxillin, with the final actin cytoskeleton regulation that is responsible for migration and invasion mechanisms.

Since the discovery of SRC as a proto-oncogene, the role of SRC in cancers has been largely investigated, and due to the rare cases of gene mutation and amplification, it has remained unclear for a long time. Then, much evidence supported the oncogenic role of SRC mainly due to the interaction with various signaling molecules activating pathways for the promotion, maintenance, and progression of several cancers. Deregulation of SRC was not only associated with central nervous system cancers, but also with several others, including prostate, colorectal, breast, lung, head-neck, and pancreatic cancers [16]. In addition to

SRC, also other proteins among the non-receptor tyrosine kinase family have been associated with tumor development, including Fgr, Fyn, Yes, and Lyn [16].

In GBM, the absence of gene amplification and mutation confirmed that the hyperactivation of SRC is linked to aberrant activation of RTKs and surface receptors [17]. Indeed, FAK and other RTKs, including epidermal growth factor receptor (EGFR), platelet-derived growth factor receptor (PDGFR), and vascular endothelial growth factor receptor (VEGFR), determine the loss of SRC interdomains interactions involved in SRC inhibition, leading to most of the GBM-associated phenomena [9,18–20]. The role of SRC in GBM progression is not only directly linked to the main proliferation and survival pathways affected by deregulation of downstream RTKs; indeed, it was also found that SRC modulates the activation or the overexpression of proinflammatory transcription factors, contributing to an increase in aggressiveness and support of the complex tumor microenvironment [21]. The microenvironment has a key role in GBM; cancer cells establish a complex network with reactive stroma composed by a heterogenic cell population, including immune cells, fibroblasts, precursor cells, endothelial cells, macrophages, lymphocytes, as well as signaling molecules and ECM components [22]. For these reasons, SRC signaling in GBM holds great promise and may provide crucial insight into developing new therapeutic approaches.

3. Hypoxia and Glioblastoma

Despite hypoxia being usually associated with cell suffering and death, it has a different connotation in solid tumors, representing a common feature of increased malignancy. In fact, hypoxia can trigger the production of inflammatory mediators which potentiate neoplastic risk [23]; furthermore, in response to hypoxia, tumor tissues activate the production of VEGF, which is one of the main downstream targets of the HIF-1 α pathway, increasing vascular permeability and promoting angiogenesis. The creation of new vessels is fundamental for the stromal blood supply in order to maintain the rate of cell growth [24].

Intratumoral oxygen pressure (pO₂) values in GBM represent a critical aspect of the radiotherapy approach. The aerobic value of the brain tissue is of about 40 mmHg in physiological conditions, whereas it has been shown to be significantly lower in GBM [25]. To be defined hypoxic, a tissue must reach a pO₂ value below 10 mmHg, which is the result of the unbalanced oxygen supply and consumption rate [26]. In GBM, hypoxia ranges from mild (pO₂ = 20 to 4 mmHg) to severe condition (pO₂ = 4 to 0.75 mmHg), especially in necrotic and micronecrotic areas [26]. Hypoxia occurs when the distance to the nearest blood vessel is impeding appropriate exchanges but also when blood perfusion is altered. In general, both phenomena occur in GBM and it is considered that chronic but also cycling hypoxia take place, making it very difficult to deal with such a complex scenario [27].

4. Hypoxic Regulation of SRC in Glioblastoma Development and Invasion

Hypoxia seems to play a major role in the SRC tyrosine-kinase pathway, which is constitutively activated in several malignant human tumors, including GBM [28–30]. In fact, all the RTKs described above are targets of the transcription factors hypoxia-inducible factor-1 α (HIF-1 α), which is induced under conditions of low oxygen. The oxygen-sensitive subunits of HIF transcription factors are normally synthesized in normoxic condition, but they are unstable and targeted for ubiquitination and degradation by the von Hippel–Lindau protein (VHL). VHL is able to recognize HIF-1 α /HIF-2 α thanks to their hydroxylation that is performed by prolyl hydroxylases, which use molecular oxygen as a cofactor; for this reason, under hypoxic condition, HIF-1 α and HIF-2 α cannot be hydroxylated and they bind the HIF-1 β subunit, allowing gene transcription regulation [31]. Indeed, as early as 1995, it has been shown that phosphorylated SRC protein is highly active in GBM cells, particularly under hypoxic conditions [32]. In this study, it has also been shown that the increase in SRC activity in hypoxia causes the VEGF upregulation, which therefore represents a downstream transcription of the SRC pathway induced by hypoxia [32]. Moreover, a correlation between angiogenesis and hypoxia was also sustained by the observation of a significant increase in vascularization related to the hypoxia-signaling pathway involving integrin upregulation [33,34]. The integrin overexpression in hypoxic GBM cells was correlated to the activation of FAK, which promotes the activation of small GTPase such as RhoB. RhoB increases the phosphorylation leading to the inhibition of glycogen synthase kinase-3 β (GSK-3 β) pathway, involved in the degradation

of HIF-1 α [35]. This evidence supported angiogenesis inhibition as a strategy for GBM therapy; however, it was shown that in response to the anti-VEGF antibody (Bevacizumab), further cell survival mechanisms were activated due to increased SRC signaling [36]. The robust invasion in response to anti-VEGF may be, at least partially, associated with neo-vascular loss, low perfusion, and consequent hypoxia, which induces SRC activation [37]. In addition to angiogenesis, metabolism alteration has been identified as a typical hallmark of GBM, mainly due to the hypoxic condition that promotes the upregulation of glycolysis by HIFs and sustains the so-called Warburg effect [38]. In this scenario, there is not a direct link between the metabolism alteration and the SRC activity in GBM; among the factors influencing GBM metabolism, the MYC oncoprotein has been shown to increase glycolysis in GBM and its regulation has been associated with the SRC pathway in other tumors. Therefore, there is likely an involvement of the SRC-MYC axis in driving metabolic reprogramming, in addition to the RTKs expression by HIF-1 α [39].

GBM is a highly infiltrating tumor characterized by intense proliferation, the ability to invade surrounding tissue, and dysregulated biological pathways operating in both intra- and extra-cellular compartments. Among the most crucial alterations, the dysfunction of cellular metabolism leads to a series of consecutive events which invariably affect the degree of malignancy. In particular, hypoxic conditions are known to control the expression of target genes such as VEGF, TGF- β 2, MMP-1,2, and 9, human plasminogen activator inhibitor type 1, endothelin-1, and erythropoietin (EPO), influencing angiogenesis, tumor growth, and GBM invasiveness [40–42].

Hypoxia also supports a complex remodeling of cytoskeleton, which includes a number of linked events such as i) alteration of cell adhesion, ii) activation of cell motility, iii) production of proteolytic enzymes. Cell adhesion modification occurs through the modulation of E-cadherin expression, which is commonly altered in tumors [43], generally as a result of mutation or gene suppression by hypermethylation [44]. It has been reported that E-cadherin expression decreases in high grade brain tumor as compared to healthy tissue [45]. In particular, a shift occurs from E-cadherin to N-cadherin expression, which increases the interaction between cancer and stromal cells [46], promoting the activation of cell motility as part of the complex epithelial-mesenchymal transition (EMT) [46]. Several pathways are involved in the cadherin switching, consisting in the upregulation of N-cadherin, which creates less efficient adherent junctions than E-cadherin. In this context, it has been demonstrated that zinc finger E-box binding homeobox 1 (ZEB1) was upregulated in U87 cells under hypoxic conditions, with the consequent nuclear accumulation with HIF-1 α and HIF-2 α . Roundabout guidance receptor 1 (ROBO) is a downstream effector of ZEB1, which takes part in the process of loss of N-cadherin adhesion to the cytoskeleton, thus promoting motility and finally supporting the EMT process [47,48].

After cell adhesion loss, cancer cells increase their motility by a number of processes such as stimulating the activity of cytoskeleton, autocrine/paracrine chemotaxis or proteolysis activity, and ECM degradation [49]. Cancer cells are stimulated to move via interactions between adhesion molecules (i.e., integrins) and the products of ECM degradation. Under hypoxic condition, GBM cells increase interactions between the mutated form of epidermal growth factor receptor vIII (EGFR-vIII) and α v β 3 and α v β 5 integrins [50,51] which are recruited on the cell membrane surface, leading to invasion enhancement mediated by FAK activation [35]. Such a process generates the so-called adhesion plate, where integrins interact with FAK promoting cytoskeleton contraction and proliferative effects by intracellular signal transduction. It is noteworthy that phosphorylation of FAK is induced in hypoxia by a pathway that involved the procollagen-lysine 2-oxoglutarate 5-dioxygenase (PLOD2) [52].

The production of proteolytic enzymes is a crucial event during invasion. In particular, increased activity of matrix metalloproteases (MMPs) is associated with higher grade glioma and correlated with shorter overall survival in GBM patients [53,54], even if in vitro studies on GBM cell lines provided evidence of a heterogeneous expression of MMPs [55,56]. On this aspect, a well-characterized effect is mediated by hypoxia. Indeed, low oxygenation indirectly promotes MMP-9 and MMP-2 upregulation and increased proteolytic activity, by reducing pH levels in the tumor microenvironment. This condition is related to the increased metabolic activity of the tumor that, based on glycolysis in hypoxic conditions, increases the lactic acid levels by gradually reducing the pH [57]. In addition, induction of type A lactate dehydrogenase (LDH-A), regulating the transforming growth factor- β 2 (TGF- β 2), has been shown to trigger the cascade of transcriptional regulation of MMP-2 and integrin α v β 3 expression, strongly influencing the tumor

invasiveness [58]. It is noteworthy that the tissue inhibitor of metalloproteases (TIMP) and TIMP-like molecules, which are synthesized and released by resident cells, counteracting ECM degradation including MMPs, inhibit GBM invasion [59,60].

SRC drives GBM invasion and progression [9,61]. The hypoxia-induced SRC pathway entirely influences the process described above, finally resulting in fostered invasiveness. In fact, it primarily involves EGFR-vIII and integrin $\beta 3$ interaction, the recruitment of $\alpha v \beta 3$ integrin on GBM cell membranes and the creation of focal adhesion complexes by FAK activation [62]. Finally, the EGFRvIII / integrin $\beta 3$ / FAK / SRC axis leads to the activation of the intracellular signaling pathway ERK1/2, MAPK, AKT, and STAT3, which determines the upregulation of MMP-2 and MMP-9, further promoting cell invasion [63]. It is also interesting that the SRC-induced TGF β pathway activation via α -SMA is associated with the promotion of cancer-associated fibroblasts (CAFs), which further increase chemotactic mediated migration of GBM cells (Figure 3) [30,64].

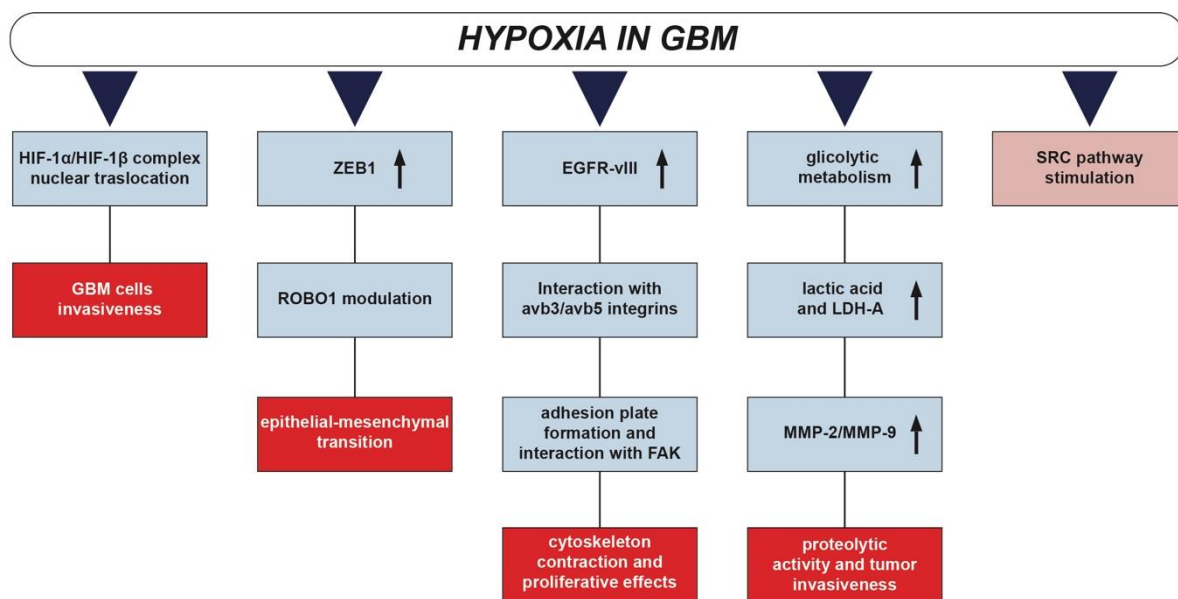


Figure 3. Schematic representation of the main pathways for the invasion process induced by hypoxia. SRC pathway stimulation under hypoxia contributes to the deregulation of the principal events required for invasion, including cell adhesion, activation of cell motility, and production of proteolytic enzymes.

5. Hypoxia-SRC Axis Promoting Glioblastoma Radioresistance

Hypoxia-induced radioresistance in GBM is a radiobiological event due to the interaction between ionizing radiation (IR) and the biological matter. IR can determine direct and indirect damage to all organelles and macromolecules of cells [65]. IR induces single strand breaks, or double strand breaks, directly on DNA molecules, which are difficult to repair and are associated with oxygen-independent-cell death. Vice versa, indirect damage is closely linked to the presence of oxygen. Indeed, IR interacting with water molecules induces the formation of reactive oxygen species (ROS) through a radiolysis reaction, which is much more efficient in well oxygenated tissues that facilitate the formation of superoxide radical and hyperoxide, leading to the amplification of damage and increased radiotherapy efficiency [66]. In particular, according to oxygen fixation hypothesis, increasing ROS concentration induces the so-called “fixed damage from oxygen” on DNA, invariably leading to cell death [67]. In hypoxic areas, the effect of cell death induced by ROS and oxygen reactions is less efficient, with the resulting radioresistance. In view of the crucial significance of the GBM hypoxic condition, the “oxygen effect” and the response to radiotherapy treatment is assessed by the oxygen enhancement ratio (OER) parameter, which is defined as the ratio between the dose in hypoxia and normoxia to reach the same biological effect [68].

It has been shown that the majority of GBM recurrences occur at the margins of surgical resection or within the high dose irradiation field, likely associated to residual cells that receive a sublethal irradiation and escape from the primary tumor, while underlying molecular mechanisms remained partially uncovered

[69,70]. Moreover, the high incidences of recurrences within the high-dose irradiation field, in close proximity (1–2 cm) to the primary tumor, is associated to the existence of a subpopulation of resistant cells with stem cell-like properties, called glioblastoma stem cells (GSCs), which are promoted in the high hypoxic site or niches [71,72]. It was reported that IR promoted the phenotypical switch from neural to mesenchymal types in GSCs in recurrences; the IR induces the production of proinflammatory factors or NF- κ B and induction of C/EBP- β , which in turn activates CD109 transcription binding its promoter. CD109 is a clear marker of the mesenchymal subtype [73]. GSCs were also implicated in the formation of new blood vessels in response to IR, enhancing their trans-differentiation in tumor derived endothelial cells, by the activation of the Tie2 signaling pathway [74]. SRC was found highly expressed in GSCs, where they can enhance the migratory ability [75] and potentiate the stemness properties being a downstream target, together with transcription 3 (STAT3)-Kirsten rat sarcoma viral oncogene homolog (KRAS), in the MerTK pathway. Indeed, MerTK is upregulated in GBM and it was reported that the silencing of KRAS and SRC suppressed mesenchymal markers and GSC features in MerTK-overexpressing X01 GBM stem-like cells [76].

Besides being active during hypoxia, SRC activation has been found to promote invasiveness and motility of cancer cells in response to radiotherapy; in breast cancer cells it has been shown that fractional irradiation caused an increase in SRC phosphorylation [77]. In the same study, it has been observed that SRC inhibition reduced cell migration and the expression of markers associated with the EMT process [77]. The activation of malignant phenotypes of GBM in response to radiation was reported through the induction of MMP-2, involving pathways mediated by the interaction of SRC with EGFR. In this study, it has been reported that IR induced phosphorylation of SRC kinase and that SRC inhibition by PP2 reduced MMP-2 secretion, AKT activation, and SRC phosphorylation in irradiated cells. Moreover, PP2 was able to block IR-induced EGFR phosphorylation, whereas inhibition of EGFR did not affect the phosphorylation of SRC, identifying the possibility that radiation may stimulate the SRC activation regardless of EGFR/AKT pathway [78]. It has been also reported that IR-induced invasion modulating the ECM protein, is not only due to MMP action, but also to high production of other components such as hyaluronic acid, which acts as an extracellular signaling molecule for the mesenchymal shift of GBM, in response to radiation; hyaluronic acid is recognized by the CD44 receptor, which is a clear marker of the mesenchymal subtype. The interaction of hyaluronic acid and the CD44 receptor, leads to SRC activation, promoting tumor progression and radioresistance [79]. Moreover, IR-SRC activation promotes invasion processes also due to FAK, ephrin type-A receptor 2 (EphA2), and EGFR-vIII signaling [80]. The EGFR-vIII expressing cells have been shown to release ligands such as hepatocyte growth factor (HGF) and interleukin 6 (IL6), activating SRC in EGFR expressing cells, thus increasing diffusion and infiltration [81].

The SRC pathways induced by IR have been also evaluated in relation to the intercellular communication systems in the context of signal molecules transmission by connexin-based channel and extracellular vesicles [82–84]. It has been shown *in vitro* that connexin43 (Cx43)-gap junction and -hemichannel activity is implicated in invadopodia formation and function responsible for invasion capacity and MMP-2 activity by Cx43 dynamic interactions with partners including SRC [85,86]. It has also been shown that following irradiation, GBM cells can release exosomes, which stimulate the migration of recipient cells. In this condition, cells increase the expression of proteins involved in cell migration, including SRC, in addition to focal adhesion kinase (FAK), paxillin, and T neurotrophic tyrosine kinase receptor type 1 (TrkA) [87].

6. New Frontiers to Improve Radiotherapy: Evaluating the Potential of Synergistic Approaches

It is well known that hypoxia is associated with increased resistance to IR, contributing to treatment failures after radiotherapy based on X-rays. The need for new strategies to improve radiotherapy has become increasingly urgent and research efforts are currently focusing on studying synergistic approaches to overcome current limitations.

An action plan adopted to counteract hypoxia-induced radioresistance involves a model known as “hypoxia dose painting”, based on providing a personalized radiation dose according to local phenotypic or microenvironmental variations of the tumor, influenced by spatial and temporal heterogeneity of hypoxia [26,88]. Other aspects take into consideration the IR physical features including specific linear energy transfer (LET), which also have an impact on radiotherapy efficacy and biological effects. LET is a measure

of ionization density and it is defined as the average energy (keV) transferred by a particle along the 1 μm path [89]. High LET particles show high ionization density, thus inducing increased direct cell damage, but display lower indirect effects mediated by ROS and other radicals [89,90]. Another main advantage of particle-based radiation therapy is the finite dose deposition in the tissue that allows sparing the normal brain tissue. Consequently, a frontier in radiotherapy is to combine multiple ion beams simultaneously, in order to deliver low-LET radiation in normoxic tumor areas and high-LET radiation in the hypoxic tumor microenvironment, in so doing optimizing IR-induced cell damage in a microenvironment-dependent manner [91]. Reoxygenation strategies have been also developed to improve radiotherapy efficacy both during the course of irradiation and by radiosensitizing drugs or nanoparticles delivered into the tumor to improve oxygenation [92,93].

Targeting the molecular mechanisms regulated by hypoxia represents a promising way to sensitize GBM cells to treatments. In general, the rationale to use radiosensitizing agents is to reduce the dose of IR maintaining similar biological effects in terms of cell death and reducing radiotherapy side-effects. Such a concept is expressed as dose modifying factor or sensitized enhancement ratio, both indicating the ratio between the dose alone and in the presence of the radiosensitizer to determine the same biological effect [94]. Radiosensitive agents also hold great potential to increase effectiveness of radiotherapy reducing OER with multivariate effects, such as blocking specific pathway induced by hypoxia, or enhancing DNA damage by affecting self-repairing mechanisms [95]. In addition to radiosensitive agents designed for specific biological targets, further promising candidates for synergistic approaches include sodium borocaptate (BSH) and boron phenylalanine (BPA). The combination of BSH/BPA with IR can determine an increase in therapeutic efficacy by increasing the LET, due to a selective accumulation of the Boron isotope ^{10}B inside cancer cells that react with the thermal neutron to produce high-energy alpha particles, leading to the so-called boron neutron capture therapy (BNCT) [96]. Good results have been obtained, especially in Japan, thanks to imaging techniques labeling the BPA [97]; the main challenge for this promising therapy is not only related to the cost and availability of the neutron sources in clinical settings but also to the research of new boron carriers capable to cross the blood brain barrier [98]. A similar strategy using BSH/BPA combined with protons for proton boron capture therapy (PBCT) has revealed the possibility to enhance the proton therapy effectiveness, but preliminary results have been obtained and no clinical trials for GBM have been proposed so far [99].

Hypoxia induces a number of intracellular reactions such as the activation of the transcription factor HIF, which in turn activate a variety of cellular process in response to the lowering oxygen level [100]. Several molecular targets have been described as radiosensitizing agents in hypoxic conditions. For instance, EPO transcription is regulated by the HIF-1 α /HIF-1 β complex and it has a key role in GBM proliferation and survival through the AKT/PI3K pathway and the upregulation of Bcl-2/Bcl-xL anti apoptotic factors. Therefore, EPO receptor silencing not only increases the sensitivity of glioma cells to chemotherapy (temozolomide) as well as X-rays, but also counteracts the hypoxia-induced chemo- and radio-resistance [101]; for this reason, targeted therapy, such as specific antibodies, may be applied directly to EPO, EPO receptor, or to another downstream mediator of EPO receptor signaling pathway such as STAT3. Likewise, the hypoxic cell radiosensitizer doranidazole (PR-350) administration in malignant significantly enhanced radiation-induced reproductive cell death in vitro under hypoxia, suggesting a potent strategy for improving the clinical outcome of radiotherapy, reducing related side effects [102]. A promising strategy to enhance the radiosensitivity of GBM is represented by the application of targeted molecules that weaken the DNA damage response (DDR) signaling pathway. DDR can be considered as a group of highly interconnected signaling pathways, that cooperate to preserve the survival in response to the DNA damage by irradiation; DDR activation contributes to enhance radioresistance of GBM, which is able to reach high levels of double strand DNA break repair proficiency. The most representative agents belonging to this radiosensitizers group are inhibitors of the poly(ADP-ribose) polymerase (PARP) proteins; PARP are involved in DNA repair pathways, especially for DNA single-strand breaks [103]. Veliparib and olaparib are PARP inhibitors, largely evaluated at both the preclinical and clinical stages. However, despite some promising results, veliparib has not been shown to be effective in combination with temozolomide and radiotherapy in new diagnosed GBM [104]; clinical trials for olaparib are currently ongoing, and additional

upstream or downstream DDR biomarkers, including DNA-dependent protein kinase and cell cycle checkpoint inhibitors are attractive target for the radiosensitization of GBM [105].

Beside radiosensitizing agents, novel strategies have also been tested as molecularly targeted drugs. Cilengitide is a drug that selectively blocks activation of the $\alpha v\beta 3$ and $\alpha v\beta 5$ integrins, amplifying the effect of IR and triggering an enhanced apoptotic response and tumor growth suppression [106]. Unfortunately, the results of two large phase-III clinical trials showed that combination of cilengitide, radiotherapy, and temozolomide for newly diagnosed GBM does not improve progression free survival and overall survival as compared to radiotherapy and temozolomide alone [107]. As previously reported, FAK participates with SRC in adhesion and migration signaling network; moreover, they are upregulated and activated in GBM influencing growth and motility. The combination of radiotherapy and FAK inhibition also provided promising results, showing radiosensitization in GBM cell lines in vitro [108]. Further studies encouraged the development of a potent, ATP-competitive, reversible inhibitor of FAK, called GSK2256098. A phase I clinical trial evaluated the tolerability for GBM treatment and additional clinical trials are evaluating the therapeutic efficiency of such an approach [109]. Likewise, inhibition of MMP-14 in combination with radiotherapy and temozolomide improved the survival of glioma-bearing mice as compared to single treatment group [110]; nevertheless, the main MMP inhibitor, marimastat, was tested with temozolomide, but not with radiotherapy, in a phase II trial for recurrent GBM [111].

SRC activation leads to different pathways activation, promoting cell adhesion, motility, survival, proliferation, and angiogenesis. Moreover, SRC is also activated in response to IR, promoting invasiveness and malignancy of GBM as a consequence. For this reason, SRC inhibition combined with RT represents a promising approach to increase the therapeutic effect as well as to block GBM progression. The SRC pathway is targeted by radiosensitizing strategies tested to treat GBM in preclinical studies or at different phases of active clinical trials. Several SRC inhibitors were tested to treat GBM and they have been recently reviewed by Cirotti et al. [21]. Noteworthy, dasatinib (Sprycel, by Bristol-Myers Squibb) was the most used in clinical trial. It is a dual inhibitor SRC/ABL proto-oncogene 1-non-receptor tyrosine kinase, also inhibiting other SRC family kinases, such as LYN proto-oncogene and FYN proto-oncogene SRC. In a single-arm phase II trial, dasatinib was tested as monotherapy and was considered ineffective to proceed to stage 2 [112]. The evidences of SRC inhibition to reduce invasiveness induced by anti-VGFA led to perform an additional trial, in which dasatinib was tested in combination with bevacizumab [36]. Even in this trial, dasatinib does not show a significant improvement as compared with bevacizumab alone [36]; no additional improvements were provided in combination with EGFR (erlotinib) [113] and cyclonexyl-chloroethyl-nitrosourea (CCNU) [114]. Recently, a clinical trial evaluating dasatinib in combination with temozolomide and radiotherapy on newly diagnosed glioblastoma did not show promising results (NCT00869401). The current efforts in evaluating SRC inhibition potential are coupled with research in drug design to develop optimized SRC inhibitors for combinatorial approaches with radiotherapy. Such a field benefits from the current knowledge on the limitations of previously tested drugs. For example, it is now clear that pharmacodynamic issues, such as overexpression of efflux transporters P-gp at the blood-brain barrier levels, strongly affects dasatinib efficiency [115]. Current efforts aim at the design of new SRC inhibitor drugs aiming at the optimization of combinatorial approaches with radiotherapy.

A new SRC inhibitor, belonging to the pyrazolo[3'-d] pyrimidines series (i.e. Si306, Lead Discovery Siena, Italy) showed an excellent pharmacodynamic profile and was able to significantly inhibit GBM cell growth in highly P-gp expressing cells as compared to dasatinib [116]. We previously demonstrated that Si306 showed a synergic radiosensitive effect with proton irradiation in GBM cell lines [117]. We also identified up- or down-regulated genes associated with the SRC pathway modulation in GBM cells after irradiation with proton therapy [117]. After 2 or 10 Gy irradiation with protons, we detected that the GBM cell cycle, motility, survival, and proliferation rate were strongly affected by Si306, also showing increased overall radiation efficiency [117]. Moreover, Si306 has been tested in combination with X-ray both in normoxic and hypoxic conditions, demonstrating a significantly increased effect as compared to radiotherapy alone [30,118]. These findings are encouraging the investigations on SRC mechanisms in order to discover a valuable approach to develop new effective therapy against GBM. Most of the trials with targeted therapy were conducted in patients with recurrent GBM and rarely were tested in combination with radiotherapy. Further studies and evidence from in vitro and preclinical studies could enhance the

importance of molecularly targeted drugs in association with radiotherapy, increasing the number of clinical trials, in order to propose new solution to GBM treatment.

7. Conclusions

The dynamic GBM profile is still limiting our knowledge on its progression and invasion. Nevertheless, the remarkable progress that is gradually being made allows us to have some clear conditions on which to focus our attention. Indeed, it is now widely accepted that the microenvironment, which can be defined hostile for its hypoxic and necrotic characteristics, paradoxically proves to be a survival stimulus for cancer cells able to reprogram molecules and pathways and above all migrate to new sites, so arguing, in short, the aggressive phenotype and invasiveness of the tumor.

Classical therapeutic approaches are facing strong limitations due to the intrinsic characteristics of GBM, such as heterogeneity, high invasiveness, and marked angiogenesis, but also due to physiological barriers protecting the central nervous system, such as the blood-brain barrier, and off target and side effects. The ideal approach therefore would be a synergistic combination of therapies specifically developed to counteract this aggressive brain tumor. Hypoxia-induced pathways dysregulation certainly represents the beating heart of GBM. Optimizing radiotherapy and its functional variables using target therapy against specific molecular actors, such as SRC, represents a promising path that needs to be smoothed out in the shortest possible time.

Author Contributions: Conceptualization, F.T., N.V., R.P.; writing—original draft preparation, F.T., N.V., F.P.C., R.G., S.V., G.M., R.P.; writing—review and editing, F.T., N.V., F.M.S., F.P.C., L.M., L.S., G.R., G.C., S.V., R.G., G.M., R.P. All authors have read and agreed to the published version of the manuscript

Funding: F.T. was supported by the PhD programme in Biotechnology (Biometec, University of Catania, Italy). N.V. was supported by the PON AIM R&I 2014–2020 - E66C18001240007. F.M.S. was supported by the International PhD programme in Neuroscience and PO FSE 2014–2020 Fellow (Biometec, University of Catania, Italy). The research was supported by PRIN 2017, Grant no.: 2017XKWWK9_004 to R.P., G.R. and G.C. from Italian “Ministero dell’Istruzione, dell’Università e della Ricerca”.

Conflicts of Interest: The authors declare no conflict of interest.

Abbreviations

BPA	Boron phenylalanine
BSH	Sodium borocaptate
Cx43	Connexin43
DDR	DNA damage response
ECM	Extracellular matrix
EGF	Epidermal growth factor receptor
EMT	Epithelial–mesenchymal transition
EPO	Erythropoietin
FAK	Focal adhesion kinases
GBM	Glioblastoma
HIF-1 α	Hypoxia-inducible factor-1 α
IR	Ionizing radiation
LET	Linear energy transfer
MMPs	Matrix metalloproteases
OER	Oxygen enhancement ratio
ROS	Reactive oxygen species
RTKs	Receptors tyrosine kinases
SH	SRC homology domains
SRC	SRC proto-oncogene non-receptor tyrosine kinase
TIMPs	Tissue inhibitor of metalloproteases
VEGFR	Vascular endothelial growth factor receptor

References

1. Wen, P.Y.; Weller, M.; Lee, E.Q.; Alexander, B.; Barnholtz-Sloan, J.S.; Barthel, F.P.; Batchelor, T.T.; Bindra, R.S.; Chang, S.M.; Chiocca, E.A.; et al. Glioblastoma in Adults: A Society for Neuro-Oncology (SNO) and European Society of Neuro-Oncology (EANO) Consensus Review on Current Management and Future Directions. *Neuro-Oncology* **2020**, *22*, 1073–1113, doi:10.1093/neuonc/noaa106.
2. Verhaak, R.G.; Hoadley, K.A.; Purdom, E.; Wang, V.; Qi, Y.; Wilkerson, M.D.; Miller, C.R.; Ding, L.; Golub, T.; Mesirov, J.P.; et al. Integrated Genomic Analysis Identifies Clinically Relevant Subtypes of Glioblastoma Characterized by Abnormalities in PDGFRA, IDH1, EGFR, and NF1. *Cancer Cell* **2010**, *17*, 98–110, doi:10.1016/j.ccr.2009.12.020.
3. Neftel, C.; Laffy, J.; Filbin, M.G.; Hara, T.; Shore, M.E.; Rahme, G.J.; Richman, A.R.; Silverbush, D.; Shaw, M.L.; Hebert, C.M.; et al. An Integrative Model of Cellular States, Plasticity, and Genetics for Glioblastoma. *Cell* **2019**, *178*, 835–849.e21, doi:10.1016/j.cell.2019.06.024.
4. Louis, D.N.; Perry, A.; Reifenberger, G.; Von Deimling, A.; Figarella-Branger, M.; Cavenee, W.K.; Ohgaki, H.; Wiestler, O.D.; Kleihues, P.; Ellison, D.W. The 2016 World Health Organization Classification of Tumors of the Central Nervous System: a summary. *Acta Neuropathol.* **2016**, *131*, 803–820, doi:10.1007/s00401-016-1545-1.
5. Cabrera, A.R.; Kirkpatrick, J.; Fiveash, J.B.; Shih, H.A.; Koay, E.J.; Lutz, S.; Petit, J.; Chao, S.T.; Brown, P.D.; Vogelbaum, M.; et al. Radiation therapy for glioblastoma: Executive summary of an American Society for Radiation Oncology Evidence-Based Clinical Practice Guideline. *Pr. Radiat. Oncol.* **2016**, *6*, 217–225, doi:10.1016/j.prro.2016.03.007.
6. Fernandes, C.; Costa, A.; Osório, L.; Lago, R.C.; Linhares, P.; Carvalho, B.; Caeiro, C.; De Vleeschouwer, S. Current Standards of Care in Glioblastoma Therapy. *Glioblastoma* **2017**, 197–241.
7. Ohno, M.; Miyakita, Y.; Takahashi, M.; Igaki, H.; Matsushita, Y.; Ichimura, K.; Narita, Y. Survival benefits of hypofractionated radiotherapy combined with temozolomide or temozolomide plus bevacizumab in elderly patients with glioblastoma aged ≥ 75 years. *Radiat. Oncol.* **2019**, *14*, 200–10, doi:10.1186/s13014-019-1389-7.
8. Monteiro, A.R.; Hill, R.; Pilkington, G.J.; Madureira, P.A. The Role of Hypoxia in Glioblastoma Invasion. *Cells* **2017**, *6*, 45, doi:10.3390/cells6040045.
9. Ahluwalia, M.S.; De Groot, J.F.; Liu, W. (Michael); Gladson, C.L. Targeting SRC in glioblastoma tumors and brain metastases: Rationale and preclinical studies. *Cancer Lett.* **2010**, *298*, 139–149, doi:10.1016/j.canlet.2010.08.014.
10. Roskoski, R. Src protein-tyrosine kinase structure, mechanism, and small molecule inhibitors. *Pharmacol. Res.* **2015**, *94*, 9–25, doi:10.1016/j.phrs.2015.01.003.
11. Sen, B.; Johnson, F.M. Regulation of Src Family Kinases in Human Cancers. *J. Signal Transduct.* **2011**, *2011*, 1–14, doi:10.1155/2011/865819.
12. Deakin, N.O.; Turner, C.E. Paxillin comes of age. *J. Cell Sci.* **2008**, *121*, 2435–44, doi:10.1242/jcs.018044.
13. Guan, J.-L. Integrin signaling through FAK in the regulation of mammary stem cells and breast cancer. *IUBMB Life* **2010**, *62*, 268–276, doi:10.1002/iub.303.
14. Huveneers, S.; Danen, E.H. Adhesion signaling - crosstalk between integrins, Src and Rho. *J Cell Sci* **2009**, *122*, 1059–1069, doi:10.1242/jcs.039446.
15. Lieu, C.; Kopetz, S. The SRC family of protein tyrosine kinases: a new and promising target for colorectal cancer therapy. *Clin. Color. Cancer* **2010**, *9*, 89–94, doi:10.3816/CCC.2010.n.012.
16. Wheeler, D.L.; Iida, M.; Dunn, E.F. The Role of Src in Solid Tumors. *Oncol.* **2009**, *14*, 667–678, doi:10.1634/theoncologist.2009-0009.
17. Mitra, S.K.; Schlaepfer, D.D. Integrin-regulated FAK-Src signaling in normal and cancer cells. *Curr Opin Cell Biol* **2006**, *18*, 516–523, doi:10.1016/j.ceb.2006.08.011.
18. Bolós, V. The dual kinase complex FAK-Src as a promising therapeutic target in cancer. *OncoTargets Ther.* **2010**, *3*, 83, doi:10.2147/OTT.S6909.
19. An, Z.; Aksoy, O.; Zheng, T.; Fan, Q.-W.; Weiss, W.A. Epidermal growth factor receptor and EGFRvIII in glioblastoma: signaling pathways and targeted therapies. *Oncogene* **2018**, *37*, 1561–1575, doi:10.1038/s41388-017-0045-7.
20. Ding, Q.; Stewart, J.; Olman, M.A.; Klobe, M.R.; Gladson, C.L.; Jr., J.S. The Pattern of Enhancement of Src Kinase Activity on Platelet-derived Growth Factor Stimulation of Glioblastoma Cells Is Affected by the Integrin Engaged. *J. Biol. Chem.* **2003**, *278*, 39882–39891, doi:10.1074/jbc.m304685200.
21. Cirotti, C.; Contadini, C.; Barilà, D. SRC Kinase in Glioblastoma News from an Old Acquaintance. *Cancers* **2020**, *12*, 12, doi:10.3390/cancers12061558.

22. Valtorta, S.; Salvatore, D.; Rainone, P.; Belloli, S.; Bertoli, G.; Moresco, R.M. Molecular and Cellular Complexity of Glioma. Focus on Tumour Microenvironment and the Use of Molecular and Imaging Biomarkers to Overcome Treatment Resistance. *Int. J. Mol. Sci.* **2020**, *21*, 5631, doi:10.3390/ijms21165631.
23. Coussens, L.M.; Werb, Z. Inflammation and cancer. *Nat.* **2002**, *420*, 860–867, doi:10.1038/nature01322.
24. Krock, B.L.; Skuli, N.; Simon, M.C. Hypoxia-Induced Angiogenesis. *Genes Cancer* **2011**, *2*, 1117–1133, doi:10.1177/1947601911423654.
25. Valable, S.; Corroyer-Dulmont, A.; Chakhoyan, A.; Durand, L.; Toutain, J.; Divoux, D.; Barré, L.; MacKenzie, E.T.; Petit, E.; Bernaudin, M.; et al. Imaging of brain oxygenation with magnetic resonance imaging: A validation with positron emission tomography in the healthy and tumoural brain. *Br. J. Pharmacol.* **2016**, *37*, 2584–2597, doi:10.1177/0271678X16671965.
26. Gérard, M.; Corroyer-Dulmont, A.; Lesueur, P.; Collet, S.; Chérel, M.; Bourgeois, M.; Stefan, D.; Limkin, E.J.; Perrio, C.; Guillamo, J.-S.; et al. Hypoxia Imaging and Adaptive Radiotherapy: A State-of-the-Art Approach in the Management of Glioma. *Front. Med.* **2019**, *6*, doi:10.3389/fmed.2019.00117.
27. Mendichovszky, I.; Jackson, A. Imaging hypoxia in gliomas. *Br. J. Radiol.* **2011**, *84*, S145–S158, doi:10.1259/bjr/82292521.
28. Fianco, G.; Cenci, C.; Barilà, D. Caspase-8 expression and its Src-dependent phosphorylation on Tyr380 promote cancer cell neoplastic transformation and resistance to anoikis. *Exp. Cell Res.* **2016**, *347*, 114–122, doi:10.1016/j.yexcr.2016.07.013.
29. Lluís, J.M.; Buricchi, F.; Chiarugi, P.; Morales, A.; Fernández-Checa, J.C. Dual Role of Mitochondrial Reactive Oxygen Species in Hypoxia Signaling: Activation of Nuclear Factor- κ B via c-SRC and Oxidant-Dependent Cell Death. *Cancer Res.* **2007**, *67*, 7368–7377, doi:10.1158/0008-5472.can-07-0515.
30. Calgani, A.; Vignaroli, G.; Zamperini, C.; Coniglio, F.; Festuccia, C.; Di Cesare, E.; Gravina, G.L.; Mattei, C.; Vitale, F.; Schenone, S.; et al. Suppression of SRC signaling is effective in reducing synergy between glioblastoma and stromal cells. *Mol. Cancer Ther.* **2016**, *15*, 1535–1544, doi:10.1158/1535-7163.MCT-15-1011.
31. Huang, W.-J.; Chen, W.-W.; Zhang, X. Glioblastoma multiforme: Effect of hypoxia and hypoxia inducible factors on therapeutic approaches. *Oncol. Lett.* **2016**, *12*, 2283–2288, doi:10.3892/ol.2016.4952.
32. Mukhopadhyay, D.; Tsiokas, L.; Zhou, X.-M.; Foster, D.; Brugge, J.S.; Sukhatme, V.P. Hypoxic induction of human vascular endothelial growth factor expression through c-Src activation. *Nat.* **1995**, *375*, 577–581, doi:10.1038/375577a0.
33. Delamarre, E.; Taboubi, S.; Mathieu, S.; Berenguer, C.; Rigot, V.; Lissitzky, J.-C.; Figarella-Branger, M.; Ouafik, L.; Luis, J. Expression of Integrin α 6 β 1 Enhances Tumorigenesis in Glioma Cells. *Am. J. Pathol.* **2009**, *175*, 844–855, doi:10.2353/ajpath.2009.080920.
34. Da Ponte, K.F.; Berro, D.H.; Collet, S.; Constans, J.-M.; Valable, S.; Emery, E.; Guillamo, J.-S. In Vivo Relationship Between Hypoxia and Angiogenesis in Human Glioblastoma: A Multimodal Imaging Study. *J. Nucl. Med.* **2017**, *58*, 1574–1579, doi:10.2967/jnumed.116.188557.
35. Skuli, N.; Monferran, S.; Delmas, C.; Favre, G.; Bonnet, J.; Toulas, C.; Moyal, E.C.-J. v3/ v5 Integrins-FAK-RhoB: A Novel Pathway for Hypoxia Regulation in Glioblastoma. *Cancer Res.* **2009**, *69*, 3308–3316, doi:10.1158/0008-5472.can-08-2158.
36. Huvelde, D.; Lewis-Tuffin, L.J.; Carlson, B.L.; Schroeder, M.A.; Rodríguez, F.; Giannini, C.; Galanis, E.; Sarkaria, J.N.; Anastasiadis, P.Z. Targeting Src Family Kinases Inhibits Bevacizumab-Induced Glioma Cell Invasion. *PLOS ONE* **2013**, *8*, e56505, doi:10.1371/journal.pone.0056505.
37. Keunen, O.; Johansson, M.; Oudin, A.; Sanzey, M.; Rahim, S.A.A.; Fack, F.; Thorsen, F.; Taxt, T.; Bartoš, M.; Jirik, R.; et al. Anti-VEGF treatment reduces blood supply and increases tumor cell invasion in glioblastoma. *Proc. Natl. Acad. Sci.* **2011**, *108*, 3749–3754, doi:10.1073/pnas.1014480108.
38. Libby, C.J.; Tran, A.N.; Scott, S.E.; Griguer, C.; Hjelmeland, A.B. The pro-tumorigenic effects of metabolic alterations in glioblastoma including brain tumor initiating cells. *Biochim. et Biophys. Acta (BBA) - Bioenerg.* **2018**, *1869*, 175–188, doi:10.1016/j.bbcan.2018.01.004.
39. Tateishi, K.; Iafrate, A.J.; Ho, Q.; Curry, W.T.; Batchelor, T.T.; Flaherty, K.T.; Onozato, M.L.; Lelic, N.; Sundaram, S.; Cahill, D.P.; et al. Myc-Driven Glycolysis Is a Therapeutic Target in Glioblastoma. *Clin. Cancer Res.* **2016**, *22*, 4452–65, doi:10.1158/1078-0432.CCR-15-2274.
40. Kaur, B.; Khwaja, F.W.; Severson, E.A.; Matheny, S.L.; Brat, D.J.; Van Meir, E.G. Hypoxia and the hypoxia-inducible-factor pathway in glioma growth and angiogenesis. *Neuro-oncology* **2005**, *7*, 134–153, doi:10.1215/S1152851704001115.

41. Gabriely, G.; Wheeler, M.A.; Takenaka, M.C.; Quintana, F.J. Role of AHR and HIF-1 α in Glioblastoma Metabolism. *Trends Endocrinol. Metab.* **2017**, *28*, 428–436, doi:10.1016/j.tem.2017.02.009.
42. Méndez, O.; Zavadil, J.; Esencay, M.; Lukyanov, Y.; Santovasi, D.; Wang, S.-C.; Newcomb, E.W.; Zagzag, D. Knock down of HIF-1 α in glioma cells reduces migration in vitro and invasion in vivo and impairs their ability to form tumor spheres. *Mol. Cancer* **2010**, *9*, 133, doi:10.1186/1476-4598-9-133.
43. Jeanes, A.; Gottardi, C.J.; Yap, A.S. Cadherins and cancer: how does cadherin dysfunction promote tumor progression? *Oncogene* **2008**, *27*, 6920–6929, doi:10.1038/onc.2008.343.
44. Alsaleem, M.; Toss, M.S.; Joseph, C.; Aleskandarany, M.; Kurozumi, S.; Alshankyty, I.; Ogden, A.; Rida, P.C.G.; Ellis, I.; Aneja, R.; et al. The molecular mechanisms underlying reduced E-cadherin expression in invasive ductal carcinoma of the breast: high throughput analysis of large cohorts. *Mod. Pathol.* **2019**, *32*, 967–976, doi:10.1038/s41379-019-0209-9.
45. Lewis-Tuffin, L.J.; Rodríguez, F.; Giannini, C.; Scheithauer, B.; Necela, B.M.; Sarkaria, J.N.; Anastasiadis, P.Z. Misregulated E-Cadherin Expression Associated with an Aggressive Brain Tumor Phenotype. *PLOS ONE* **2010**, *5*, e13665, doi:10.1371/journal.pone.0013665.
46. Noh, M.-G.; Oh, S.-J.; Ahn, E.-J.; Kim, Y.-J.; Jung, T.-Y.; Jung, S.; Kim, K.K.; Lee, J.-H.; Lee, K.-H.; Moon, K.-S. Prognostic significance of E-cadherin and N-cadherin expression in Gliomas. *BMC Cancer* **2017**, *17*, 583, doi:10.1186/s12885-017-3591-z.
47. Siebzehnrübl, F.A.; Silver, D.J.; Tugertimur, B.; Deleyrolle, L.P.; Siebzehnrubl, D.; Sarkisian, M.R.; Devers, K.G.; Yachnis, A.T.; Kupper, M.D.; Neal, D.; et al. The ZEB1 pathway links glioblastoma initiation, invasion and chemoresistance. *EMBO Mol. Med.* **2013**, *5*, 1196–1212, doi:10.1002/emmm.201302827.
48. Joseph, J.V.; Conroy, S.; Pavlov, K.; Sontakke, P.; Tomar, T.; Eggens-Meijer, E.; Balasubramaniyan, V.; Wagemakers, M.; Dunnen, W.F.A.D.; Kruyt, F.A. Hypoxia enhances migration and invasion in glioblastoma by promoting a mesenchymal shift mediated by the HIF1 α -ZEB1 axis. *Cancer Lett.* **2015**, *359*, 107–116, doi:10.1016/j.canlet.2015.01.010.
49. Bravo-Cordero, J.J.; Hodgson, L.; Condeelis, J. Directed cell invasion and migration during metastasis. *Curr. Opin. Cell Boil.* **2012**, *24*, 277–283, doi:10.1016/j.ceb.2011.12.004.
50. Liu, Z.; Han, L.; Dong, Y.; Tan, Y.; Li, Y.; Zhao, M.; Xie, H.; Ju, H.; Wang, H.; Zhao, Y.; et al. EGFRvIII/integrin β 3 interaction in hypoxic and vitronectinenriching microenvironment promote GBM progression and metastasis. *Oncotarget* **2015**, *7*, 4680–4694, doi:10.18632/oncotarget.6730.
51. Malric, L.; Monferran, S.; Gilhodes, J.; Boyrie, S.; Dahan, P.; Skuli, N.; Sesen, J.; Filleron, T.; Kowalski-Chauvel, A.; Moyal, E.C.-J.; et al. Interest of integrins targeting in glioblastoma according to tumor heterogeneity and cancer stem cell paradigm: an update. *Oncotarget* **2017**, *8*, 86947–86968, doi:10.18632/oncotarget.20372.
52. Xu, Y.; Zhang, L.; Wei, Y.; Zhang, X.; Xu, R.; Han, M.; Huang, B.; Chen, A.; Li, W.; Zhang, Q.; et al. Procollagenlysinase 2-oxoglutarate 5-dioxygenase 2 promotes hypoxia-induced glioma migration and invasion. *Oncotarget* **2017**, *8*, 23401–23413, doi:10.18632/oncotarget.15581.
53. Aaberg-Jessen, C.; Christensen, K.; Offenberg, H.; Bartels, A.; Dreehsen, T.; Hansen, S.; Schröder, H.D.; Brünner, N.; Kristensen, B.W. Low expression of tissue inhibitor of metalloproteinases-1 (TIMP-1) in glioblastoma predicts longer patient survival. *J. Neuro-Oncology* **2009**, *95*, 117–128, doi:10.1007/s11060-009-9910-8.
54. Crocker, M.; Ashley, S.; Giddings, I.; Petrik, V.; Hardcastle, A.; Aherne, W.; Pearson, A.; Bell, B.A.; Zacharoulis, S.; Papadopoulos, M.C. Serum angiogenic profile of patients with glioblastoma identifies distinct tumor subtypes and shows that TIMP-1 is a prognostic factor. *Neuro-oncology* **2010**, *13*, 99–108, doi:10.1093/neuonc/noq170.
55. Stamenkovic, I. Matrix metalloproteinases in tumor invasion and metastasis. *Semin. Cancer Boil.* **2000**, *10*, 415–433, doi:10.1006/scbi.2000.0379.
56. Hagemann, C.; Anacker, J.; Ernestus, R.-I.; Vince, G.H. A complete compilation of matrix metalloproteinase expression in human malignant gliomas. *World J. Clin. Oncol.* **2012**, *3*, 67–79, doi:10.5306/wjco.v3.i5.67.
57. Cassim, S.; Pouyssegur, J. Tumor Microenvironment: A Metabolic Player that Shapes the Immune Response. *Int. J. Mol. Sci.* **2019**, *21*, 157, doi:10.3390/ijms21010157.
58. Baumann, F.; Leukel, P.; Doerfelt, A.; Beier, C.P.; Dettmer, K.; Oefner, P.J.; Kastenberger, M.; Kreutz, M.; Nickl-Jockschat, T.; Bogdahn, U.; et al. Lactate promotes glioma migration by TGF- β 2-dependent regulation of matrix metalloproteinase-2. *Neuro-Oncology* **2009**, *11*, 368–380, doi:10.1215/15228517-2008-106.
59. Jiang, Y.; Goldberg, I.D.; Shi, Y.E. Complex roles of tissue inhibitors of metalloproteinases in cancer. *Oncogene* **2002**, *21*, 2245–2252, doi:10.1038/sj.onc.1205291.

60. Lampert, K.; Machein, U.; Machein, M.R.; Conca, W.; Peter, H.H.; Volk, B. Expression of Matrix Metalloproteinases and Their Tissue Inhibitors in Human Brain Tumors. *Am. J. Pathol.* **1998**, *153*, 429–437, doi:10.1016/s0002-9440(10)65586-1.
61. Lewis-Tuffin, L.J.; Feathers, R.; Hari, P.; Durand, N.; Li, Z.; Rodriguez, F.J.; Bakken, K.; Carlson, B.; Schroeder, M.; Sarkaria, J.N.; et al. Src family kinases differentially influence glioma growth and motility. *Mol. Oncol.* **2015**, *9*, 1783–1798, doi:10.1016/j.molonc.2015.06.001.
62. Ellert-Miklaszewska, A.; Poleszak, K.; Pasierbinska, M.; Kaminska, B. Integrin Signaling in Glioma Pathogenesis: From Biology to Therapy. *Int. J. Mol. Sci.* **2020**, *21*, 888, doi:10.3390/ijms21030888.
63. Keller, S.; Schmidt, M.H.H. EGFR and EGFRvIII Promote Angiogenesis and Cell Invasion in Glioblastoma: Combination Therapies for an Effective Treatment. *Int. J. Mol. Sci.* **2017**, *18*, 1295, doi:10.3390/ijms18061295.
64. Trylcova, J.; Busek, P.; Smetana, K.; Balaziová, E.; Dvorankova, B.; Mifkova, A.; Šedo, A. Effect of cancer-associated fibroblasts on the migration of glioma cells in vitro. *Tumor Boil.* **2015**, *36*, 5873–5879, doi:10.1007/s13277-015-3259-8.
65. Reisz, J.A.; Bansal, N.; Qian, J.; Zhao, W.; Furdui, C.M. Effects of Ionizing Radiation on Biological Molecules—Mechanisms of Damage and Emerging Methods of Detection. *Antioxidants Redox Signal.* **2014**, *21*, 260–292, doi:10.1089/ars.2013.5489.
66. Azzam, E.I.; Jay-Gerin, J.-P.; Pain, D. Ionizing radiation-induced metabolic oxidative stress and prolonged cell injury. *Cancer Lett.* **2012**, *327*, 48–60, doi:10.1016/j.canlet.2011.12.012.
67. Grimes, D.R.; Partridge, M. A mechanistic investigation of the oxygen fixation hypothesis and oxygen enhancement ratio. *Biomed. Phys. Eng. Express* **2015**, *1*, 045209, doi:10.1088/2057-1976/1/4/045209.
68. Wenzl, T.; Wilkens, J.J. Theoretical analysis of the dose dependence of the oxygen enhancement ratio and its relevance for clinical applications. *Radiat. Oncol.* **2011**, *6*, 171, doi:10.1186/1748-717X-6-171.
69. Wank, M.; Schilling, D.; Schmid, T.E.; Meyer, B.; Gempt, J.; Barz, M.; Schlegel, J.; Liesche, F.; Kessel, K.A.; Wiestler, B.; et al. Human Glioma Migration and Infiltration Properties as a Target for Personalized Radiation Medicine. *Cancers* **2018**, *10*, 456, doi:10.3390/cancers10110456.
70. Kargiotis, O.; Geka, A.; Rao, J.S.; Kyritsis, A.P. Effects of irradiation on tumor cell survival, invasion and angiogenesis. *J. Neuro-Oncology* **2010**, *100*, 323–338, doi:10.1007/s11060-010-0199-4.
71. Rivera, M.; Sukhdeo, K.; Yu, J.S. Ionizing Radiation in Glioblastoma Initiating Cells. *Front. Oncol.* **2013**, *3*, 74,, doi:10.3389/fonc.2013.00074.
72. Fine, H.A. Glioma stem cells: not all created equal. *Cancer Cell* **2009**, *15*, 247–9, doi:10.1016/j.ccr.2009.03.010.
73. Minata, M.; Audia, A.; Shi, J.; Lu, S.; Bernstock, J.D.; Pavlyukov, M.S.; Das, A.; Kim, S.-H.; Shin, Y.J.; Lee, Y.; et al. Phenotypic Plasticity of Invasive Edge Glioma Stem-like Cells in Response to Ionizing Radiation. *Cell Rep.* **2019**, *26*, 1893–1905.e7, doi:10.1016/j.celrep.2019.01.076.
74. Deshors, P.; Toulas, C.; Arnauduc, F.; Malric, L.; Siegfried, A.; Nicaise, Y.; Lemarié, A.; Larrieu, D.; Tosolini, M.; Moyal, E.C.-J.; et al. Ionizing radiation induces endothelial transdifferentiation of glioblastoma stem-like cells through the Tie2 signaling pathway. *Cell Death Dis.* **2019**, *10*, 816–15, doi:10.1038/s41419-019-2055-6.
75. Han, X.; Zhang, W.; Yang, X.; Wheeler, C.G.; Langford, C.P.; Wu, L.; Filippova, N.; Friedman, G.K.; Ding, Q.; Fathallah-Shaykh, H.M.; et al. The role of Src family kinases in growth and migration of glioma stem cells. *Int. J. Oncol.* **2014**, *45*, 302–310, doi:10.3892/ijco.2014.2432.
76. Eom, H.; Kaushik, N.; Yoo, K.-C.; Shim, J.-K.; Kwon, M.; Choi, M.-Y.; Yoon, T.; Kang, S.-G.; Lee, S.-J. MerTK mediates STAT3–KRAS/SRC-signaling axis for glioma stem cell maintenance. *Artif. Cells, Nanomedicine, Biotechnol.* **2018**, *46*, 87–95, doi:10.1080/21691401.2018.1452022.
77. Kim, R.-K.; Cui, Y.-H.; Yoo, K.-C.; Kim, I.-G.; Lee, M.; Choi, Y.H.; Suh, Y.; Lee, S.-J. Radiation promotes malignant phenotypes through SRC in breast cancer cells. *Cancer Sci.* **2014**, *106*, 78–85, doi:10.1111/cas.12574.
78. Park, C.-M.; Park, M.-J.; Kwak, H.-J.; Lee, H.-C.; Kim, M.-S.; Lee, S.-H.; Park, I.-C.; Rhee, C.H.; Hong, S.-I. Ionizing Radiation Enhances Matrix Metalloproteinase-2 Secretion and Invasion of Glioma Cells through Src/Epidermal Growth Factor Receptor–Mediated p38/Akt and Phosphatidylinositol 3-Kinase/Akt Signaling Pathways. *Cancer Res.* **2006**, *66*, 8511–8519, doi:10.1158/0008-5472.can-05-4340.
79. Yoo, K.-C.; Suh, Y.; An, Y.; Lee, H.-J.; Jeong, Y.J.; Uddin, N.; Cui, Y.-H.; Roh, T.H.; Shim, J.-K.; Chang, J.H.; et al. Proinvasive extracellular matrix remodeling in tumor microenvironment in response to radiation. *Oncogene* **2018**, *37*, 3317–3328, doi:10.1038/s41388-018-0199-y.
80. Kegelman, T.P.; Wu, B.; Das, S.K.; Talukdar, S.; Beckta, J.M.; Hu, B.; Emdad, L.; Valerie, K.; Sarkar, D.; Furnari, F.; et al. Inhibition of radiation-induced glioblastoma invasion by genetic and pharmacological targeting of

- MDA-9/Syntenin. In *Proceedings of the National Academy of Sciences*; Proceedings of the National Academy of Sciences, 2016; Vol. 114, pp. 370–375.
81. Jubran, M.R.; Rubinstein, A.M.; Cojocari, I.; Adejumbi, I.A.; Mogilevsky, M.; Tibi, S.; Sionov, R.V.; Verreault, M.; Idbaih, A.; Karni, R.; et al. Dissecting the role of crosstalk between glioblastoma subpopulations in tumor cell spreading. *Oncog.* **2020**, *9*, 11–15, doi:10.1038/s41389-020-0199-y.
 82. Ohshima, Y.; Tsukimoto, M.; Harada, H.; Kojima, S. Involvement of connexin43 hemichannel in ATP release after γ -irradiation. *J. Radiat. Res.* **2012**, *53*, 551–557, doi:10.1093/jrr/rrs014.
 83. Spitale, F.M.; Vicario, N.; Di Rosa, M.; Tibullo, D.; Vecchio, M.; Gulino, R.; Parenti, R. Increased expression of connexin 43 in a mouse model of spinal motoneuronal loss. *Aging* **2020**, *12*, 12598–12608, doi:10.18632/aging.103561.
 84. Vicario, N.; Calabrese, G.; Zappalà, A.; Parenti, C.; Forte, S.; Graziano, A.C.E.; Vanella, L.; Pellitteri, R.; Cardile, V.; Parenti, R. Inhibition of Cx43 mediates protective effects on hypoxic/reoxygenated human neuroblastoma cells. *J. Cell. Mol. Med.* **2017**, *21*, 2563–2572, doi:10.1111/jcmm.13177.
 85. Chepied, A.; Daoud-Omar, Z.; Meunier-Balandre, A.-C.; Laird, D.; Mesnil, M.; Defamie, N. Involvement of the Gap Junction Protein, Connexin43, in the Formation and Function of Invadopodia in the Human U251 Glioblastoma Cell Line. *Cells* **2020**, *9*, 117, doi:10.3390/cells9010117.
 86. Vicario, N.; Turnaturi, R.; Spitale, F.M.; Torrisi, F.; Zappalà, A.; Gulino, R.; Pasquinucci, L.; Chiechio, S.; Parenti, C.; Parenti, R. Intercellular communication and ion channels in neuropathic pain chronicization. *Inflamm. Res.* **2020**, *69*, 841–850, doi:10.1007/s00011-020-01363-9.
 87. Arcsott, W.T.; Tandle, A.T.; Zhao, S.; Shabason, J.E.; Gordon, I.K.; Schlaff, C.D.; Zhang, G.; Tofilon, P.J.; Camphausen, K.A. Ionizing Radiation and Glioblastoma Exosomes: Implications in Tumor Biology and Cell Migration. *Transl. Oncol.* **2013**, *6*, 638–IN6, doi:10.1593/tlo.13640.
 88. Bentzen, S.M.; Gregoire, V. Molecular Imaging–Based Dose Painting: A Novel Paradigm for Radiation Therapy Prescription. *Semin. Radiat. Oncol.* **2011**, *21*, 101–110, doi:10.1016/j.semradonc.2010.10.001.
 89. Antonovic, L.; Brahme, A.; Furusawa, Y.; Toma-Dasu, I. Radiobiological description of the LET dependence of the cell survival of oxic and anoxic cells irradiated by carbon ions. *J. Radiat. Res.* **2012**, *54*, 18–26, doi:10.1093/jrr/rrs070.
 90. Tsai, J.-Y.; Chen, F.-H.; Hsieh, T.-Y.; Hsiao, Y.-Y. Effects of indirect actions and oxygen on relative biological effectiveness: estimate of DSB induction and conversion induced by gamma rays and helium ions. *J. Radiat. Res.* **2015**, *56*, 691–699, doi:10.1093/jrr/rrv025.
 91. Sokol, O.; Krämer, M.; Hild, S.; Durante, M.; Scifoni, E.; Krämer, M. Kill painting of hypoxic tumors with multiple ion beams. *Phys. Med. Boil.* **2019**, *64*, 045008, doi:10.1088/1361-6560/aafe40.
 92. Clarke, R.H.; Moosa, S.; Anzivino, M.; Wang, Y.; Floyd, D.H.; Puro, B.W.; Lee, K.S. Sustained Radiosensitization of Hypoxic Glioma Cells after Oxygen Pretreatment in an Animal Model of Glioblastoma and In Vitro Models of Tumor Hypoxia. *PLOS ONE* **2014**, *9*, e111199, doi:10.1371/journal.pone.0111199.
 93. Hong, B.-J.; Kim, J.; Jeong, H.; Bok, S.; Kim, Y.-E.; Ahn, G.-O. Tumor hypoxia and reoxygenation: the yin and yang for radiotherapy. *Radiat. Oncol. J.* **2016**, *34*, 239–249, doi:10.3857/roj.2016.02012.
 94. Subiel, A.; Ashmore, R.; Schettino, G. Standards and Methodologies for Characterizing Radiobiological Impact of High-Z Nanoparticles. *Theranostics* **2016**, *6*, 1651–1671, doi:10.7150/thno.15019.
 95. Patel, A.; Sant, S. Hypoxic tumor microenvironment: Opportunities to develop targeted therapies. *Biotechnol. Adv.* **2016**, *34*, 803–812, doi:10.1016/j.biotechadv.2016.04.005.
 96. Barth, R.F.; Mi, P.; Yang, W. Boron delivery agents for neutron capture therapy of cancer. *Cancer Commun.* **2018**, *38*, 35, doi:10.1186/s40880-018-0299-7.
 97. Miyatake, S.-I.; Kawabata, S.; Hiramatsu, R.; Kuroiwa, T.; Suzuki, M.; Kondo, N.; Ono, K. Boron Neutron Capture Therapy for Malignant Brain Tumors. *Neurol. medico-chirurgica* **2016**, *56*, 361–371, doi:10.2176/nmc.ra.2015-0297.
 98. Zavjalov, E.; Zaboronok, A.; Kanygin, V.; Kasatova, A.; Kichigin, A.I.; Mukhamadiyarov, R.; Razumov, I.; Sycheva, T.; Mathis, B.J.; Maezono, S.E.B.; et al. Accelerator-based boron neutron capture therapy for malignant glioma: a pilot neutron irradiation study using boron phenylalanine, sodium borocaptate and liposomal borocaptate with a heterotopic U87 glioblastoma model in SCID mice. *Int. J. Radiat. Boil.* **2020**, *96*, 1–11, doi:10.1080/09553002.2020.1761039.
 99. Cirrone, G.A.P.; Manti, L.; Margarone, D.; Petringa, G.; Giuffrida, L.; Minopoli, A.; Picciotto, A.; Russo, G.; Cammarata, F.; Pisciotto, P.; et al. First experimental proof of Proton Boron Capture Therapy (PBCT) to enhance protontherapy effectiveness. *Sci. Rep.* **2018**, *8*, 1141, doi:10.1038/s41598-018-19258-5.

100. Lee, P.; Chandel, N.S.; Simon, M.C. Cellular adaptation to hypoxia through hypoxia inducible factors and beyond. *Nat. Rev. Mol. Cell Biol.* **2020**, *21*, 268–283, doi:10.1038/s41580-020-0227-y.
101. Pérès, E.A.; Gérault, A.N.; Valable, S.; Roussel, S.; Toutain, J.; Divoux, D.; Guillamo, J.-S.; Sanson, M.; Bernaudin, M.; Petit, E. Silencing erythropoietin receptor on glioma cells reinforces efficacy of temozolomide and X-rays through senescence and mitotic catastrophe. *Oncotarget* **2014**, *6*, 2101–2119, doi:10.18632/oncotarget.2937.
102. Yasui, H.; Asanuma, T.; Kino, J.; Yamamori, T.; Meike, S.; Nagane, M.; Kubota, N.; Kuwabara, M.; Inanami, O. The prospective application of a hypoxic radiosensitizer, doranidazole to rat intracranial glioblastoma with blood brain barrier disruption. *BMC Cancer* **2013**, *13*, 106, doi:10.1186/1471-2407-13-106.
103. Gupta, S.K.; Smith, E.J.; Mladek, A.C.; Tian, S.; Decker, P.A.; Kizilbash, S.H.; Kitange, G.J.; Sarkaria, J.N. PARP Inhibitors for Sensitization of Alkylation Chemotherapy in Glioblastoma: Impact of Blood-Brain Barrier and Molecular Heterogeneity. *Front. Oncol.* **2019**, *8*, 670,, doi:10.3389/fonc.2018.00670.
104. Khasraw, M.; McDonald, K.L.; Rosenthal, M.; Lwin, Z.; Ashley, D.; Wheeler, H.; Barnes, E.; Foote, M.; Koh, E.-S.; Sulman, E.; et al. ACTR-24. A RANDOMIZED PHASE II TRIAL OF VELIPARIB (V), RADIOTHERAPY (RT) AND TEMOZOLOMIDE (TMZ) IN PATIENTS (PTS) WITH UNMETHYLATED MGMT (uMGMT) GLIOBLASTOMA (GBM): THE VERTU STUDY. *Neuro-Oncology* **2019**, *21*, vi18, doi:10.1093/neuonc/noz175.067.
105. Ferri, A.; Stagni, V.; Barilà, D. Targeting the DNA Damage Response to Overcome Cancer Drug Resistance in Glioblastoma. *Int. J. Mol. Sci.* **2020**, *21*, 4910, doi:10.3390/ijms21144910.
106. Scaringi, C.; Minniti, G.; Caporello, P.; Enrici, R.M. Integrin inhibitor cilengitide for the treatment of glioblastoma: a brief overview of current clinical results. *Anticancer. Res.* **2012**, *32*, 4213–4223.
107. Eisele, G.; Wick, A.; Eisele, A.-C.; Clement, P.M.; Tonn, J.; Tabatabai, G.; Ochsenein, A.; Schlegel, U.; Neyns, B.; Krex, D.; et al. Cilengitide treatment of newly diagnosed glioblastoma patients does not alter patterns of progression. *J. Neuro-Oncology* **2014**, *117*, 141–145, doi:10.1007/s11060-014-1365-x.
108. Storch, K.; Sagerer, A.; Cordes, N. Cytotoxic and radiosensitizing effects of FAK targeting in human glioblastoma cells in vitro. *Oncol. Rep.* **2015**, *33*, 2009–2016, doi:10.3892/or.2015.3753.
109. Brown, N.; Williams, M.; Arkenau, H.-T.; A Fleming, R.; Tolson, J.; Yan, L.; Zhang, J.; Singh, R.; Auger, K.R.; Lenox, L.; et al. A study of the focal adhesion kinase inhibitor GSK2256098 in patients with recurrent glioblastoma with evaluation of tumor penetration of [11C]GSK2256098. *Neuro-Oncology* **2018**, *20*, 1634–1642, doi:10.1093/neuonc/noy078.
110. Ulasov, I.; Thaci, B.; Sarvaiya, P.; Yi, R.; Guo, D.; Auffinger, B.; Pytel, P.; Zhang, L.; Kim, C.K.; Borovjagin, A.; et al. Inhibition of MMP14 potentiates the therapeutic effect of temozolomide and radiation in gliomas. *Cancer Med.* **2013**, *2*, 457–467, doi:10.1002/cam4.104.
111. Groves, M.D.; Puduvalli, V.K.; Hess, K.R.; Jaeckle, K.A.; Peterson, P.; Yung, W.K.; Levin, V.A. Phase II Trial of Temozolomide Plus the Matrix Metalloproteinase Inhibitor, Marimastat, in Recurrent and Progressive Glioblastoma Multiforme. *J. Clin. Oncol.* **2002**, *20*, 1383–1388, doi:10.1200/jco.2002.20.5.1383.
112. Lassman, A.B.; Pugh, S.L.; Gilbert, M.R.; Aldape, K.D.; Geinoz, S.; Beumer, J.H.; Christner, S.M.; Komaki, R.; DeAngelis, L.M.; Gaur, R.; et al. Phase 2 trial of dasatinib in target-selected patients with recurrent glioblastoma (RTOG 0627). *Neuro-Oncology* **2015**, *17*, 992–998, doi:10.1093/neuonc/nov011.
113. Reardon, D.A.; Vredenburgh, J.J.; Desjardins, A.; Peters, K.B.; Sathornsumetee, S.; Threath, S.; Sampson, J.H.; Herndon, J.E.; Coan, A.; McSherry, F.; et al. Phase 1 trial of dasatinib plus erlotinib in adults with recurrent malignant glioma. *J. Neuro-Oncology* **2012**, *108*, 499–506, doi:10.1007/s11060-012-0848-x.
114. Franceschi, E.; Stupp, R.; Bent, M.J.V.D.; Van Herpen, C.; Donadey, F.L.; Gorlia, T.; Hegi, M.; Lhermitte, B.; Strauss, L.C.; Allgeier, A.; et al. EORTC 26083 phase I/II trial of dasatinib in combination with CCNU in patients with recurrent glioblastoma. *Neuro-Oncology* **2012**, *14*, 1503–1510, doi:10.1093/neuonc/nos256.
115. Agarwal, S.; Mittapalli, R.K.; Zellmer, D.M.; Gallardo, J.L.; Donelson, R.; Seiler, C.; Decker, S.A.; Santacruz, K.S.; Pokorny, J.L.; Sarkaria, J.N.; et al. Active efflux of Dasatinib from the brain limits efficacy against murine glioblastoma: broad implications for the clinical use of molecularly targeted agents. *Mol. Cancer Ther.* **2012**, *11*, 2183–92, doi:10.1158/1535-7163.MCT-12-0552.
116. Fallacara, A.L.; Zamperini, C.; Podolski-Renić, A.; Dinić, J.; Andjelković, T.; Nešović, M.; Mancini, A.; Rango, E.; Iovenitti, G.; Molinari, A.; et al. A New Strategy for Glioblastoma Treatment: In Vitro and In Vivo Preclinical Characterization of Si306, a Pyrazolo[3,4-d]Pyrimidine Dual Src/P-Glycoprotein Inhibitor. *Cancers* **2019**, *11*, 848, doi:10.3390/cancers11060848.
117. Cammarata, F.P.; Torrisi, F.; I Forte, G.; Minafra, L.; Bravatà, V.; Pisciotta, P.; Savoca, G.; Calvaruso, M.; Petringa, G.; Cirrone, G.A.P.; et al. Proton Therapy and Src Family Kinase Inhibitor Combined Treatments on U87 Human Glioblastoma Multiforme Cell Line. *Int. J. Mol. Sci.* **2019**, *20*, 4745, doi:10.3390/ijms20194745.

118. Torrisi, F.; Minafra, L.; Cammarata, F.P.; Savoca, G.; Calvaruso, M.; Vicario, N.; Maccari, L.; Pérès, E.A.; Özçelik, H.; Bernaudin, M.; et al. SRC Tyrosine Kinase Inhibitor and X-rays Combined Effect on Glioblastoma Cell Lines. *Int. J. Mol. Sci.* **2020**, *21*, 3917, doi:10.3390/ijms21113917.



© 2020 by the authors. Licensee MDPI, Basel, Switzerland. This article is an open access article distributed under the terms and conditions of the Creative Commons Attribution (CC BY) license (<http://creativecommons.org/licenses/by/4.0/>).

8. DISCUSSION AND CONCLUDING REMARKS

The main factors that make GBM an highly malignant disease may be listed in four interconnected points: 1) late diagnosis; 2) tumor aggressiveness; 3) absence of complete eradication with remission of the disease; 4) high incidence of recurrences. A resolution can hardly be found for the first point, because GBM is a pathology with no clear and distinguished risk factors, except for previous exposures to IR, especially in brain pediatric cancer; therefore, there are no prevention or screening tools to advance early diagnosis of this awful pathology. Consequently, at the moment of diagnosis, tumor have already reached the high grade of aggressiveness due to the establishment of well-developed hallmarks of cancer. The main factors of malignancy are the huge proliferation, the high vascularization index and the heterogeneous tumor microenvironment [132]. Besides these characteristics of malignancy, the distinctive feature of GBM aggressiveness is represented by the infiltrating and invasive ability, which is the main reason for the treatment failure and relapses. In fact, although generally GBM dissemination is not outside the central nervous system, as normally occur in metastatic tumors, it develops classical mechanisms that give rise the invasive pattern and the spreading from the primary growth site, such as: the phenotypic shift towards the mesenchymal type, the modulation of the cell adhesion, cell to cell communication or extracellular matrix (ECM)-mediated communication altered signaling, protease up regulation for the degradation of the ECM and the structural/mechanical cytoskeleton remodeling with the loss of cell adhesion and the activation of cell motility [133]. The infiltrating pattern of GBM makes difficult, if not impossible, the complete eradication of the tumor, both with surgical resection and with RT, because of the intricacy to define the area to be removed or irradiated, especially due to susceptible anatomical site and radioresistance pathways activation. For this reason, despite the current aggressive multimodal treatment of chemotherapy and RT, GBM recurrences have an high incidence, showing that GBM cancer cells exhibit both pharmacological and RT resistance.

Technological progress in the field of RT has been supported not only by the improvement of diagnostic imaging but also by the development of new conformational irradiation systems. Nonetheless, the clinical guidelines continue to maintain conventional irradiation methods as gold standard for new diagnosed GBM, whereas potential conformal radiation techniques application are aimed to limit the damage of compromised tissue rather than finding a definitive cure. It is also true that, despite the advances of imaging techniques support the planning of radiation therapy treatment, the safeguarding for healthy tissues preserve the priority in the risk/benefit assessment. The need to maintain under control the organs at risk and the difficulty in identifying GBM tumor target lead to the release of an ineffective dose, which is defined as sub-lethal dose. Therefore, the

GBM cells resist to the treatment, also due to the mechanisms of damage repair regulation and activation of the detoxification cell systems [134] [135]. The absence of a cure for a complete remission confirms the existence of radioresistance mechanisms in GBM cells that hamper the effectiveness of RT.

The application of synergistic therapy with molecularly targeted drugs and RT is one of the most promising approaches for the treatment of radioresistant tumors, such as GBM. So far, the radiosensitizing effects has been mainly related to the application of cytotoxic substances, DNA repair systems inhibitors, and oxygen-mimicking compounds. Most of these potential GBM radiosensitizers have not progressed to clinical trials due to a lack of promising preclinical data [48]. Therefore, it is mandatory to fully investigate the biological mechanisms of radioresistance that occur at the cellular level in response to radiation, in order to find appropriate pharmacological targets. In this scenario, it is known that GBM cells activate complex pathways in response to irradiation that favour their aggressive behaviour as well as they manifest an adaptation to the hypoxic microenvironment, which promotes invasiveness [136] [54]. The SRC protein is considered as a key factor for the promotion of these pathways, being at the centre of a network that regulates and supports the main hallmarks of GBM, through a complex inter- and intracellular signalling [14].

Through my works, it has been demonstrated that SRC inhibition reduced the radioresistance induced by hypoxia (expressed by OER) with X-rays, and increased the cellular radiosensitivity thus reducing the required dose to have an effective therapeutic response, expressed by the dose modifying factor (DMF) either with X-rays or protons. Moreover, the activation of radioresistance pathways in response to proton irradiation and their modulation with the Si306 molecule were analyzed. The results reported that, following the PT combined with Si306, several genes involved in the key pathways, which are sustained by the SRC activity, were downregulated, leading to a suppression of the main hallmarks of GBM, such as proliferation, survival, cell cycle promotion and motility. Such studies open the way for further perspectives to broaden the researches and to shed light on new insights. Firstly, the analysis of candidate genes and proteins by qRT-PCR and western blot respectively, can be performed to validate the results and to better understand the modulation of SRC pathways in combined treatments with proton therapy and with X-ray. From the experiments by cDNA microarray with proton and Si306 treatment, specific genes, can be selected to evaluate the cell-cycle progression, the cell survival and death, and the immunomodulation. Therefore, the evaluation of genes belonging to the human leukocyte antigen class family, to PI3K/AKT pathway and genes correlated with proteoglycan signaling may elucidate the SRC mechanisms induced by proton irradiation. Moreover, the evaluation of genes controlling phagosome, cell adhesion

molecules, inflammation and calcium signaling induced by proton irradiation combined with Si306 may clarify the radiosensitizing role of SRC inhibition. From the study with X-ray and Si306 treatment in normoxic and hypoxic conditions, the following genes can be selected: c-SRC to validate the oncogenic role of this nRTK induced by irradiation and/or hypoxic condition; HIF1- α to confirm the adaptive response to oxygen lack with transcriptional activation of hypoxia response elements (HRE); EGFR, PDGFR, PTK2 (gene of FAK) to evaluate key factors involved in SRC pathway activation; PXN (gene of paxillin) and CD44 to evaluate the acquisition of motility and migration ability; CDH1 (gene of E-cadherin), CDH2 (gene of N-cadherin), MMP-2, FN1 (gene of Fibronectin 1), SNAI1, VIM (gene of Vimentin), ACTA2 (gene of α -SMA) to evaluate EMT and invasion processes; MKI67 (gene of Ki67) MAPK1 to evaluate proliferation; AKT1 to evaluate one of the main pathways connected with SRC activation.

Few previous preclinical studies evaluated the synergistic value of SRC-targeting compounds in combination with RT for GBM treatment. Among them, only the pyrazolo[3,4-d]pyrimidine PP2 compound, has been shown to increase radiosensitivity of GBM cell lines and to improve the therapeutic effect of X-ray radiation in human GBM xenograft mouse model [137]. Two other drugs ATP-competitive of SRC, Bosutinib and Ponatinib, were evaluated in combination with RT and with TMZ in GBM cell lines, in order to test a reduction of invadopodia but not to analyze the radiosensitive effect [138]. To date, the SRC inhibitors proposed in clinical trials for the GBM treatment are the following: Dasatinib, Bosutinib, Ponatinib and NEO100, but the results on their therapeutic efficacy are still not convincing [139]. Noteworthy, among them, Dasatinib was the only one tested in combination with RT. In a first clinical trial, it was tested with the EGFR inhibitor, Vandetanib, during and after X-ray radiation, in children affected by newly diagnosed diffuse intrinsic pontine glioma, but no results were published [140]. The aim of the second clinical trial was to evaluate the effects of Dasatinib combined with radiotherapy and TMZ in newly-diagnosed GBM. The primary objectives of the first phase, were only related to characterize the safety profile of the treatment rather than evaluate its effectiveness; this study didn't progress to the phase II and only the first one was completed [141]. However, a comparable clinical study evaluating Dasatinib with radiotherapy was recently completed and the latest results were published in February 2020: there are no significant differences between Dasatinib+RT and placebo+RT in overall survival and progression-free survival [142].

One of the main reasons at the basis of the current failure of Dasatinib is the multidrug resistance and inefficient delivery beyond the blood-brain barrier due to the overexpression of P-glycoprotein and breast cancer resistance protein [143]. Recent preclinical studies demonstrated that Si306 was able to penetrate in the brain overcoming the ATP-binding cassette (ABC) transporters efflux [130].

Moreover additional experiments were performed in order to improve the water solubility enhancement and a polymer formulation strategy involving the novel 2D inkjet printing technology seem to be successful [127].

The results of this thesis, linked with these pharmacological advancements, support the idea that SRC inhibition is still a viable strategy to treat GBM synergistically with RT. Nonetheless, before envisaging any clinical application of Si306, there are still some key points to address. The extensive cellular heterogeneity of GBM is an additional issue for the effectiveness of the treatments. Indeed, on one side, SRC has central role in the multiple connection between the signaling pathways, involved in radioresistance promoted by hypoxia and by the response to IR. However, the loss of SRC activity may be compensated by further upstream or downstream factors that belongs to alternative cell line-specific pathways. Future studies will need to address these issues and to investigate cell characteristics, additional druggable targets and irradiation dosages to maximize the success of molecular targeted with radiation-based therapies in the clinic field.

In conclusion, the key role of radiobiology in the field of radiation oncology, for the treatment of aggressive cancers deserves a special consideration from the scientific community, which has been mild for many years. Through the advancements of the beam precision delivery systems and the reduction of the inaccuracy in the total irradiated volume, the suitability of radiation will tend to increase over the time. However, the recent insights obtained through research in radiobiology, suggest that, the technological progression need to walk together with the incessant investigation of the cellular and molecular mechanisms, in order to gain a favorable approach for the treatment of radioresistant tumors.

9. APPENDIX: MATERIALS AND METHODS

A fully description of material and method procedures is reported in the articles above. However, some specifications were implied. In this paragraph some experimental details are added to provide a complete knowledge of the activities performed.

Clonogenic Survival Assay set up

The core of the radiobiological experiments is represented by the clonogenic assay, that it is considered the radiobiological gold standard test for the cellular response evaluation to treatment with IR and for the creation of survival curves that are analyzed with mathematic model, such as the linear quadratic model (LQ).

According to the maintenance of the proliferative capacity that allows tumor regrowth, a single cell is defined as “clonogenic” or “colony-forming cell” when it generate at least 50 cells, which include 5 or 6 generations. Therefore, the clonogenic cells that survive to IR exposure are defined as *surviving clonogenic cells* that generate the surviving fraction (SF) in the dose-response fashion. The clonogenic survival assay was performed according to the protocol of Franken et al. [144], that suggests two options for the cell plating set up in order to obtain a correct data for the plating efficiency (PE) estimation, that is defined as the ratio between the colonies counted and the seeded cells. Therefore, the cell seeding step is critical because the number of cells that are plated for each condition should be accurate and as precise as possible. According to these options, it is possible to plate the correct number of cells before or after the irradiation. The choice of the two ways depend on the configuration of irradiator systems. In fact, the beam of the proton therapy system is delivered horizontally, and, for this reason, cells are irradiated in flasks with filtered caps, and after the irradiation, they are seeded in multiwell-6 plates; conversely, in case of X-Ray radiation system, the beam is delivered vertically from the up side, allowing the plating in multiwell-6 plates before the irradiation. Therefore, the experimental design take into account the different irradiation system between protons and X-rays, as summarized in the figure 9.

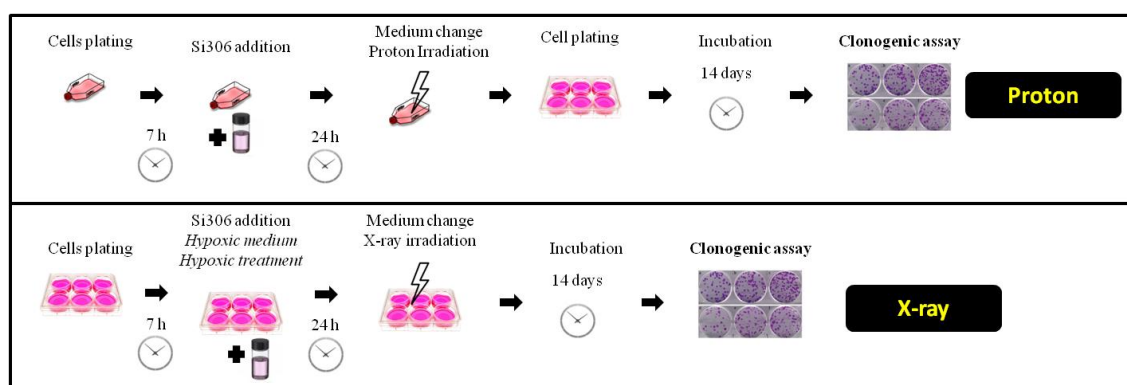


Figure 9. Scheme experimental setup with protons and X-rays. The main difference is that, for protons, the cell plating for clones formation in multiwell 6 plates occurred after irradiation; conversely, in X-ray irradiation, the cells were seeded at the beginning of the experiment (before irradiation); in hypoxic condition, the plates were transferred inside the hypoxic chamber where the Si306 was added in fresh medium previously equilibrated with the gas mixture containing 1% O₂ in order to maintain this concentration from the beginning of the treatment with the drug. In both irradiation fresh medium was added to eliminate the drug and to maintain exposure for only 24 hours.

Apposite dilutions were used to plate the cells in each condition, according to the dose delivered and to the vehicle or drug concentration. The number of the plated cells was determined from both literature data and preliminary experiments. In fact, the dose of irradiation and the cytotoxicity of the drug could have led to the failure of colonies formation or too low colonies, due to an excessive amount of cell death with consequent errors. For this reason,

preliminary evaluation were performed with the aim to assess the cytotoxic contribution of Si306 for GBM cells, especially for the experiments that included the hypoxic treatment, which might affect their first growth phase. In order to perform these preliminary studies, 2×10^4 cells/cm² were plated for 24 hours and then treated with Si306 in both hypoxic and normoxic conditions. Pictures were taken on the day after the Si306 administration and a representative fields of each group is shown (Figure 10). Morphologically the cells showed evident changes in their typical shape, with a loss of protrusions only at the highest concentration of 20 μ M, especially in hypoxic condition, but no significant changes in relation to treatment were observed in the other samples.

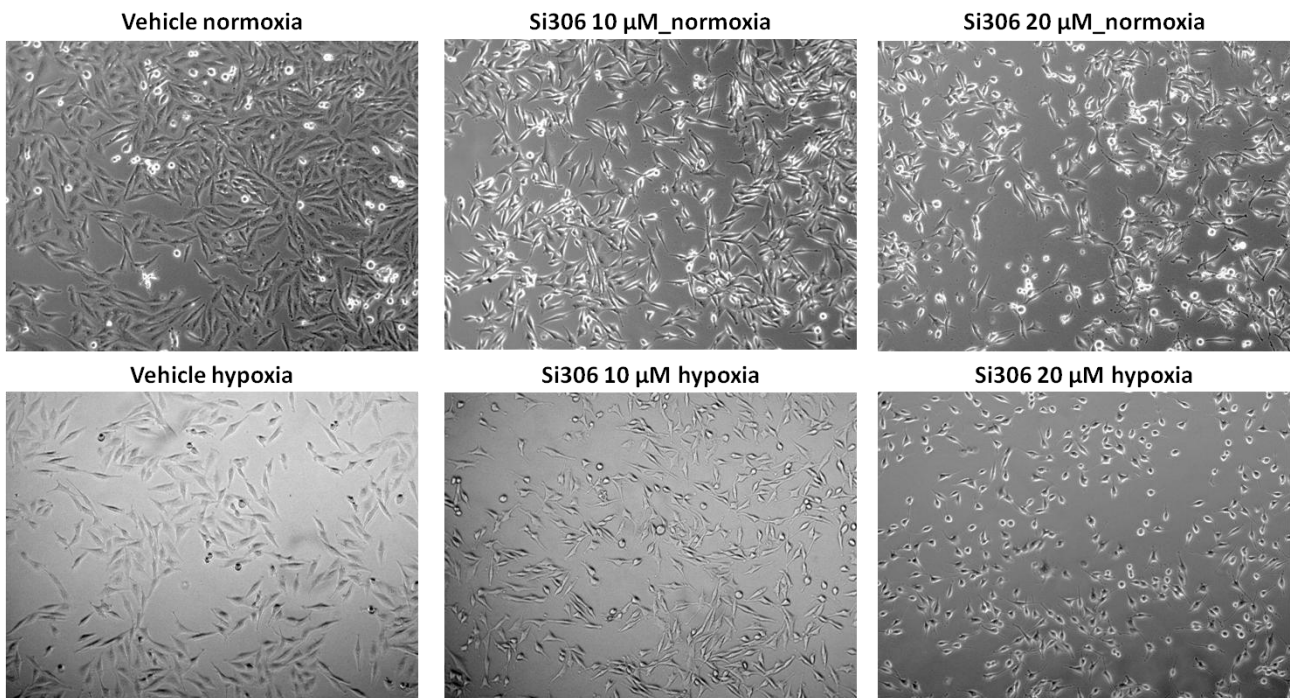


Figure 10. U251-MG cells treated with 10 μ M and 20 μ M Si306 at normoxic and hypoxic condition.

The cell vitality was also evaluated with the cristal violet (CV) assay. Before the CV assay, the growth of cells was tested with the calculation of the area covered in each well by the spectrophotometer (Spark microplate reader, Tecan Group Ltd., Switzerland) (Figure 11). The cell confluence was reduced with the Si306 exposure in a dose response fashion, and it was also affected by the hypoxia. Indeed the treatment with only vehicle in hypoxia, determined a decrease of 16,7% of confluence compared to control group in normoxic condition.

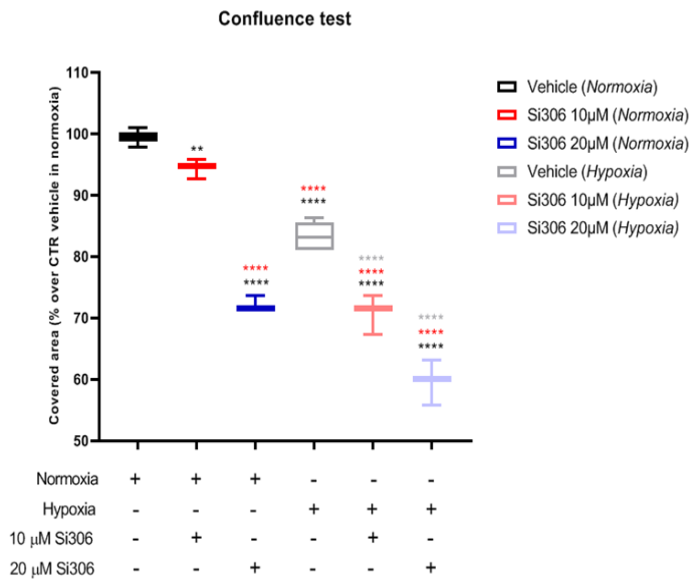


Figure 11. Percentage of covered area of U251-MG cells with Si306 exposure in normoxia and hypoxia. Mean \pm SEM, three independent experiments; black **p-value < 0.01 and **** p-value < 0.0001 versus vehicle in normoxia; red **** p-value < 0.0001 versus Si306 at 10 μ M in normoxia; grey **** p-value < 0.0001 versus vehicle in hypoxia. Two-way ANOVA with Holm-Šídák post-hoc test).

The analysis of crystal violet confirmed the cytotoxic effect of Si306 and the hypoxic condition. Indeed, the reduction of vitality was significant in all the groups treated with Si306 and it was more evident in hypoxic condition (Figure 12).

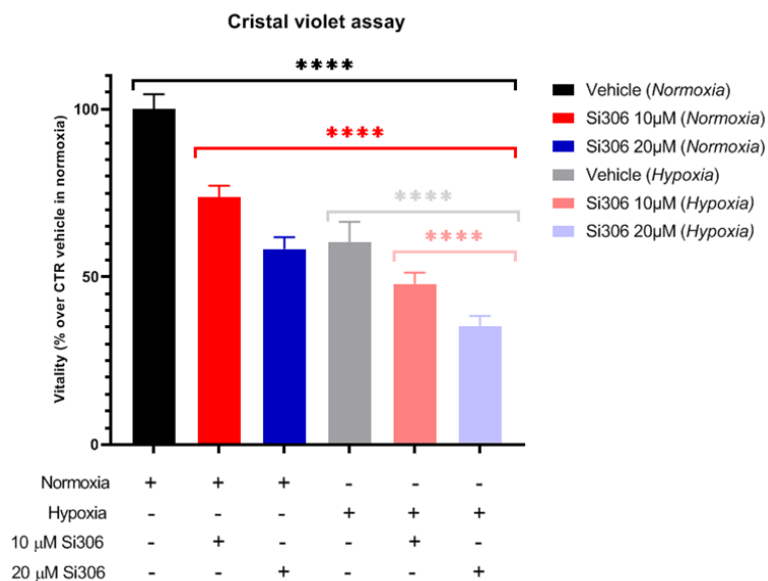


Figure 12. Percentage of vitality of U251-MG cells with Si306 exposure in normoxia and hypoxia. Mean \pm SEM, three independent experiments; black **** p-value < 0.0001 versus vehicle in normoxia; red **** p-value < 0.0001 versus Si306 at 10 μ M in normoxia.; grey **** p-value < 0.0001 versus vehicle in hypoxia; light red **** p-value < 0.0001 versus Si306 at 10 μ M in hypoxia. Two-way ANOVA with Holm-Šídák post-hoc test.

Therefore it was clearly observed that cell survival was affected by hypoxia compared to normoxia condition and that the Si306 molecule showed a dose dependent decrease in proliferation in both oxygen conditions. These findings were considered the starting point to plan the radiobiological experiments in order to plate the appropriate number of cells for the clonogenic assay (Table1).

X-RAY IRRADIATION IN NORMOXIC CONDITION				X-RAY IRRADIATION IN HYPOXIC CONDITION			
Dose (Gy)	Number of plated cells			Dose (Gy)	Number of plated cells		
	Vehicle	Si306 10 μ M	Si306 20 μ M		Vehicle	Si306 10 μ M	Si306 20 μ M
0	800	800	1600	0	1600	1600	2400
2	800	800	1800	2	1600	1800	2800
4	800	800	2000	4	1600	2000	3200
6	800	800	2200	6	1600	2200	3600
8	800	800	2400	8	1600	2400	4000

Table 1. In the table are listed the number of cells that were chosen to plate in each experimental condition. The starting number in normoxic condition was 800, and it was maintained also for the treatment with Si306 at 10 μ M ; based on our preliminary results, the double of cell number was used to start from 0 Gy + Si306 at 20 μ M and it was increased of 200 cells for each dose, up to 8 Gy. In case of hypoxia, 1600 cells were also used for vehicle and the number of cells for Si306 at 10 μ M was the same of the 20 μ M in normoxic condition. Finally the number of cell for the experimental group of Si306 at 20 μ M was quadrupled and increased for 400 in each dose up to 8 Gy.

Unlike the preliminary tests conducted on the U251-MG cell line for X-ray irradiation, U87-MG cells exhibited a less cytotoxic response to Si306. In fact, the evaluation of viability by trypan blue exclusion assay revealed that after 24 hours with Si306, the cells did not show a clear survival reduction (Figure 13).

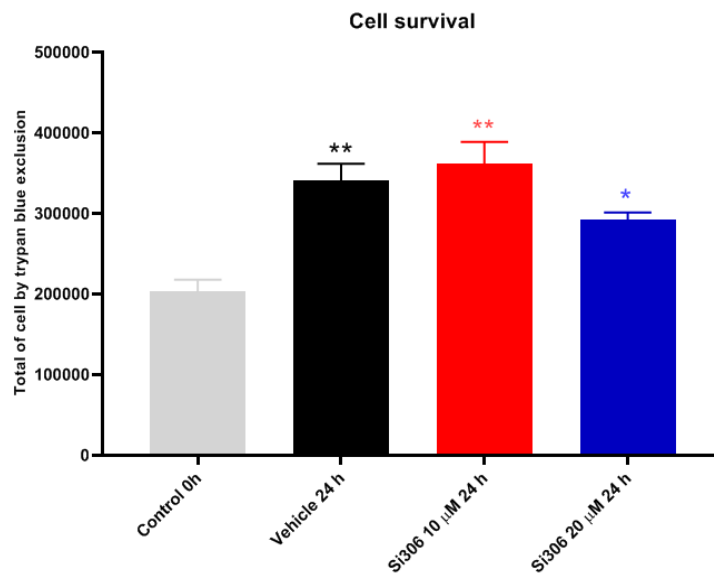


Figure 13. Number of viable cells of each condition by Trypan Blue dye exclusion test. Mean \pm SEM, three independent experiments in triplicate; black or red ** p-value < 0.01 and * p-value < 0.05 versus control 0 hour; Two-way ANOVA with Holm–Šídák post-hoc test).

The number of plated cells in the clonogenic experiments with U87-MG was maintained low, in order to perform a clonogenic-low colony density assay (Table 2). This type of assay, for the U87-MG line is also suggested because of their colony pattern which is highly scattered. Therefore it is preferred to plate few cells in order to avoid the clones overlap with contiguous cells and no longer discriminable as colony-forming units (Figure 14).

PROTON IRRADIATION IN NORMOXIC CONDITION			
Dose (Gy)	Number of plated cells		
	Vehicle	Si306 10 μ m	Si306 20 μ M
0	100	150	150
2	250	350	350
4	450	550	550
10	1500	1500	1500
21	1500	2500	2500

Table 2. In the table are listed the number of cells that was chosen to plate in each experimental condition for proton irradiation. The starting number was 100 and 150 for vehicle and Si306 respectively; for each dose 100/150 cells were added, except for the high doses of 10 and 21 Gy in which 1500 and 2500 cells were used respectively.

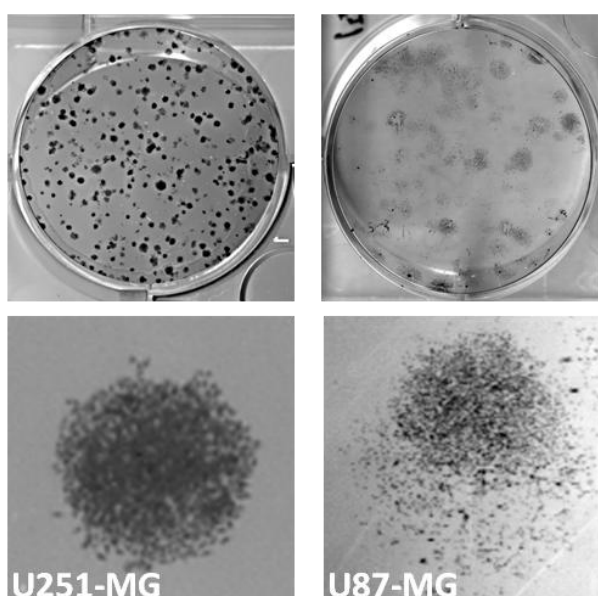


Figure 14. The clones of U251 and U87 showed a different morphology and here are reported two representative images of appearance of their clones took from multiwell 6 plate after fixation and coloration. U87-MG clones are not compact and rounded as U251-MG.

γ -H2AX Immunofluorescence Analysis

One of the most useful methods applied in radiobiology to measure DNA damage induced by IR, is represented by the detection of phosphorylated histone H2AX (γ H2AX) in the cell nucleus. H2AX is a variant of the H2A protein family that is activated in the repair process of damaged DNA. The protein H2AX is phosphorylated and recruited to damage sites to generate the so called foci γ H2AX. After DNA is repaired, γ H2AX is dephosphorylated and the percentage of tumour cells that retain γ H2AX foci during the time can be used to identify the radiosensitivity of cells or their ability to recover from damage that is induced by IR.

Briefly, images were analysed using FIJI application software (version 2.0.0-rc-69/1.52p). Each region of interest was analysed applying the iso-data threshold on immunofluorescence images of γ -H2AX; data were expressed as percentage of γ -H2AX positive nuclei over total Hoechst positive cells. Investigators blinded to the treatment groups

performed all quantifications. More in detail, the images were stacked using the *Image>Stacks>Stacked to Images* tool and for γ -H2AX-Alexa fluor 488 positive signal, the threshold was set using the *Image>Adjust>Threshold* tool. Then, images were converted in black and white by *Process>Binary>Make binary* and each pixel was replaced with the median values by *Process>Filters>Median*. The addition of segmentation allowed to separate fused nuclei of contiguous cells by *Process>Binary>Watershed* tool. In conclusion, the positive pixel were counted by *Analyze>Analyze Particles*. The procedure for Hoechst analysis was the same, even though the initial threshold was set just for segmentation and not for discriminate positive cells. The process is summarized in the figure 15.

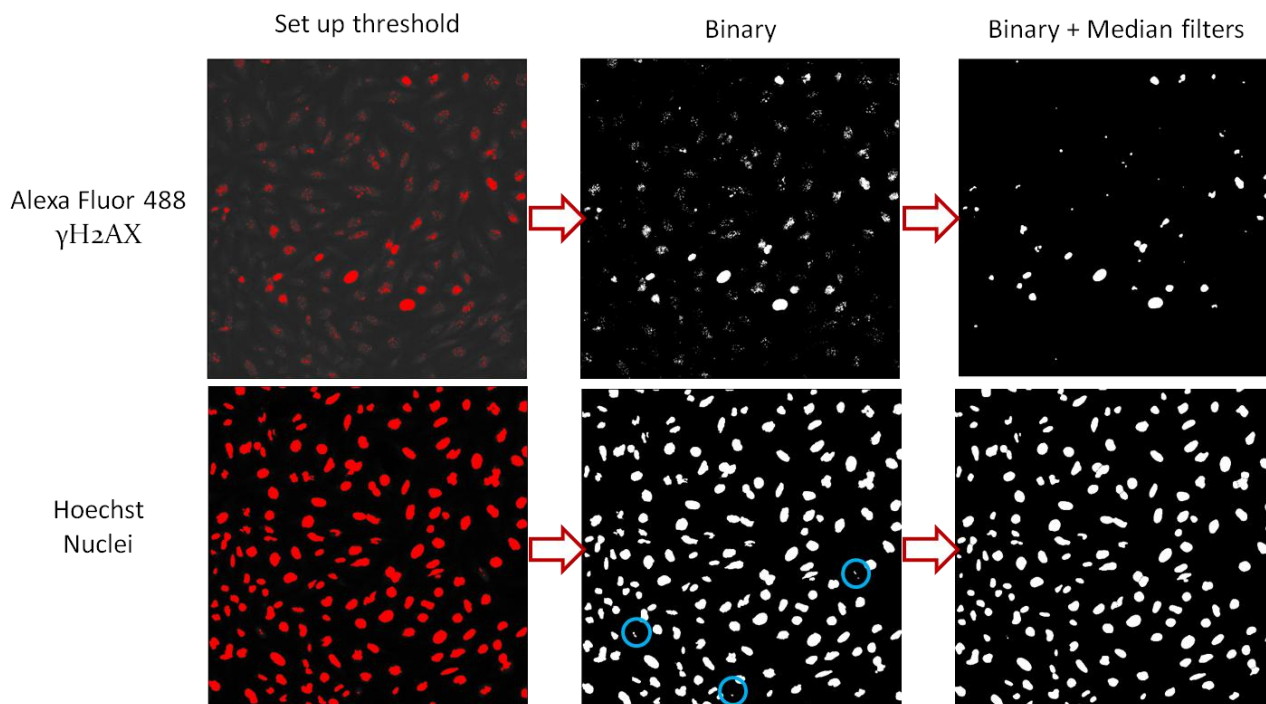


Figure 15. The main steps for the automated counting of γ H2AX positive nuclei. A common threshold is applied to determine positive cells. The removal of background and non-specific signals is performed after the creation of binary images and with the application of filters; in the images with DAPI filter is more difficult to notice the presence of non-specific signals, for this reason they are pointed out with blue rounds.

Calculation of migration index

For the calculation of migration index, the cell-free area was measured at 0 hours and 24 hours after the scratch. For each sample, 3 photos were acquired on the top, middle and bottom of the well in order to capture the entire scratch area inside the well and to reduce errors of measurement. The quantification were done using FIJI application software (version 2.0.0-rc-69 / 1.52p): briefly, the *Paintbrush tool* was used to segment the uncovered area; then *Wand (tracing) tool* was applied to select the segmented area and the background was removed with *Edit>Clear outside*. Finally the area was calculated by *Analyze>Measure*. The process is summarized in the figure 16.

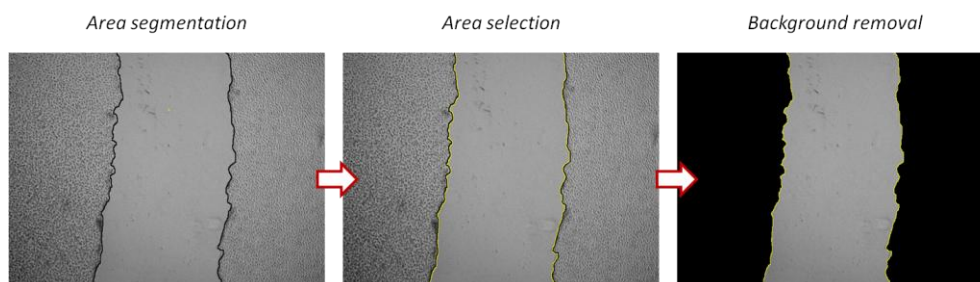


Figure 16. Representative images that show the process to calculate migration index by FIJI application software.

Whole Genome cDNA Microarray Expression Analysis

Total RNA was extracted from cells using Trizol and the RNeasy mini kit according to the manufacturer's guidelines (Invitrogen). RNA concentration and purity were determined spectrophotometrically using a Nanodrop ND-1000 (Thermo Scientific Open Biosystems, Lafayette, CO, USA) and RNA integrity, measured as RNA integrity number (RIN) values, was assessed using a Bioanalyzer 2100 (Agilent Technologies, Santa Clara, CA, USA). Only samples with a maximum RIN of 10 were used for further microarray analysis. Five hundred nanograms of total RNA were used for cRNA synthesis and labeling according to the Agilent Two-Color Microarray-Based Gene Expression Analysis protocol. Statistical data analysis, background correction, normalization and summary of expression measures were conducted with GeneSpring GX 10.0.2 software (Agilent Technologies). Data were filtered using a two-step procedure: first the entities were filtered based on their flag values P (present) and M (marginal) and then filtered based on their signal intensity values, this enables very low signal values or those that have reached saturation to be removed. Statistically significant differences were computed by Student's t test and the significance level was set at $p < 0.05$. The false discovery rate (FDR) was used as a multiple test correction method. Average gene expression values of experimental groups were compared (on log scale) by means of a modified ANOVA ($p < 0.05$). Genes were identified as being differentially expressed if they showed a foldchange (FC) of at least 1.5 with a p-value < 0.05 compared to untreated cells used as reference sample. Microarray experiments conducted by using the protocol Two-Color Microarray-Based Gene Expression Analysis (Agilent Technologies, Santa Clara, CA, USA), statistical analyzes carried out with GeneSpring GX 10.0.2 software (Agilent Technologies), and pathway analysis were conducted by using DAVID database. The data showed in this work were deposited in the Gene Expression Omnibus (GEO) database (NCBI) [145] and are available by using the GEO Series accession number GSE127989 in compliance with Minimum Information About a Microarray Experiment standards.

10. REFERENCES

1. Ostrom, Q.T., et al., *CBTRUS Statistical Report: Primary Brain and Other Central Nervous System Tumors Diagnosed in the United States in 2012-2016*. Neuro Oncol, 2019. **21**(Suppl 5): p. v1-v100.
2. Stupp, R., et al., *Radiotherapy plus concomitant and adjuvant temozolomide for glioblastoma*. N Engl J Med, 2005. **352**(10): p. 987-96.
3. Das, K.K. and R. Kumar, *Pediatric Glioblastoma*, in *Glioblastoma*, S. De Vleeschouwer, Editor. 2017, Codon Publications
Copyright: The Authors.: Brisbane (AU).
4. Ladomersky, E., et al., *The Coincidence Between Increasing Age, Immunosuppression, and the Incidence of Patients With Glioblastoma*. Front Pharmacol, 2019. **10**: p. 200.
5. Tamimi, A.F. and M. Juweid, *Epidemiology and Outcome of Glioblastoma*, in *Glioblastoma*, S. De Vleeschouwer, Editor. 2017, Codon Publications
Copyright: The Authors.: Brisbane (AU).
6. Yan, H., et al., *IDH1 and IDH2 mutations in gliomas*. N Engl J Med, 2009. **360**(8): p. 765-73.
7. Yang, W., et al., *Sex differences in GBM revealed by analysis of patient imaging, transcriptome, and survival data*. Sci Transl Med, 2019. **11**(473).
8. Wang, Y., et al., *A Risk Classification System With Five-Gene for Survival Prediction of Glioblastoma Patients*. Front Neurol, 2019. **10**: p. 745.
9. Prasad, G. and D.A. Haas-Kogan, *Radiation-induced gliomas*. Expert Rev Neurother, 2009. **9**(10): p. 1511-7.
10. Nelson, J.S., et al., *Potential risk factors for incident glioblastoma multiforme: the Honolulu Heart Program and Honolulu-Asia Aging Study*. J Neurooncol, 2012. **109**(2): p. 315-21.
11. Backes, C., et al., *New insights into the genetics of glioblastoma multiforme by familial exome sequencing*. Oncotarget, 2015. **6**(8): p. 5918-31.
12. Nizamutdinov, D., et al., *Prognostication of Survival Outcomes in Patients Diagnosed with Glioblastoma*. World Neurosurg, 2018. **109**: p. e67-e74.
13. Hanif, F., et al., *Glioblastoma Multiforme: A Review of its Epidemiology and Pathogenesis through Clinical Presentation and Treatment*. Asian Pac J Cancer Prev, 2017. **18**(1): p. 3-9.
14. Torrisi, F., et al., *The Role of Hypoxia and SRC Tyrosine Kinase in Glioblastoma Invasiveness and Radioresistance*. Cancers (Basel), 2020. **12**(10).
15. Louis, D.N., et al., *The 2007 WHO classification of tumours of the central nervous system*. Acta Neuropathol, 2007. **114**(2): p. 97-109.
16. Louis, D.N., et al., *The 2016 World Health Organization Classification of Tumors of the Central Nervous System: a summary*. Acta Neuropathol, 2016. **131**(6): p. 803-20.
17. Cohen, A.L., S.L. Holmen, and H. Colman, *IDH1 and IDH2 mutations in gliomas*. Curr Neurol Neurosci Rep, 2013. **13**(5): p. 345.
18. Parsons, D.W., et al., *An integrated genomic analysis of human glioblastoma multiforme*. Science, 2008. **321**(5897): p. 1807-12.
19. Pisapia, D.J., *The Updated World Health Organization Glioma Classification: Cellular and Molecular Origins of Adult Infiltrating Gliomas*. Arch Pathol Lab Med, 2017. **141**(12): p. 1633-1645.
20. Verhaak, R.G., et al., *Integrated genomic analysis identifies clinically relevant subtypes of glioblastoma characterized by abnormalities in PDGFRA, IDH1, EGFR, and NF1*. Cancer Cell, 2010. **17**(1): p. 98-110.
21. Brat, D.J., et al., *cIMPACT-NOW update 3: recommended diagnostic criteria for "Diffuse astrocytic glioma, IDH-wildtype, with molecular features of glioblastoma, WHO grade IV"*. Acta Neuropathol, 2018. **136**(5): p. 805-810.
22. Behnan, J., G. Finocchiaro, and G. Hanna, *The landscape of the mesenchymal signature in brain tumours*. Brain, 2019. **142**(4): p. 847-866.

23. Weller, M., et al., *European Association for Neuro-Oncology (EANO) guideline on the diagnosis and treatment of adult astrocytic and oligodendroglial gliomas*. *Lancet Oncol*, 2017. **18**(6): p. e315-e329.
24. Olson, R.A., P.K. Brastianos, and D.A. Palma, *Prognostic and predictive value of epigenetic silencing of MGMT in patients with high grade gliomas: a systematic review and meta-analysis*. *J Neurooncol*, 2011. **105**(2): p. 325-35.
25. Herrlinger, U., et al., *Lomustine-temozolomide combination therapy versus standard temozolomide therapy in patients with newly diagnosed glioblastoma with methylated MGMT promoter (CeTeG/NOA-09): a randomised, open-label, phase 3 trial*. *Lancet*, 2019. **393**(10172): p. 678-688.
26. Fernandes, C., et al., *Current Standards of Care in Glioblastoma Therapy*, in *Glioblastoma*, S. De Vleeschouwer, Editor. 2017, Codon Publications

Copyright: The Authors.: Brisbane (AU).

27. Mallick, S., et al., *Management of glioblastoma after recurrence: A changing paradigm*. *J Egypt Natl Canc Inst*, 2016. **28**(4): p. 199-210.
28. Song, J., et al., *Effectiveness of lomustine and bevacizumab in progressive glioblastoma: a meta-analysis*. *Onco Targets Ther*, 2018. **11**: p. 3435-3439.
29. Gilbert, M.R., et al., *A randomized trial of bevacizumab for newly diagnosed glioblastoma*. *N Engl J Med*, 2014. **370**(8): p. 699-708.
30. Wen, P.Y., et al., *Glioblastoma in adults: a Society for Neuro-Oncology (SNO) and European Society of Neuro-Oncology (EANO) consensus review on current management and future directions*. *Neuro Oncol*, 2020. **22**(8): p. 1073-1113.
31. Stupp, R., et al., *Effects of radiotherapy with concomitant and adjuvant temozolomide versus radiotherapy alone on survival in glioblastoma in a randomised phase III study: 5-year analysis of the EORTC-NCIC trial*. *Lancet Oncol*, 2009. **10**(5): p. 459-66.
32. Cabrera, A.R., et al., *Radiation therapy for glioblastoma: Executive summary of an American Society for Radiation Oncology Evidence-Based Clinical Practice Guideline*. *Pract Radiat Oncol*, 2016. **6**(4): p. 217-225.
33. Fitzek, M.M., et al., *Accelerated fractionated proton/photon irradiation to 90 cobalt gray equivalent for glioblastoma multiforme: results of a phase II prospective trial*. *J Neurosurg*, 1999. **91**(2): p. 251-60.
34. Baumann, M., et al., *Radiation oncology in the era of precision medicine*. *Nat Rev Cancer*, 2016. **16**(4): p. 234-49.
35. Niyazi, M., et al., *ESTRO-ACROP guideline "target delineation of glioblastomas"*. *Radiother Oncol*, 2016. **118**(1): p. 35-42.
36. Mayer, R. and P. Sminia, *Reirradiation tolerance of the human brain*. *Int J Radiat Oncol Biol Phys*, 2008. **70**(5): p. 1350-60.
37. Amelio, D. and M. Amichetti, *Radiation therapy for the treatment of recurrent glioblastoma: an overview*. *Cancers (Basel)*, 2012. **4**(1): p. 257-80.
38. Mitin, T. and A.L. Zietman, *Promise and pitfalls of heavy-particle therapy*. *J Clin Oncol*, 2014. **32**(26): p. 2855-63.
39. Chen, H., et al., *Interactions between synchrotron radiation X-ray and biological tissues - theoretical and clinical significance*. *Int J Physiol Pathophysiol Pharmacol*, 2011. **3**(4): p. 243-8.
40. Newhauser, W.D. and R. Zhang, *The physics of proton therapy*. *Phys Med Biol*, 2015. **60**(8): p. R155-209.
41. Tommasino, F. and M. Durante, *Proton radiobiology*. *Cancers (Basel)*, 2015. **7**(1): p. 353-81.
42. Hadziahmetovic, M., K. Shirai, and A. Chakravarti, *Recent advancements in multimodality treatment of gliomas*. *Future Oncol*, 2011. **7**(10): p. 1169-83.
43. Mohan, R., et al., *Radiobiological issues in proton therapy*. *Acta Oncol*, 2017. **56**(11): p. 1367-1373.
44. McNamara, A.L., J. Schuemann, and H. Paganetti, *A phenomenological relative biological effectiveness (RBE) model for proton therapy based on all published in vitro cell survival data*. *Phys Med Biol*, 2015. **60**(21): p. 8399-416.

45. Paganetti, H. and P. van Luijk, *Biological considerations when comparing proton therapy with photon therapy*. Semin Radiat Oncol, 2013. **23**(2): p. 77-87.
46. Durante, M., *Proton beam therapy in Europe: more centres need more research*. Br J Cancer, 2019. **120**(8): p. 777-778.
47. Shergalis, A., et al., *Current Challenges and Opportunities in Treating Glioblastoma*. Pharmacol Rev, 2018. **70**(3): p. 412-445.
48. Ali, M.Y., et al., *Radioresistance in Glioblastoma and the Development of Radiosensitizers*. Cancers (Basel), 2020. **12**(9).
49. Subiel, A., R. Ashmore, and G. Schettino, *Standards and Methodologies for Characterizing Radiobiological Impact of High-Z Nanoparticles*. Theranostics, 2016. **6**(10): p. 1651-71.
50. Pilié, P.G., et al., *State-of-the-art strategies for targeting the DNA damage response in cancer*. Nat Rev Clin Oncol, 2019. **16**(2): p. 81-104.
51. Seol, H.J., et al., *Prognostic implications of the DNA damage response pathway in glioblastoma*. Oncol Rep, 2011. **26**(2): p. 423-30.
52. Jackson, S.P. and J. Bartek, *The DNA-damage response in human biology and disease*. Nature, 2009. **461**(7267): p. 1071-8.
53. Ruan, K., G. Song, and G. Ouyang, *Role of hypoxia in the hallmarks of human cancer*. J Cell Biochem, 2009. **107**(6): p. 1053-62.
54. Gupta, K. and T.C. Burns, *Radiation-Induced Alterations in the Recurrent Glioblastoma Microenvironment: Therapeutic Implications*. Front Oncol, 2018. **8**: p. 503.
55. Gerstner, E.R., et al., *ACRIN 6684: Assessment of Tumor Hypoxia in Newly Diagnosed Glioblastoma Using 18F-FMISO PET and MRI*. Clin Cancer Res, 2016. **22**(20): p. 5079-5086.
56. Valable, S., et al., *Imaging of brain oxygenation with magnetic resonance imaging: A validation with positron emission tomography in the healthy and tumoural brain*. J Cereb Blood Flow Metab, 2017. **37**(7): p. 2584-2597.
57. Mendichovszky, I. and A. Jackson, *Imaging hypoxia in gliomas*. Br J Radiol, 2011. **84 Spec No 2**(Spec Iss 2): p. S145-58.
58. Gérard, M., et al., *Hypoxia Imaging and Adaptive Radiotherapy: A State-of-the-Art Approach in the Management of Glioma*. Front Med (Lausanne), 2019. **6**: p. 117.
59. Qiang, L., et al., *HIF-1 α is critical for hypoxia-mediated maintenance of glioblastoma stem cells by activating Notch signaling pathway*. Cell Death Differ, 2012. **19**(2): p. 284-94.
60. Wang, X., et al., *Reciprocal Signaling between Glioblastoma Stem Cells and Differentiated Tumor Cells Promotes Malignant Progression*. Cell Stem Cell, 2018. **22**(4): p. 514-528.e5.
61. Reisz, J.A., et al., *Effects of ionizing radiation on biological molecules--mechanisms of damage and emerging methods of detection*. Antioxid Redox Signal, 2014. **21**(2): p. 260-92.
62. Azzam, E.I., J.P. Jay-Gerin, and D. Pain, *Ionizing radiation-induced metabolic oxidative stress and prolonged cell injury*. Cancer Lett, 2012. **327**(1-2): p. 48-60.
63. Grimes, D.R. and M. Partridge, *A mechanistic investigation of the oxygen fixation hypothesis and oxygen enhancement ratio*. Biomed Phys Eng Express, 2015. **1**(4): p. 045209.
64. Wenzl, T. and J.J. Wilkens, *Theoretical analysis of the dose dependence of the oxygen enhancement ratio and its relevance for clinical applications*. Radiat Oncol, 2011. **6**: p. 171.
65. Gabriely, G., et al., *Role of AHR and HIF-1 α in Glioblastoma Metabolism*. Trends Endocrinol Metab, 2017. **28**(6): p. 428-436.
66. Kaur, B., et al., *Hypoxia and the hypoxia-inducible-factor pathway in glioma growth and angiogenesis*. Neuro Oncol, 2005. **7**(2): p. 134-53.
67. Méndez, O., et al., *Knock down of HIF-1 α in glioma cells reduces migration in vitro and invasion in vivo and impairs their ability to form tumor spheres*. Mol Cancer, 2010. **9**: p. 133.
68. Jeanes, A., C.J. Gottardi, and A.S. Yap, *Cadherins and cancer: how does cadherin dysfunction promote tumor progression?* Oncogene, 2008. **27**(55): p. 6920-9.
69. Alsaleem, M., et al., *The molecular mechanisms underlying reduced E-cadherin expression in invasive ductal carcinoma of the breast: high throughput analysis of large cohorts*. Mod Pathol, 2019. **32**(7): p. 967-976.

70. Lewis-Tuffin, L.J., et al., *Misregulated E-cadherin expression associated with an aggressive brain tumor phenotype*. PLoS One, 2010. **5**(10): p. e13665.
71. Noh, M.G., et al., *Prognostic significance of E-cadherin and N-cadherin expression in Gliomas*. BMC Cancer, 2017. **17**(1): p. 583.
72. Siebzehnruhl, F.A., et al., *The ZEB1 pathway links glioblastoma initiation, invasion and chemoresistance*. EMBO Mol Med, 2013. **5**(8): p. 1196-212.
73. Joseph, J.V., et al., *Hypoxia enhances migration and invasion in glioblastoma by promoting a mesenchymal shift mediated by the HIF1 α -ZEB1 axis*. Cancer Lett, 2015. **359**(1): p. 107-16.
74. Bravo-Cordero, J.J., L. Hodgson, and J. Condeelis, *Directed cell invasion and migration during metastasis*. Curr Opin Cell Biol, 2012. **24**(2): p. 277-83.
75. Skuli, N., et al., *Alphavbeta3/alphavbeta5 integrins-FAK-RhoB: a novel pathway for hypoxia regulation in glioblastoma*. Cancer Res, 2009. **69**(8): p. 3308-16.
76. Liu, Z., et al., *EGFRvIII/integrin β 3 interaction in hypoxic and vitronectin-enriching microenvironment promote GBM progression and metastasis*. Oncotarget, 2016. **7**(4): p. 4680-94.
77. Malric, L., et al., *Interest of integrins targeting in glioblastoma according to tumor heterogeneity and cancer stem cell paradigm: an update*. Oncotarget, 2017. **8**(49): p. 86947-86968.
78. Xu, Y., et al., *Procollagen-lysine 2-oxoglutarate 5-dioxygenase 2 promotes hypoxia-induced glioma migration and invasion*. Oncotarget, 2017. **8**(14): p. 23401-23413.
79. Aaberg-Jessen, C., et al., *Low expression of tissue inhibitor of metalloproteinases-1 (TIMP-1) in glioblastoma predicts longer patient survival*. J Neurooncol, 2009. **95**(1): p. 117-128.
80. Crocker, M., et al., *Serum angiogenic profile of patients with glioblastoma identifies distinct tumor subtypes and shows that TIMP-1 is a prognostic factor*. Neuro Oncol, 2011. **13**(1): p. 99-108.
81. Cassim, S. and J. Pouyssegur, *Tumor Microenvironment: A Metabolic Player that Shapes the Immune Response*. Int J Mol Sci, 2019. **21**(1).
82. Baumann, F., et al., *Lactate promotes glioma migration by TGF-beta2-dependent regulation of matrix metalloproteinase-2*. Neuro Oncol, 2009. **11**(4): p. 368-80.
83. Jiang, Y., I.D. Goldberg, and Y.E. Shi, *Complex roles of tissue inhibitors of metalloproteinases in cancer*. Oncogene, 2002. **21**(14): p. 2245-52.
84. Lampert, K., et al., *Expression of matrix metalloproteinases and their tissue inhibitors in human brain tumors*. Am J Pathol, 1998. **153**(2): p. 429-37.
85. Roche, J., *The Epithelial-to-Mesenchymal Transition in Cancer*. Cancers (Basel), 2018. **10**(2).
86. Iwadate, Y., *Epithelial-mesenchymal transition in glioblastoma progression*. Oncol Lett, 2016. **11**(3): p. 1615-1620.
87. Mahabir, R., et al., *Sustained elevation of Snail promotes glial-mesenchymal transition after irradiation in malignant glioma*. Neuro Oncol, 2014. **16**(5): p. 671-85.
88. Otomo, T., et al., *Microarray analysis of temporal gene responses to ionizing radiation in two glioblastoma cell lines: up-regulation of DNA repair genes*. J Radiat Res, 2004. **45**(1): p. 53-60.
89. Catania, A., et al., *Expression and localization of cyclin-dependent kinase 5 in apoptotic human glioma cells*. Neuro Oncol, 2001. **3**(2): p. 89-98.
90. Jeon, H.Y., et al., *Irradiation induces glioblastoma cell senescence and senescence-associated secretory phenotype*. Tumour Biol, 2016. **37**(5): p. 5857-67.
91. Brocard, E., et al., *Radiation-induced PGE2 sustains human glioma cells growth and survival through EGF signaling*. Oncotarget, 2015. **6**(9): p. 6840-9.
92. Seo, Y.S., et al., *Radiation-Induced Changes in Tumor Vessels and Microenvironment Contribute to Therapeutic Resistance in Glioblastoma*. Front Oncol, 2019. **9**: p. 1259.
93. Sangwan, V. and M. Park, *Receptor tyrosine kinases: role in cancer progression*. Curr Oncol, 2006. **13**(5): p. 191-3.
94. Du, Z. and C.M. Lovly, *Mechanisms of receptor tyrosine kinase activation in cancer*. Mol Cancer, 2018. **17**(1): p. 58.
95. Jackson, M., et al., *The genetic basis of disease*. Essays Biochem, 2018. **62**(5): p. 643-723.
96. Siveen, K.S., et al., *Role of Non Receptor Tyrosine Kinases in Hematological Malignancies and its Targeting by Natural Products*. Mol Cancer, 2018. **17**(1): p. 31.

97. Stehelin, D., et al., *Detection and enumeration of transformation-defective strains of avian sarcoma virus with molecular hybridization*. *Virology*, 1977. **76**(2): p. 675-84.
98. Irby, R.B. and T.J. Yeatman, *Role of Src expression and activation in human cancer*. *Oncogene*, 2000. **19**(49): p. 5636-42.
99. Roskoski, R., Jr., *Src protein-tyrosine kinase structure, mechanism, and small molecule inhibitors*. *Pharmacol Res*, 2015. **94**: p. 9-25.
100. Sen, B. and F.M. Johnson, *Regulation of SRC family kinases in human cancers*. *J Signal Transduct*, 2011. **2011**: p. 865819.
101. Guan, J.L., *Integrin signaling through FAK in the regulation of mammary stem cells and breast cancer*. *IUBMB Life*, 2010. **62**(4): p. 268-76.
102. Lieu, C. and S. Kopetz, *The SRC family of protein tyrosine kinases: a new and promising target for colorectal cancer therapy*. *Clin Colorectal Cancer*, 2010. **9**(2): p. 89-94.
103. *Comprehensive genomic characterization defines human glioblastoma genes and core pathways*. *Nature*, 2008. **455**(7216): p. 1061-8.
104. Ahluwalia, M.S., et al., *Targeting SRC in glioblastoma tumors and brain metastases: rationale and preclinical studies*. *Cancer Lett*, 2010. **298**(2): p. 139-49.
105. Bolós, V., et al., *The dual kinase complex FAK-Src as a promising therapeutic target in cancer*. *Onco Targets Ther*, 2010. **3**: p. 83-97.
106. Ding, Q., et al., *The pattern of enhancement of Src kinase activity on platelet-derived growth factor stimulation of glioblastoma cells is affected by the integrin engaged*. *J Biol Chem*, 2003. **278**(41): p. 39882-91.
107. Han, X., et al., *The role of Src family kinases in growth and migration of glioma stem cells*. *Int J Oncol*, 2014. **45**(1): p. 302-10.
108. Eom, H., et al., *MerTK mediates STAT3-KRAS/SRC-signaling axis for glioma stem cell maintenance*. *Artif Cells Nanomed Biotechnol*, 2018. **46**(sup2): p. 87-95.
109. Fianco, G., C. Cenci, and D. Barilà, *Caspase-8 expression and its Src-dependent phosphorylation on Tyr380 promote cancer cell neoplastic transformation and resistance to anoikis*. *Exp Cell Res*, 2016. **347**(1): p. 114-122.
110. Lluís, J.M., et al., *Dual role of mitochondrial reactive oxygen species in hypoxia signaling: activation of nuclear factor- κ B via c-SRC and oxidant-dependent cell death*. *Cancer Res*, 2007. **67**(15): p. 7368-77.
111. Calgani, A., et al., *Suppression of SRC Signaling Is Effective in Reducing Synergy between Glioblastoma and Stromal Cells*. *Mol Cancer Ther*, 2016. **15**(7): p. 1535-44.
112. Huang, W.J., W.W. Chen, and X. Zhang, *Glioblastoma multiforme: Effect of hypoxia and hypoxia inducible factors on therapeutic approaches*. *Oncol Lett*, 2016. **12**(4): p. 2283-2288.
113. Mukhopadhyay, D., et al., *Hypoxic induction of human vascular endothelial growth factor expression through c-Src activation*. *Nature*, 1995. **375**(6532): p. 577-81.
114. Delamarre, E., et al., *Expression of integrin alpha6beta1 enhances tumorigenesis in glioma cells*. *Am J Pathol*, 2009. **175**(2): p. 844-55.
115. Huvelde, D., et al., *Targeting Src family kinases inhibits bevacizumab-induced glioma cell invasion*. *PLoS One*, 2013. **8**(2): p. e56505.
116. Keunen, O., et al., *Anti-VEGF treatment reduces blood supply and increases tumor cell invasion in glioblastoma*. *Proc Natl Acad Sci U S A*, 2011. **108**(9): p. 3749-54.
117. Keller, S. and M.H.H. Schmidt, *EGFR and EGFRvIII Promote Angiogenesis and Cell Invasion in Glioblastoma: Combination Therapies for an Effective Treatment*. *Int J Mol Sci*, 2017. **18**(6).
118. Trylcova, J., et al., *Effect of cancer-associated fibroblasts on the migration of glioma cells in vitro*. *Tumour Biol*, 2015. **36**(8): p. 5873-9.
119. Park, C.M., et al., *Ionizing radiation enhances matrix metalloproteinase-2 secretion and invasion of glioma cells through Src/epidermal growth factor receptor-mediated p38/Akt and phosphatidylinositol 3-kinase/Akt signaling pathways*. *Cancer Res*, 2006. **66**(17): p. 8511-9.
120. Yoo, K.C., et al., *Proinvasive extracellular matrix remodeling in tumor microenvironment in response to radiation*. *Oncogene*, 2018. **37**(24): p. 3317-3328.

121. Kegelman, T.P., et al., *Inhibition of radiation-induced glioblastoma invasion by genetic and pharmacological targeting of MDA-9/Syntenin*. Proc Natl Acad Sci U S A, 2017. **114**(2): p. 370-375.
122. Jubran, M.R., et al., *Dissecting the role of crosstalk between glioblastoma subpopulations in tumor cell spreading*. Oncogenesis, 2020. **9**(2): p. 11.
123. Ohshima, Y., et al., *Involvement of connexin43 hemichannel in ATP release after γ -irradiation*. J Radiat Res, 2012. **53**(4): p. 551-7.
124. Chepied, A., et al., *Involvement of the Gap Junction Protein, Connexin43, in the Formation and Function of Invadopodia in the Human U251 Glioblastoma Cell Line*. Cells, 2020. **9**(1).
125. Arscott, W.T., et al., *Ionizing radiation and glioblastoma exosomes: implications in tumor biology and cell migration*. Transl Oncol, 2013. **6**(6): p. 638-48.
126. Maher, M., et al., *Novel pyrazolo[3,4-d]pyrimidines: design, synthesis, anticancer activity, dual EGFR/ErbB2 receptor tyrosine kinases inhibitory activity, effects on cell cycle profile and caspase-3-mediated apoptosis*. J Enzyme Inhib Med Chem, 2019. **34**(1): p. 532-546.
127. Greco, C., et al., *Development of Pyrazolo[3,4-d]pyrimidine Kinase Inhibitors as Potential Clinical Candidates for Glioblastoma Multiforme*. ACS Med Chem Lett, 2020. **11**(5): p. 657-663.
128. Carraro, F., et al., *Pyrazolo[3,4-d]pyrimidines as potent antiproliferative and proapoptotic agents toward A431 and 8701-BC cells in culture via inhibition of c-Src phosphorylation*. J Med Chem, 2006. **49**(5): p. 1549-61.
129. Tintori, C., et al., *Combining X-ray crystallography and molecular modeling toward the optimization of pyrazolo[3,4-d]pyrimidines as potent c-Src inhibitors active in vivo against neuroblastoma*. J Med Chem, 2015. **58**(1): p. 347-61.
130. Fallacara, A.L., et al., *A New Strategy for Glioblastoma Treatment: In Vitro and In Vivo Preclinical Characterization of Si306, a Pyrazolo[3,4-d]Pyrimidine Dual Src/P-Glycoprotein Inhibitor*. Cancers (Basel), 2019. **11**(6).
131. Pearson, J.R.D. and T. Regad, *Targeting cellular pathways in glioblastoma multiforme*. Signal Transduct Target Ther, 2017. **2**: p. 17040.
132. Nørøxe, D.S., H.S. Poulsen, and U. Lassen, *Hallmarks of glioblastoma: a systematic review*. ESMO Open, 2016. **1**(6): p. e000144.
133. Vollmann-Zwerenz, A., et al., *Tumor Cell Invasion in Glioblastoma*. Int J Mol Sci, 2020. **21**(6).
134. Erasmus, H., et al., *DNA repair mechanisms and their clinical impact in glioblastoma*. Mutat Res Rev Mutat Res, 2016. **769**: p. 19-35.
135. Lo Dico, A., et al., *Intracellular Redox-Balance Involvement in Temozolomide Resistance-Related Molecular Mechanisms in Glioblastoma*. Cells, 2019. **8**(11).
136. Singh, G.K., et al., *Radiation-Induced Malignancies Making Radiotherapy a "Two-Edged Sword": A Review of Literature*. World J Oncol, 2017. **8**(1): p. 1-6.
137. Eom, K.Y., et al., *The Effect of Chemoradiotherapy with SRC Tyrosine Kinase Inhibitor, PP2 and Temozolomide on Malignant Glioma Cells In Vitro and In Vivo*. Cancer Res Treat, 2016. **48**(2): p. 687-97.
138. Whitehead, C.A., et al., *Inhibition of Radiation and Temozolomide-Induced Invadopodia Activity in Glioma Cells Using FDA-Approved Drugs*. Transl Oncol, 2018. **11**(6): p. 1406-1418.
139. Cirotti, C., C. Contadini, and D. Barilà, *SRC Kinase in Glioblastoma News from an Old Acquaintance*. Cancers (Basel), 2020. **12**(6).
140. *Clinical Trial Evaluating the Combination of Vandetanib and Dasatinib During and After Radiation Therapy (RT) in Children With Newly Diagnosed Diffuse Intrinsic Pontine Glioma (DIPG)*.
141. *Dasatinib Plus Radiation Therapy/Temozolomide in Newly-Diagnosed Glioblastoma*.
142. *Dasatinib or Placebo, Radiation Therapy, and Temozolomide in Treating Patients With Newly Diagnosed Glioblastoma Multiforme*.
143. Agarwal, S., et al., *Active efflux of Dasatinib from the brain limits efficacy against murine glioblastoma: broad implications for the clinical use of molecularly targeted agents*. Mol Cancer Ther, 2012. **11**(10): p. 2183-92.
144. Franken, N.A., et al., *Clonogenic assay of cells in vitro*. Nat Protoc, 2006. **1**(5): p. 2315-9.

145. Barrett, T., et al., *NCBI GEO: archive for functional genomics data sets--update*. *Nucleic Acids Res*, 2013. **41**(Database issue): p. D991-5.

11. LIST OF PUBLISHED PAPERS AND CONGRESS CONTRIBUTION

PUBLISHED PAPERS:

- *Scientific report. 2021 Jan (accepted for publication)*

A quantum-inspired classifier for clonogenic assay evaluations

Giuseppe Sergioli, Carmelo Militello, Leonardo Rundo , Luigi Minafra, **Filippo**

Torrise, Giorgio Russo, Keng Loon Chow, and Roberto Giuntini

Contributions:G.S. conceived the experiment, analysed the results and coordinated the research. C.M. conceived the experiment and analysed the results. L.R. conceived the experiment and analysed the results. L.M. and **F.T.**, extracted the datasets. G.R. conceived the experiment. K.L.C. conducted and analysed the experiment. R.G. conceived and conducted the experiment. All author 394 reviewed the manuscript.

- *Review Cancers (Basel). 2020 Oct 4;12(10):E2860. doi: 10.3390/cancers12102860.*

The Role of Hypoxia and SRC Tyrosine Kinase in Glioblastoma Invasiveness and Radioresistance

Filippo Torrise, Nunzio Vicario, Federica M Spitale, Francesco P Cammarata, Luigi Minafra, Lucia Salvatorelli, Giorgio Russo, Giacomo Cuttone, Samuel Valable, Rosario Gulino, Gaetano Magro, Rosalba Parenti

PMID: 33020459 DOI: 10.3390/cancers12102860

Contributions: Conceptualization, **F.T.**, N.V., R.P.; writing—original draft preparation, **F.T.**, N.V., F.P.C.,R.G., S.V., G.M., R.P.; writing—review and editing, **F.T.**, N.V., F.M.S., F.P.C., L.M., L.S., G.R., G.C., S.V., R.G., G.M.,R.P. All authors have read and agreed to the published version of the manuscript.

- *Int J Mol Sci. 2020 Sep 1;21(17):6337. doi: 10.3390/ijms21176337.*

Molecular Investigation on a Triple Negative Breast Cancer Xenograft Model Exposed to Proton Beams

Francesco P Cammarata, Giusi I Forte , Giuseppe Broggi, Valentina Bravatà, Luigi Minafra, Pietro Pisciotta, Marco Calvaruso, Roberta Tringali, Barbara Tomasello, **Filippo Torrise**, Giada Petringa, Giuseppe A P Cirrone, Giacomo Cuttone, Rosaria Acquaviva, Rosario Caltabiano, Giorgio Russo

PMID: 32882850 PMCID: PMC7503243 DOI: 10.3390/ijms21176337

Contributions: All authors participated in the conception and elaboration of the study. In particular, G.R., P.P. performed the irradiation setups and together with F.P.C. and R.T. performed the PT mice treatments. R.C. and G.B. carried out the histopathological and immunohistochemical characterizations. V.B. performed the microarray experiments and the gene expression analyses. G.I.F., V.B., F.P.C., R.C., G.B., L.M., P.P.; M.C., P.P., G.R., R.T.; B.T., **F.T.**, R.A., G.P., G.A.P.C. and G.C. were involved in the interpretation of the

findings and approved the final content of the manuscript. All authors have read and agreed to the published version of the manuscript.

- *Review Inflamm Res. 2020 Sep;69(9):841-850. doi: 10.1007/s00011-020-01363-9. Epub 2020 Jun 12.*

Intercellular communication and ion channels in neuropathic pain chronicization

Nunzio Vicario, Rita Turnaturi, Federica Maria Spitale, **Filippo Torrissi**, Agata Zappalà, Rosario Gulino, Lorella Pasquinucci, Santina Chiechio, Carmela Parenti, Rosalba Parenti

PMID: 32533221 DOI: 10.1007/s00011-020-01363-9.

Contributions: Conceptualization: NV, RT, CP, RP; Writing the original draft: NV, RT, CP, RP; Critically reviewed and edited the manuscript: NV, RT, FMS, **FT**, AZ, RG, LP, SC, CP, RP.

- *Int J Mol Sci. 2020 May 30;21(11):3917. doi: 10.3390/ijms21113917.*

SRC Tyrosine Kinase Inhibitor and X-rays Combined Effect on Glioblastoma Cell Lines

Filippo Torrissi, Luigi Minafra, Francesco P Cammarata, Gaetano Savoca, Marco Calvaruso, Nunzio Vicario, Laura Maccari, Elodie A Pérès, Hayriye Özçelik, Myriam Bernaudin, Lorenzo Botta, Giorgio Russo, Rosalba Parenti, Samuel Valable

PMID: 32486205 PMCID: PMC7312922 DOI: 10.3390/ijms21113917

Contributions: Conceptualization, **F.T.**, L.M. (Luigi Minafra), F.P.C., S.V.; methodology, **F.T.**, L.M. (Luigi Minafra), F.P.C., G.S., M.C., E.A.P., H.Ö., S.V.; investigation, **F.T.**, L.M. (Luigi Minafra), S.V.; data curation and formal analysis, **F.T.**, L.M. (Luigi Minafra), N.V. and S.V.; resources, L.M. (Laura Maccari), M.B., L.B., G.R., R.P., S.V.; writing—original draft preparation, **F.T.**; writing—review and editing, **F.T.**, L.M. (Luigi Minafra), F.P.C., N.V., R.P., S.V.; supervision, **F.T.**, L.M. (Luigi Minafra), F.P.C., M.B., G.R., R.P., S.V.; project administration, F.P.C., M.B., L.B., G.R., R.P., S.V.; funding acquisition, M.B., G.R., R.P., S.V. All authors have read and agreed to the published version of the manuscript.

- *PLoS One. 2020 May 22;15(5):e0233258. doi: 10.1371/journal.pone.0233258. eCollection 2020.*

Evaluation of proton beam radiation-induced skin injury in a murine model using a clinical SOBP

Pietro Pisciotta, Angelita Costantino, Francesco Paolo Cammarata, **Filippo Torrissi**, Giovanna Calabrese, Valentina Marchese, Giuseppe Antonio Pablo Cirrone, Giada Petringa, Giusi Irma Forte, Luigi Minafra, Valentina Bravatà, Massimo Gulisano, Fabrizio Scopelliti, Francesco Tommasino, Emanuele Scifoni, Giacomo Cuttone, Massimo Ippolito, Rosalba Parenti, Giorgio Russo

PMID: 32442228 PMCID: PMC7244158 DOI: 10.1371/journal.pone.0233258

Contributions: Conceptualization: P.P, A.C, G.R.; Data curation: P.P, A.C; Formal analysis: P.P., A.C., S.C.; Funding acquisition: G.C., G.R.; Investigation: A.C., F.P.C., V.M., G.R.; Methodology: P.P., A.C., F.P.C., M.G., G.R.; Project administration: F.P.C., R.P., G.R.; Resources: F.P.C., G.A.P.C., G.P., G.I.F., L.M., V.B., F.S.; Supervision: P.P., F.P.C., M.G., F.T. (Francesco Tommasino), E.S., G.C., M.I., R.P., G.R.; Validation: P.P., A.C., F.P.C., M.G., R.P., G.R.; Visualization: A.C. Writing – original draft: P.P., A.C., **F.T.** (Filippo Torrissi)

- *Int J Mol Sci. 2019 Sep 24;20(19):4745. doi: 10.3390/ijms20194745.*

Proton Therapy and Src Family Kinase Inhibitor Combined Treatments on U87 Human Glioblastoma Multiforme Cell Line

Francesco P Cammarata, **Filippo Torrissi**, Giusi I Forte, Luigi Minafra, Valentina Bravatà, Pietro Pisciotta, Gaetano Savoca, Marco Calvaruso, Giada Petringa, Giuseppe A P Cirrone, Anna L Fallacara, Laura Maccari, Maurizio Botta, Silvia Schenone, Rosalba Parenti, Giacomo Cuttone, Giorgio Russo

PMID: 31554327 PMCID: PMC6801826 DOI: 10.3390/ijms20194745

Contributions: All authors participated in the conception, design, interpretation, and elaboration of the findings of the study, as well as in drafting and revising the final version. In particular, G.R., P.P., G.S., G.A.P.C. and G.P. studied the irradiation setup, simulations and dose distribution. F.P.C., **F.T.**, M.C. and L.M. (Luigi Minafra), performed cell irradiations. F.P.C., L.M. (Luigi Minafra), G.I.F. and **F.T.** maintained cell cultures and carried out cell survival experiments. L.M. (Laura Maccari), A.L.F., and S.S. carried out the Si306 synthesis and IC50 determination. P.P. and G.S. performed DMF and LQ model analysis. V.B. performed whole-genome cDNA microarray experiments and gene expression profile network analyses. **F.T.** M.B, G.C., R.P., G.R. participated in the elaboration of the findings of the study, drafting and revising the final version. All authors read and approved the final content of the manuscript.

- *IL NUOVO CIMENTO C; YEAR 2018 - ISSUE 6 - NOVEMBER-DECEMBER, SIRR 2018*
DOI: 10.1393/ncc/i2018-18203-8 Published online 3 May 2019

Preliminary study of novel SRC tyrosine kinase inhibitor and proton therapy combined effect on glioblastoma multiforme cell line: In vitro evaluation of target therapy for the enhancement of protons effectiveness

Luigi Minafra, Francesco P. Cammarata, **Filippo Torrissi**, Giusi I. Forte, Valentina Bravatà, Marco Calvaruso, Pietro Pisciotta, Carmelo Militello, Giada Petringa, Giuseppe A. P. Cirrone, Anna L. Fallacara, Laura Maccari, Maurizio Botta, Giacomo Cuttone, Giorgio Russo

- *Int J Mol Sci.* 2018 Dec 7;19(12):3944. doi: 10.3390/ijms19123944.

MiR-19a Overexpression in FTC-133 Cell Line Induces a More De-Differentiated and Aggressive Phenotype

Giovanna Calabrese, Anna Dolcimascolo, **Filippo Torrisi**, Agata Zappalà, Rosario Gulino, Rosalba Parenti

PMID: 30544640 PMCID: PMC6320980 DOI:

Contributions: All authors had substantial contribution to the present work. Conceptualization, G.C. and R.P.; Data curation, G.C. and A.Z.; Funding acquisition, R.G. and R.P.; Methodology, A.D. and **F.T.**; Resources, R.P.; Supervision, R.P.; Writing—review & editing, G.C. and R.P.; G.C. is also the corresponding author. All the authors gave the final approval of the version to be published.

- *Phys Med.* 2018 Oct;54:173-178. doi: 10.1016/j.ejmp.2018.07.003. Epub 2018 Jul 20.

Monte Carlo GEANT4-based application for in vivo RBE study using small animals at LNS-INFN preclinical hadrontherapy facility

P. Pisciotta, F.P. Cammarata, A. Stefano, F. Romano, V. Marchese, **F. Torrisi**, G.I. Forte, L. Cella, G.A.P. Cirrone, G. Petringa, M.C. Gilardi, G. Cuttone, G. Russo

PMID: 30037452 DOI: 10.1016/j.ejmp.2018.07.003

CONGRESS CONTRIBUTION:

- National Congress of Società Italiana per la Ricerca sulle Radiazioni (SIRR)
Scientific poster : *Evaluation of SRC inhibition combined with X-rays in normoxic and hypoxic glioblastoma cell lines*
10-12 November 2020 (*webinar modality*)
- Annual Retreat of Dipartimento di Scienze Biomediche e Biotecnologiche (BIOMETEC), Università di Catania
Oral presentation of Ph.D. activities research
30 November - 1 December 2019; Hotel Capo Peloro, Torre Faro, Messina.
- 17th European Network for Light Ion Hadron Therapy (ENLIGHT) Annual Meeting and Training
Scientific poster: *Multicenter evaluation of hypoxia effects on OER and RBE of charged particles on glioblastoma cell lines.*
1-3 July 2019 ; Centre François Baclesse, Caen, France.
- National Congresso di Società Italiana per la Ricerca sulle Radiazioni (SIRR)
Oral presentation: *Evaluation of novel c-Src tyrosine kinase inhibitor and proton therapy combined effect: a preliminary in vitro study toward the preclinical phase for glioblastoma multiforme treatment*

10-13 September 2018; Università degli studi Roma tre

- 7th European Workshop in Drug Synthesis (EWDSy)

Scientific poster: *First National Radiopharmaceuticals and Hadrontherapy facility from preclinical molecular imaging studies to therapy.*

20 - 24 May 2018; Certosa di Pontignano, Siena

12. ACKNOWLEDGMENTS

At the end of my Ph.D, I would like to express my deepest gratitude to everyone that gave me the opportunity to realize this work. The thought to have offered a little contribution for the scientific community progression makes me proud and it is my biggest satisfaction. But, none of this would have been possible without the trust of Prof. Rosalba Parenti, my tutor, who has always shown great help, availability, care and interest for my professional growth.

I would like to thank Dr. Nunzio Vicario, for his incessant assistance, critical observations and essential suggestions, I think that I can only learn from a young, but very talented researcher as him. I also thank Prof. Rosario Gulino for his valuable scientific advices, my colleague Federica Spitale and all the students who share with me the laboratory life in a peaceful working environment.

I think to be very lucky to work and collaborate with several expert researchers, such as the group of the IBFM-CNR; a special thank to Dr. Francesco Cammarata, Dr. Giorgio Russo and Dr. Luigi Minafra, who introduced me to the fascinating field of radiobiology and guided me during my experimental activities. It was tiring but enjoyable to spend the endless nights of work during the proton beam time. Thanks to Dr. Giusi Forte, Dr. Valentina Bravatà, Dr. Gaetano Savoca and Dr. Marco Calvaruso for their significant cooperation. I would like to thank all the INFN-LNS team of physicists for their professionalism and willingness during the irradiation experiments.

Thanks to Dr. Samuel Valable, who represented my mentor for the research activities conducted in my period abroad. I am glad and honored to have taken part in his prolific and innovative laboratory, where I had the possibility to improve my scientific skills, knowledge and professional abilities. I also thank all the members of Cyceron Institute, who always made me feel at home. They gave me an unforgettable work and social experience, between the laboratory benches and the greenery of Normandy.

I enormously thank all my family, my parents and my brothers. They have been a point of reference, where I have always found a big support during the difficulties. Finally, thanks to my sweet Eleonora; she has always knew how to understand and encourage me during my troubles and the most intense periods of work; thanks for your patience and for always being there, without you I would not have preserve the internal serenity to face the work in the best way.